Supporting Information for:

Potent inhibition of nicotinamide N-methyltransferase by alkene-linked bisubstrate mimics bearing electron deficient aromatics

Yongzhi Gao,[a,‡] Matthijs J. van Haren,[a,‡] Ned Buijs,[a] Paolo Innocenti,[a] Yurui Zhang,[a] Davide Sartini,[b] Roberto Campagna,[b] Monica Emanuelli,[b] Richard B. Parsons,[c] Willem Jespers,[d,e] Hugo Gutiérrez-de-Terán,[e] Gerard J. P. van Westen,[d] Nathaniel I. Martin[a,*]

[‡]*These authors contributed equally*

[a]*Biological Chemistry Group, Institute of Biology Leiden, Leiden University, Sylviusweg 72, 2333 BE Leiden, The Netherlands;* [b]*Department of Clinical Sciences, Universitá Politecnica delle Marche, Via Ranieri 65, 60131, Ancona, Italy;* [c]*Institute of Pharmaceutical Science, King's College London, London SE1 9NH, United Kingdom;* [d]*Drug Discovery and Safety, Leiden Academic Center for Drug Research, Einsteinweg 55, 2333 CC, Leiden, The Netherlands;* [e]*Department of Cell and Molecular Biology, Uppsala University, Uppsala 75124, Sweden*

**E-mail: n.i.martin@biology.leidenuniv.nl*

Table of Contents

IC_{50} curves

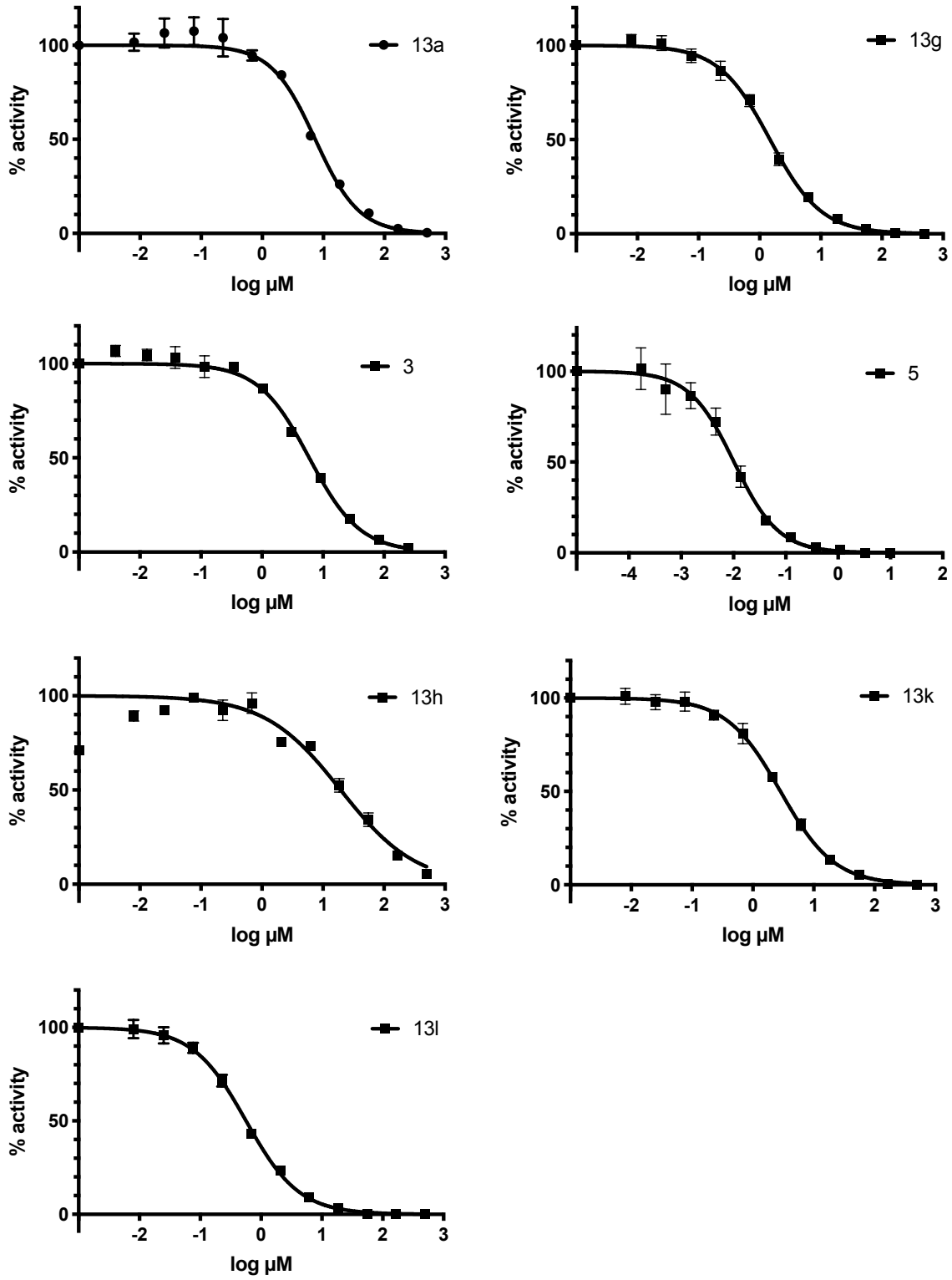

Figure S1. IC_{50} curves of reference compounds **3** and **5** and bicyclic aromatic compounds **13a-l**

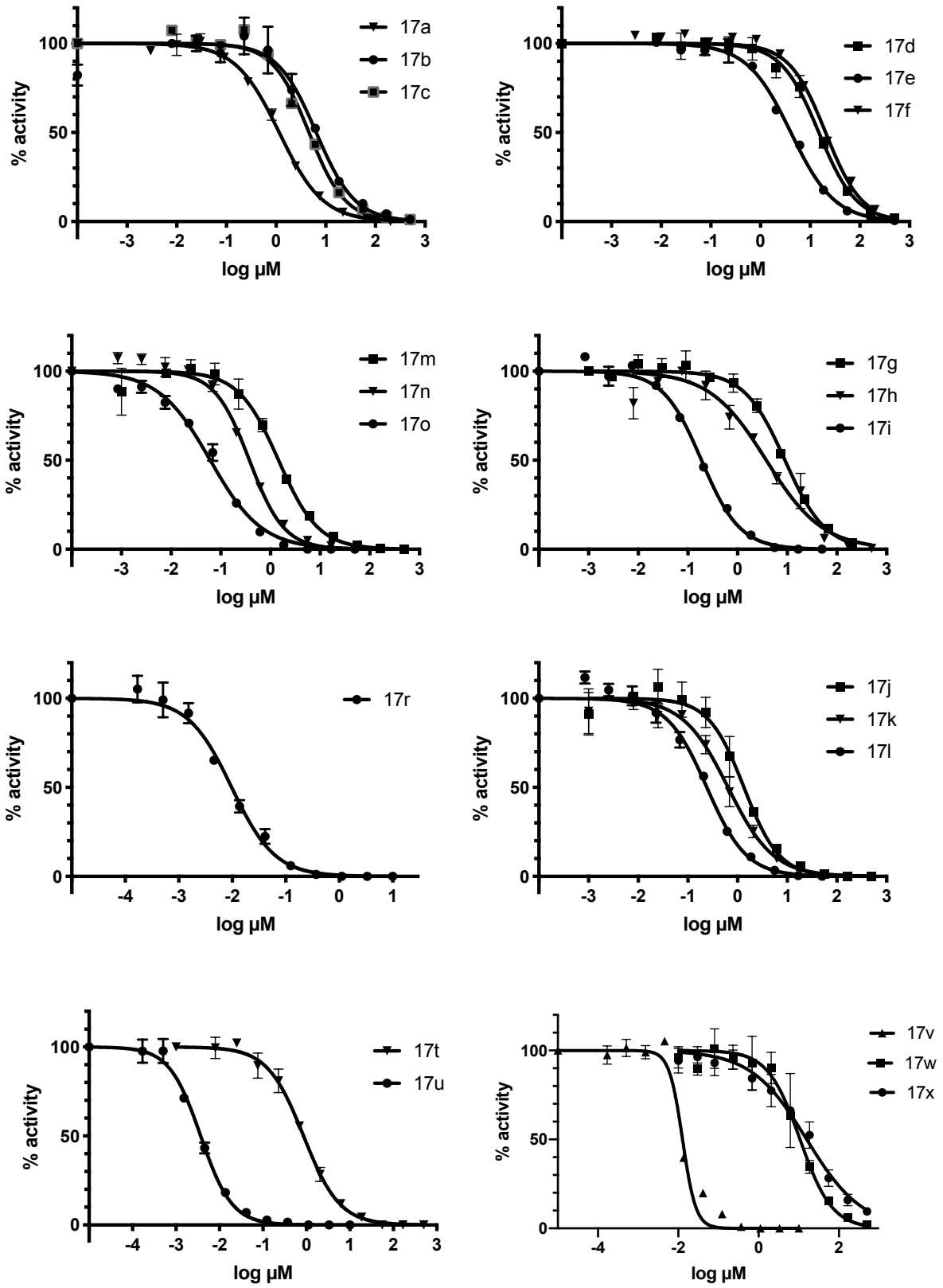

Figure S2. IC_{50} curves of alkenyl linked compounds **17a-x**.

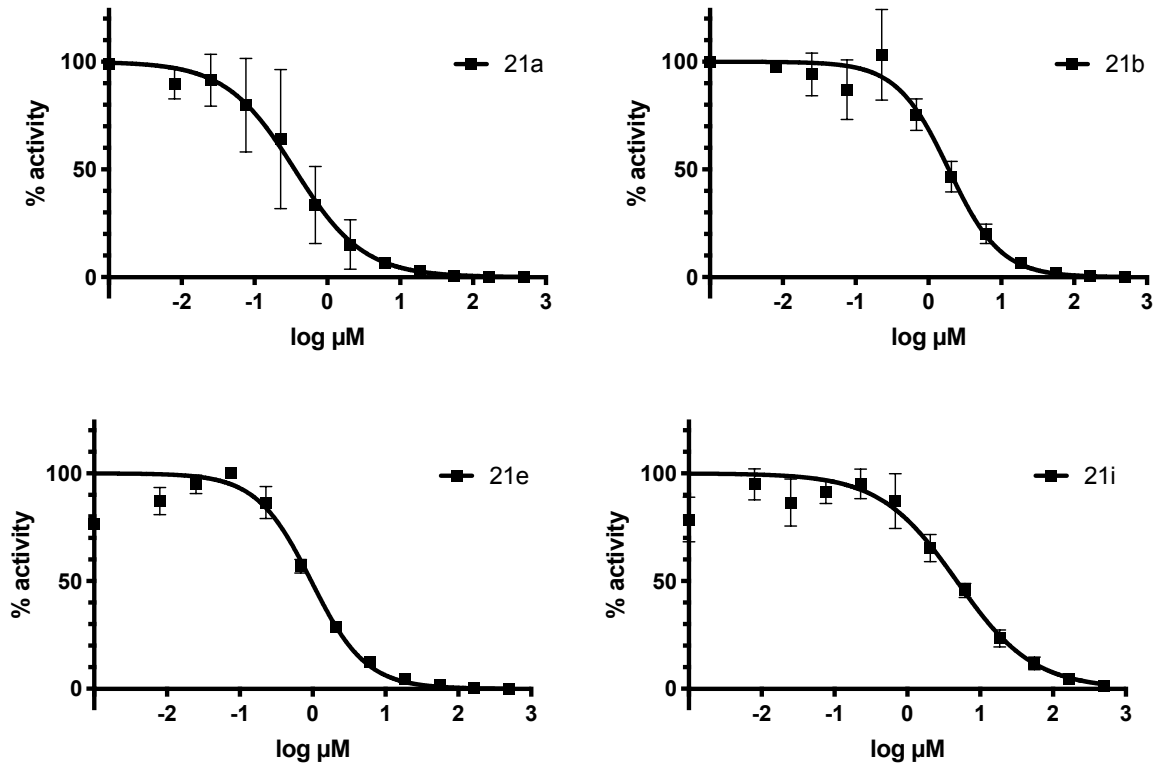

Figure S3. IC_{50} curves of compounds **21a**, **21b**, **21e** and **21i** bearing different substitutions replacing the amino acid group

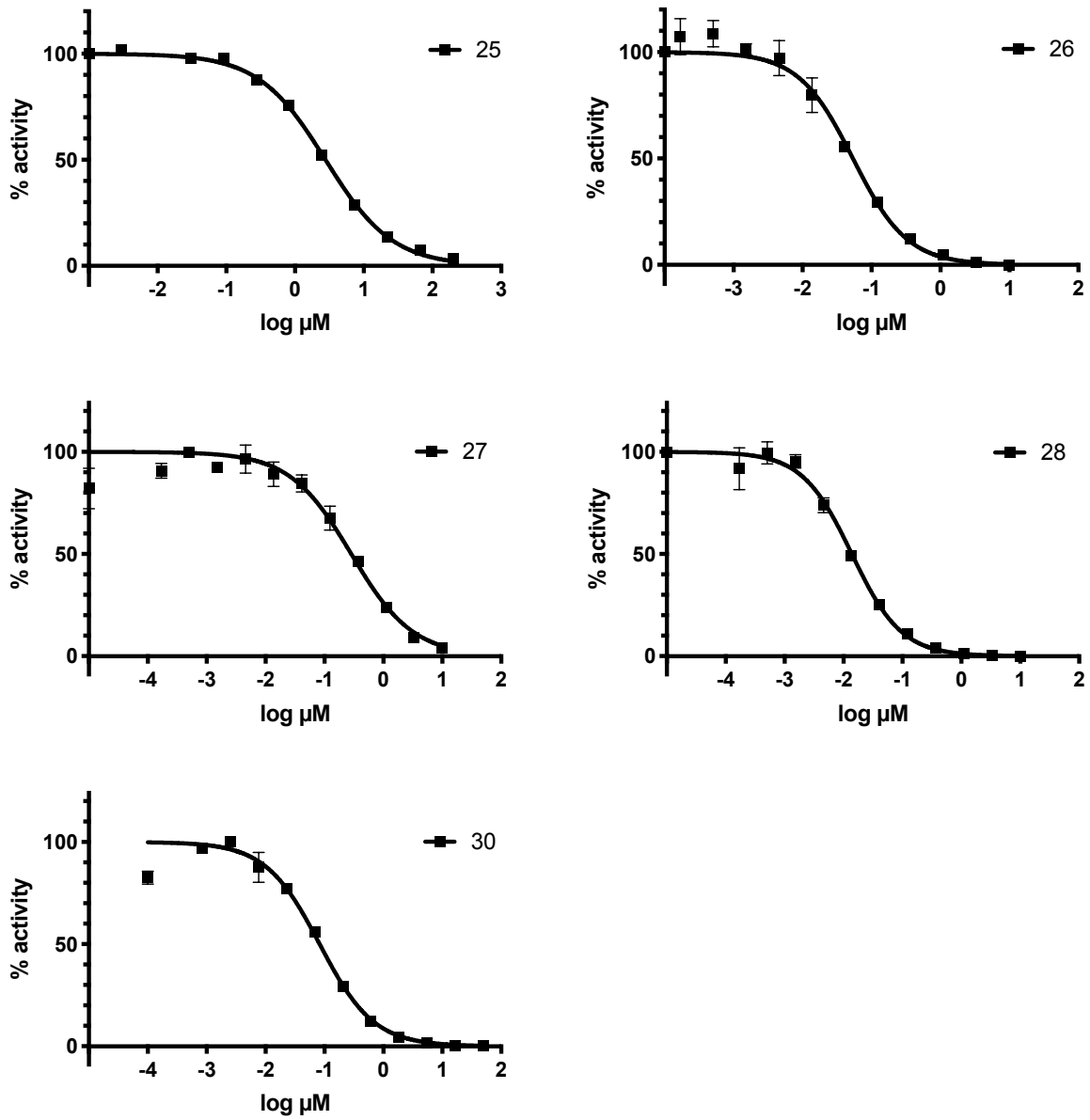

Figure S4. IC_{50} curves for compounds **25**-**28** and **30**, with varying linkers to either a *para*-cyano or *meta*-amide substituted phenyl group.

Comparative inhibition data

Table S1. IC_{50} values for para-cyano compounds **17u** and **28** and meta-amide compounds **17v** and **5** in the presence of SAM at its K_M value of 8.5 μM or 10 times its K_M value (85 μM)

			IC_{50} in nM with s.e.m.	
Compound	**substitution**	**linker**	**8.5 μM SAM**	**85 μM SAM**
17u	*para*-CN	propenyl	3.69 ± 0.17	16.00 ± 1.48
28	*para*-CN	propargyl	69.29 ± 4.42	258.25 ± 26.21
17v	*meta*-amide	propenyl	12.76 ± 0.78	39.53 ± 4.52
5	*meta*-amide	propargyl	10.23 ± 0.90	21.66 ± 1.61

Table S2. Apparent Ki values for para-cyano compounds **17u** and **28** and meta-amide compounds **17v** and **5** in the presence of SAM at its K_M value of 8.5 μM or 10 times its K_M value (85 μM) obtained using Morrison's equation for tight binding inhibitors

			Ki_{app} in nM with s.e.m.	
Compound	**substitution**	**linker**	**8.5 μM SAM**	**85 μM SAM**
17u	*para*-CN	propenyl	1.70 ± 0.12	1.49 ± 0.22
28	*para*-CN	propargyl	34.90 ± 2.58	35.38 ± 0.96
17v	*meta*-amide	propenyl	6.93 ± 1.15	5.23 ± 4.52
5	*meta*-amide	propargyl	5.11 ± 0.44	2.48 ± 0.32

Isothermal Titration Calorimetry

Thermodynamic parameters of the three independent experiments are reported in Table S3. Thermograms of the measurements are presented in Figure S5.

Table S3. Thermodynamic parameters for the three independent titrations of compound **17u** to hNNMT

		K_D	ΔH	ΔG	-TΔS
replicate	**n**	**(nM)**	**(kcal/mol)**	**(kcal/mol)**	**(kcal/mol)**
1	0.895 ± 0.008	21.60 ± 6.94	-5.56 ± 0.12	-10.50	-4.89
2	0.936 ± 0.006	20.40 ± 5.36	-5.18 ± 0.09	-10.50	-5.31
3	0.849 ± 0.006	21.70 ± 6.07	-5.38 ± 0.10	-10.50	-5.07
Average	**0.893 ± 0.006**	**21.23 ± 6.12**	**-5.37 ± 0.10**	**-10.50**	**-5.09**

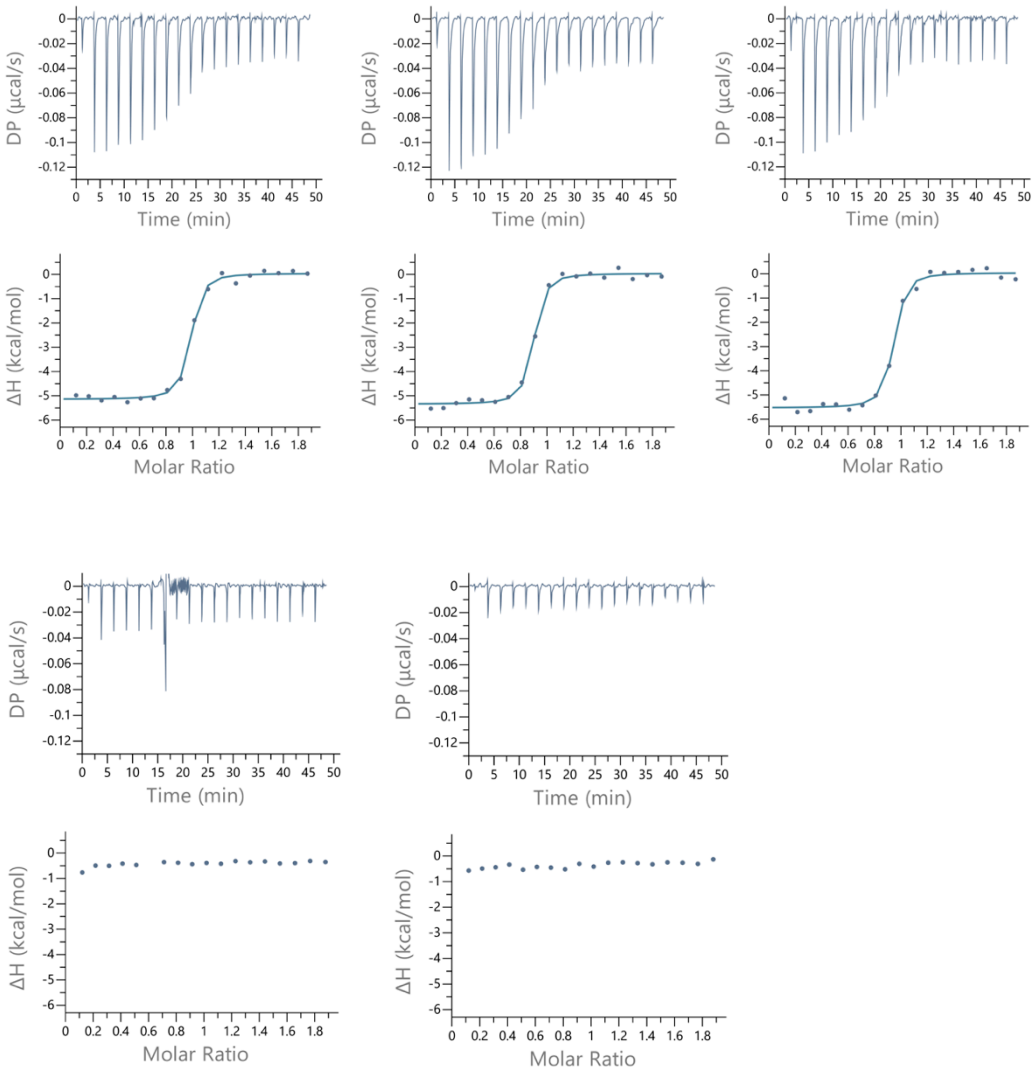

Figure S5. Isothermal Titration Calorimetry thermograms of the three independent experiments of the titration of compound **17u** to hNNMT (top) and the thermograms of the control experiments of titrations of buffer to enzyme and compound **17u** to buffer (bottom).

Selectivity studies

The results of selectivity assays against twelve different methyltransferases are summarized in Table S4 and the accompanying bar graph below.

Table S4. Selectivity data for compound 17u against a panel of 12 methyltransferases. Results are presented as % activity at the indicated concentrations. Enzyme activity <50% indicated in green.

MTase	Activity (%)						Average Activity (%)	
	@1µM			@10µM			1µM	10µM
	Exp 1	Exp 2	Exp 3	Exp 1	Exp 2	Exp 3		
PNMT*	95	96		70	67		96 ± 1	69 ± 2
CARM1	101	100	102	98	99	102	100 ± 1	100 ± 2
G9a	115	108	101	99	103	95	108 ± 7	99 ± 4
SETDB1	120	108	109	105	114	105	112 ± 7	108 ± 5
SETD2	108	109	114	94	93	91	110 ± 3	93 ± 2
MLL1	107	116	115	84	82	76	113 ± 5	81 ± 4
SMYD2	43	37	38	19	19	19	39 ± 3	19 ± 0
PRMT1	115	114	104	109	101	101	111 ± 7	104 ± 5
PRMT5	86	93	89	35	38	35	90 ± 3	36 ± 2
PRMT7	100	95	97	67	70	65	97 ± 2	67 ± 3
DNMT1	114	104	101	102	101	106	106 ± 7	103 ± 3
DOT1L	89	59	70	37	40	41	73 ± 15	39 ± 2

* Data extracted from the inhibition curve presented in figure S6

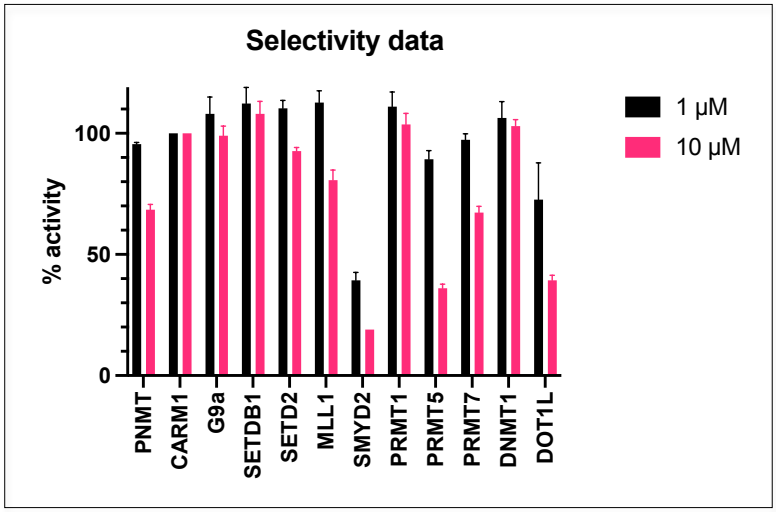

PNMT selectivity assay

The phenylethanolamine N-methyltransferase (PNMT) assay was developed using the Promega MTase-Glo™ Methyltransferase Assay (Promega Corporation, US, #V7601). In the coupled luminescence-based assay, the enzymatic product SAH is converted into ADP and subsequently into light.[1] Human recombinant PNMT was purchased from ProSpec-Tany TechnoGene Ltd, Israel (#ENZ-457). After establishing the concentration of enzyme to use in the assay, the K_M values for

cofactor SAM and substrate (+)-norepinephrine were determined. The measured K_M values were 2.6 µM for SAM and 5.9 µM for (+)-norepinephrine. The final conditions of the assay were set at 125 nM PNMT, 5 µM SAM, 10 µM (+)-norepinephrine and a reaction time of 45 minutes. The reactions were performed in half area, flat bottom, white 96 well plates (Greiner Bio-One #675074) with a final volume of the reaction mixture of 10 µL. Inhibitors (2 µL) were pre-incubated with the enzyme in the presence of substrate (4 µL) for 10 minutes before the methyltransferase reaction was initiated through addition of cofactor SAM (4 µL). After 45 minutes, the MTase Glo detection solution (10 µL) was added and incubated for 60 minutes followed by analysis of the luminescent signal in a plate reader. Compound **17u** was tested at 3.7, 11.1, 33.3 and 100 µM in duplicate.

The luminescence data were analysed using GraphPad Prism (version 8.4.3). The luminescence of the positive control (Lp) in each dataset was defined as 100% activity. This value was included in the IC_{50} graphs at a concentration of 1.5 log values below the lowest concentration tested. The luminescence data of the negative controls (Ln) in each dataset were subtracted from the obtained luminescence data. The percent activity in the presence of each inhibitor was calculated according to the following equation: % activity = (L − Ln)/(Lp − Ln), where L = the luminescence in the presence of the compound, Ln = the luminescence in the absence of the enzyme, and Lp = the luminescence in the absence of the inhibitor. The percent activity values were plotted as a function of inhibitor concentrations and fitted using non-linear regression analysis of the Sigmoidal dose–response curve generated using the equation Y=100/(1+10^((LogIC50-X)*HillSlope))). The IC_{50} value was determined by the concentration resulting in a half- maximal percent activity (Figure S6).

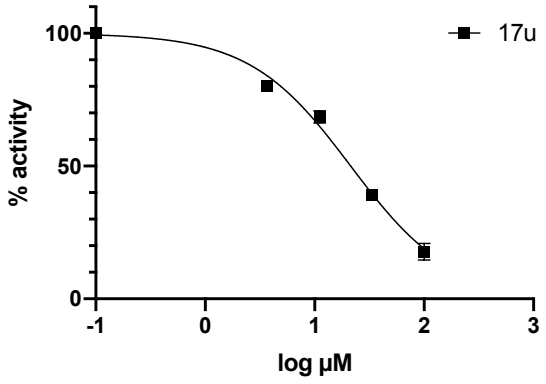

Figure S6. Inhibition curve for compound **17u** against PNMT. The experiment was performed in duplicate.

Docking and FEP simulation of compound 17v

Compound **17v** was docked in NNMT co-crystal structure 6PVE (Figure S7). The experimental values (4.11 kcal/mol) and calculated values (7.21 kcal/mol) of the differences in free binding energy (ΔG) compared to unsubstituted compound **17x** were found to be similar with a minor overestimation of the affinity in the model.

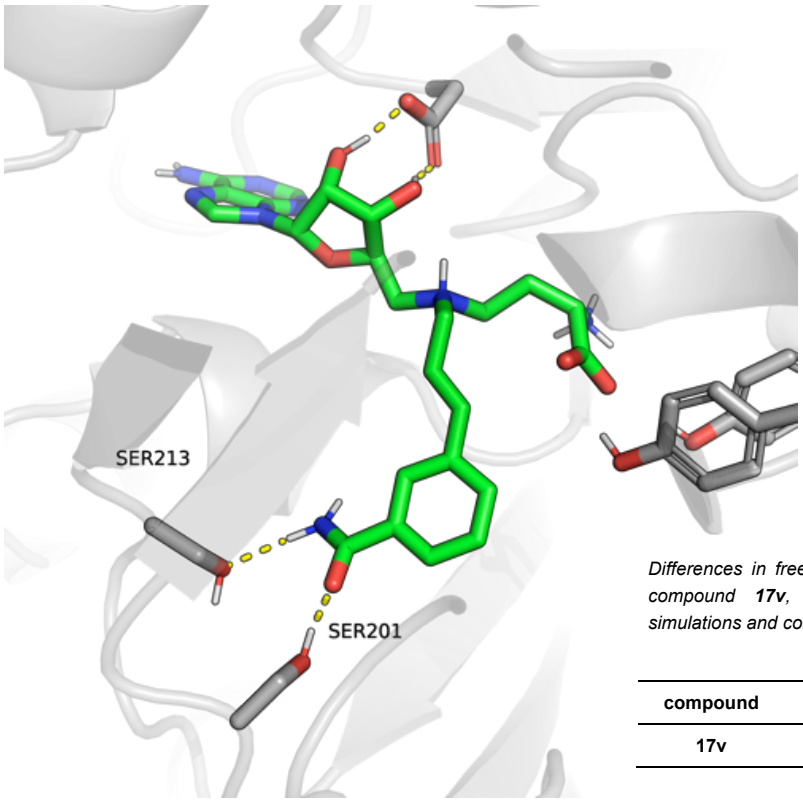

*Differences in free energy of binding (± s.e.m.) for compound **17v**, as calculated from the FEP simulations and compared to the experimental data.*

	ΔΔG (kcal/mol)	
compound	**Experimental**	**FEP**
17v	4.11 +/- 0.05	7.21 +/- 0.76

Figure S7. Result of modeling of compounds **17v**, bearing the meta-amide substituent, in the active site of NNMT (PDB ID: 6PVE). The results indicate strong hydrogen bonding interacctions with serine residues S201 and S213 similar to that predicted for para-cyano compound **17u**. The modelled predictions are supported by the similarity in the difference in Gibbs free energy (ΔΔG) compared to unsubstituted compound **17x** from the biochemical assay and the MD simulations.

Cell based data

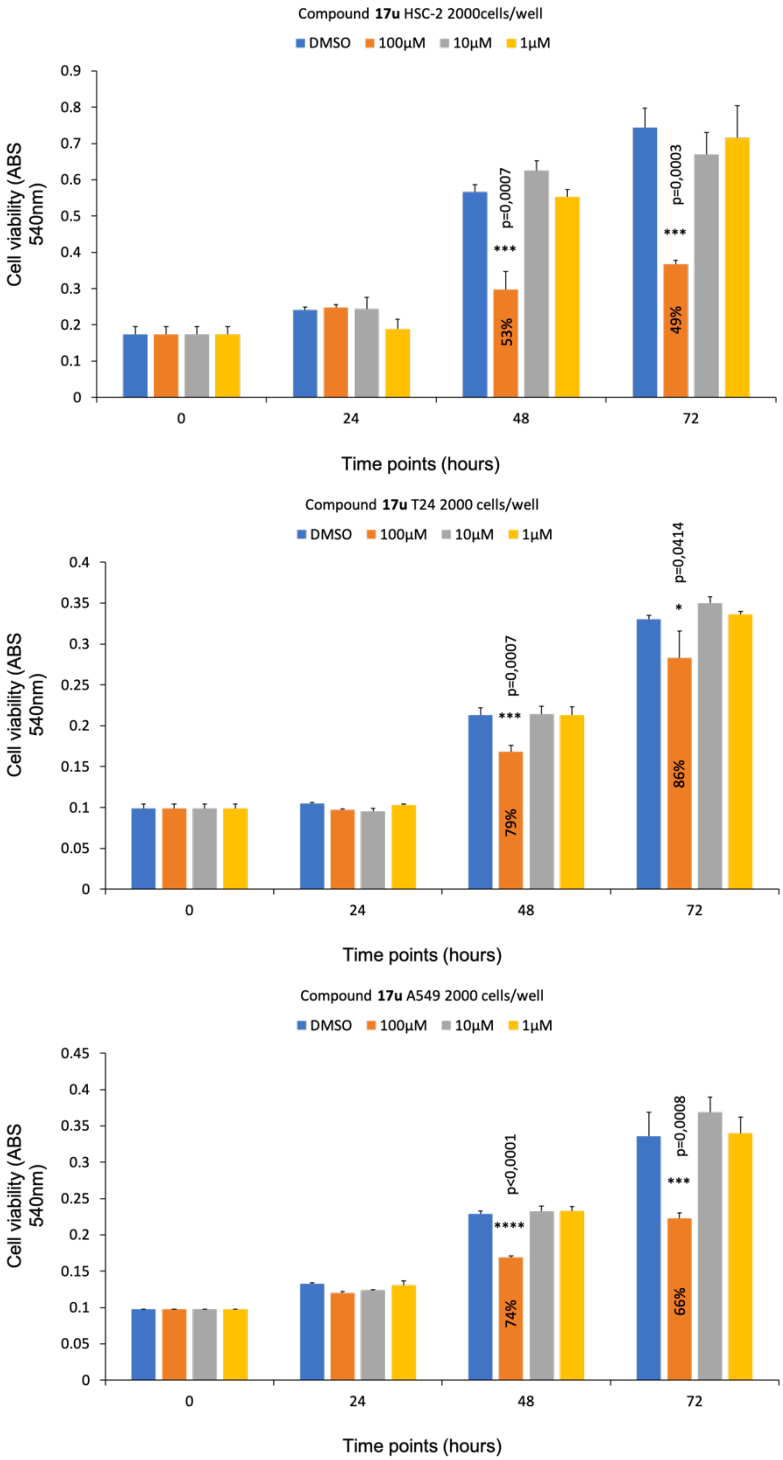

Figure S8. Cell viability data of treatment of HSC-2 human oral cancer cell line, T24 human bladder cancer cell line and A549 human lung cancer line with compound **17u** after 0, 24, 48 and 72 hours. Percentage inhibition is given at time-points and concentrations showing significant difference with the DMSO control.

PAMPA assay

The Permeability (P_e) data were calculated using the following equation:

$$P_e = \frac{-\ln\left(1 - \frac{C_A}{C_{eq}}\right)}{S * \left(\frac{1}{V_D} + \frac{1}{V_A}\right) * t}$$

where

$$C_D = C_0 * \frac{A_D - A_{buffer}}{A_0 - A_{buffer}}$$

$$C_A = C_0 * \frac{A_A - A_{buffer}}{A_0 - A_{buffer}}$$

and

$$C_{eq} = \frac{(C_D * V_D + C_A * V_A)}{V_D + V_A}$$

S Is the membrane area (0.3 cm^2), V_A is the acceptor well volume (0.2 ml), V_D is the donor well volume (0.3 ml), t is the incubation time (18480 s), C_A is the concentration of the drug in the acceptor well at time t, C_D is the concentration of drug in the donor well at time t, and C_{eq} is the equilibrium concentration (compound concentration across donor and acceptor wells if the membrane is 100% permeable to the compound). The concentration listed above are computed from the absorbances of the donor, acceptor, starting and buffer solutions (A_D, A_A, A_0 and A_{buffer} respectively).

Table S5. Cell permeability results from the PAMPA assay

Compound		**Permeability (* 10^{-6}) cm/s**[1]
Caffeine	Positive control	6.85
Furosemide	Negative control	0.06
Compound **17u**	Test compound	0.01

[1] The cut-off between low and high permeability is defined at 1.5 * 10^{-6} cm/s

HPLC traces of lead compounds

Compound **17i**

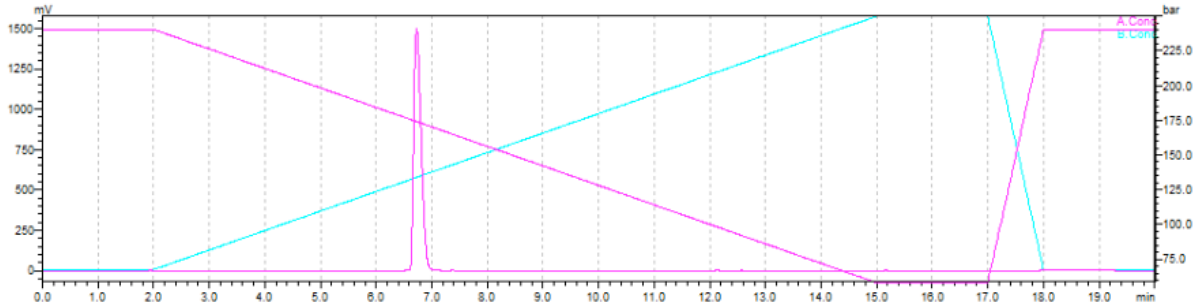

Compound **17l**

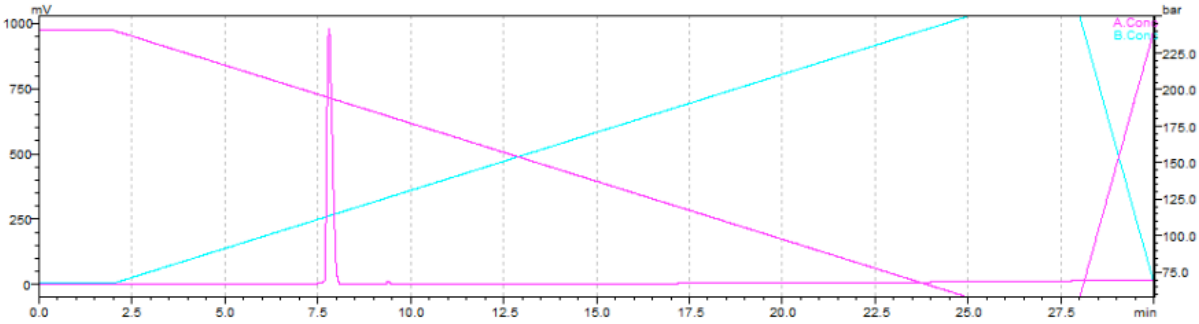

Compound **17o**

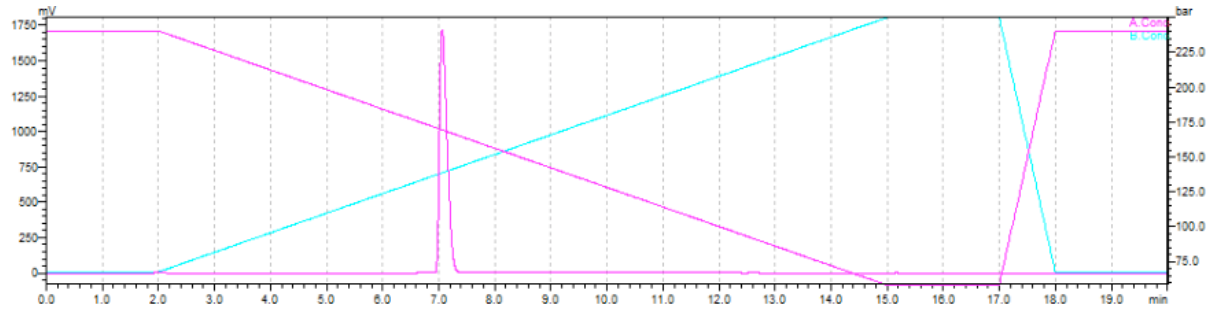

Compound **17r**

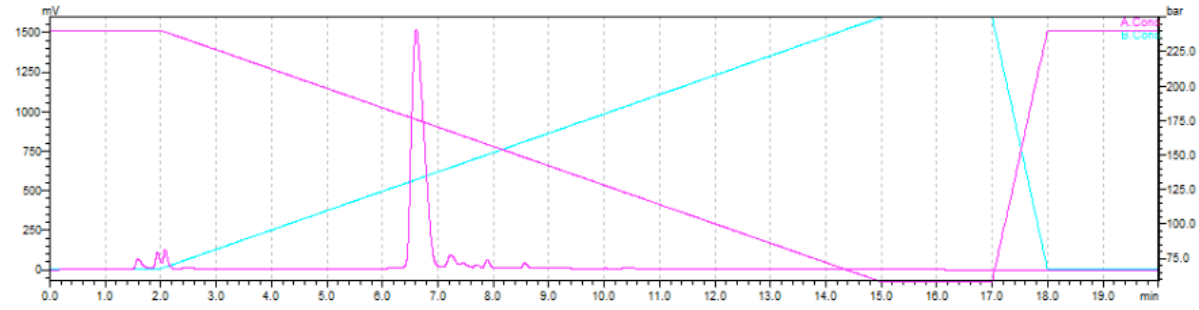

Compound **17s**

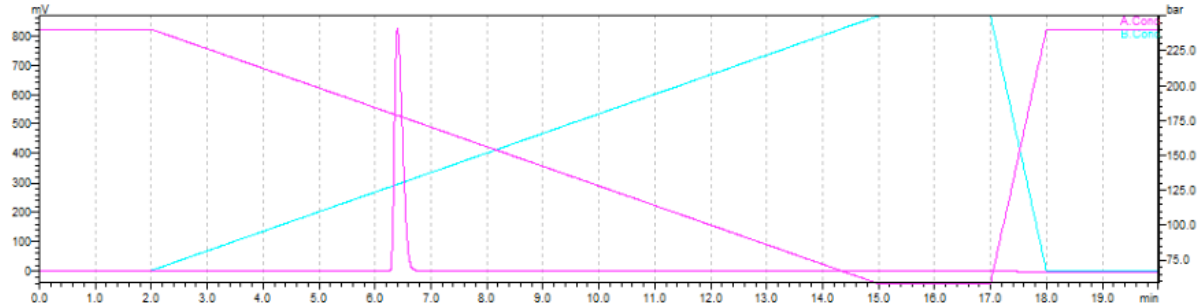

Compound **17t**

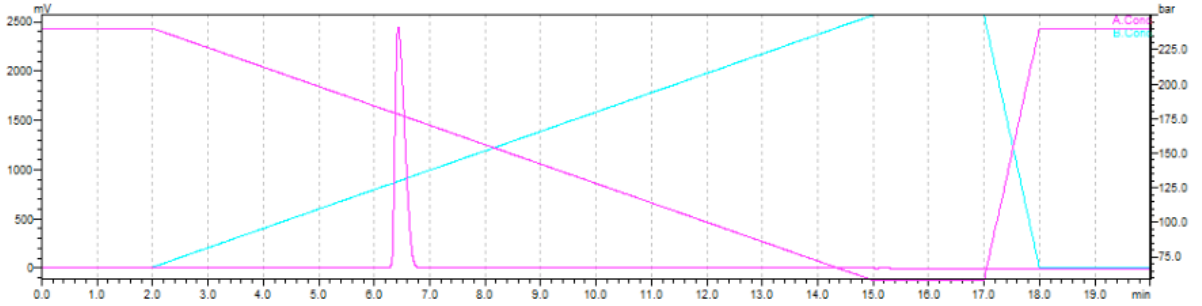

Compound **17u**

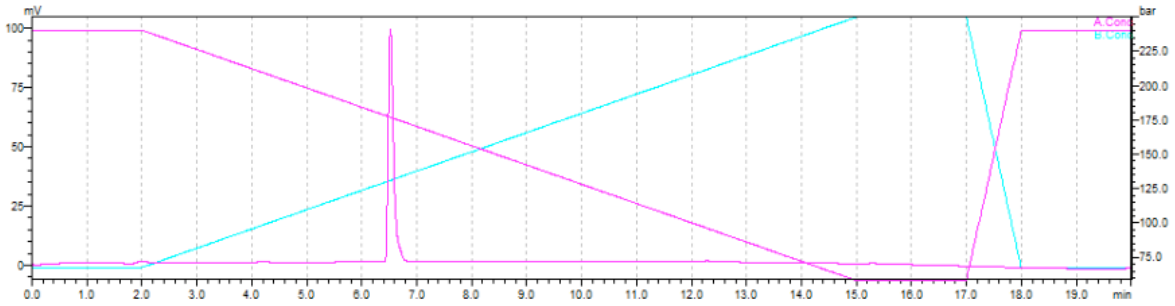

Compound **17v**

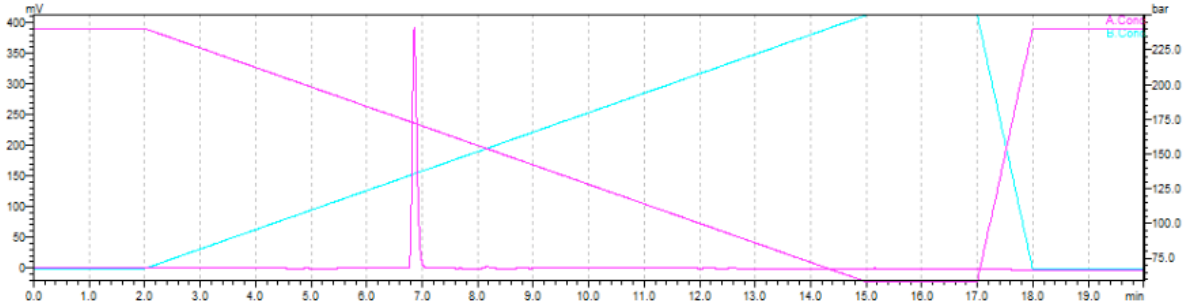

Compound **11** ^{1}H NMR (400 MHz) $CDCl_3$

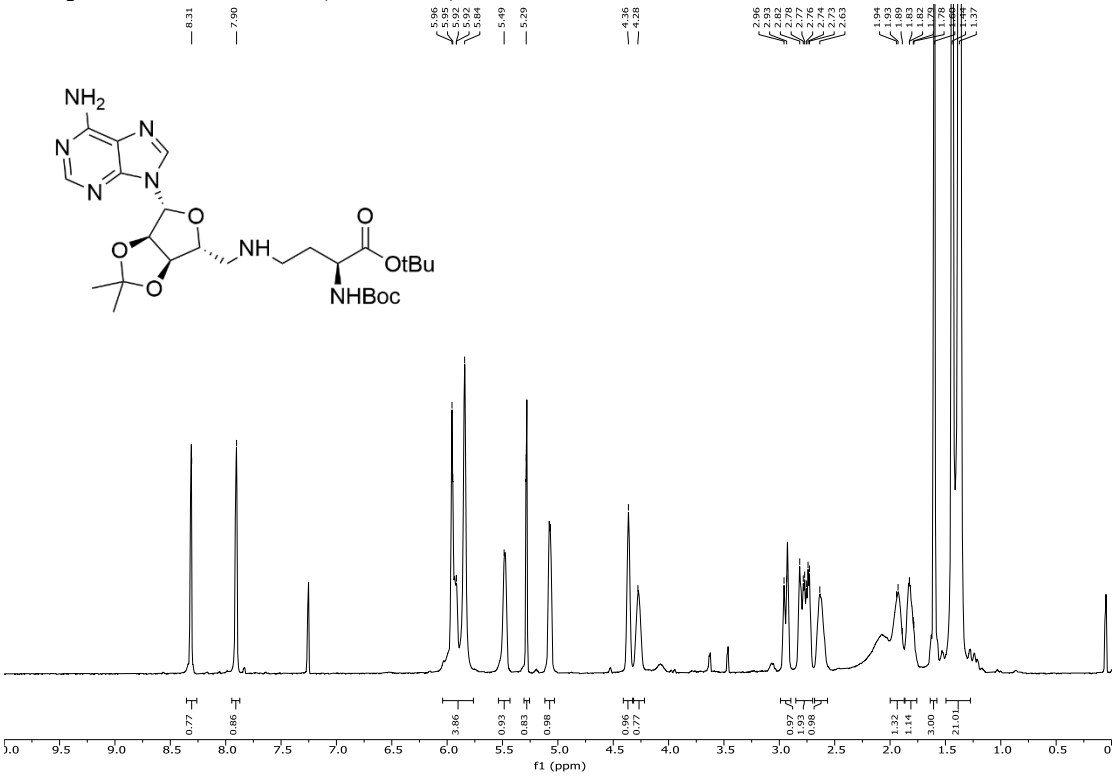

^{13}C NMR (400 MHz) $CDCl_3$

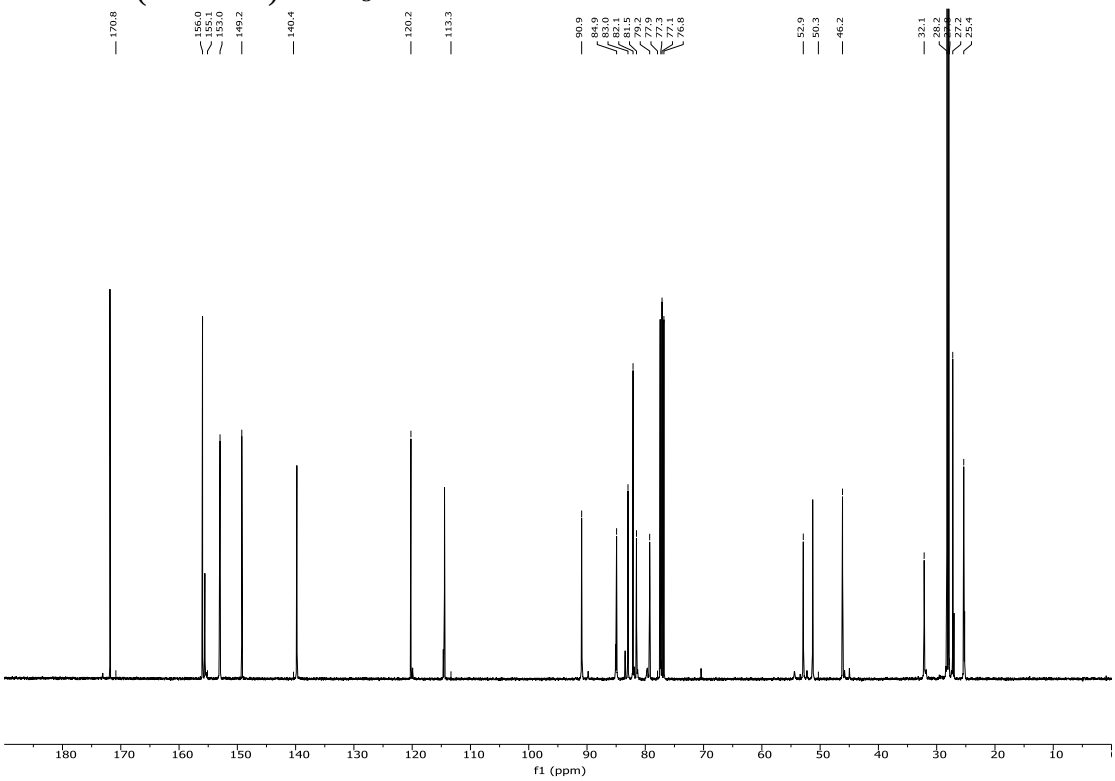

Compound **12a** ^{1}H NMR (400 MHz) $CDCl_3$

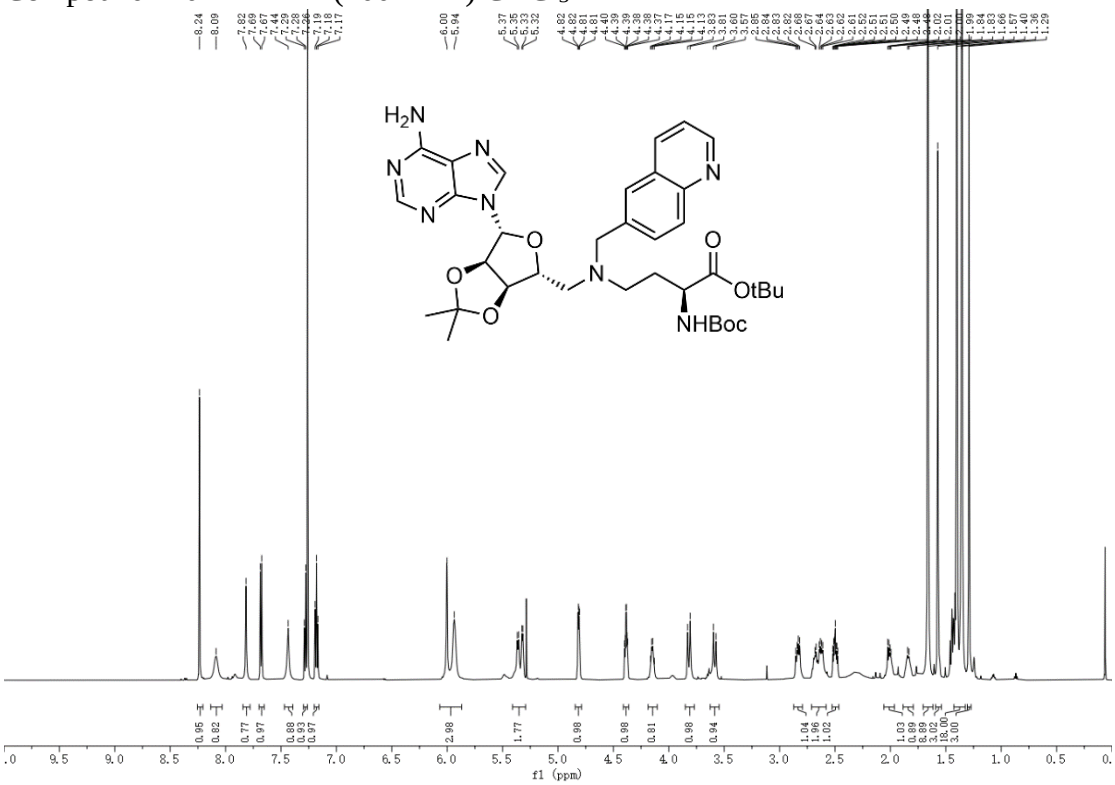

^{13}CNMR (101 MHz) $CDCl_3$

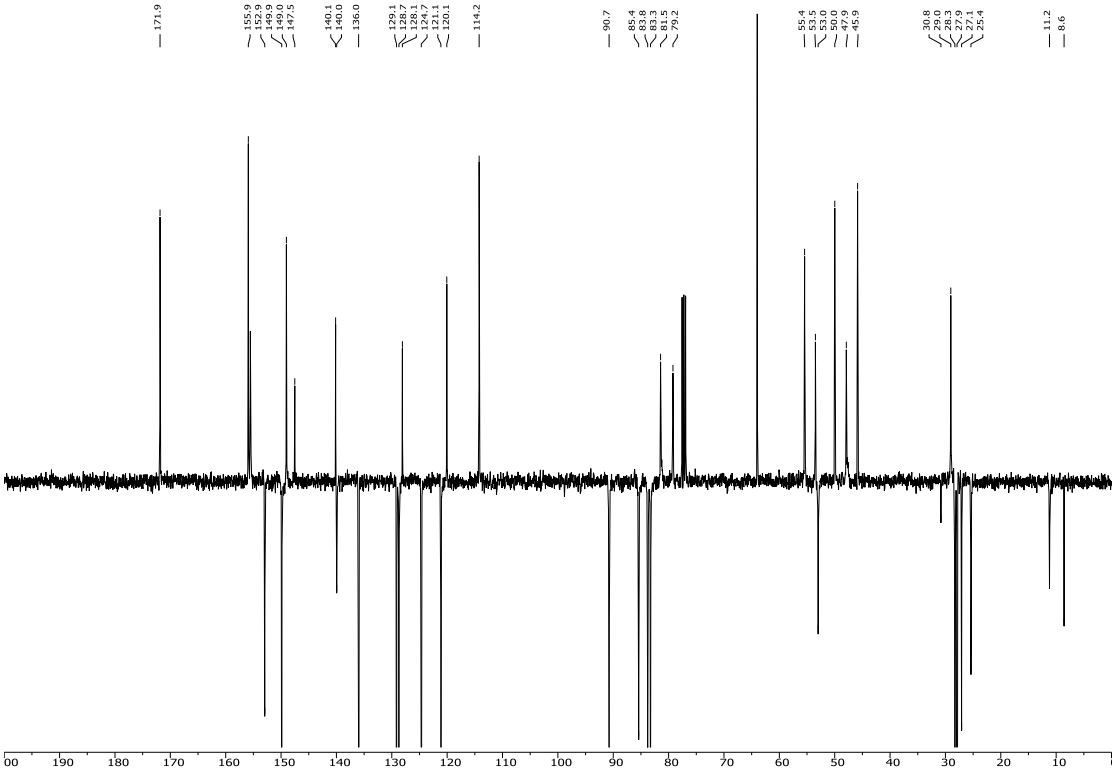

Compound **12c** ^{1}H NMR (400 MHz) $CDCl_3$

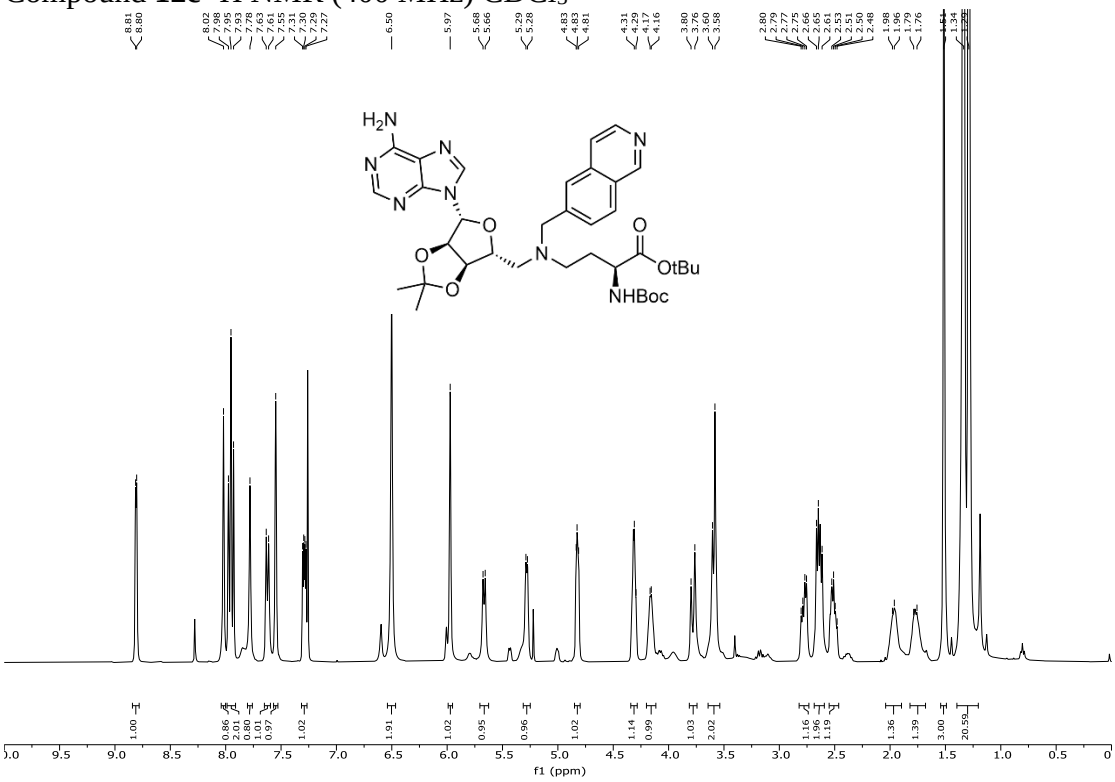

^{13}CNMR (101 MHz) $CDCl_3$

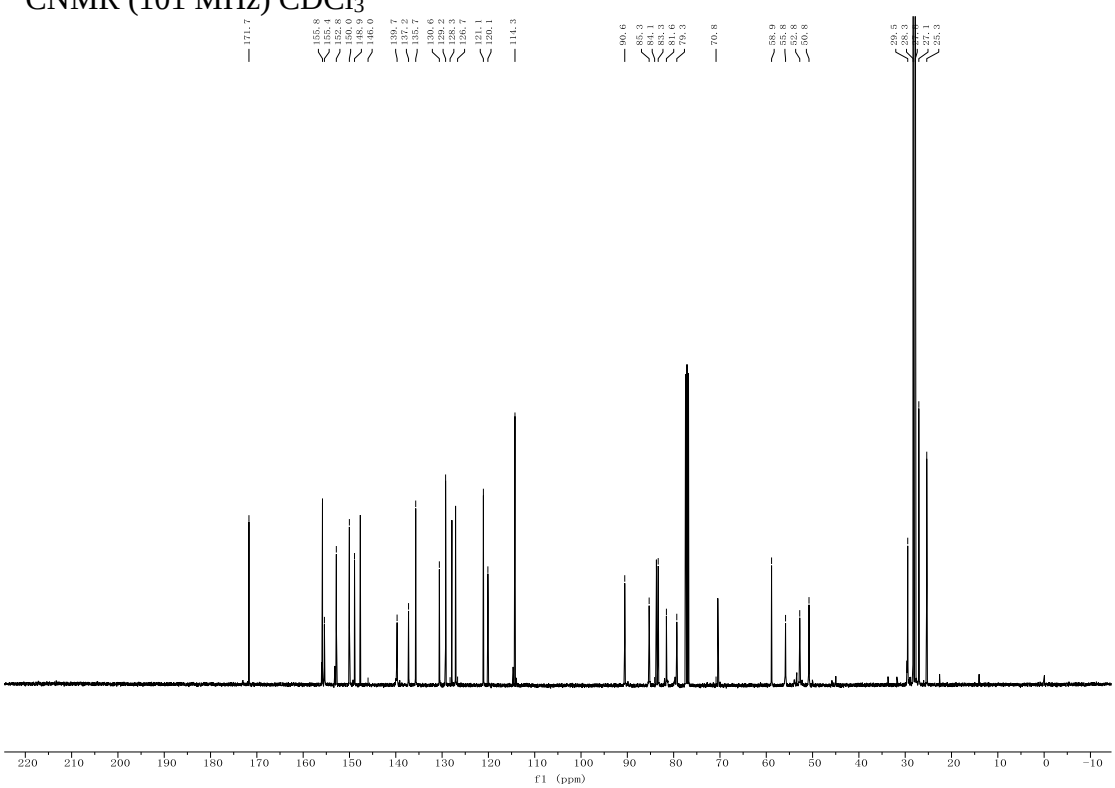

Compound **12d** ^{1}H NMR (400 MHz) $CDCl_3$

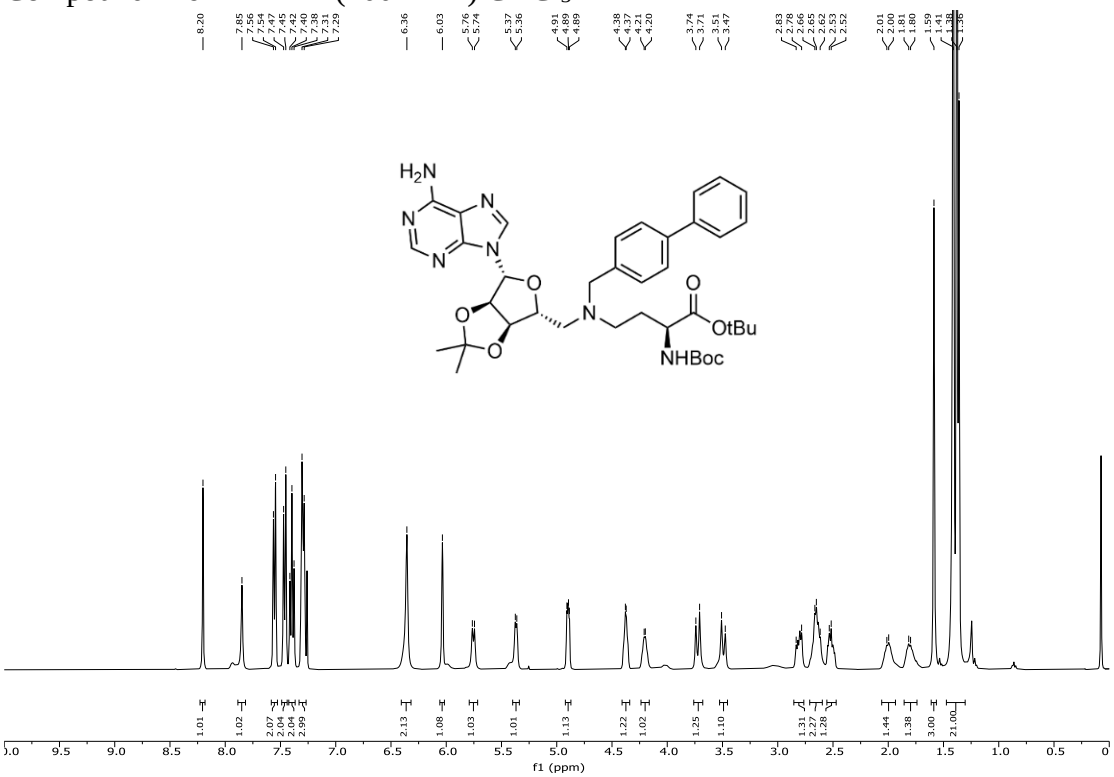

^{13}C NMR (101 MHz) $CDCl_3$

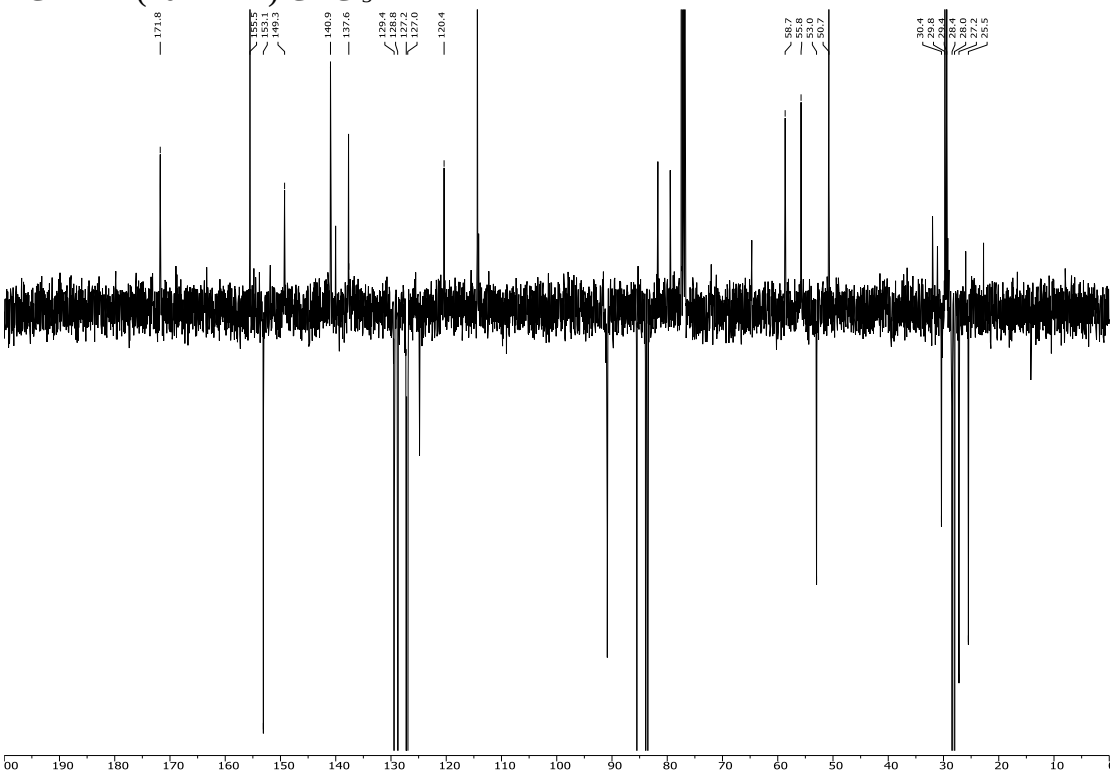

Compound **12e** ^{1}H NMR (400 MHz) $CDCl_3$

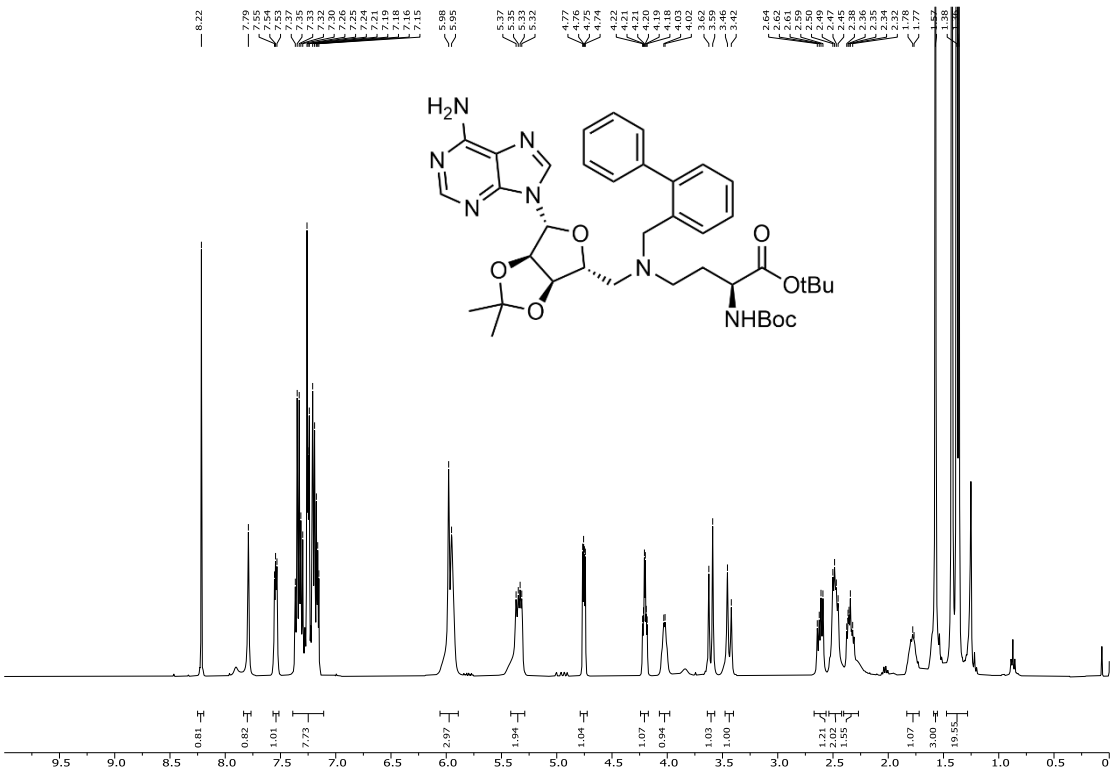

^{13}C NMR (101 MHz) $CDCl_3$

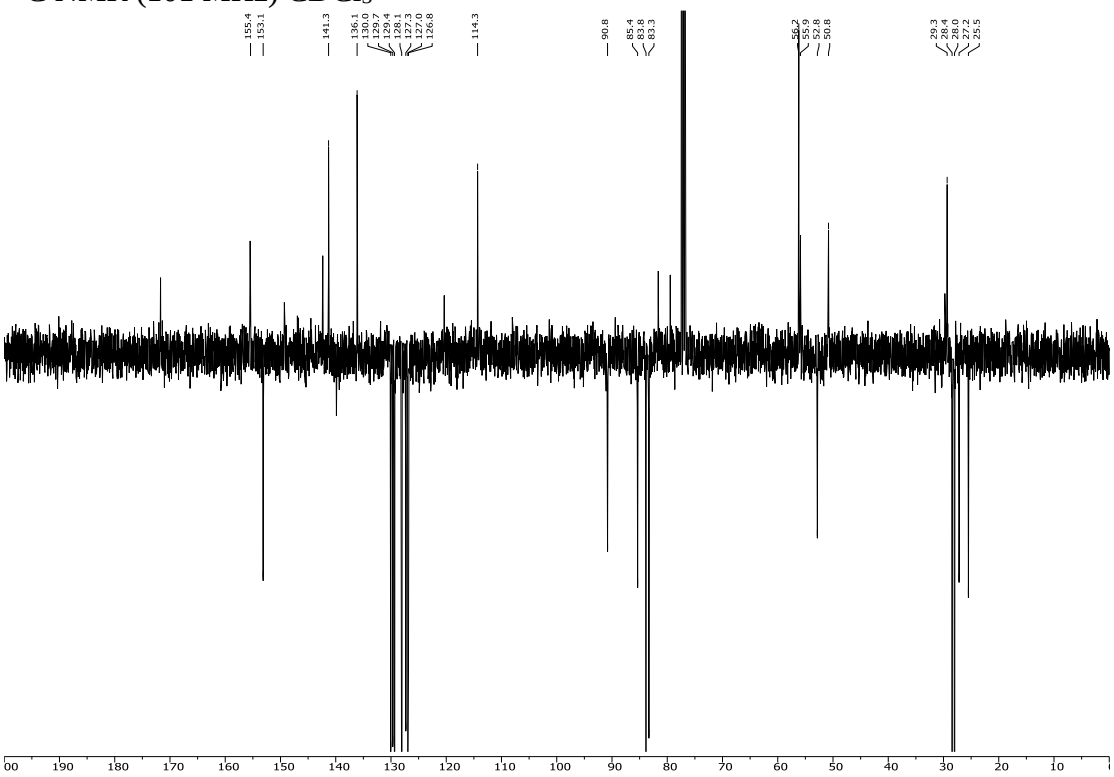

Compound **12f** ^{1}H NMR (400 MHz) $CDCl_3$

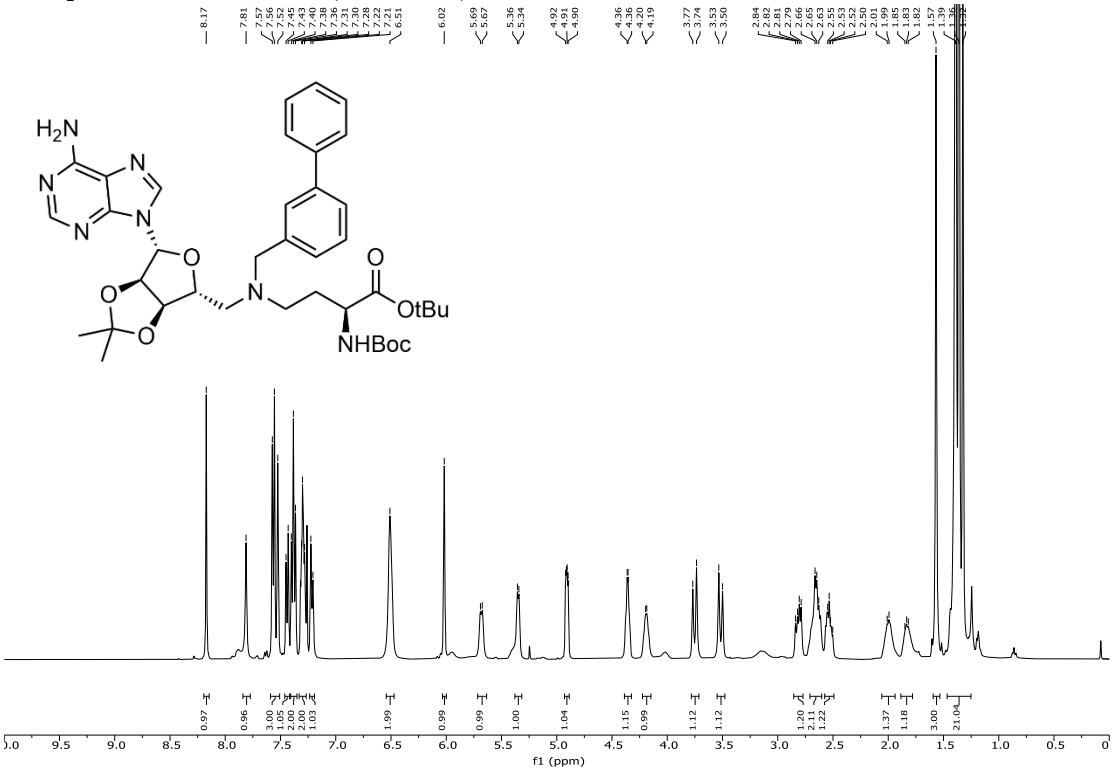

^{13}C NMR (101 MHz) $CDCl_3$

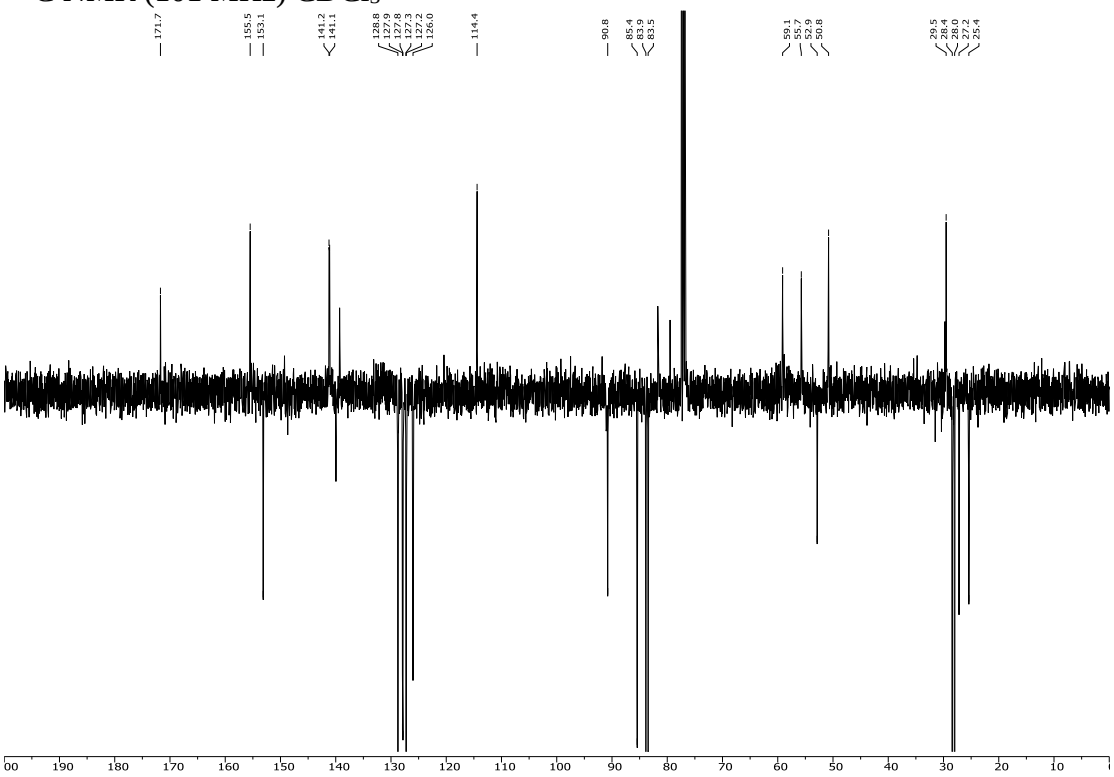

Compound **12g** ^{1}H NMR (600 MHz) $CDCl_3$

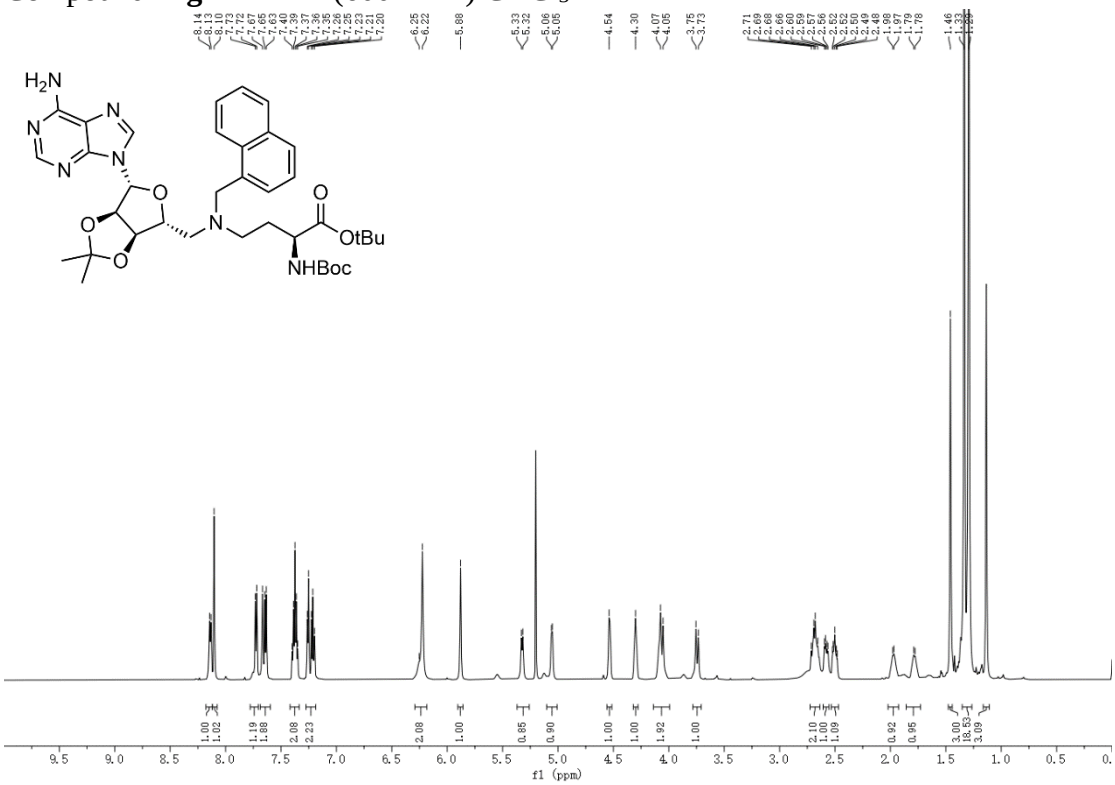

^{13}C NMR (151 MHz) $CDCl_3$

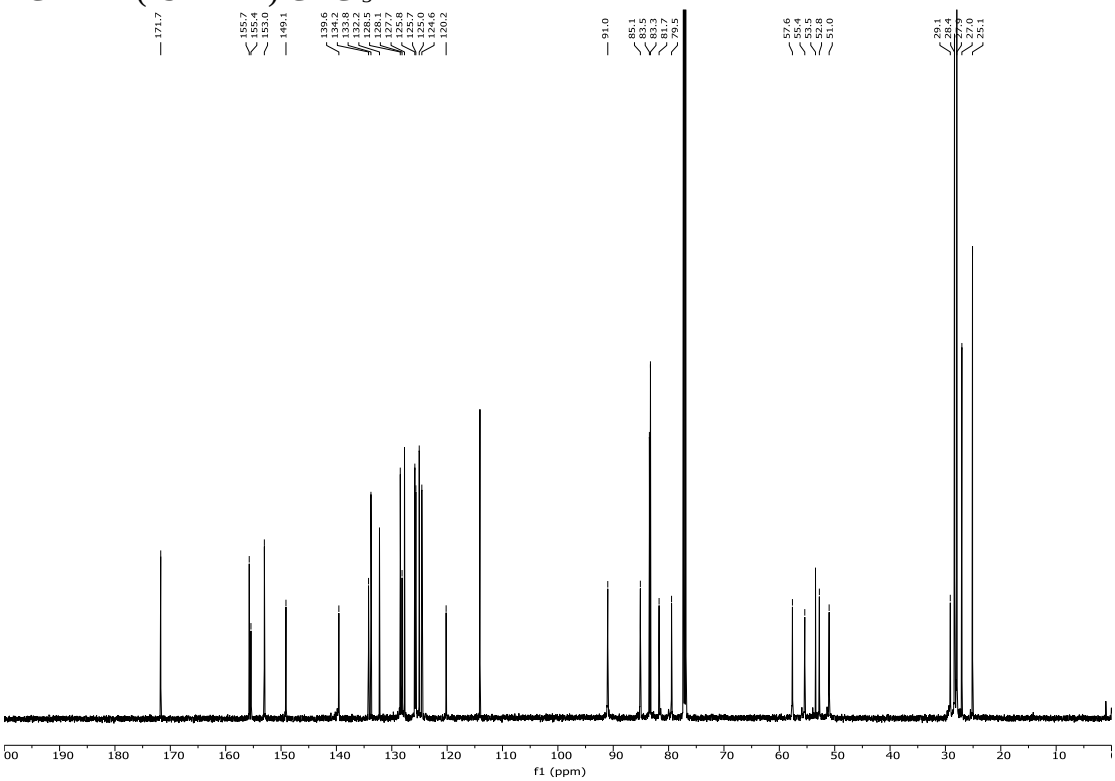

Compound **12h** ^{1}H NMR (400 MHz) $CDCl_3$

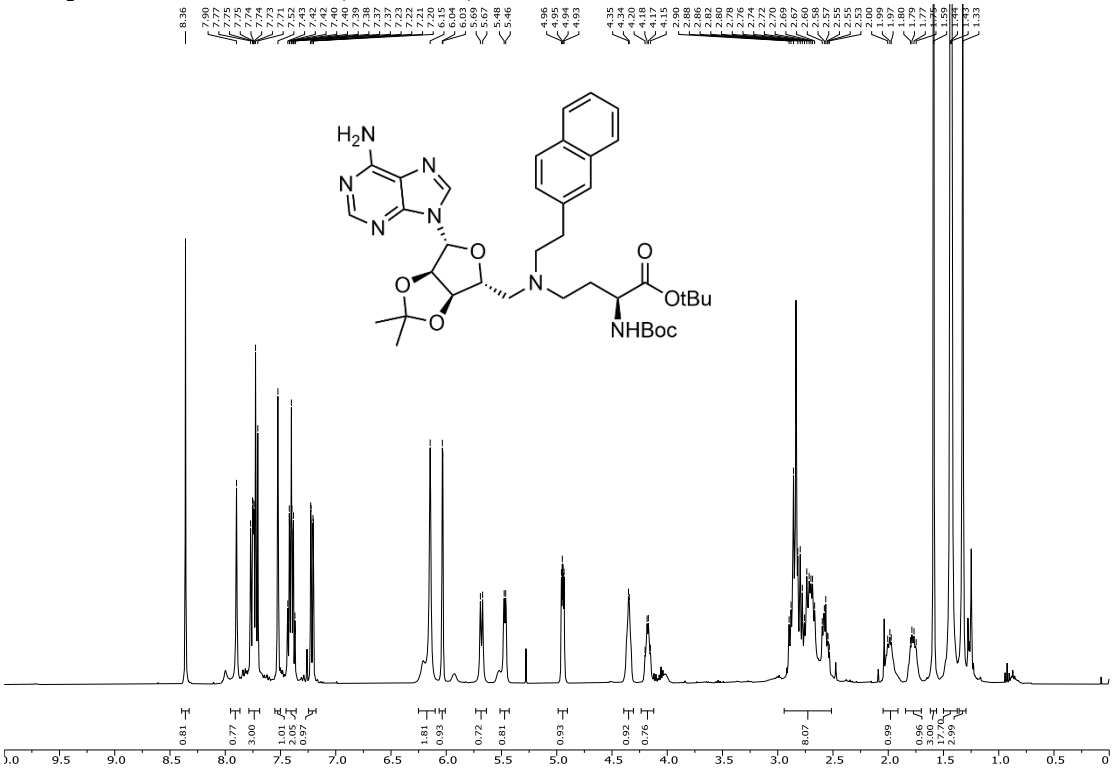

^{13}C NMR (101 MHz) $CDCl_3$

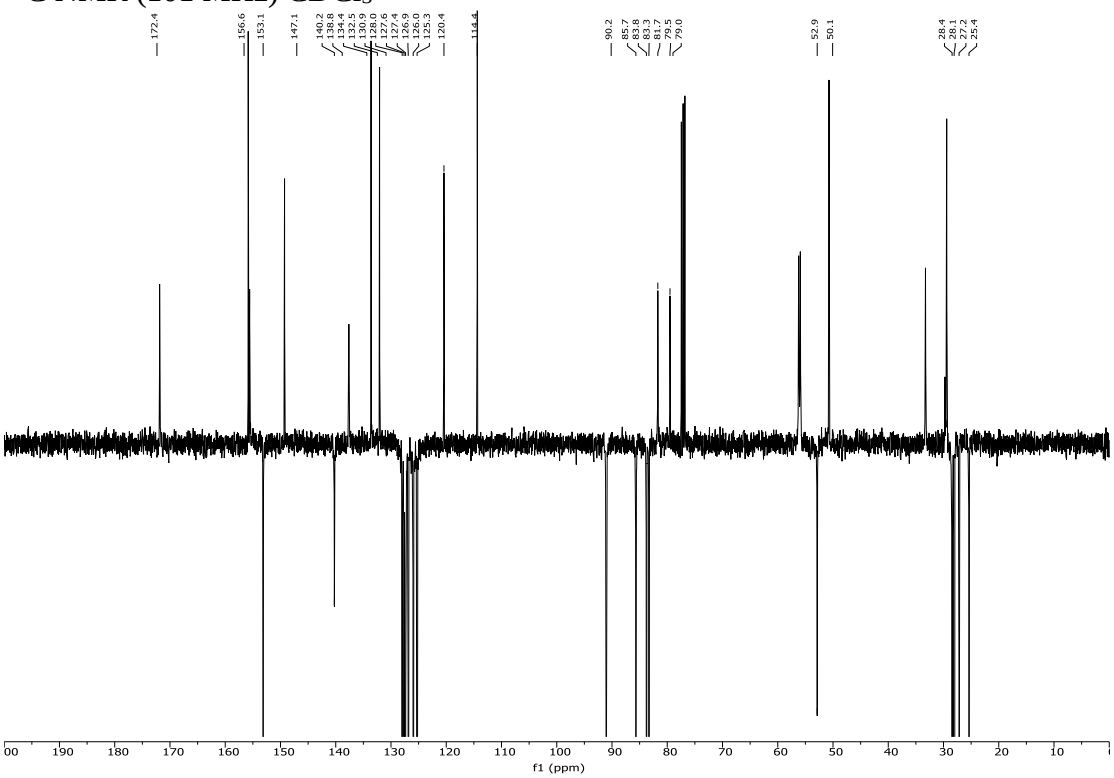

Compound **12i** ^{1}H NMR (600 MHz) $CDCl_3$

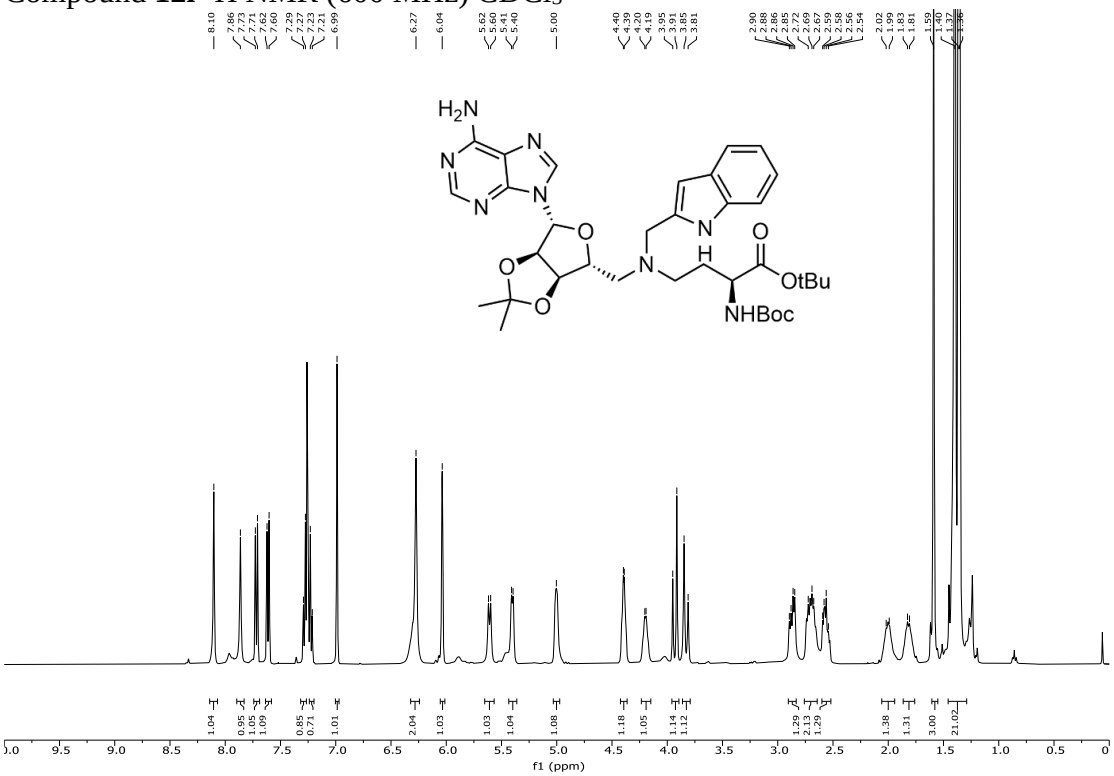

^{13}C NMR (151 MHz) $CDCl_3$

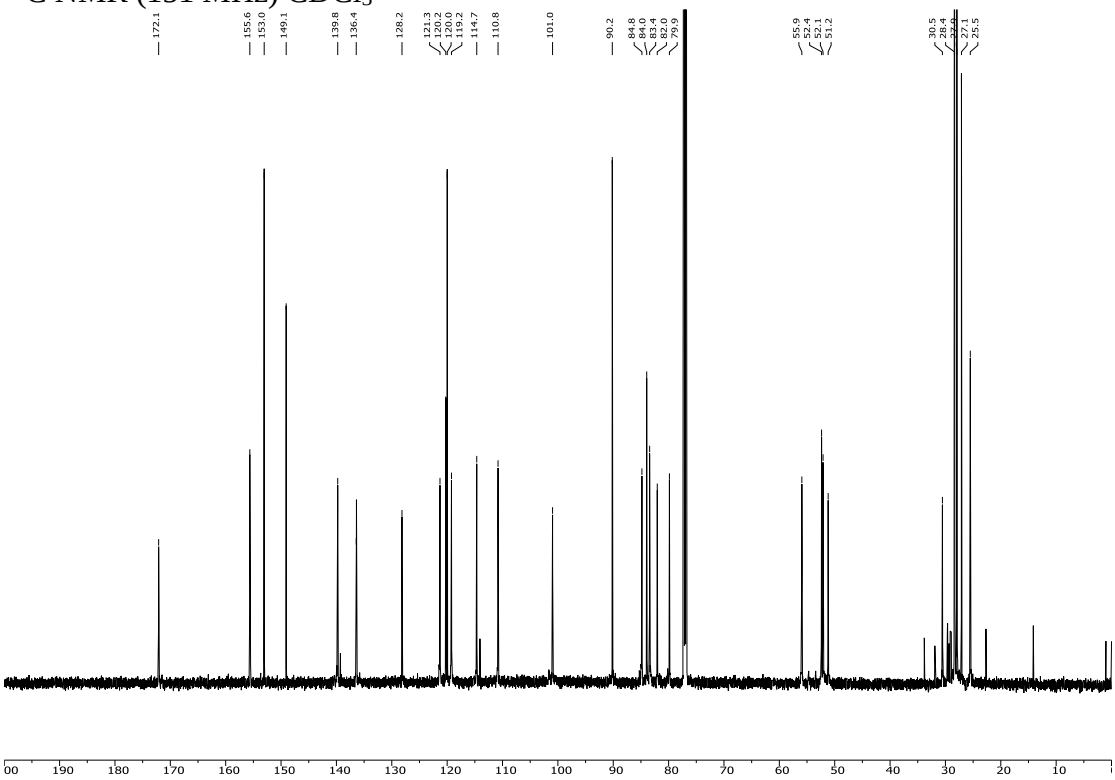

Compound **12j** ^{1}H NMR (600 MHz) $CDCl_3$

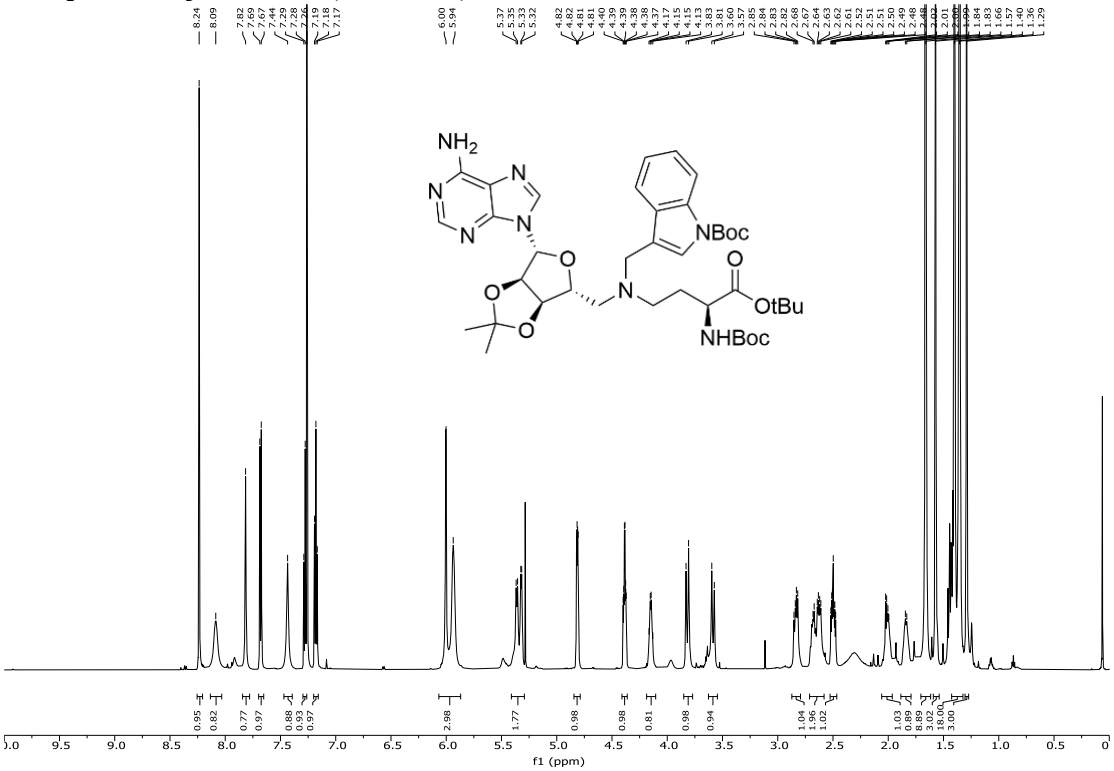

^{13}C NMR (151 MHz) $CDCl_3$

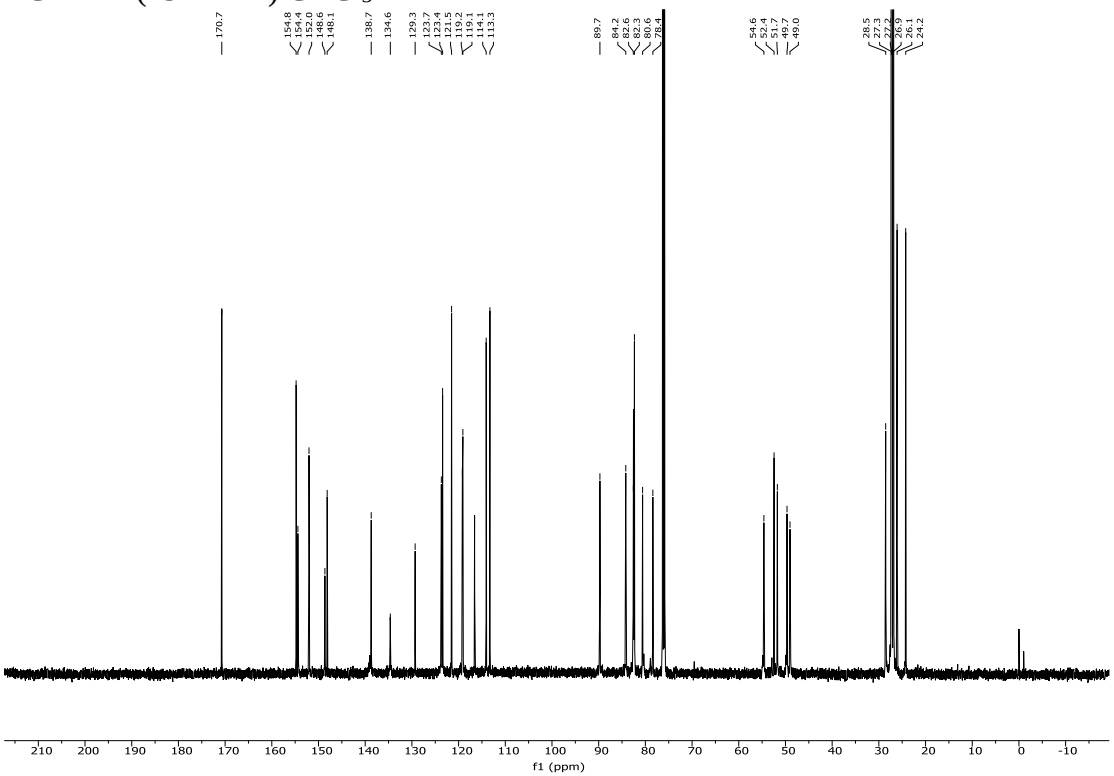

Compound **12k** ^{1}H NMR (400 MHz) $CDCl_3$

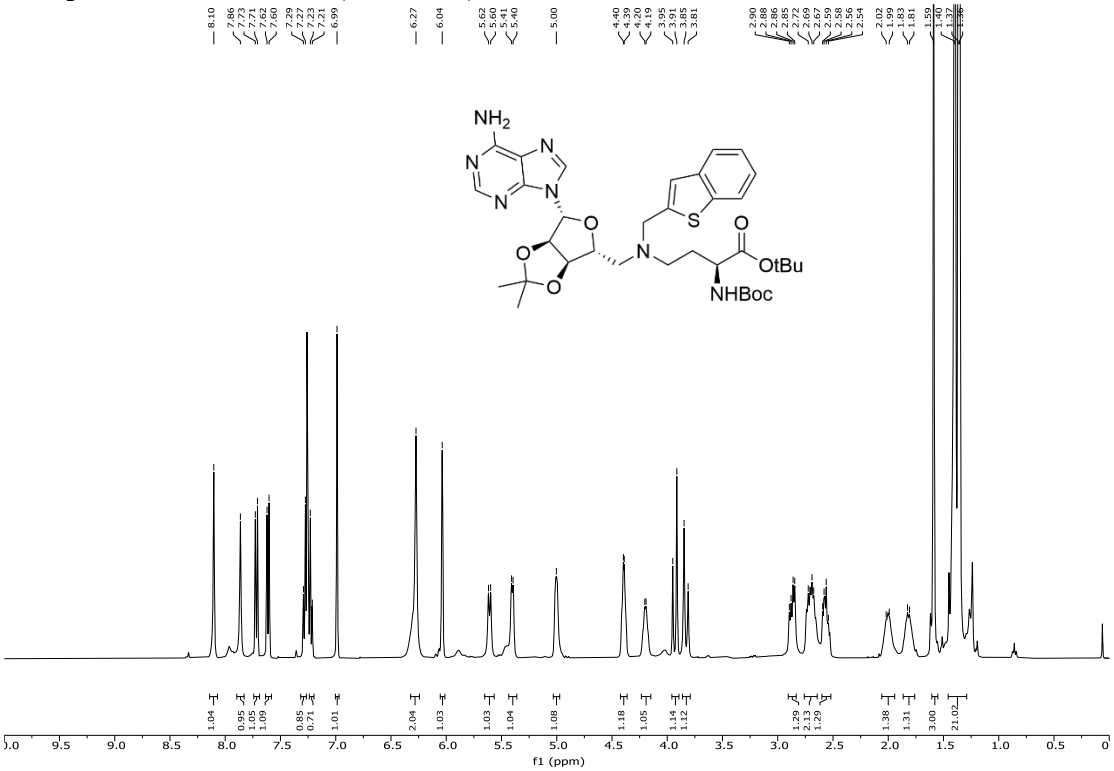

^{13}C NMR (101 MHz) $CDCl_3$

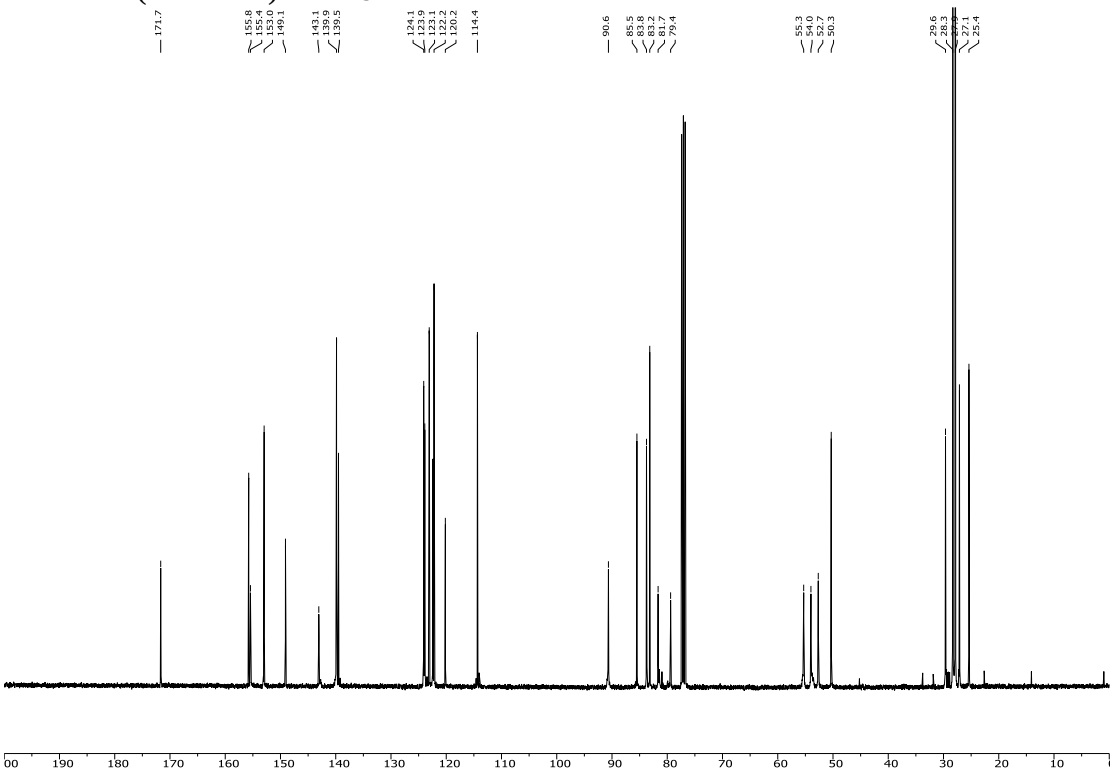

Compound **12l** ^{1}H NMR (400 MHz) $CDCl_3$

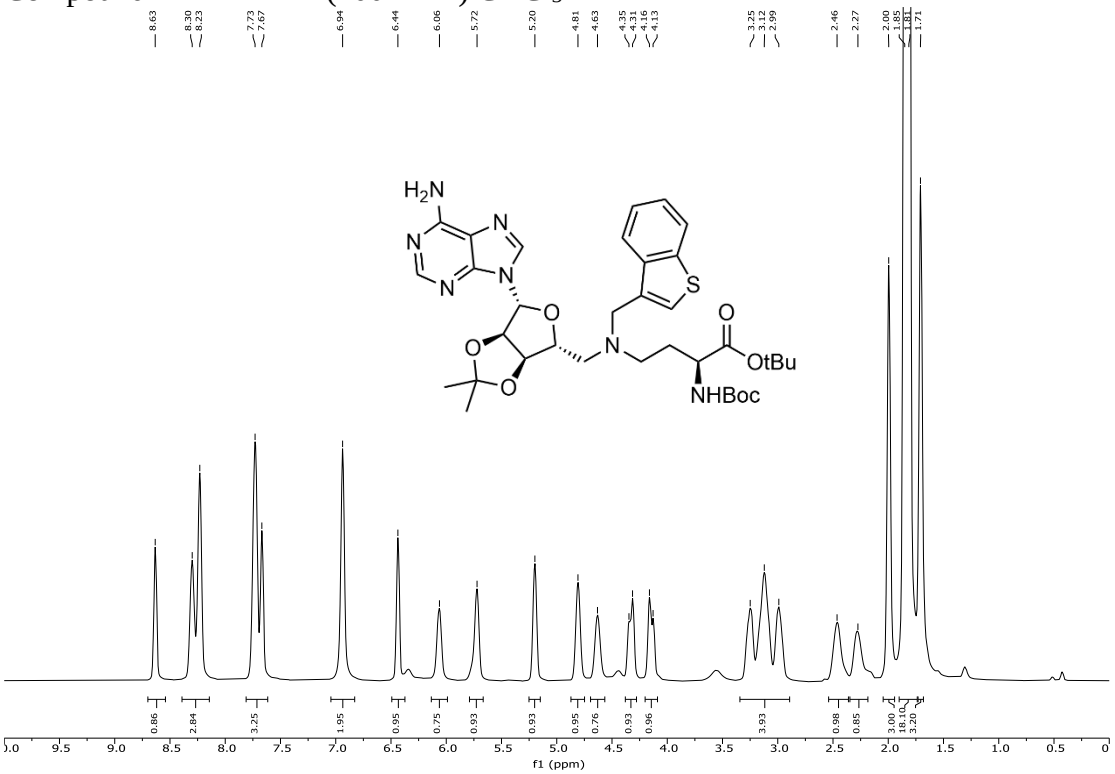

^{13}CNMR (101 MHz) $CDCl_3$

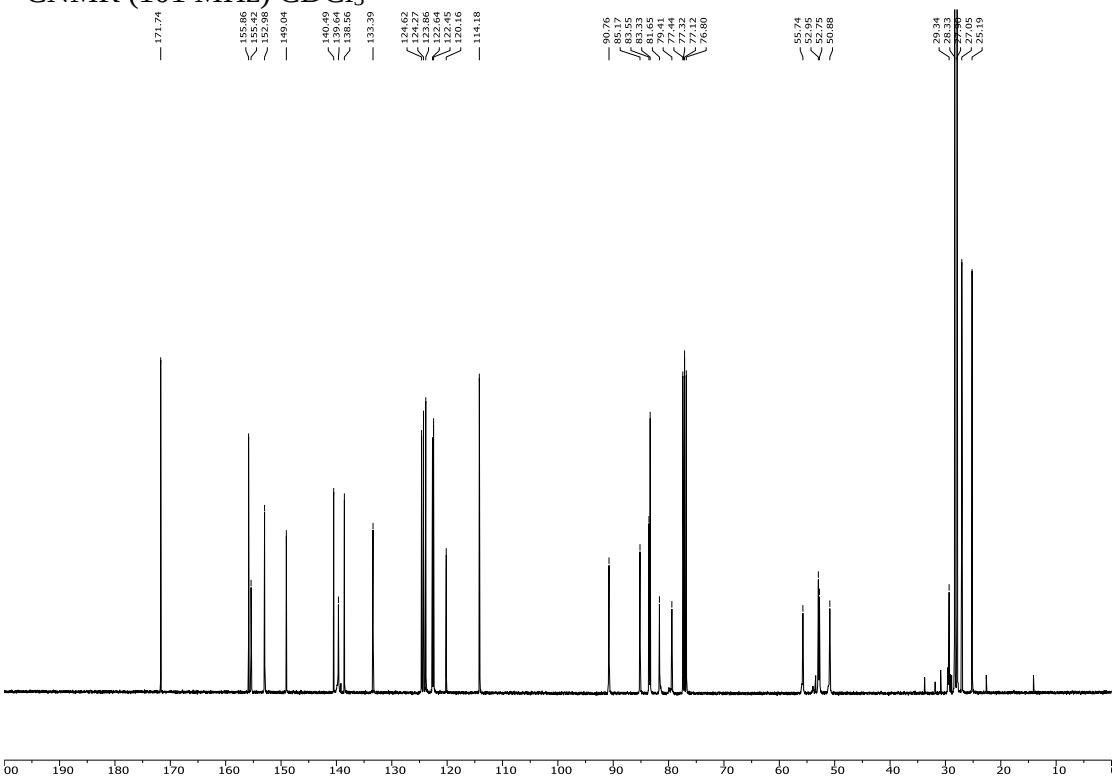

Compound **13a** ^{1}H NMR (400 MHz) D_2O

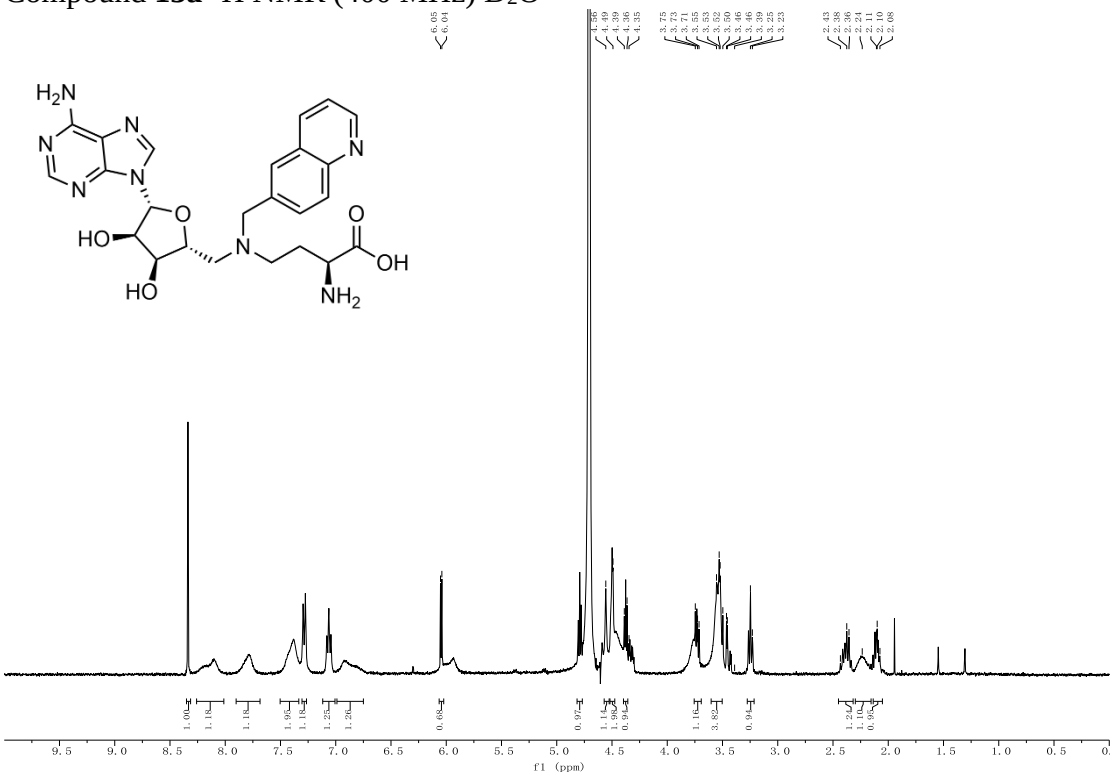

^{13}C NMR (101 MHz) D_2O

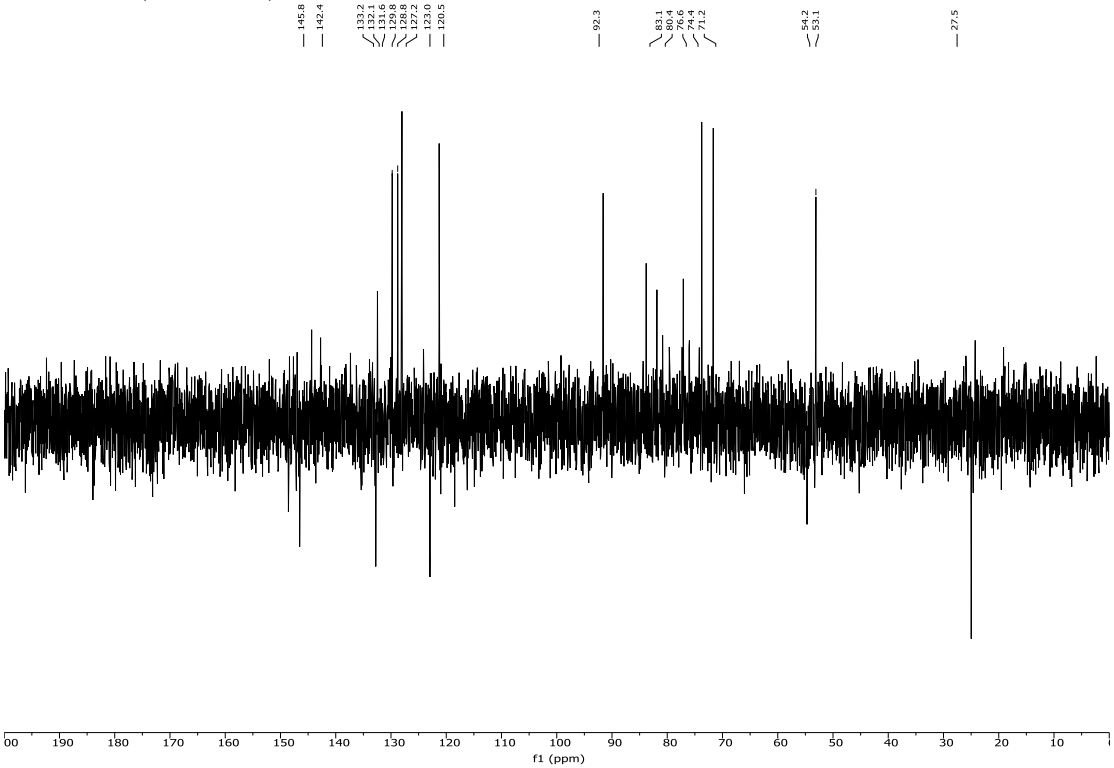

Compound **13b** ^{1}H NMR (400 MHz) D_2O

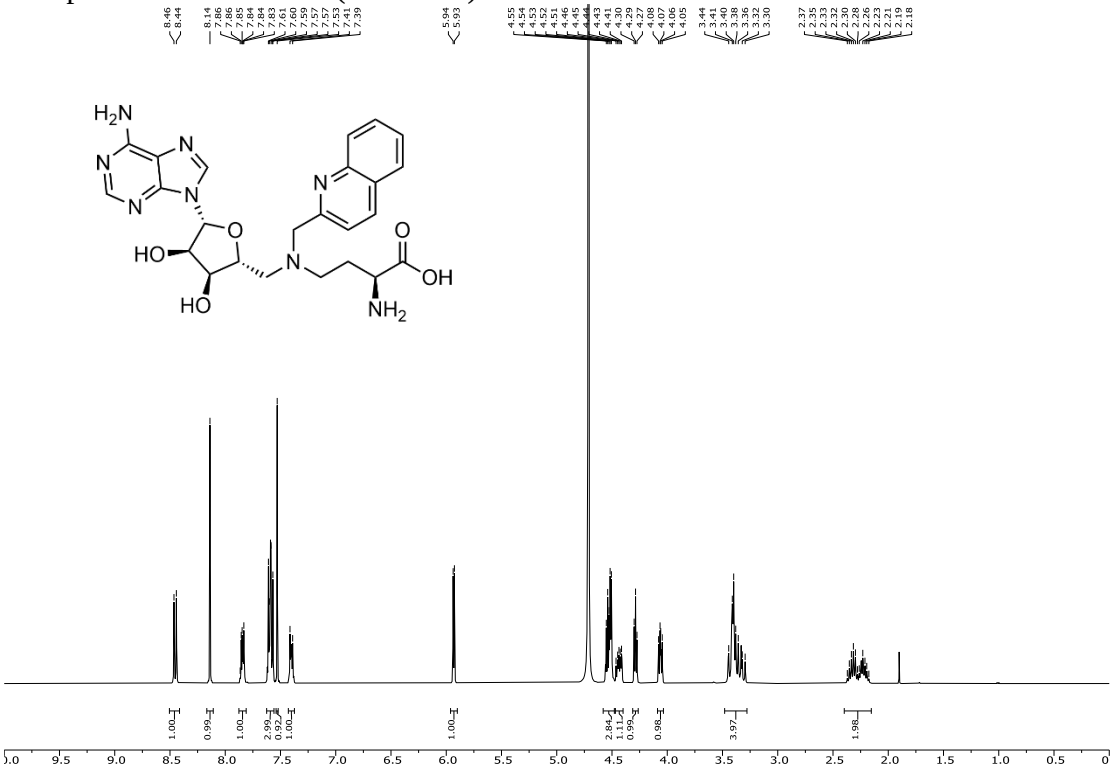

^{13}C NMR (101 MHz) D_2O

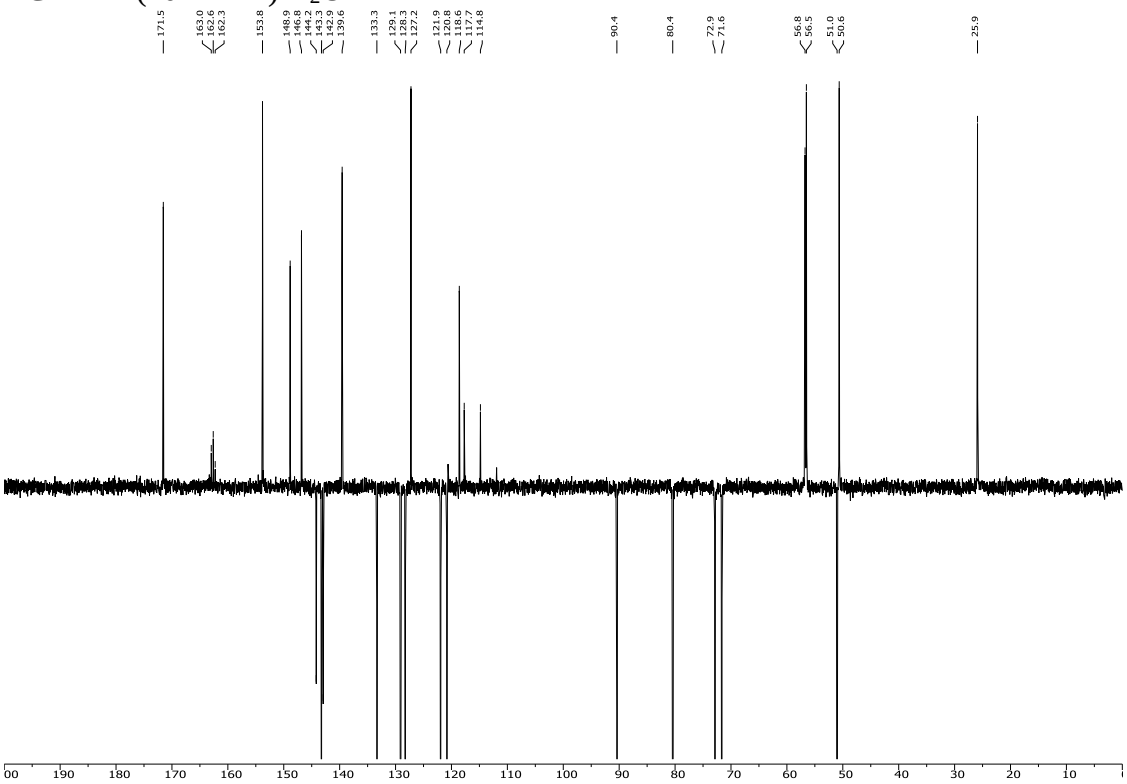

Compound **13c** ^{1}H NMR (400 MHz) D_2O

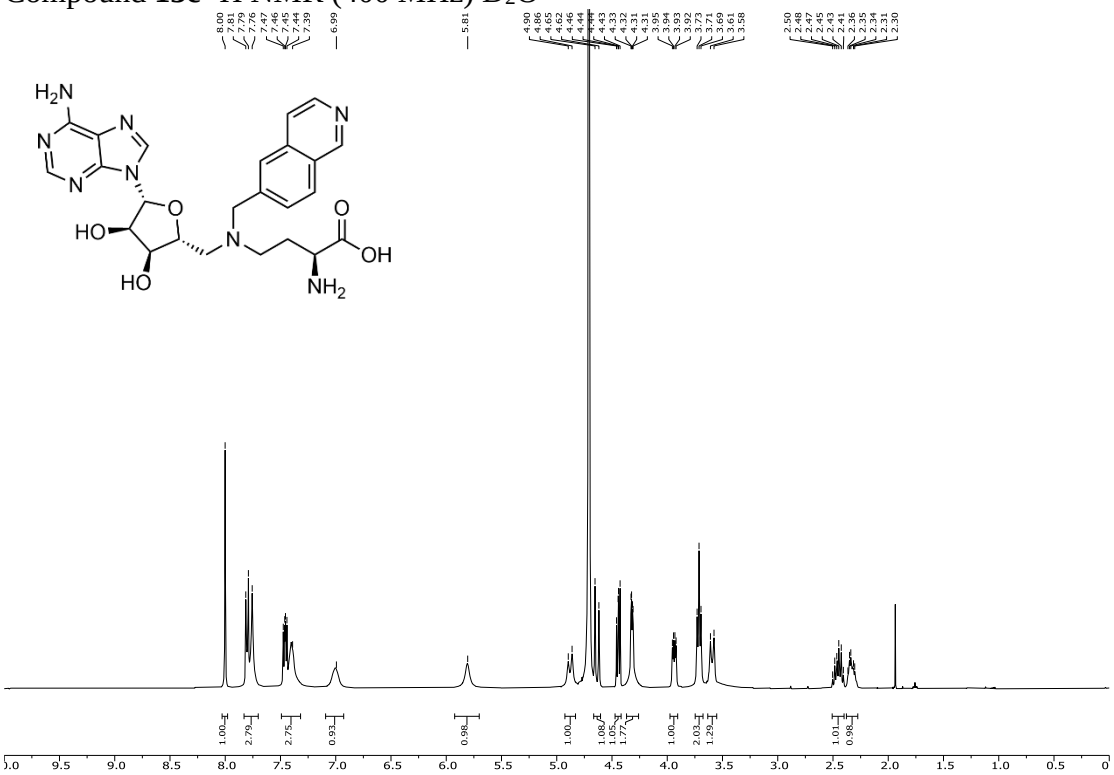

^{13}C NMR (101 MHz) D_2O

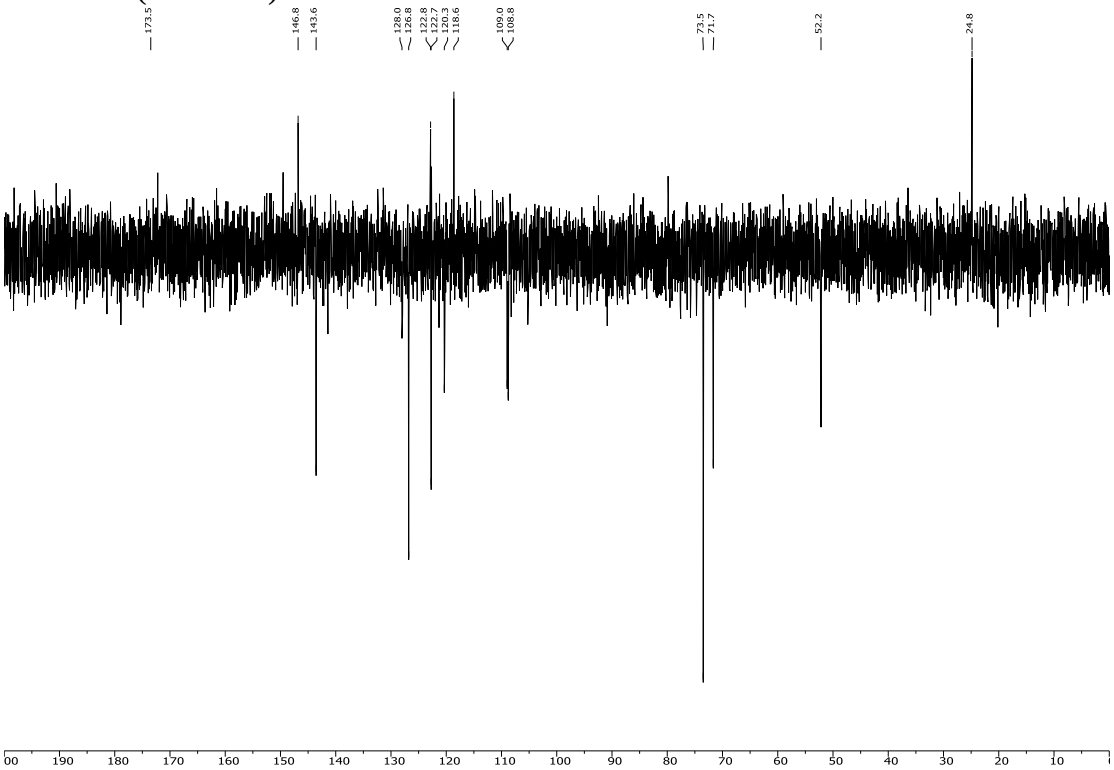

Compound **13d** ^{1}H NMR (400 MHz) D_2O

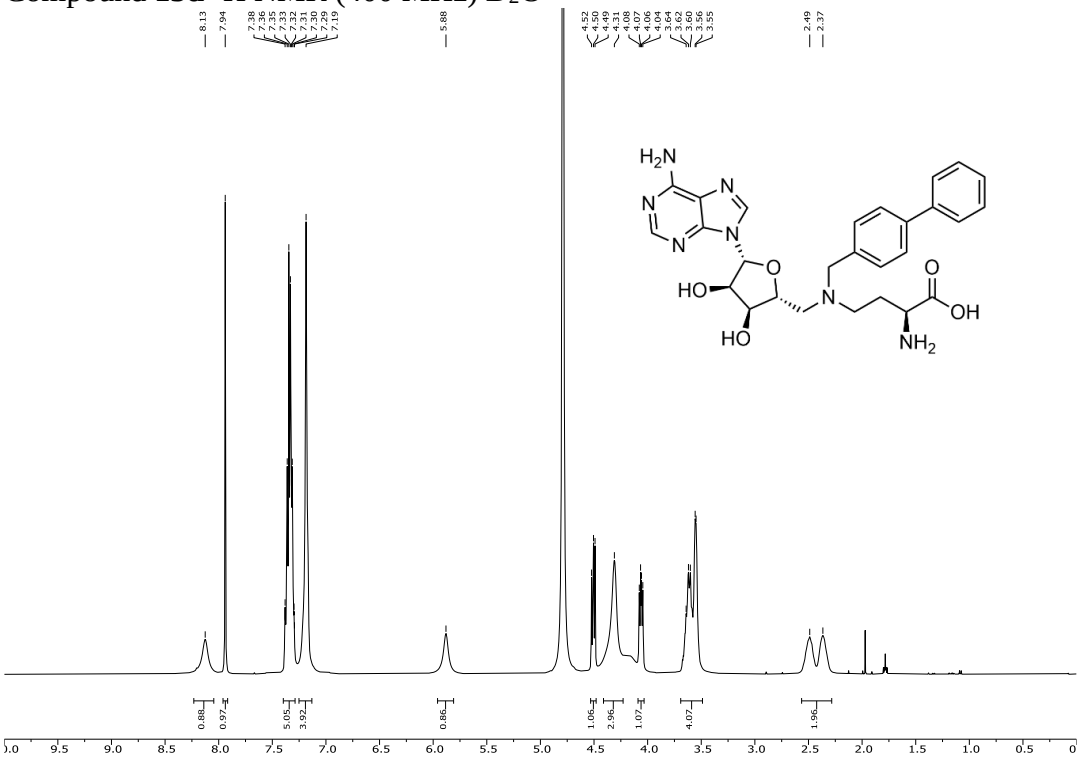

^{13}C NMR (101MHz) D_2O

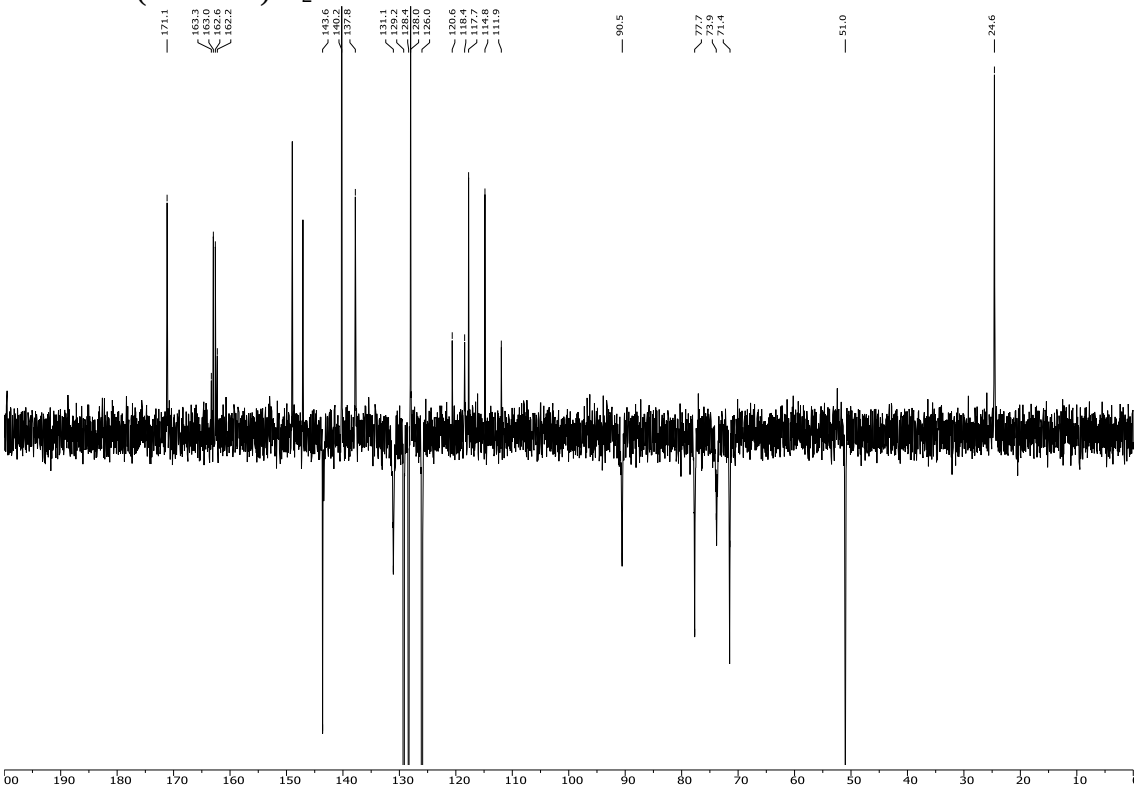

Compound **13e** ^{1}HNMR (400 MHz) D_2O

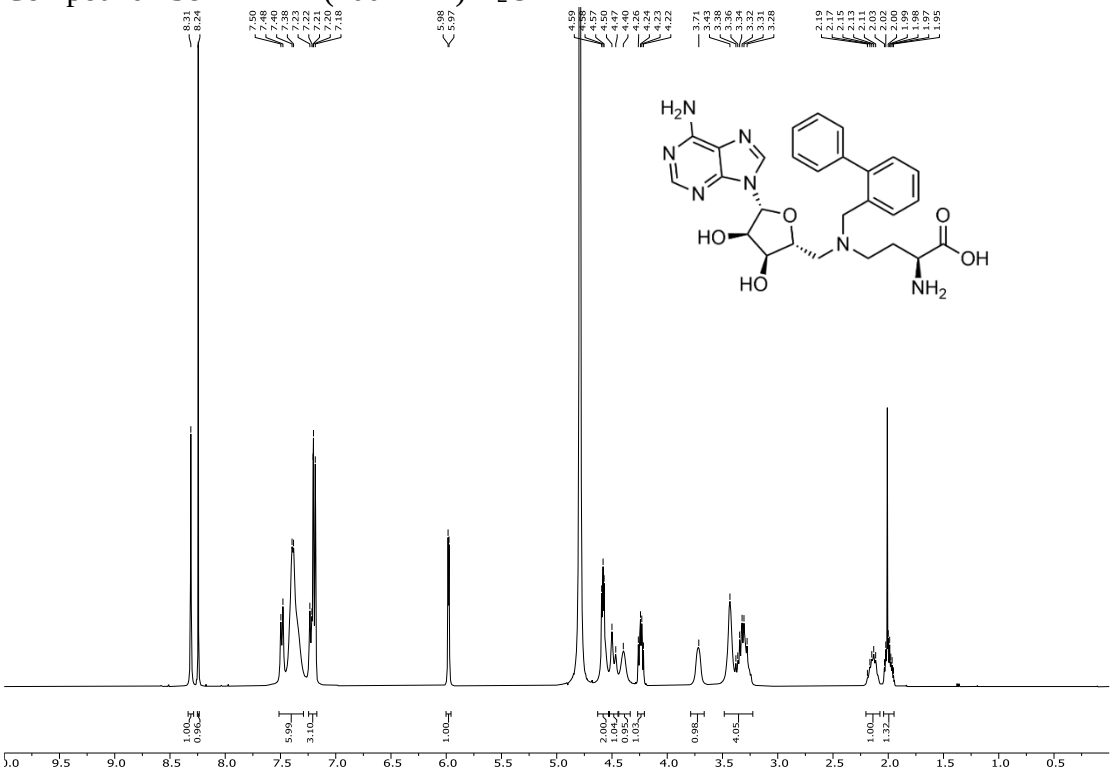

^{13}CNMR (101MHz) D_2O

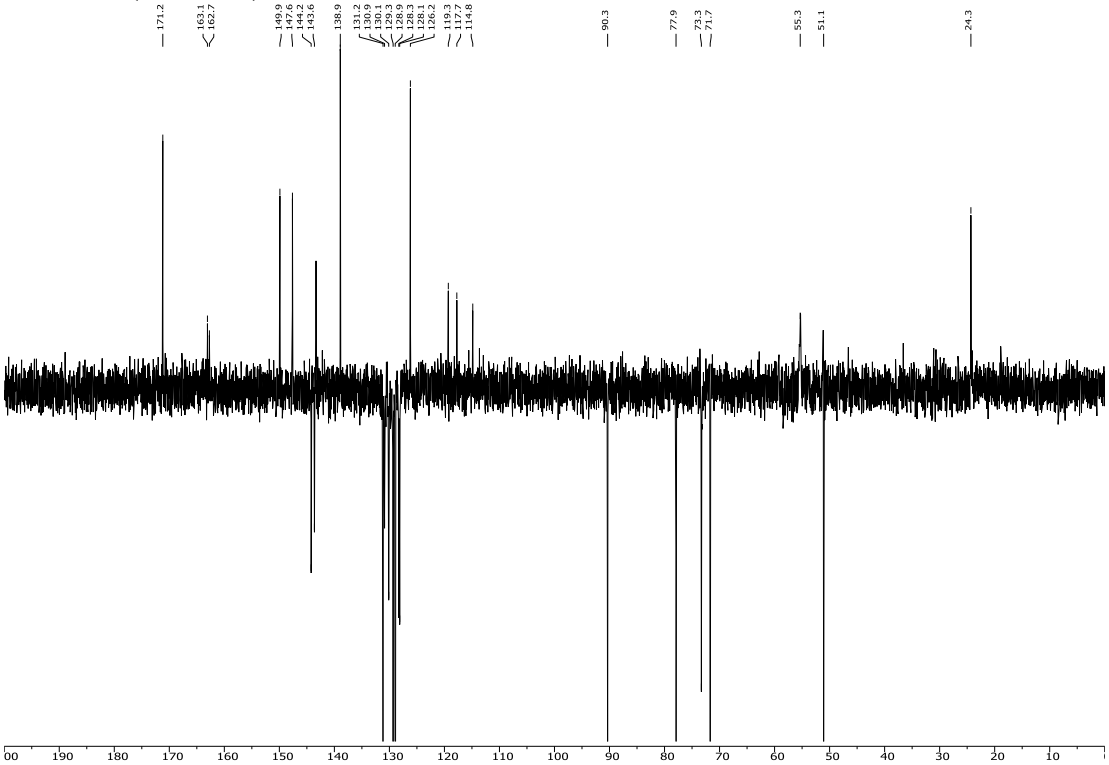

Compound **13f** ^{1}H NMR (400 MHz) D_2O

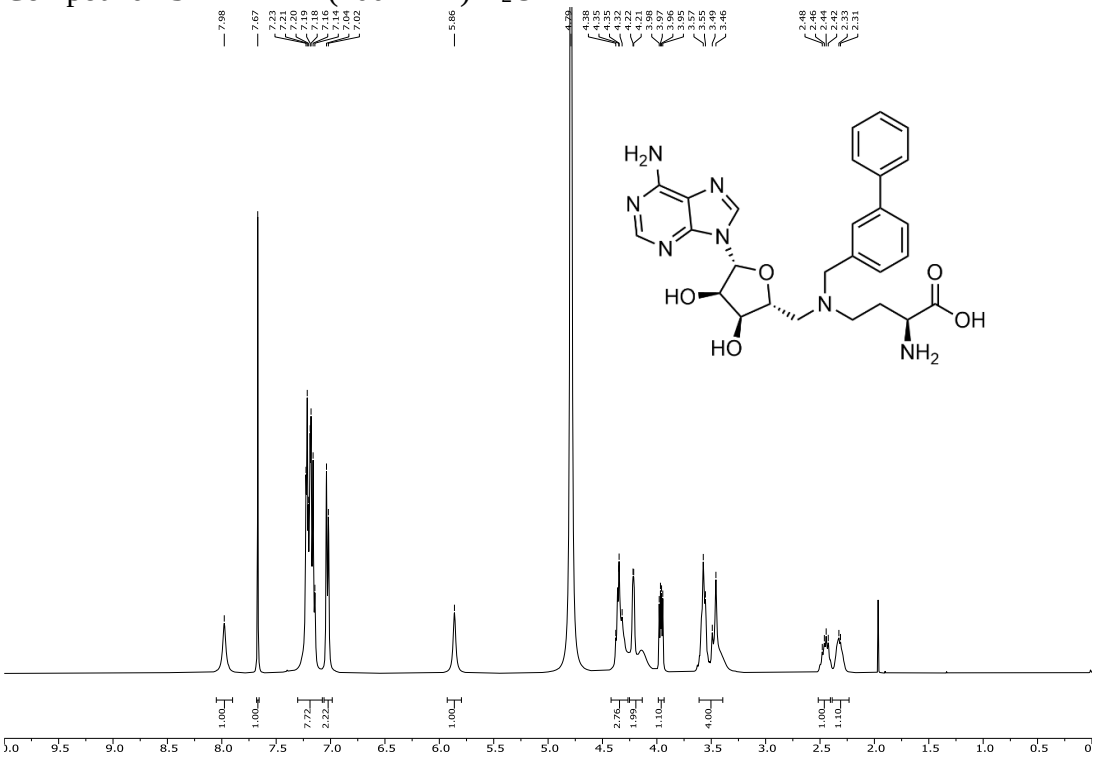

^{13}C NMR (101MHz) D_2O

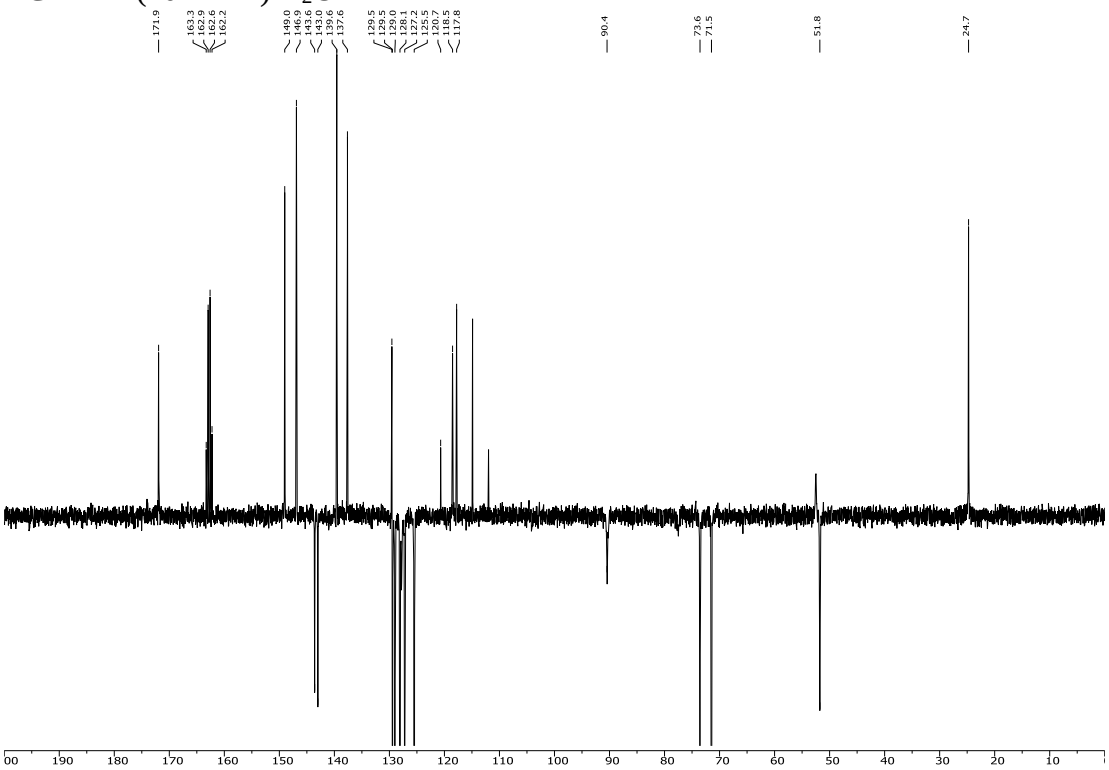

Compound **13g** ^{1}H NMR (400 MHz) D_2O

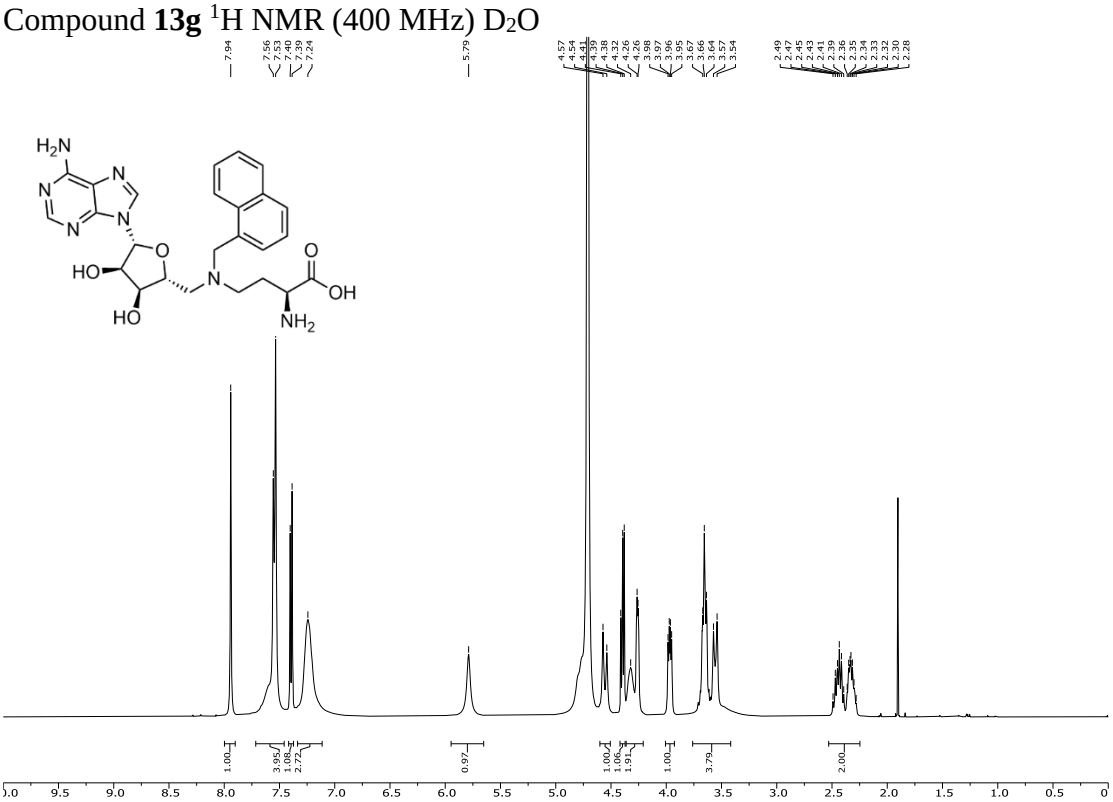

^{13}C NMR (101 MHz) D_2O

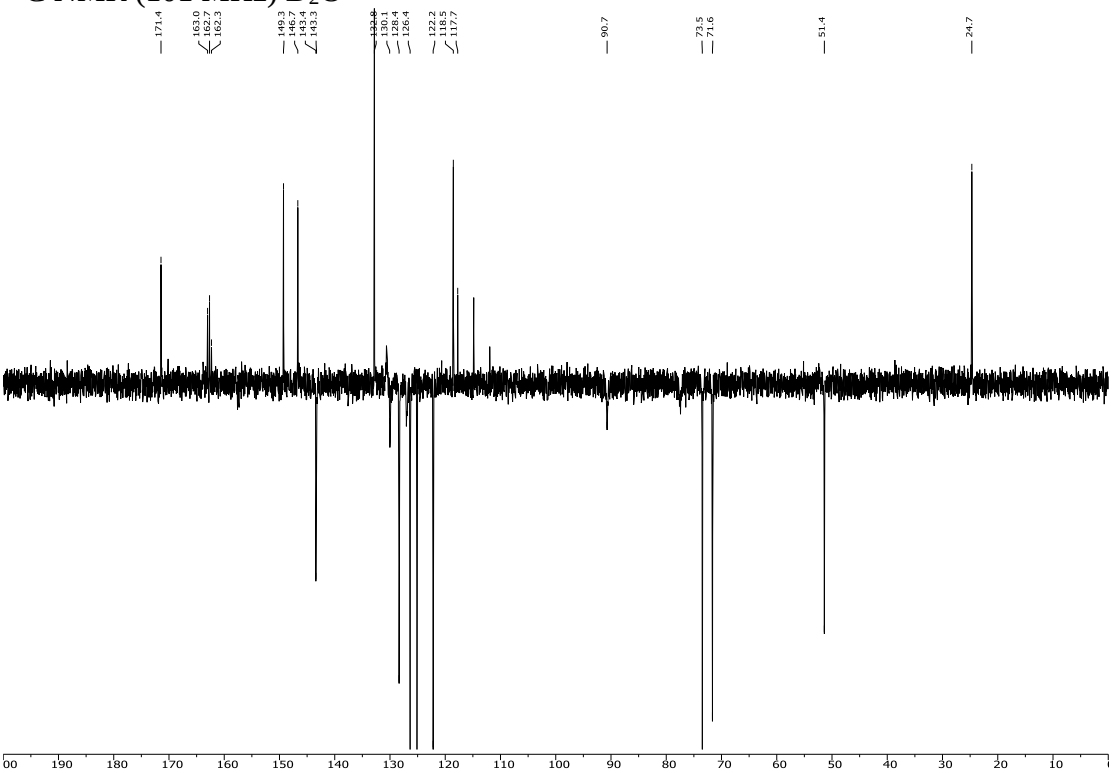

Compound **13h** ^{1}H NMR (400 MHz) CD_3OD

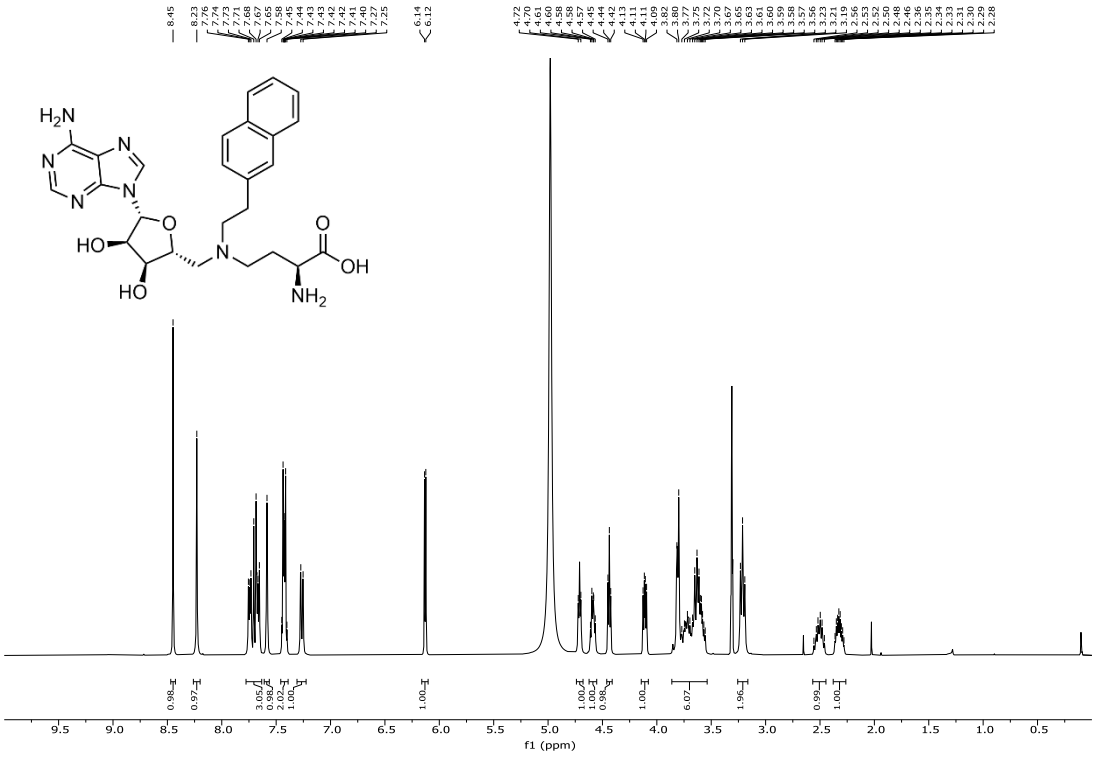

^{13}C NMR (101 MHz) CD_3OD

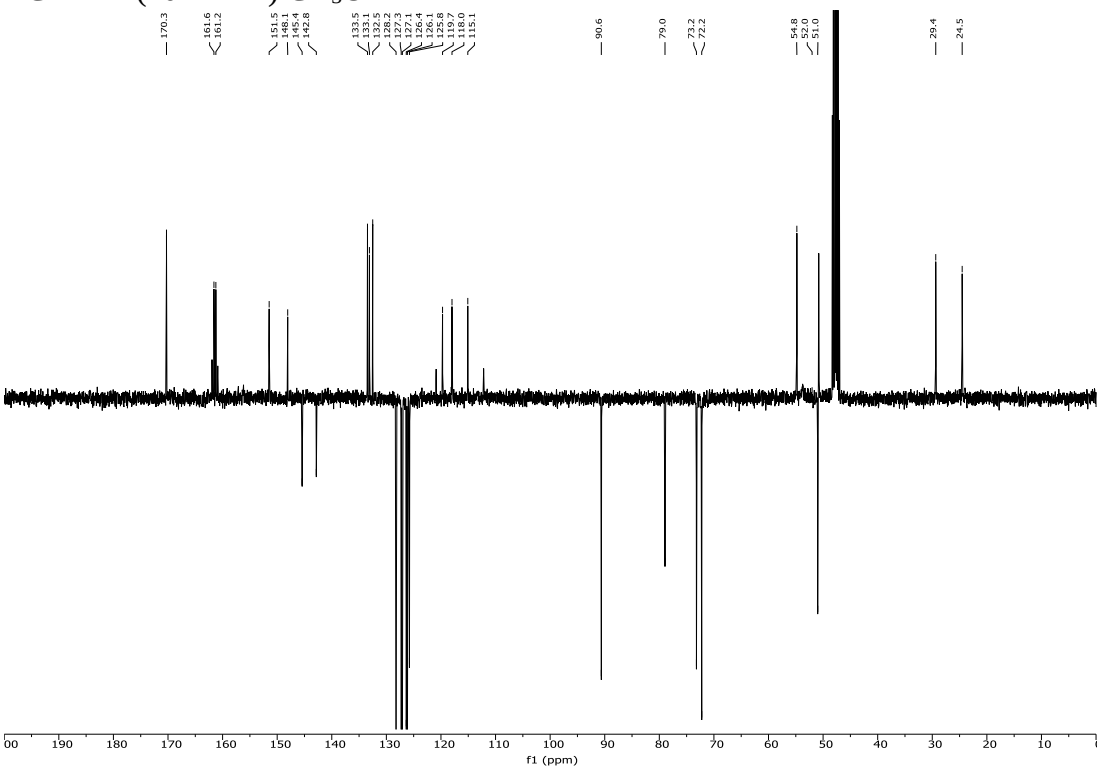

Compound **13i** ^{1}H NMR (400 MHz) D_2O

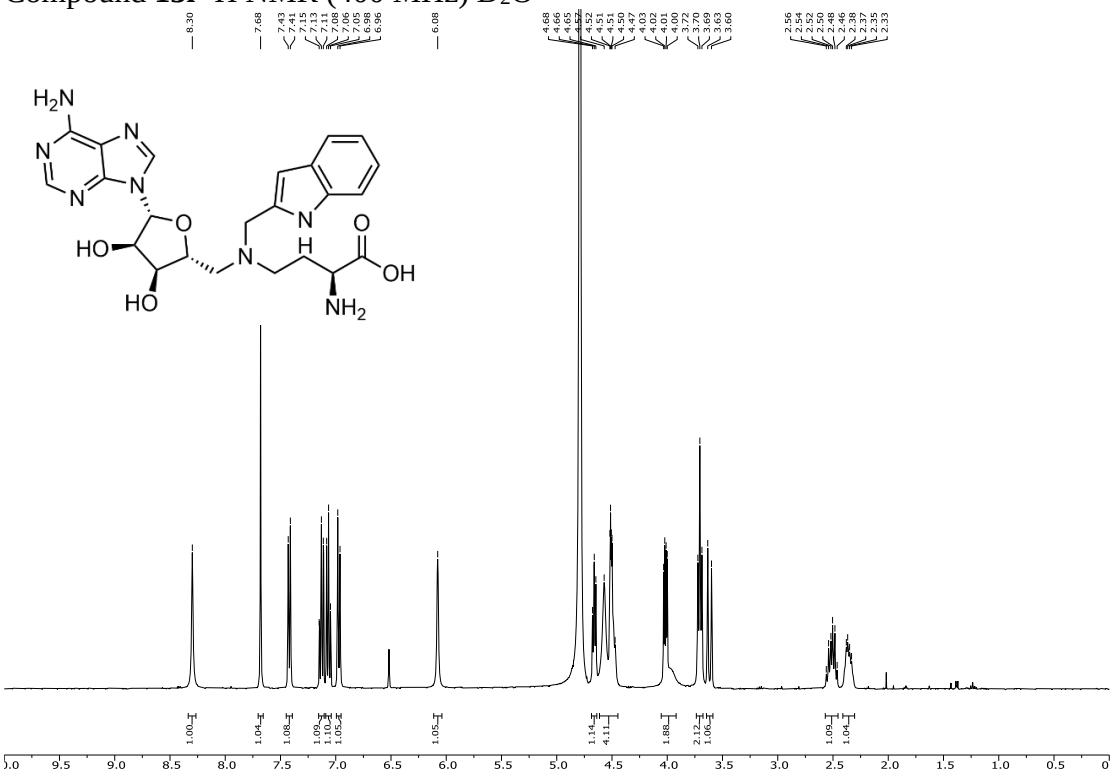

^{13}C NMR (101 MHz) D_2O

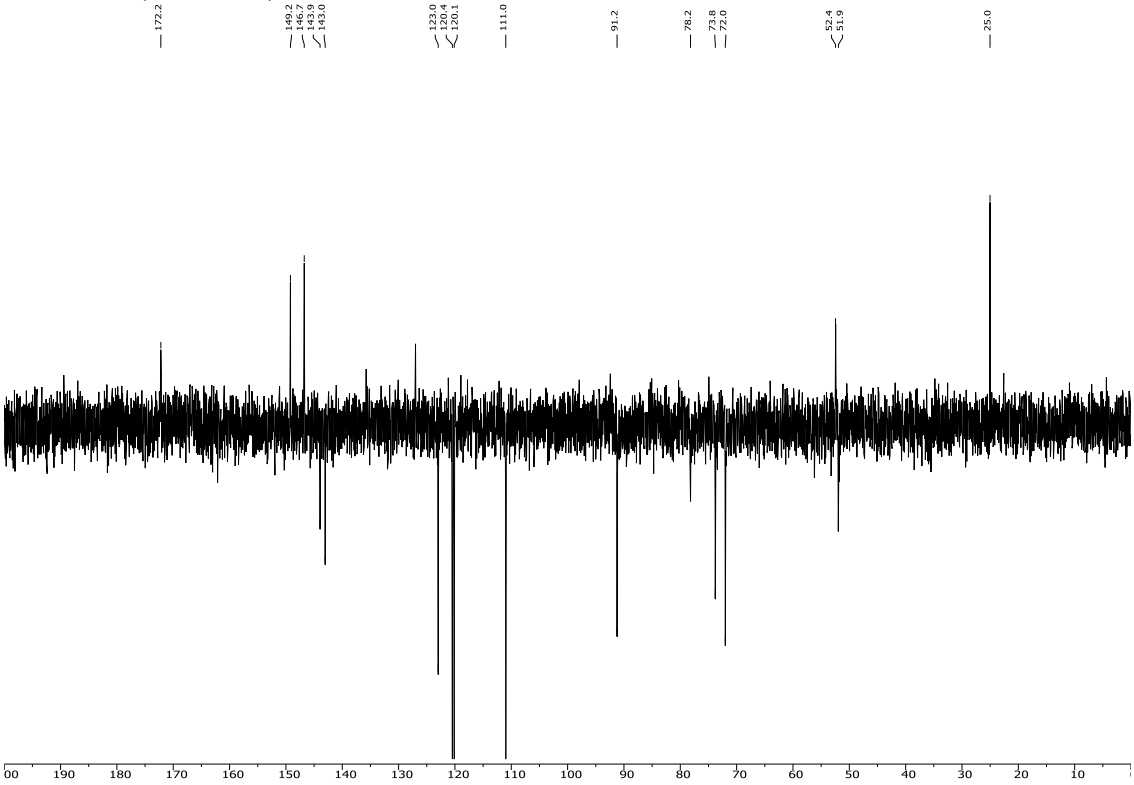

Compound **13j** ^{1}H NMR (500 MHz) CD_3OD

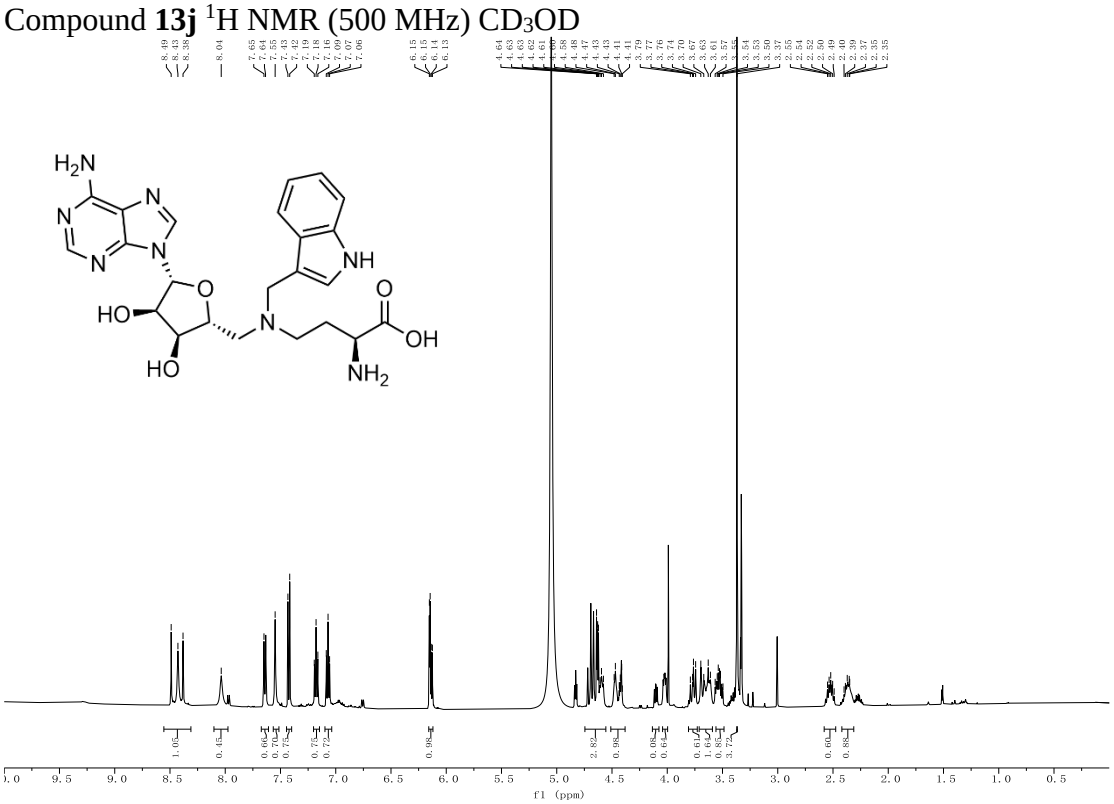

^{13}C NMR (126 MHz) CD_3OD

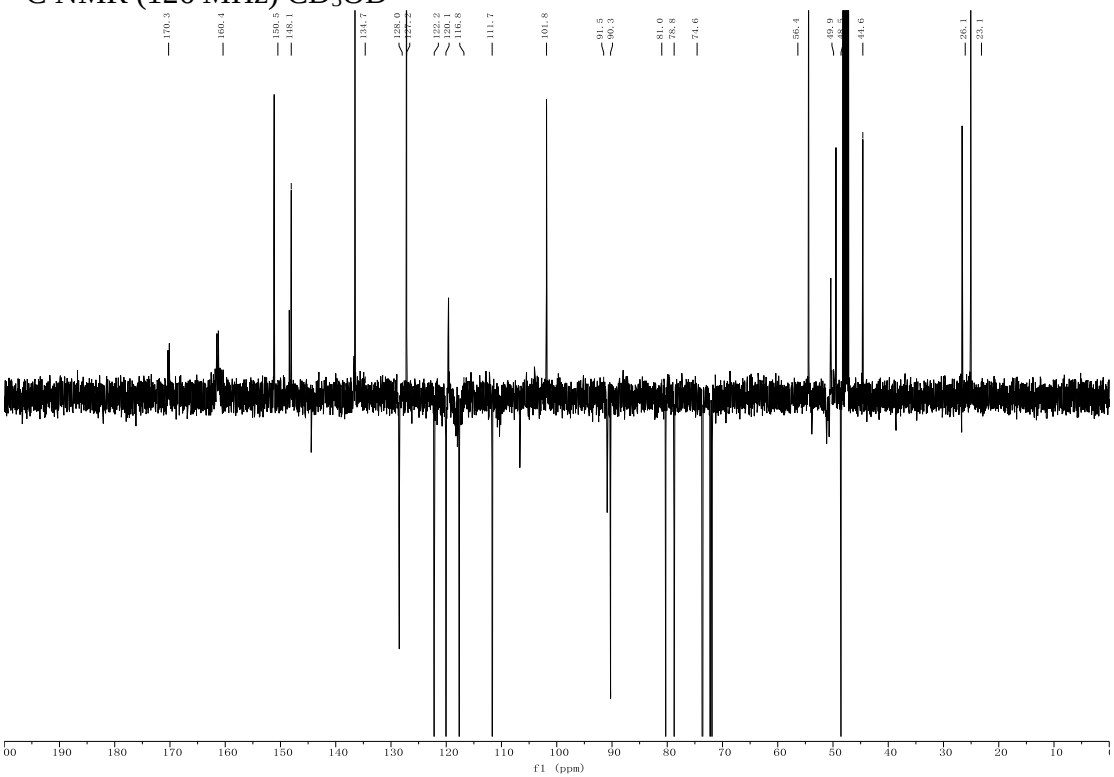

Compound **13k** ^{1}H NMR (400 MHz) D_2O

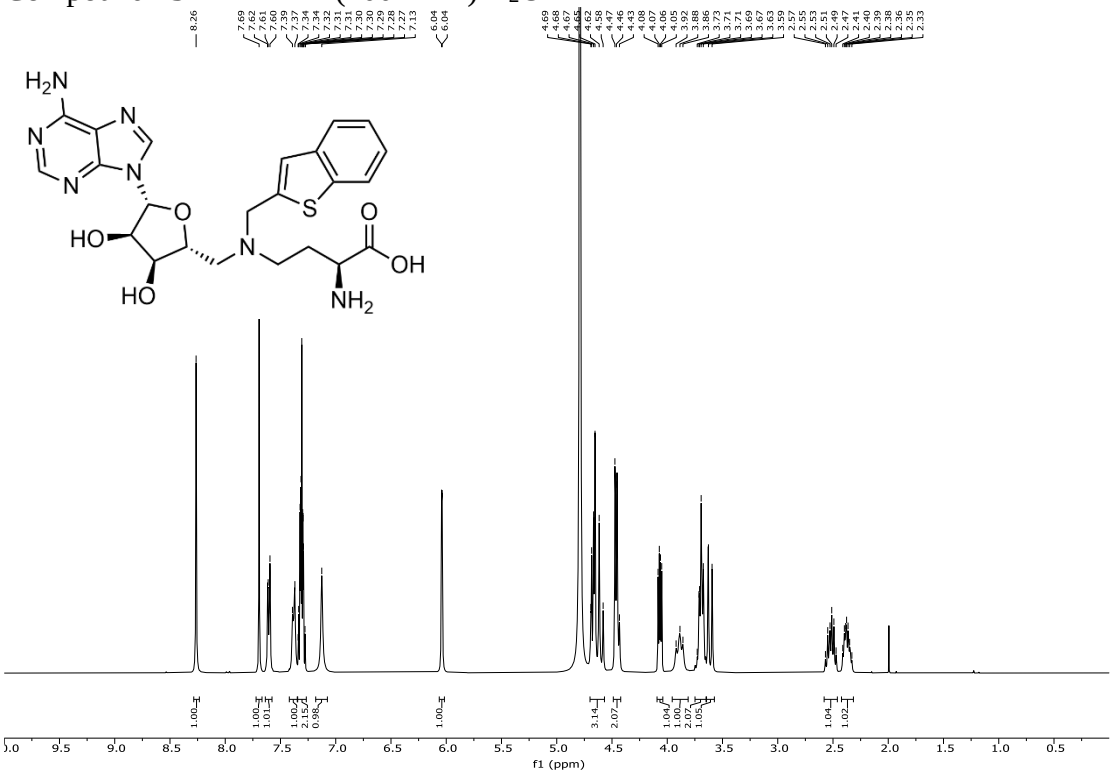

^{13}C NMR (101 MHz) D_2O

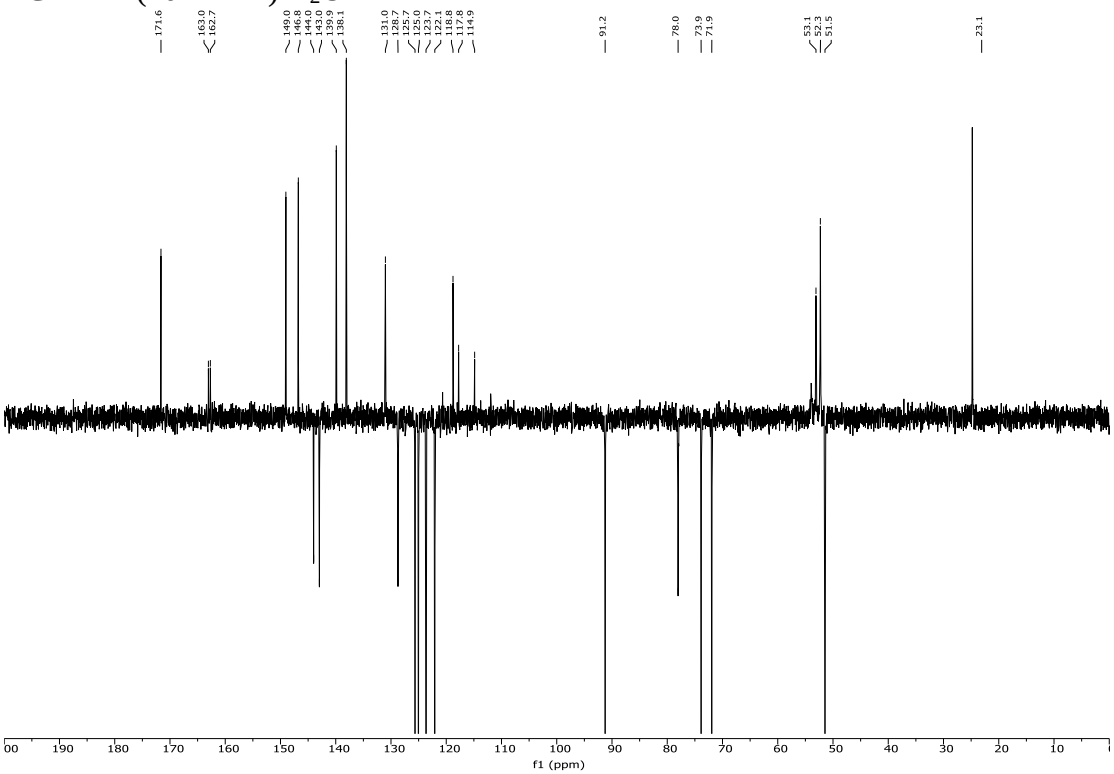

Compound **13l** ^{1}H NMR (400 MHz) CD_3OD

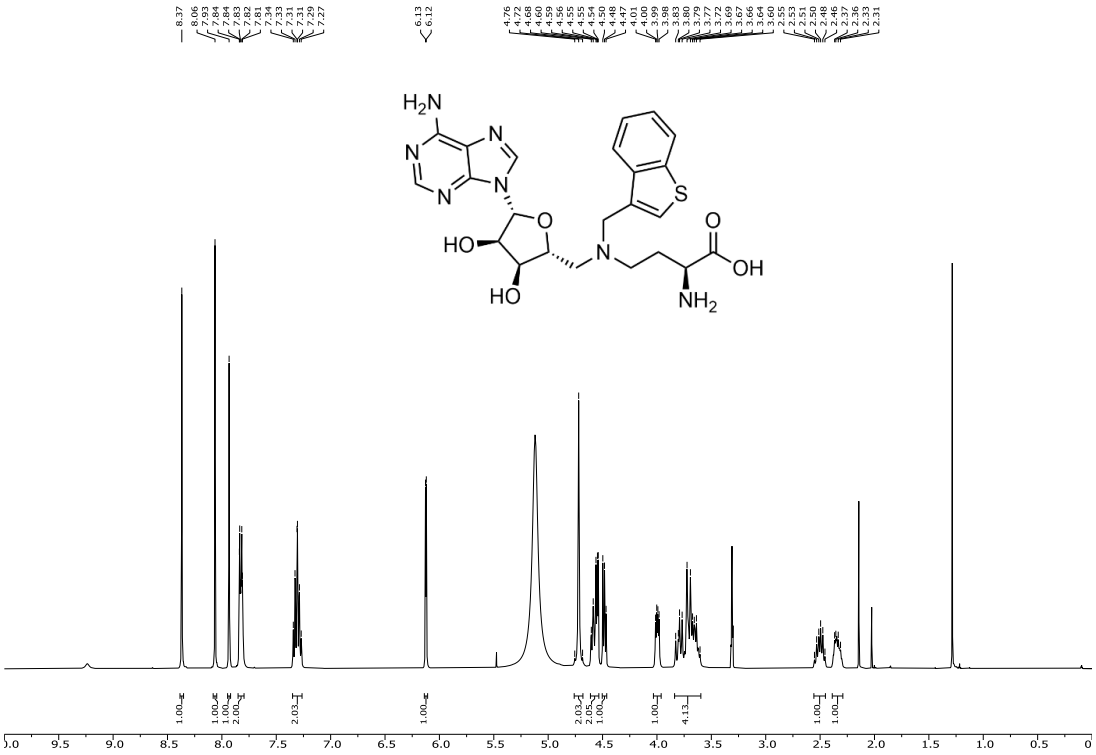

^{13}C NMR (101 MHz) CD_3OD

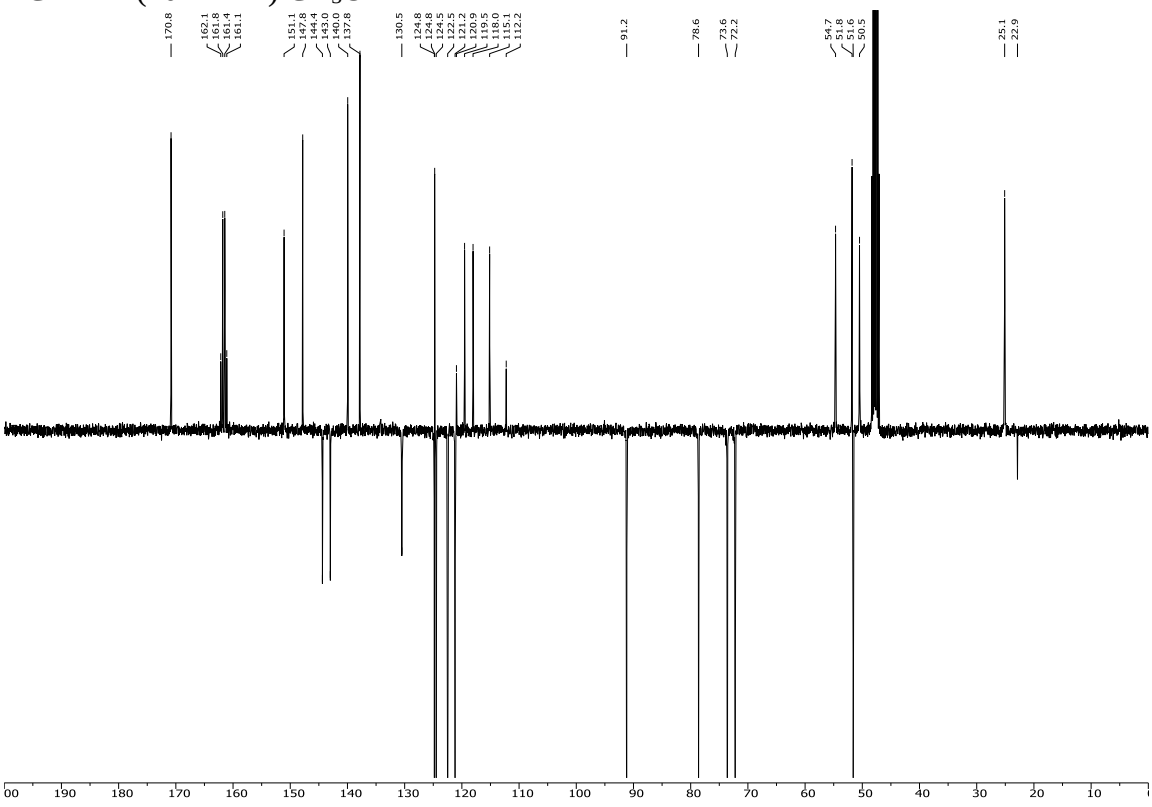

Compound **14y** ^{1}H NMR (400 MHz) $CDCl_3$

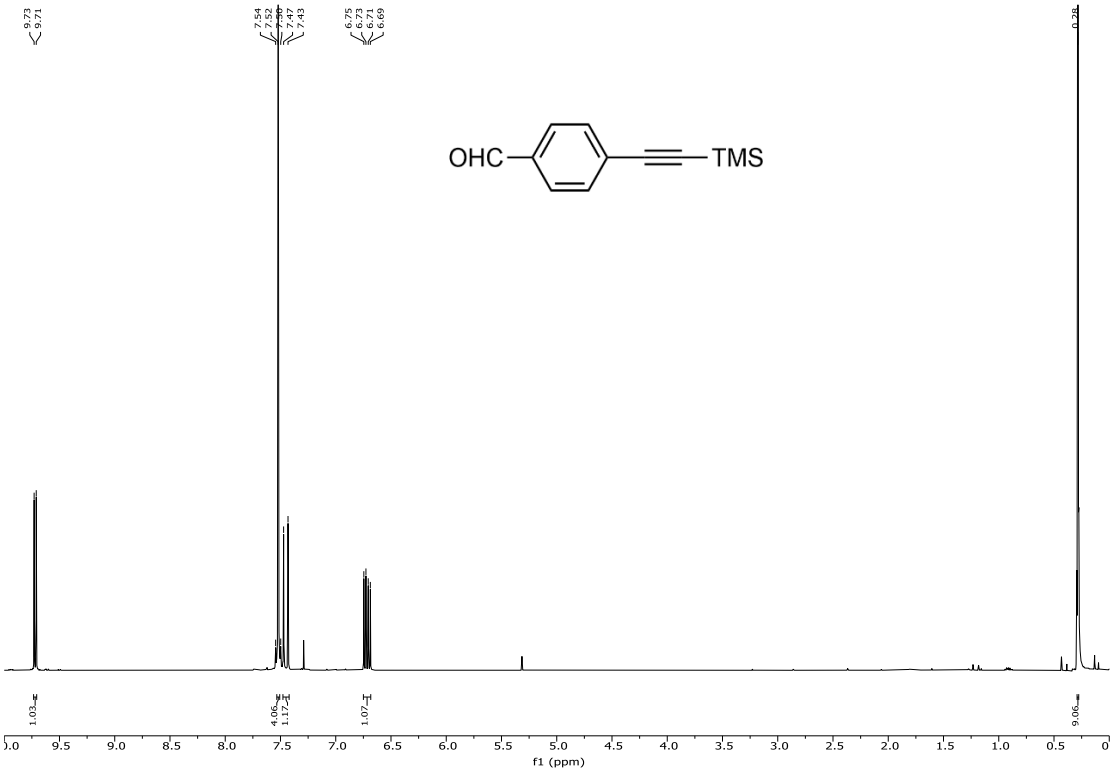

^{13}C NMR (101 MHz) $CDCl_3$

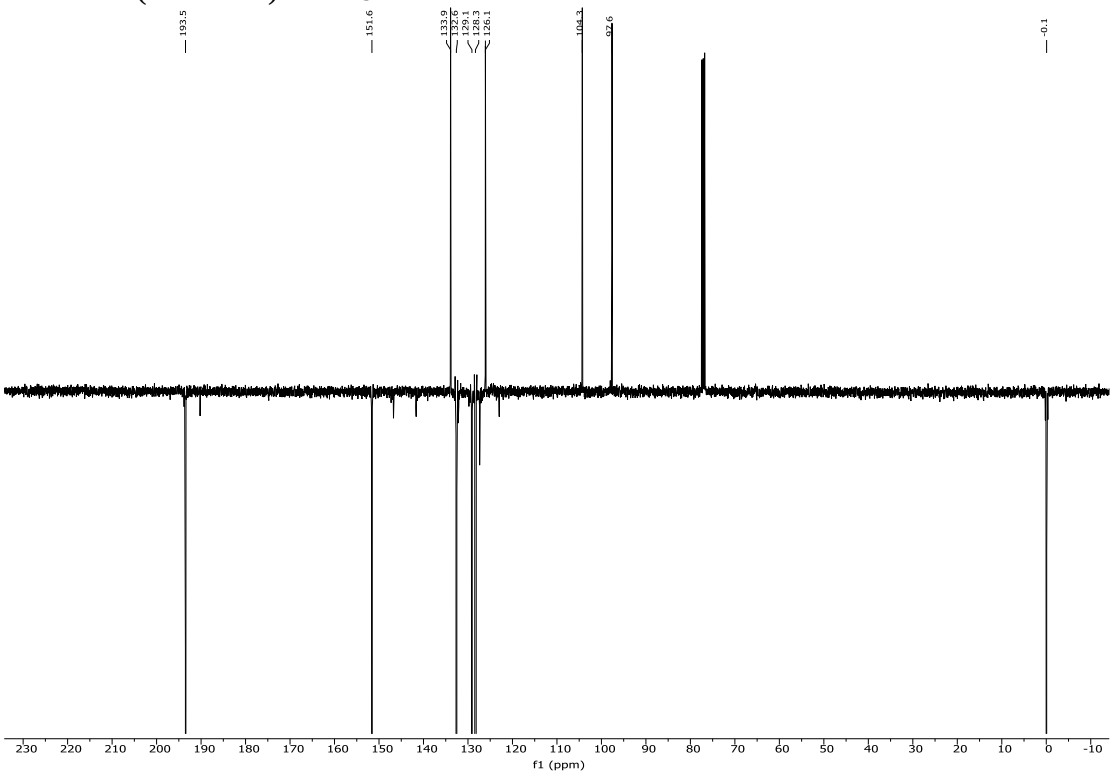

Compound **16a** ^{1}H NMR (400 MHz) $CDCl_3$

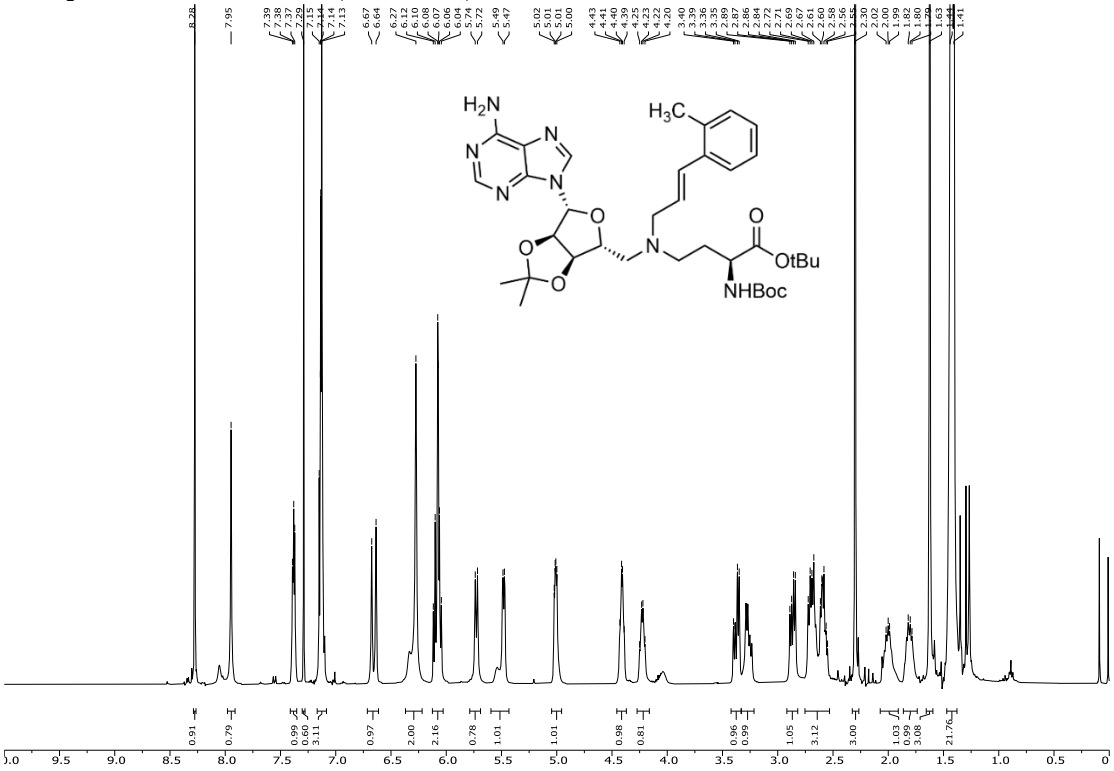

^{13}C NMR (101 MHz) $CDCl_3$

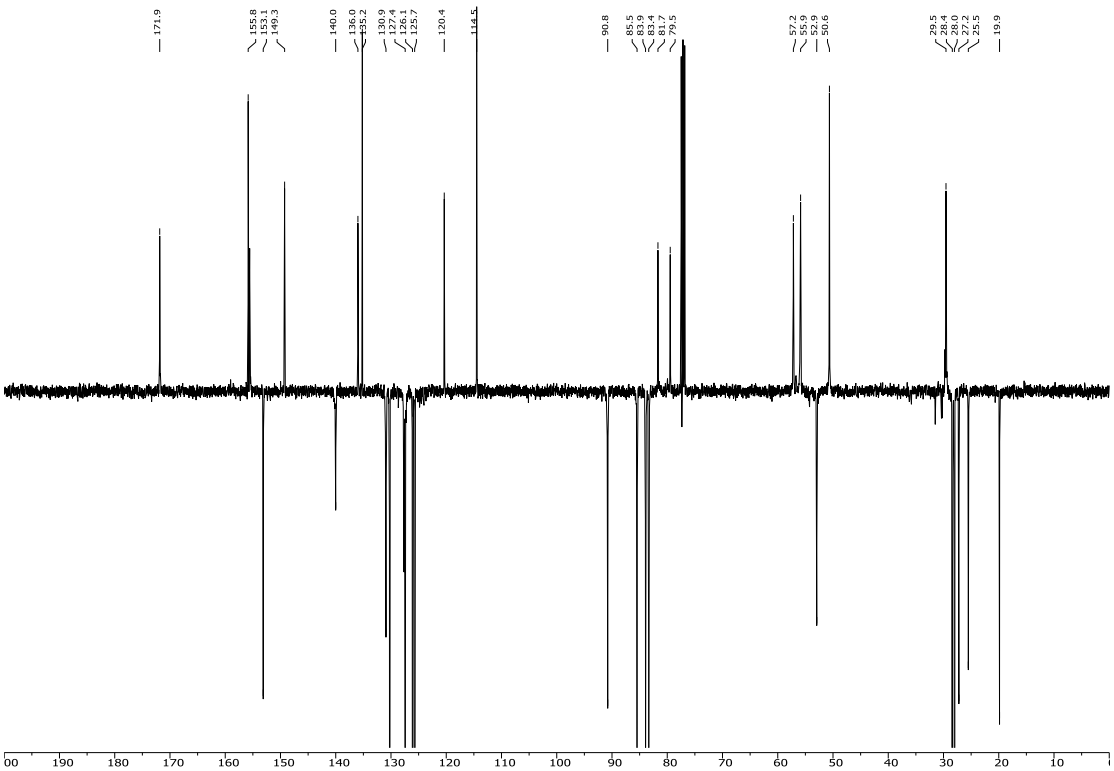

Compound **16b** ^{1}H NMR (400 MHz) $CDCl_3$

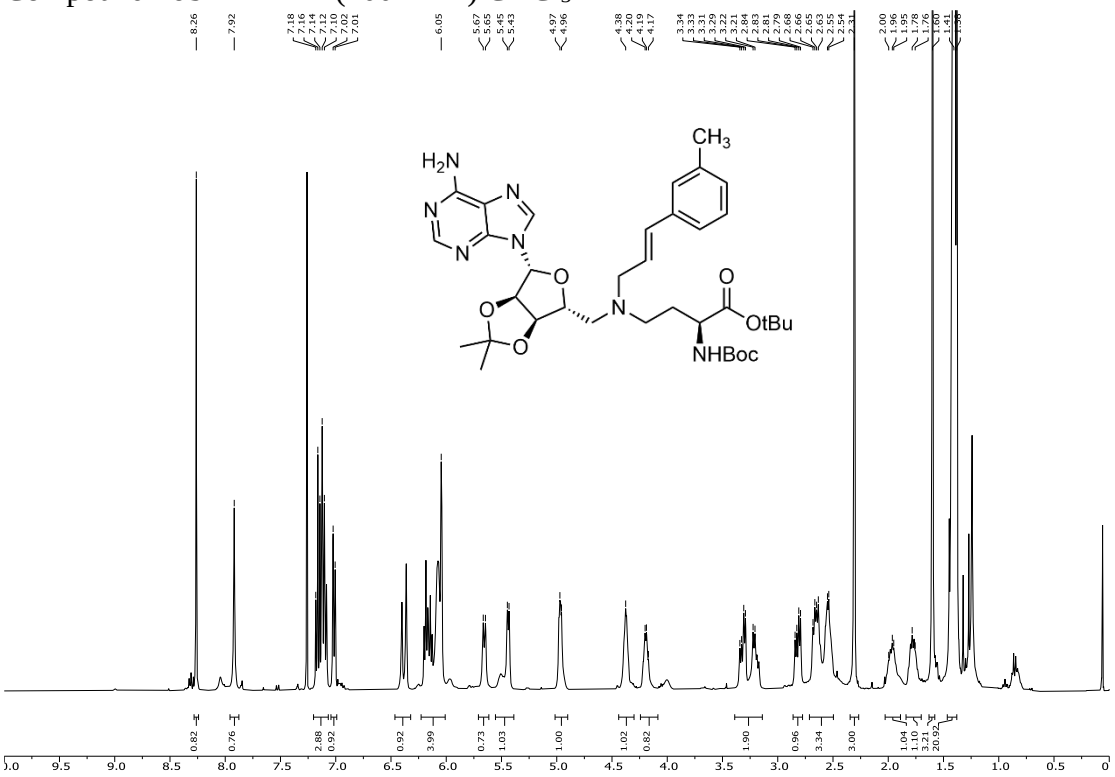

^{13}C NMR (101 MHz) $CDCl_3$

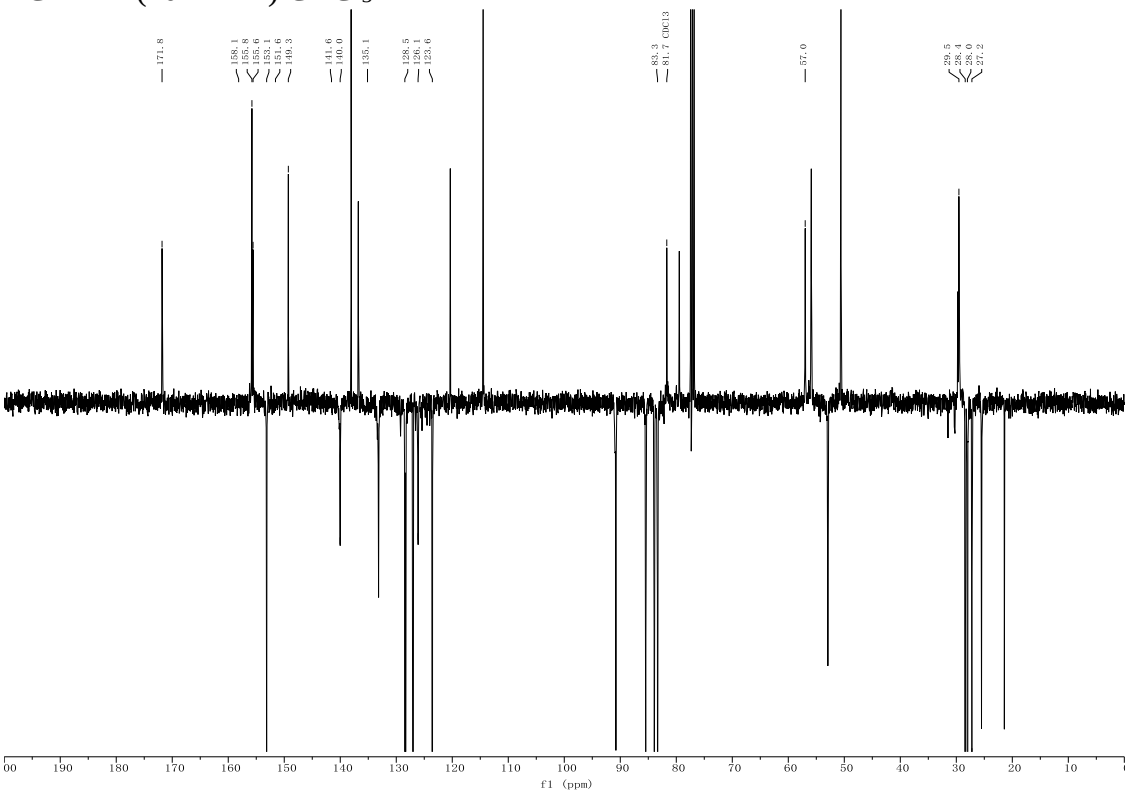

Compound **16c** ^{1}H NMR (400 MHz) $CDCl_3$

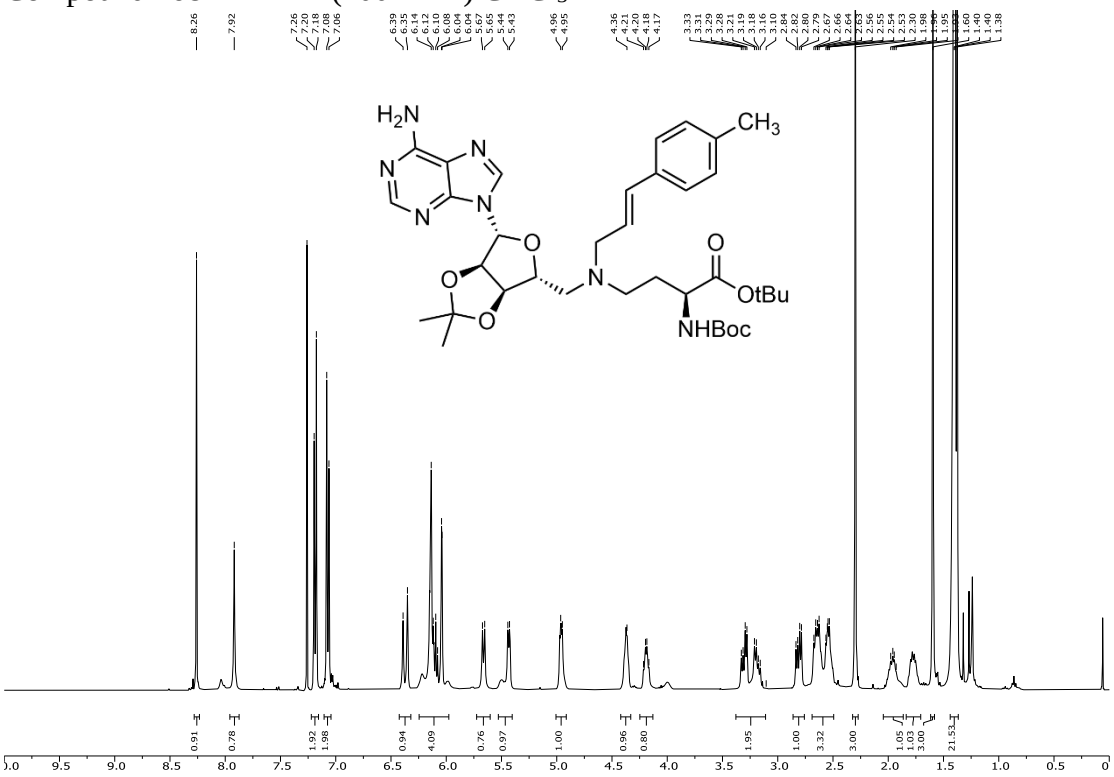

^{13}C NMR (101 MHz) $CDCl_3$

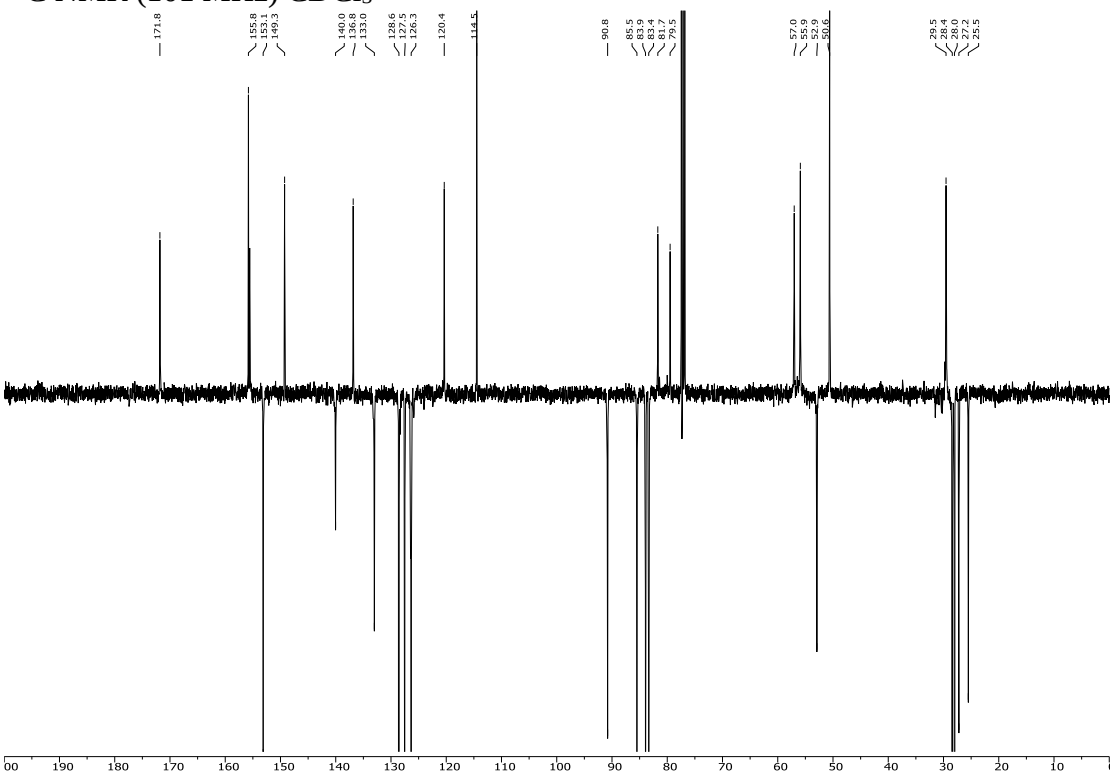

Compound **16d** ^{1}H NMR (400 MHz) $CDCl_3$

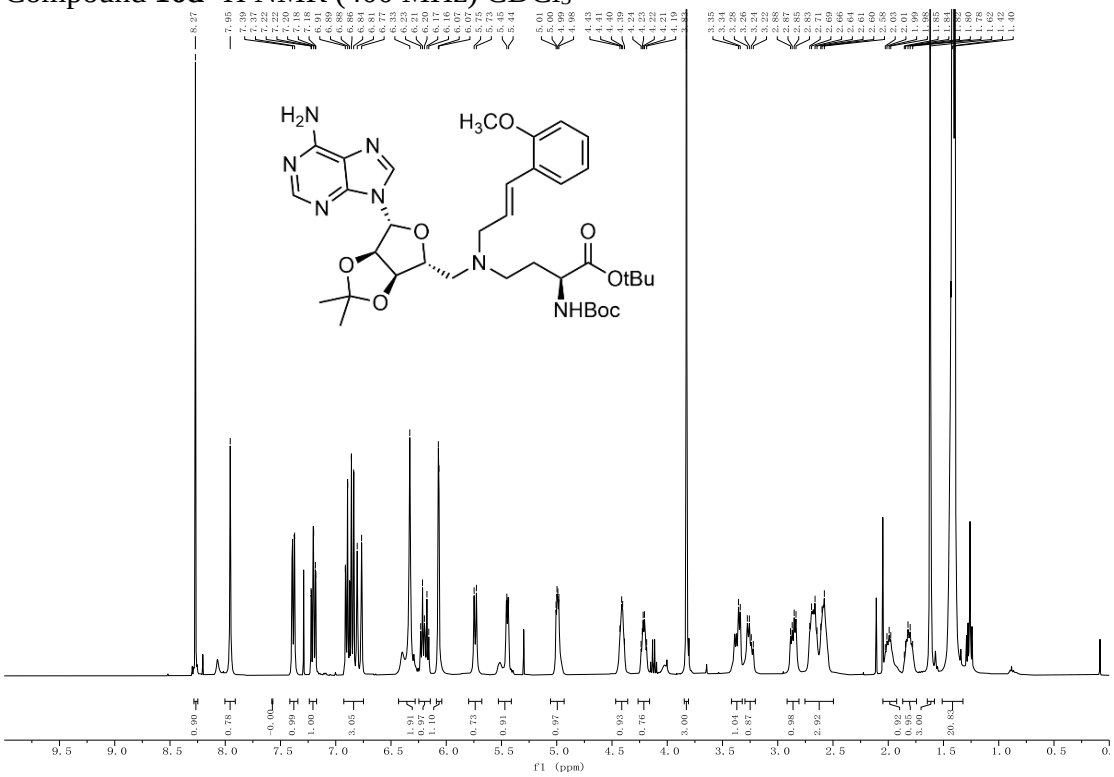

^{13}C NMR (101 MHz) $CDCl_3$

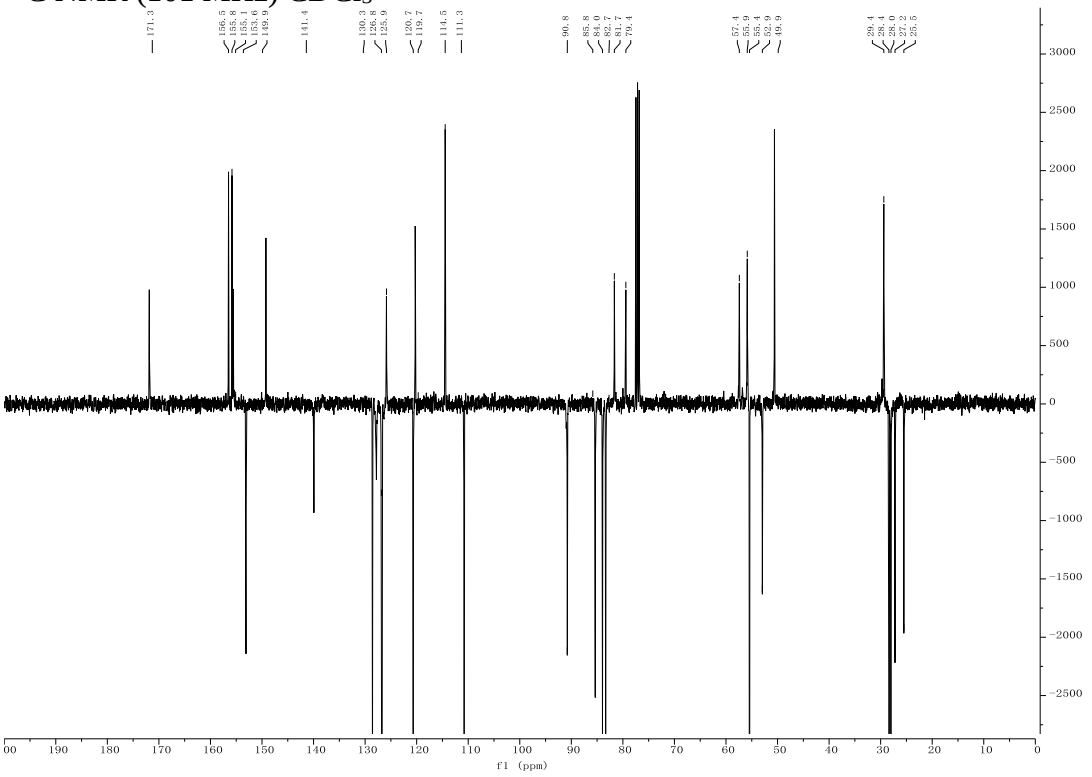

Compound **16e** ^{1}H NMR (400 MHz) $CDCl_3$

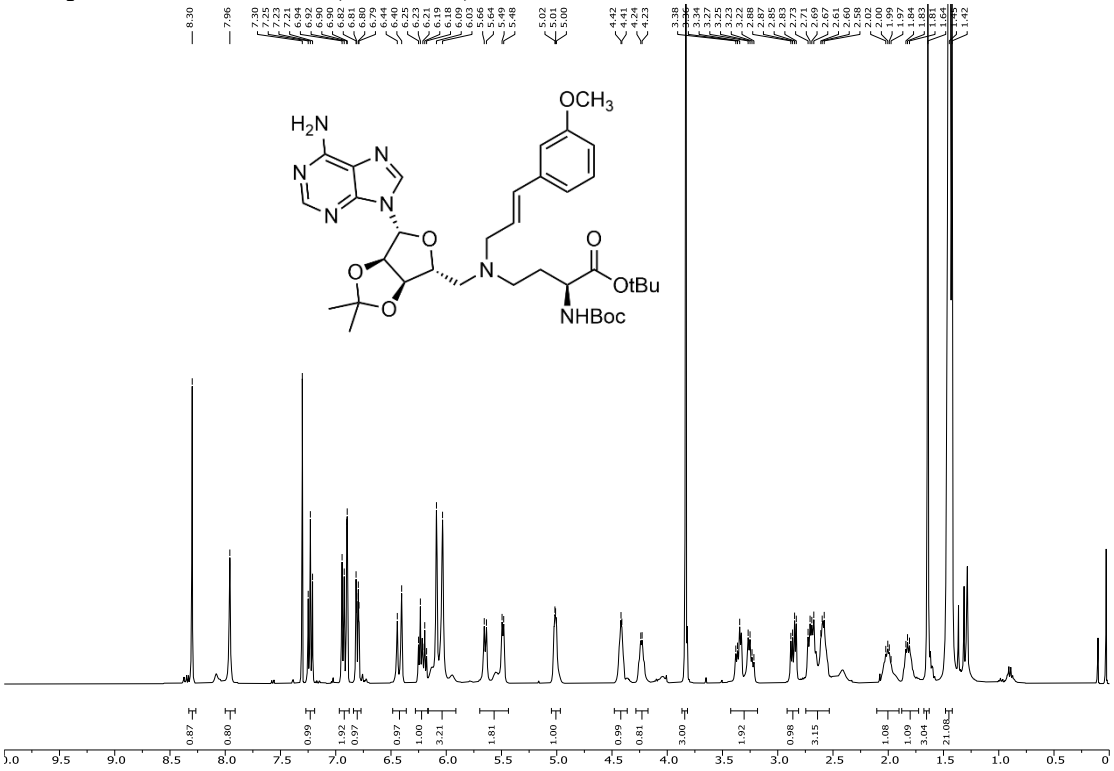

^{13}C NMR (101 MHz) $CDCl_3$

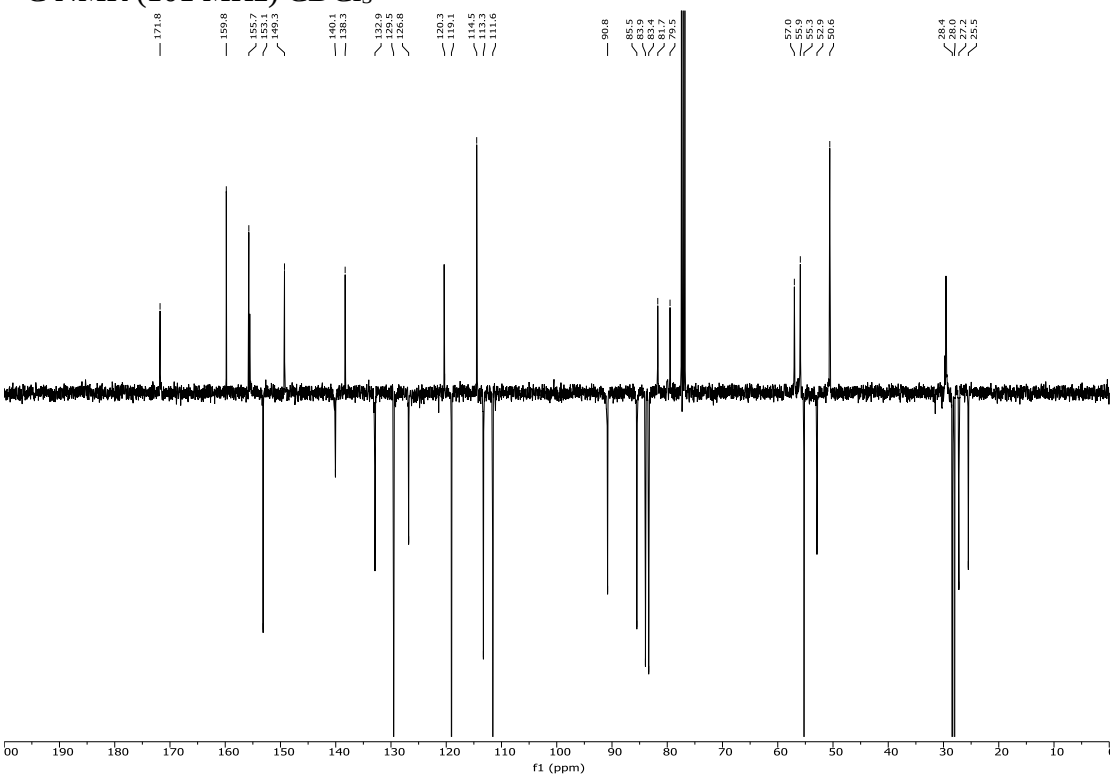

Compound **16f** ^{1}H NMR (400 MHz) $CDCl_3$

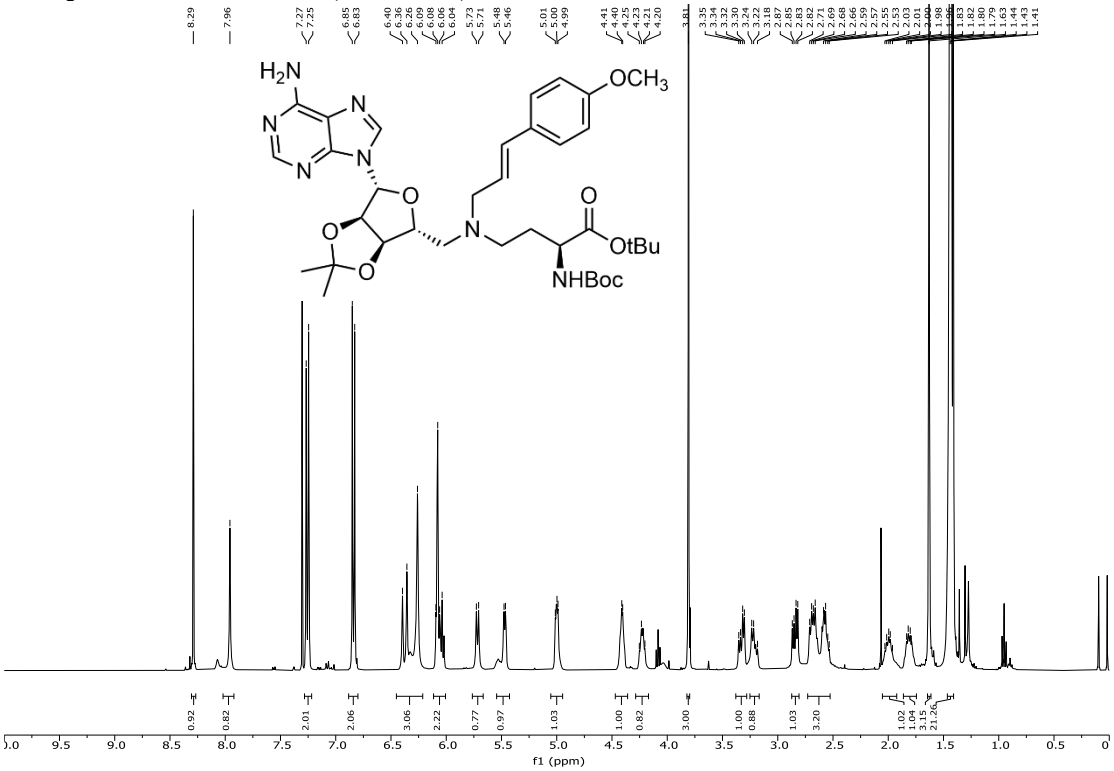

^{13}C NMR (400 MHz) $CDCl_3$

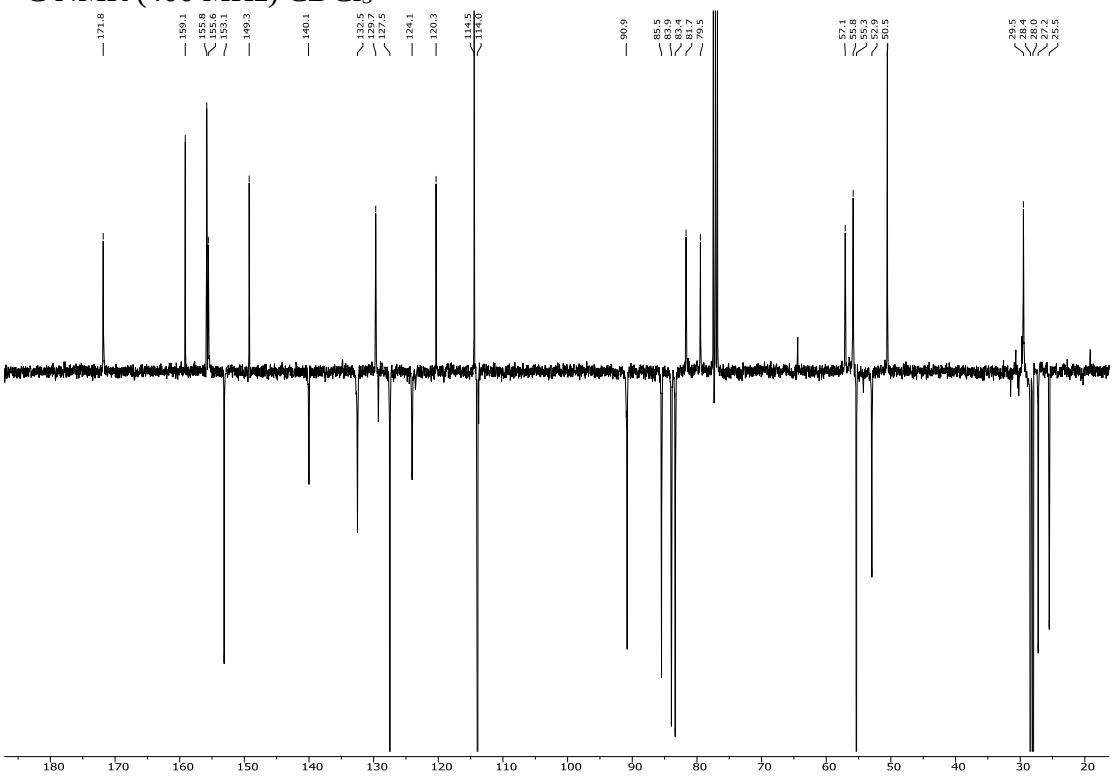

Compound **16g** ^{1}H NMR $CDCl_3$

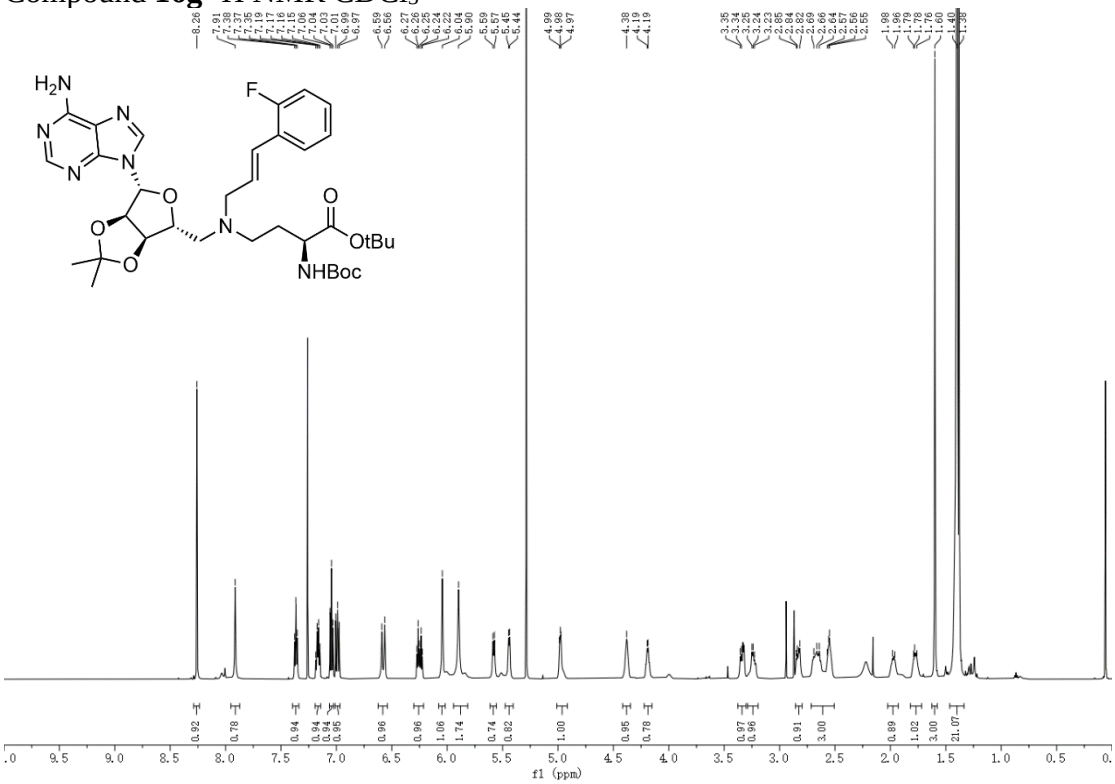

^{13}C NMR (101 MHz) $CDCl_3$

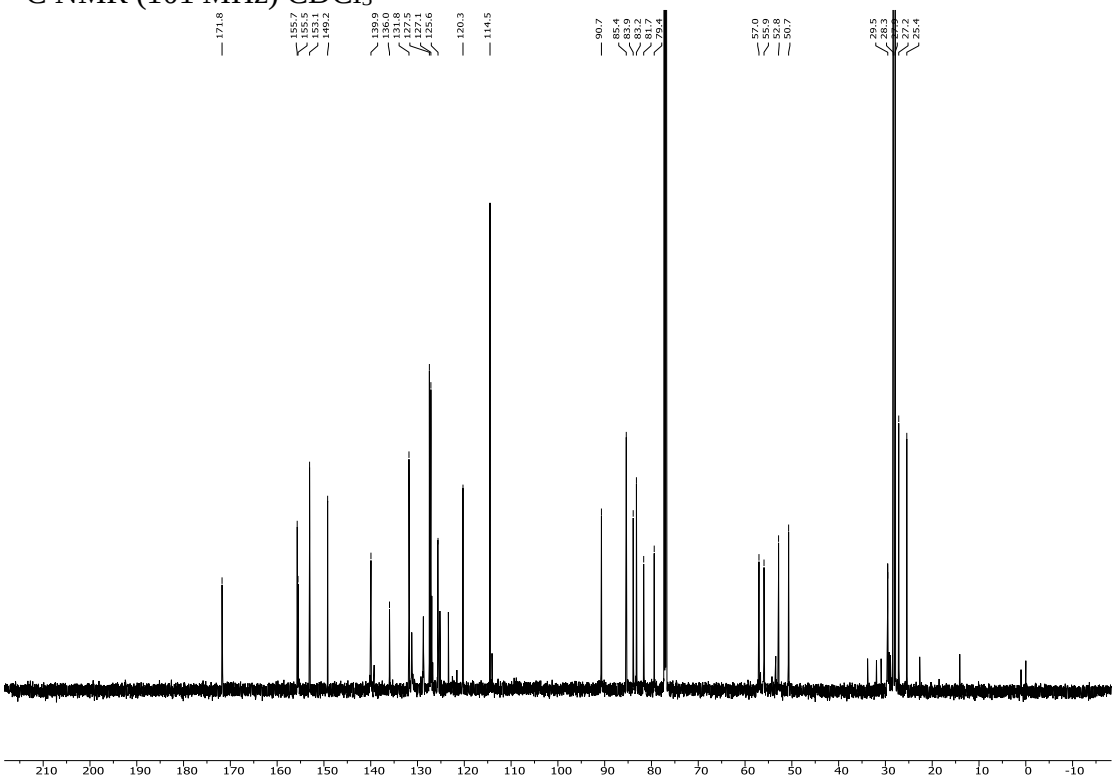

Compound **16h** ^{1}H NMR (600 MHz) $CDCl_3$

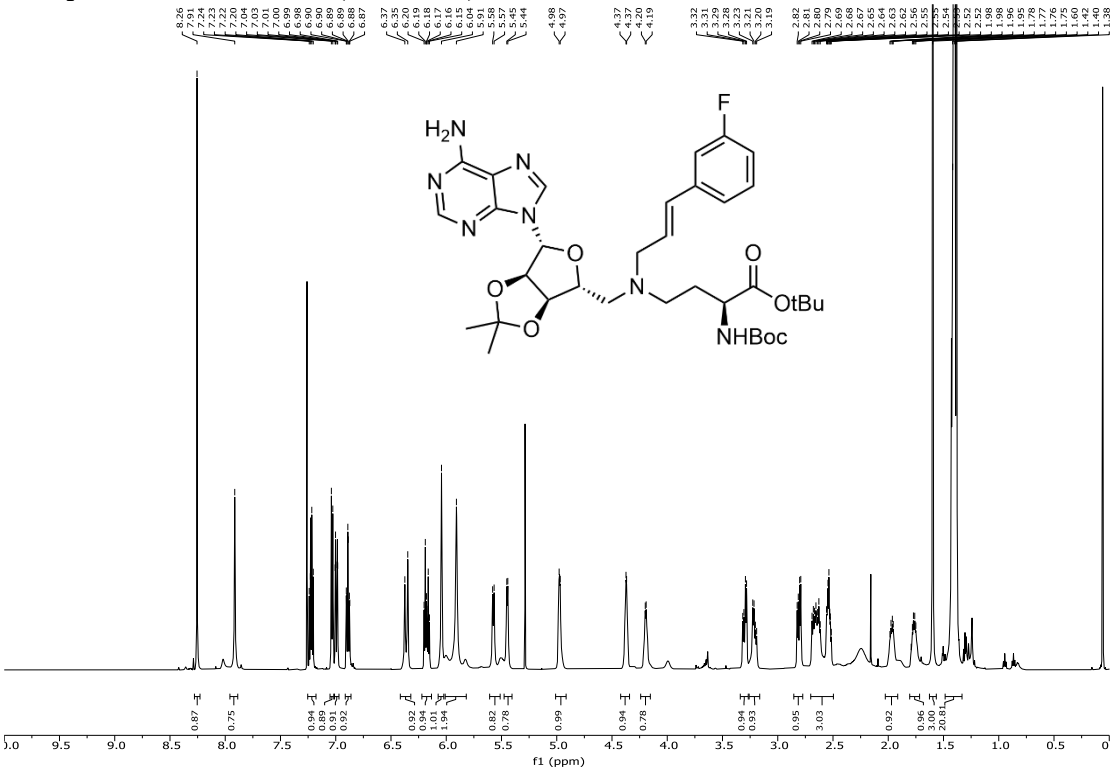

^{13}CNMR (151 MHz) $CDCl_3$

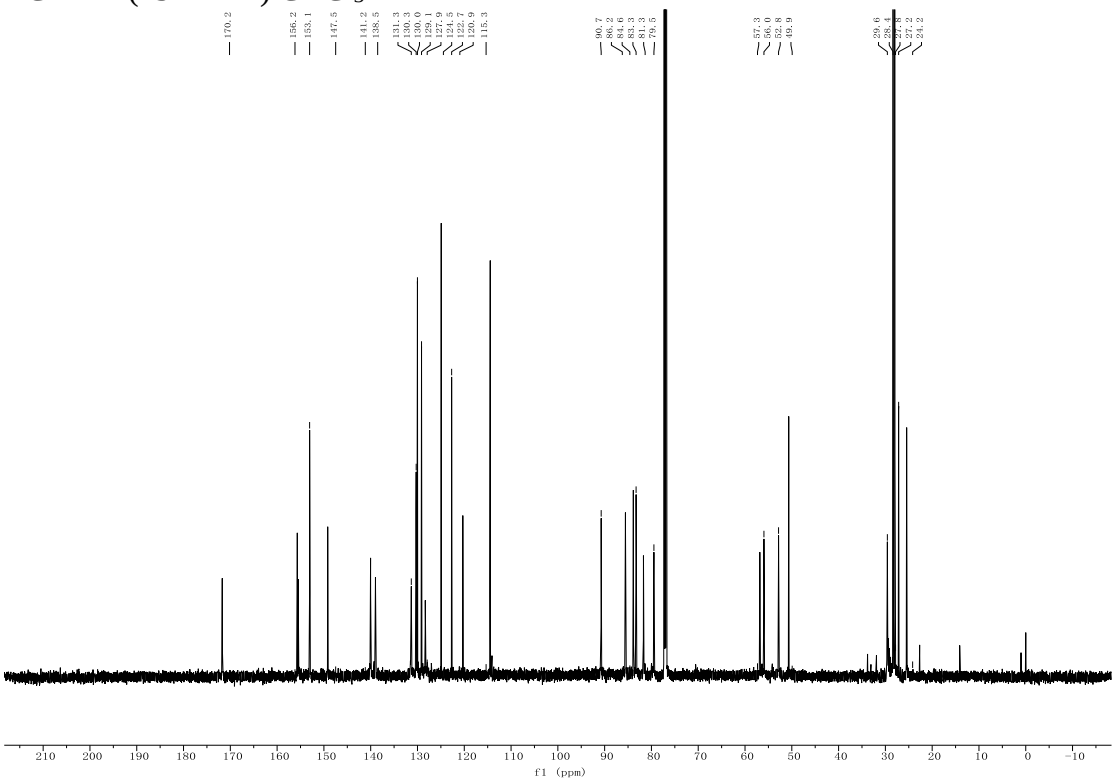

Compound **16i** ^{1}H NMR (400 MHz) $CDCl_3$

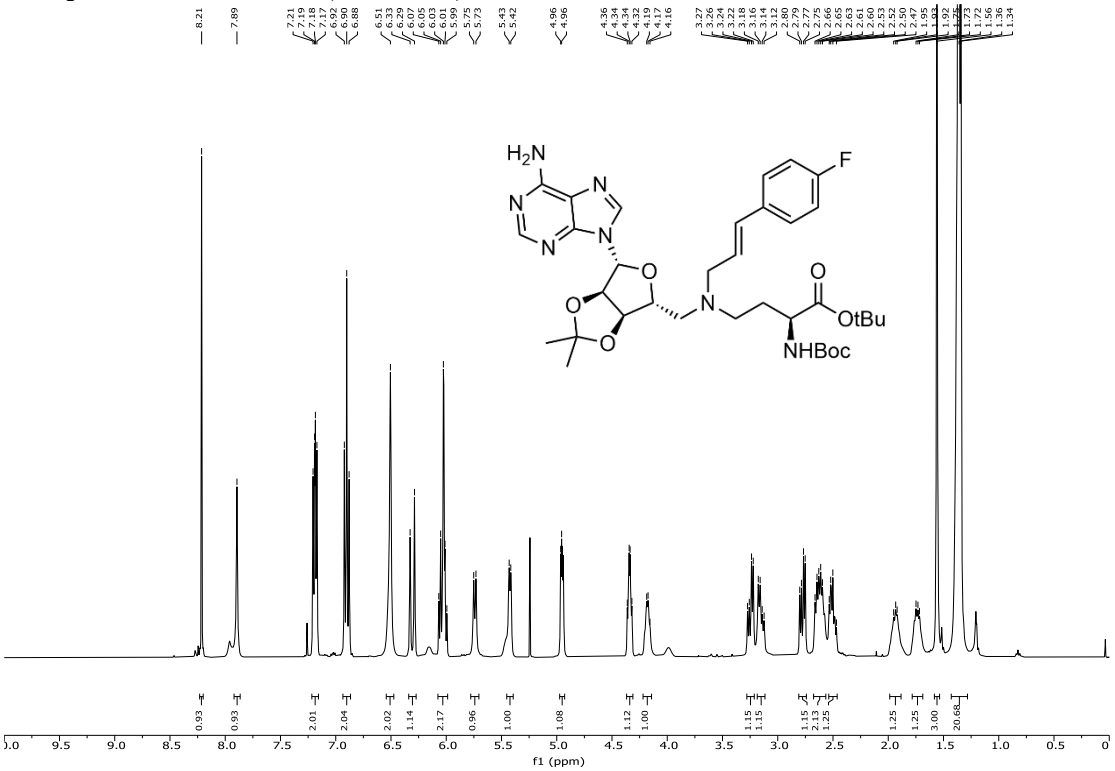

^{13}C NMR (101 MHz) $CDCl_3$

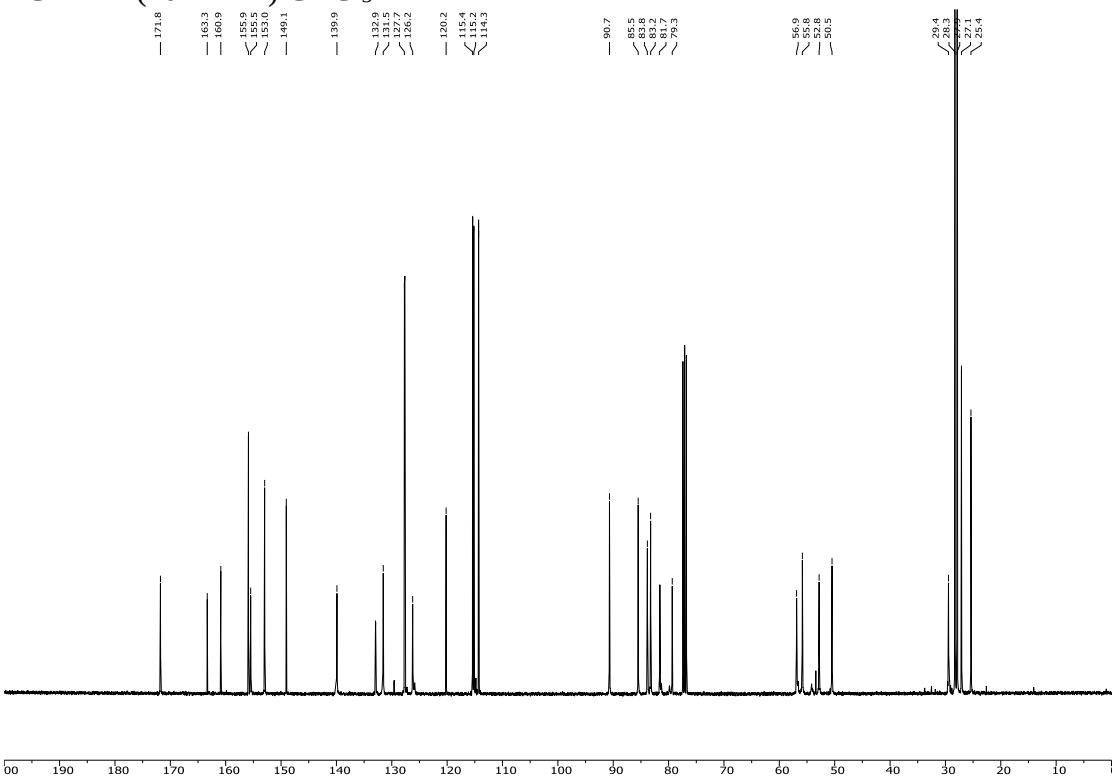

Compound **16j** ^{1}H NMR (400 MHz) $CDCl_3$

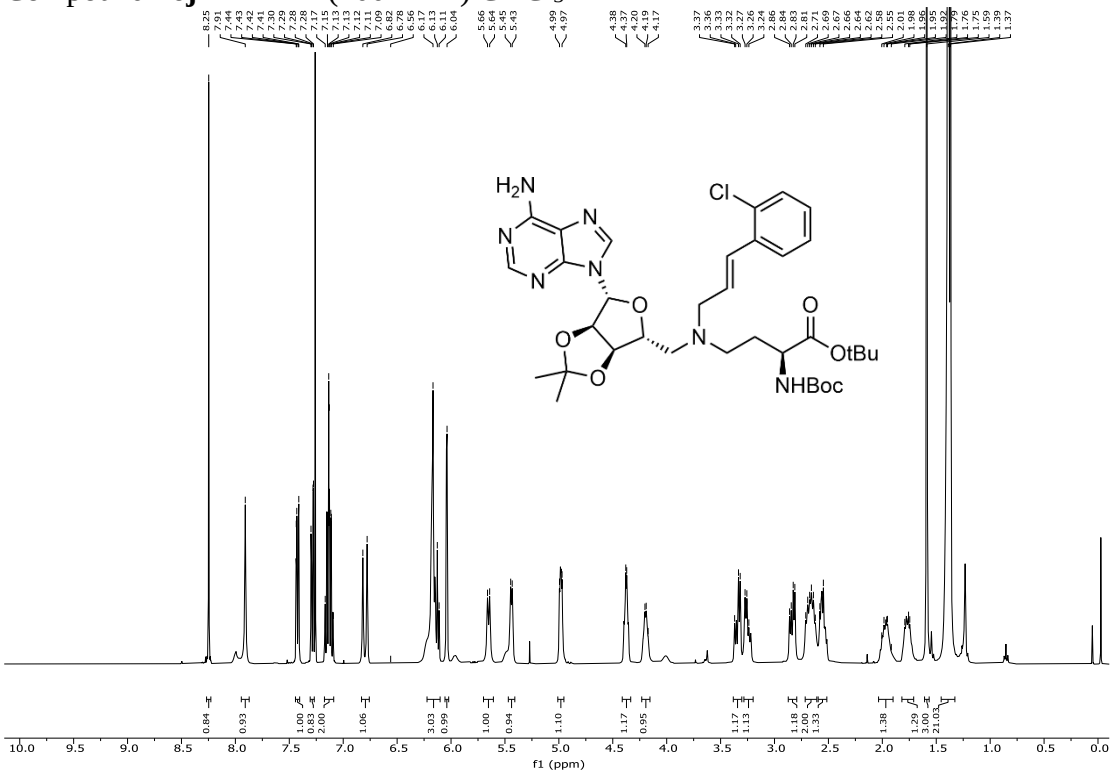

^{13}C NMR (101 MHz) $CDCl_3$

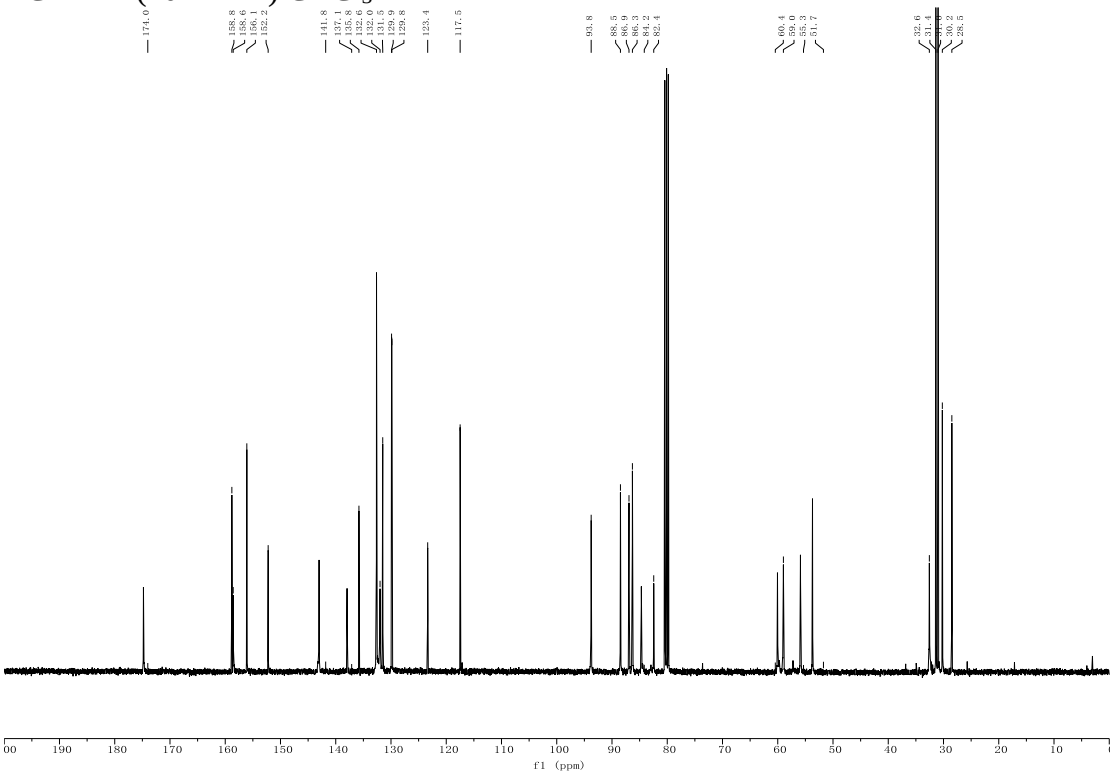

Compound **16k** ^{1}H NMR (400 MHz) $CDCl_3$

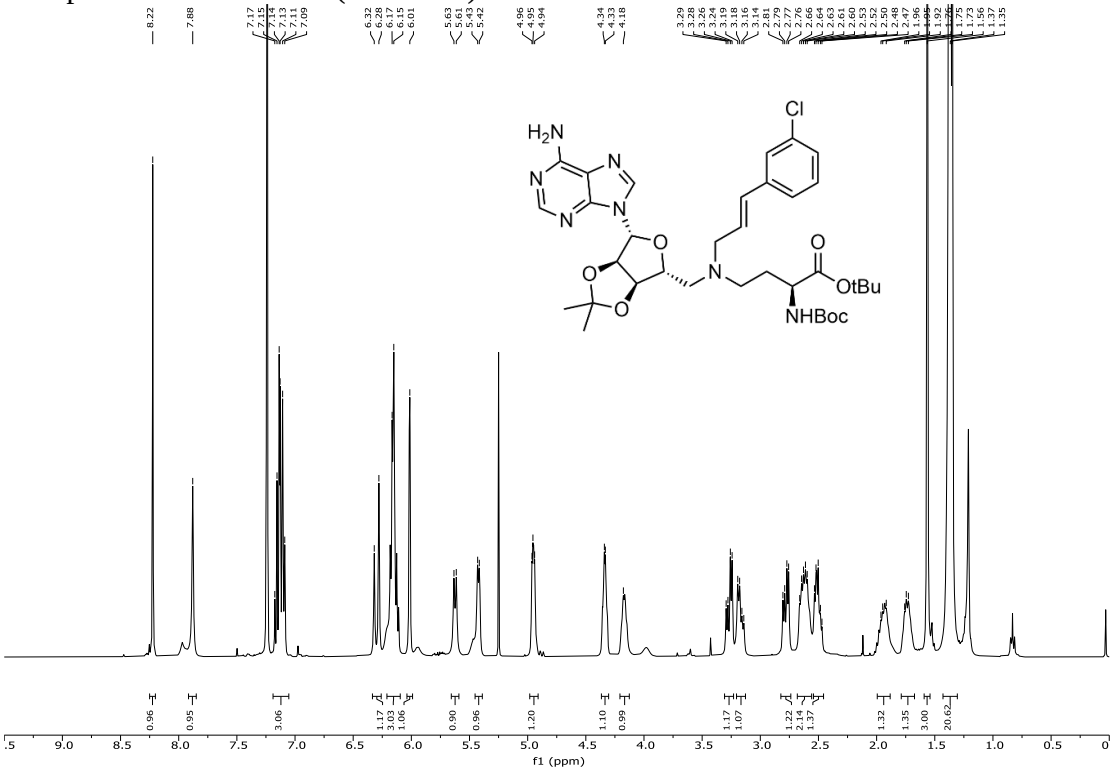

^{13}C NMR (101 MHz) $CDCl_3$

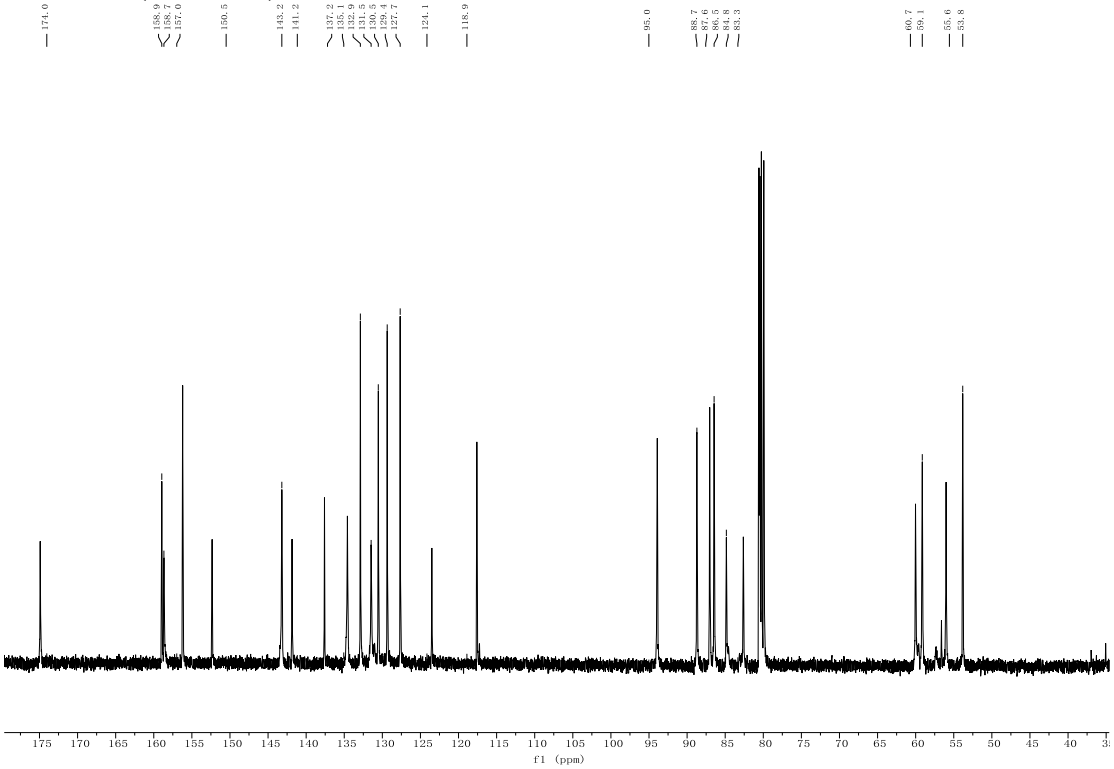

Compound **16l** ^{1}H NMR (400 MHz) $CDCl_3$

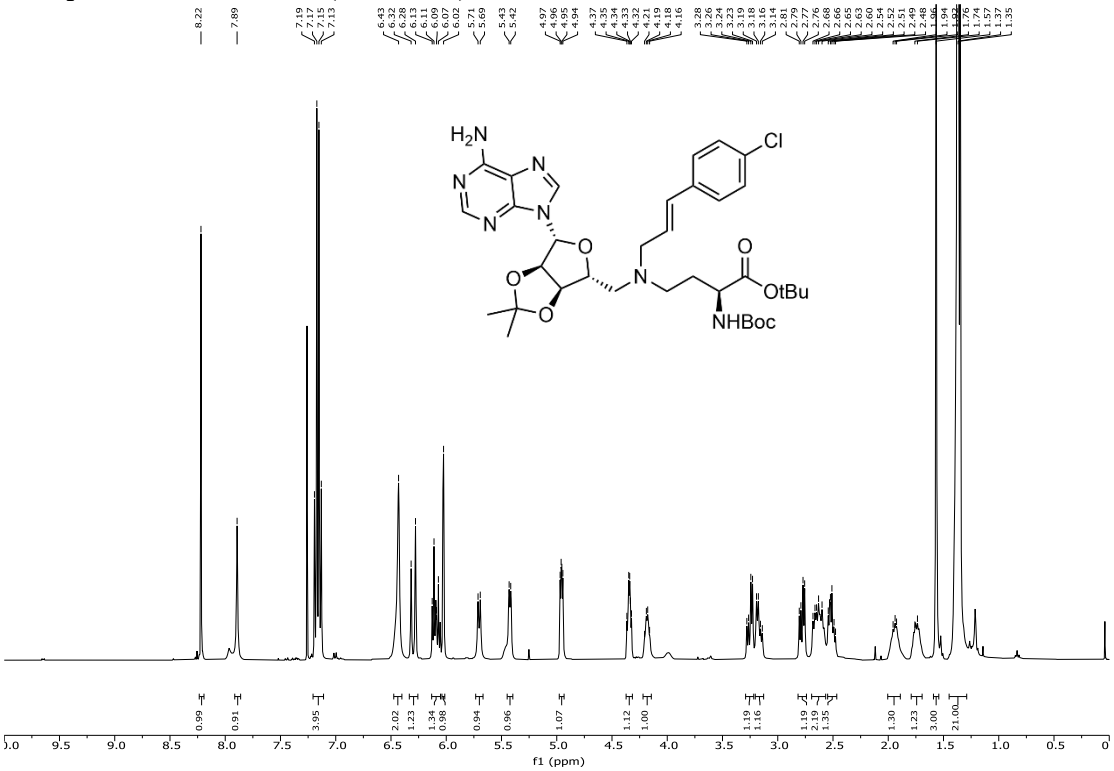

^{13}C NMR (101MHz) $CDCl_3$

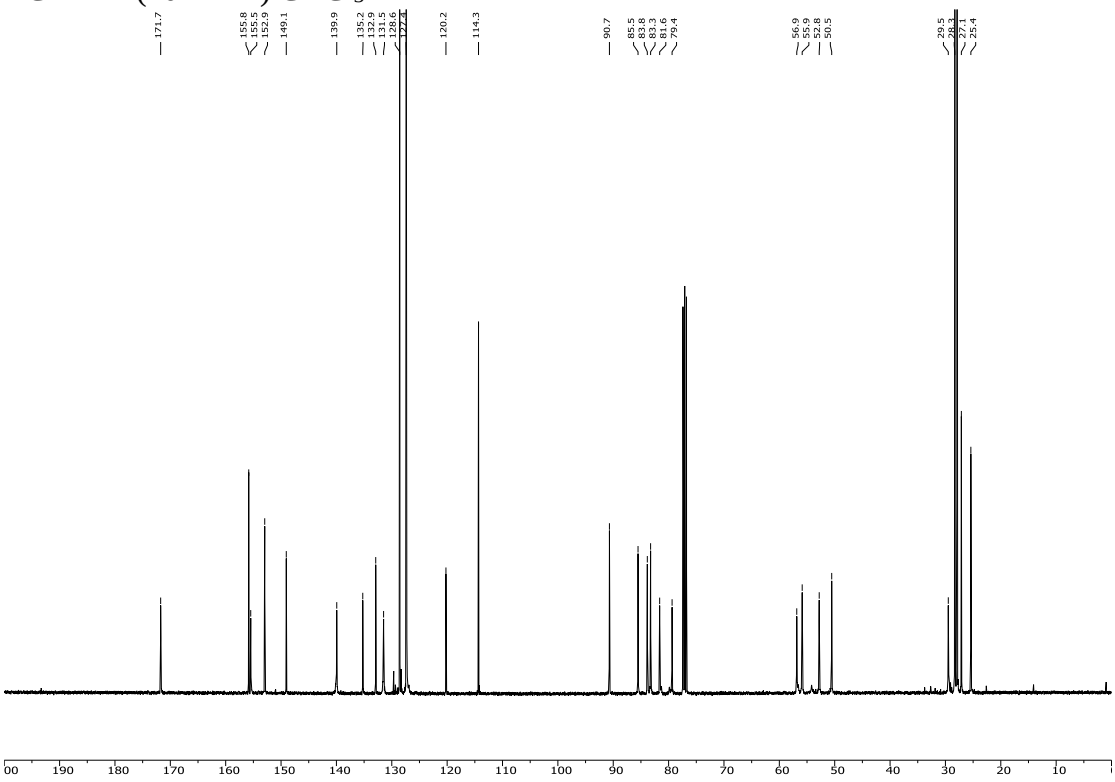

Compound **16m** ^{1}H NMR (400 MHz) $CDCl_3$

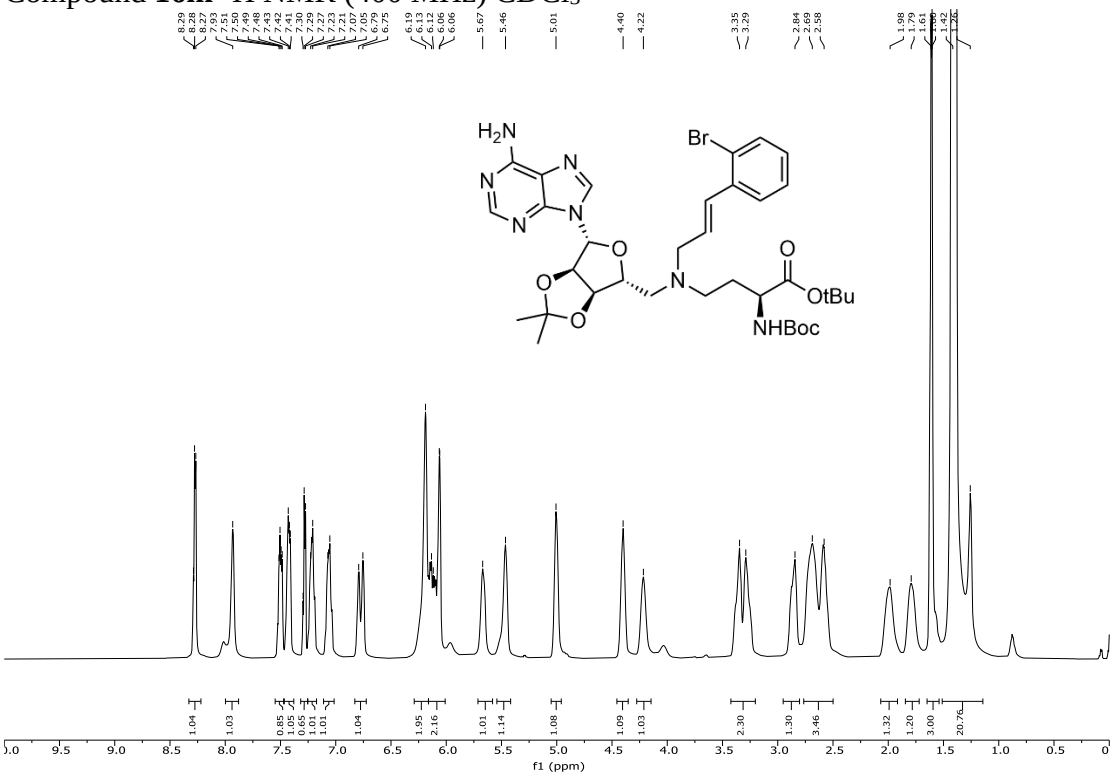

^{13}C NMR (101 MHz) $CDCl_3$

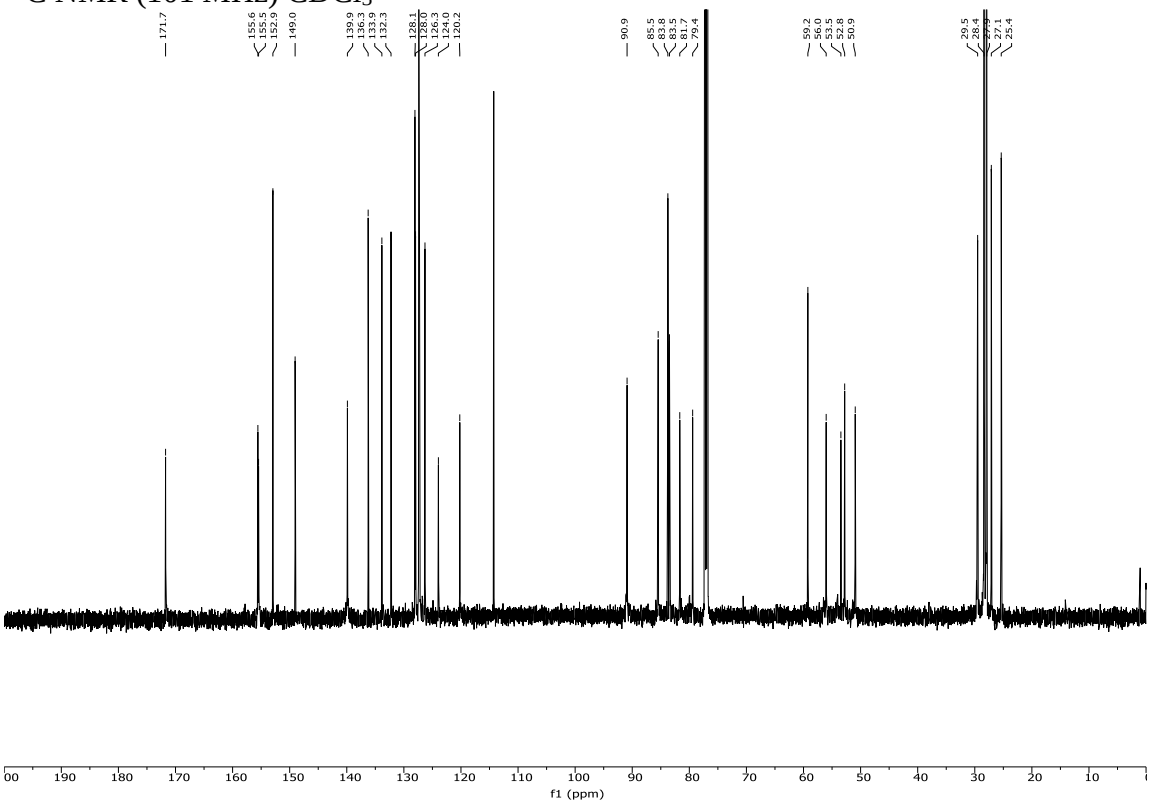

Compound **16n** ^{1}H NMR (600 MHz) $CDCl_3$

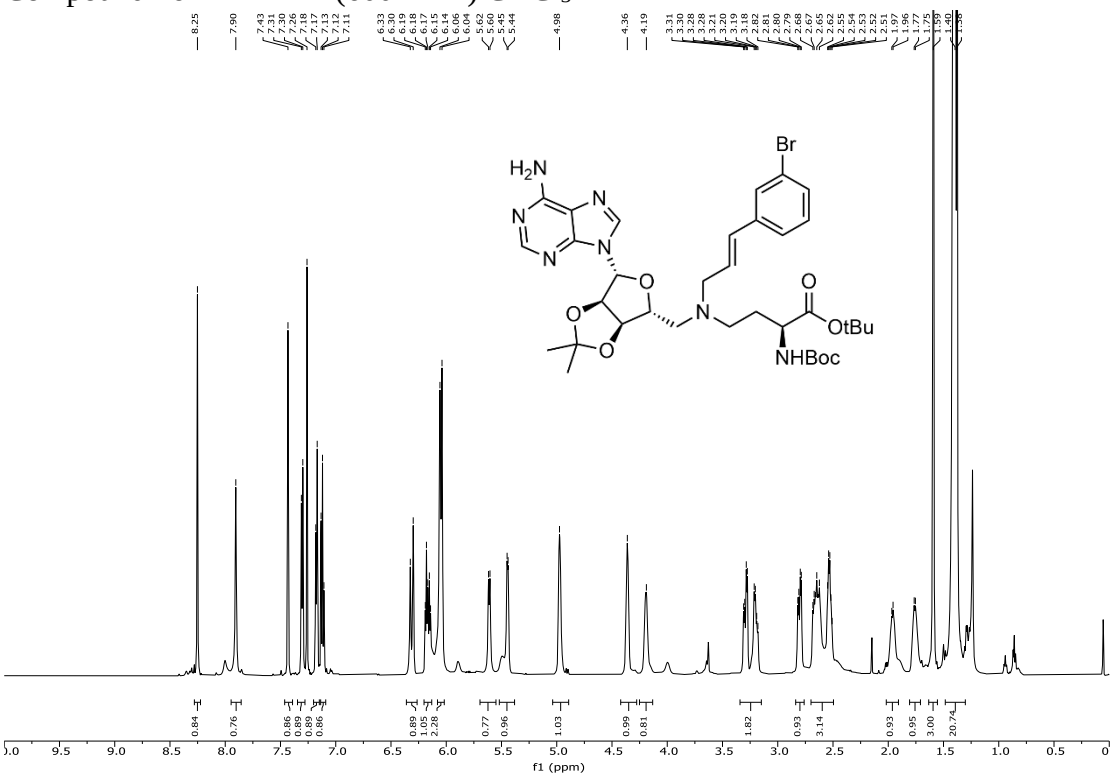

^{13}C NMR (151 MHz) $CDCl_3$

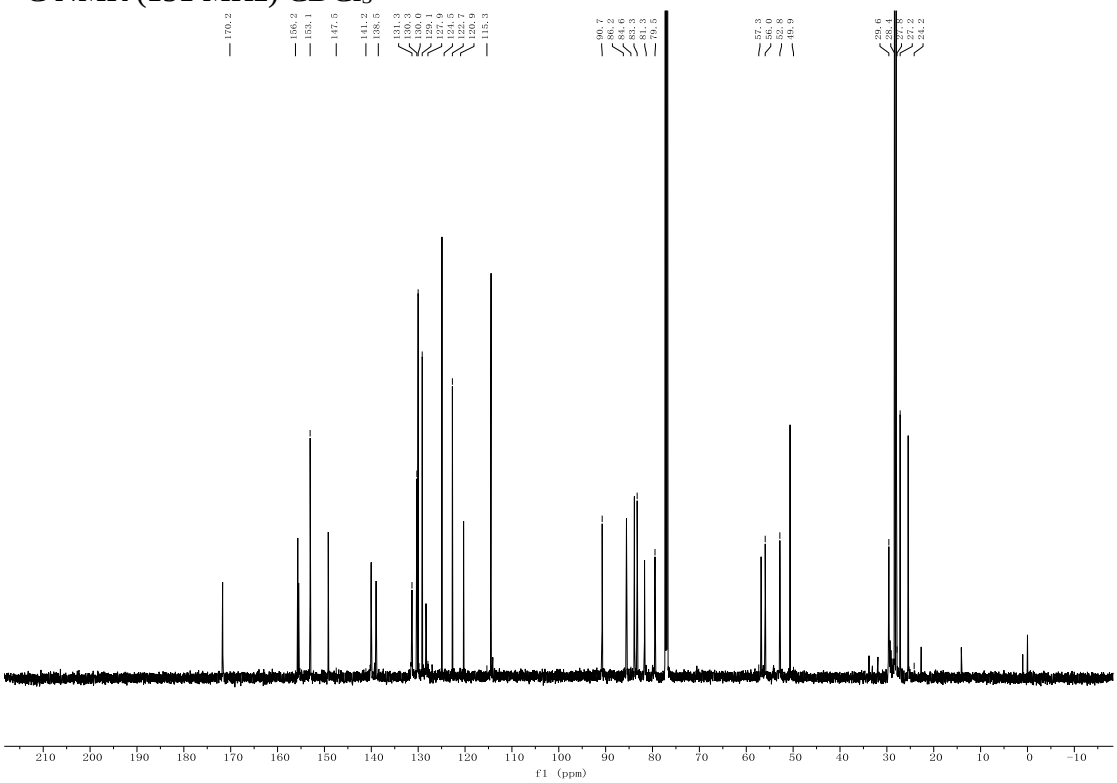

Compound **16o** ^{1}H NMR (400 MHz) $CDCl_3$

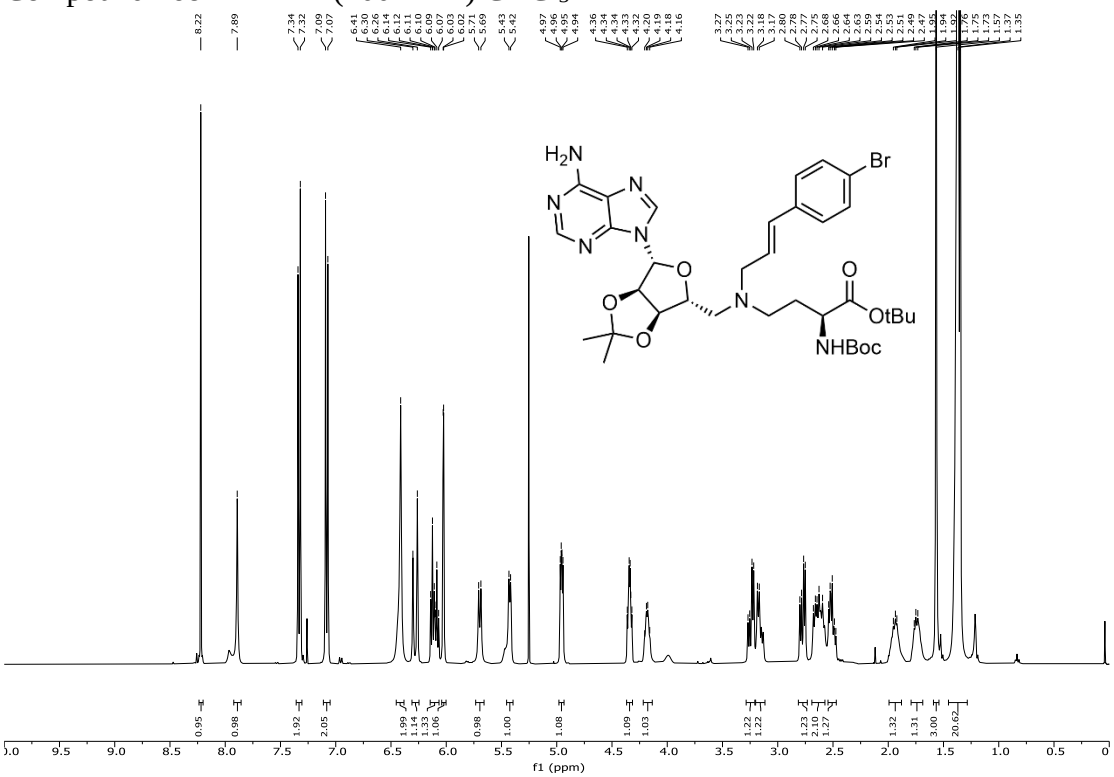

^{13}C NMR (101 MHz) $CDCl_3$

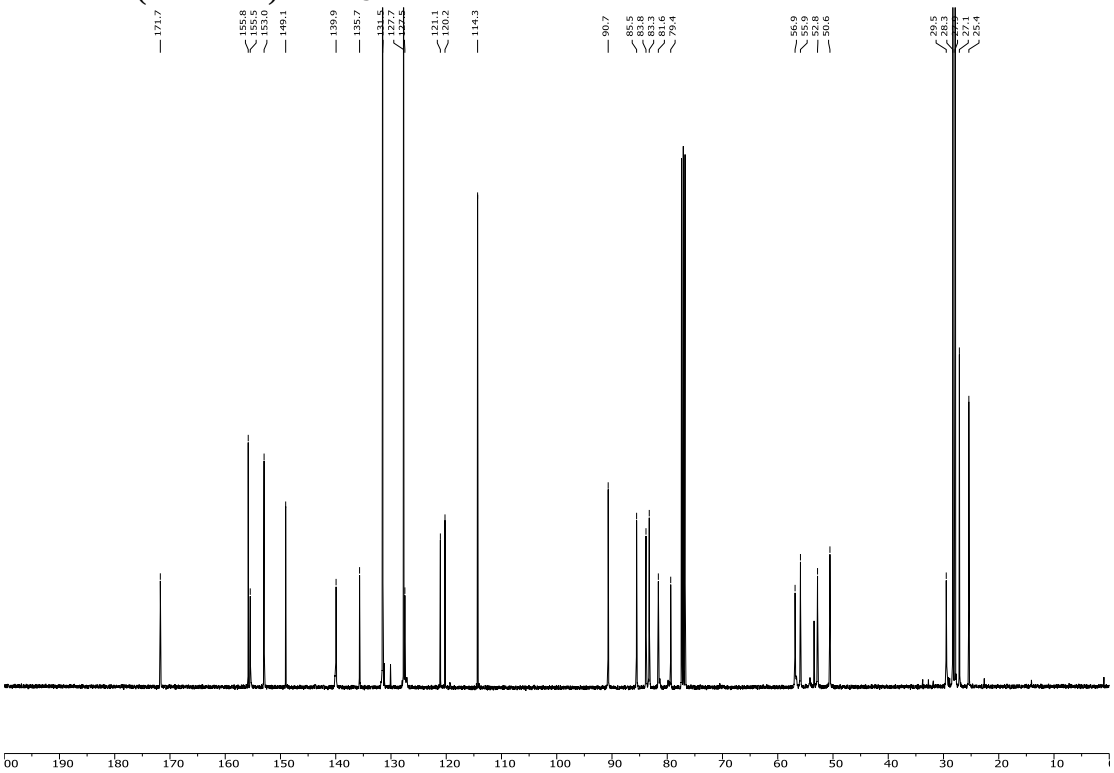

Compound **16p** ^{1}H NMR (400 MHz) $CDCl_3$

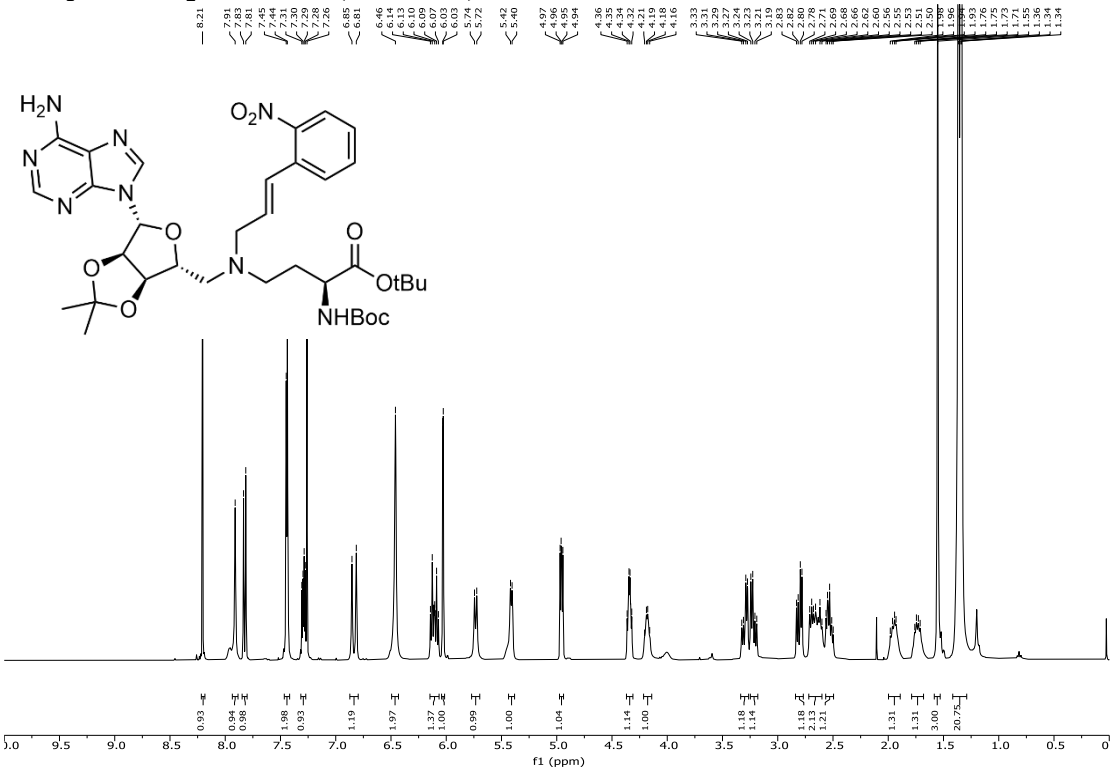

^{13}C NMR (101 MHz) $CDCl_3$

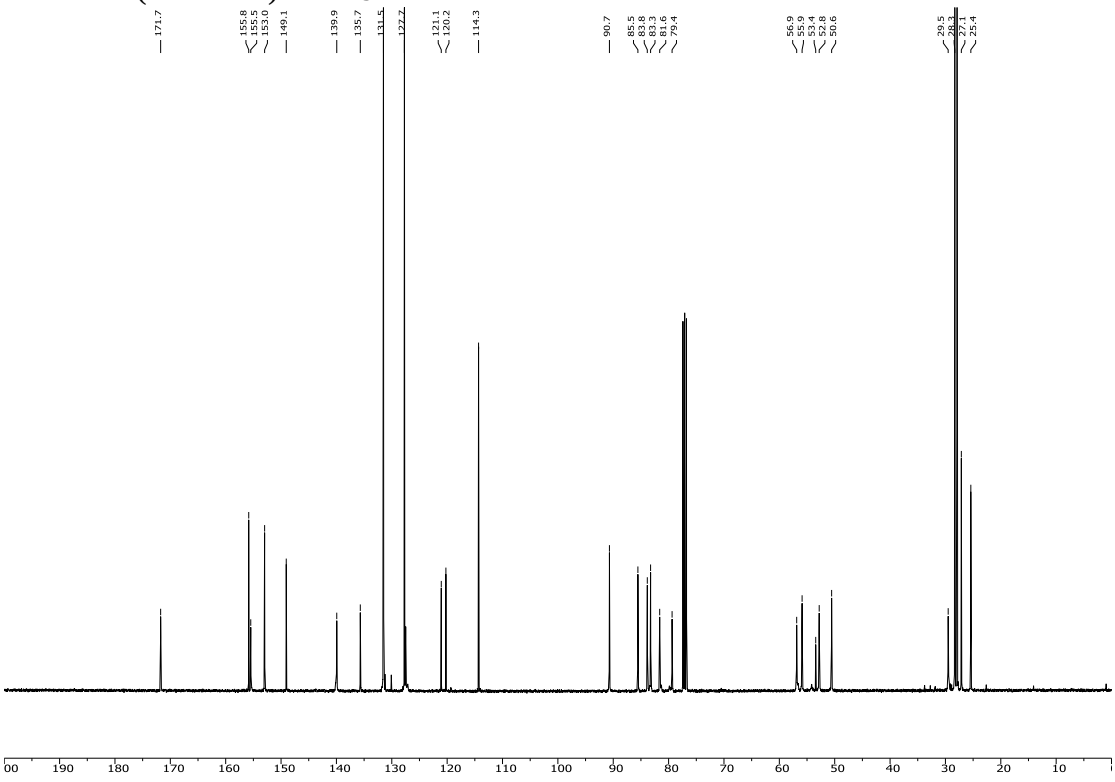

Compound **16q** ^{1}H NMR (400 MHz) $CDCl_3$

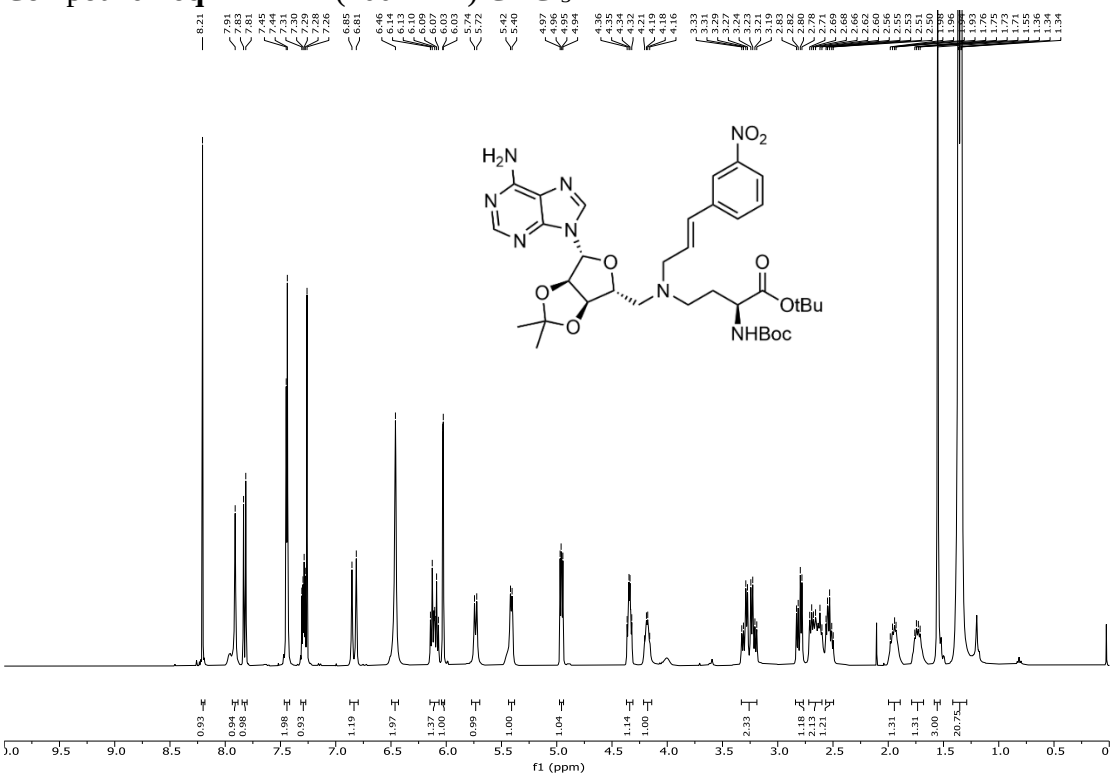

^{13}C NMR (101 MHz) $CDCl_3$

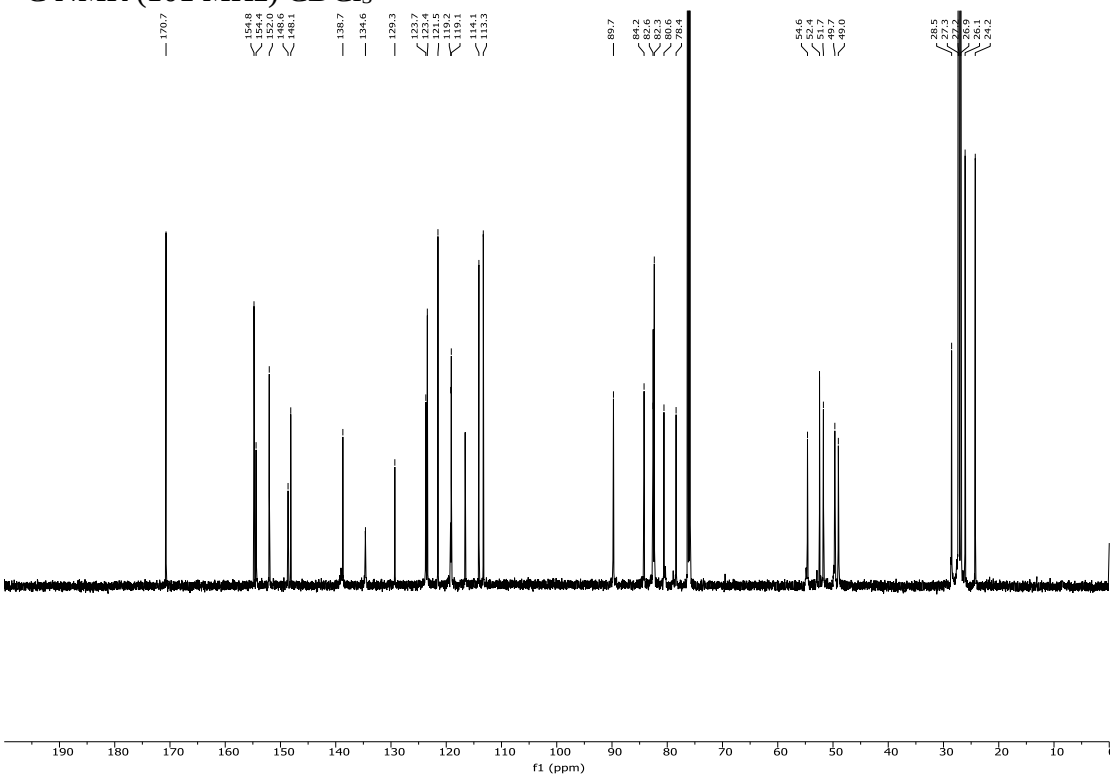

Compound **16r** ^{1}H NMR (600 MHz) $CDCl_3$

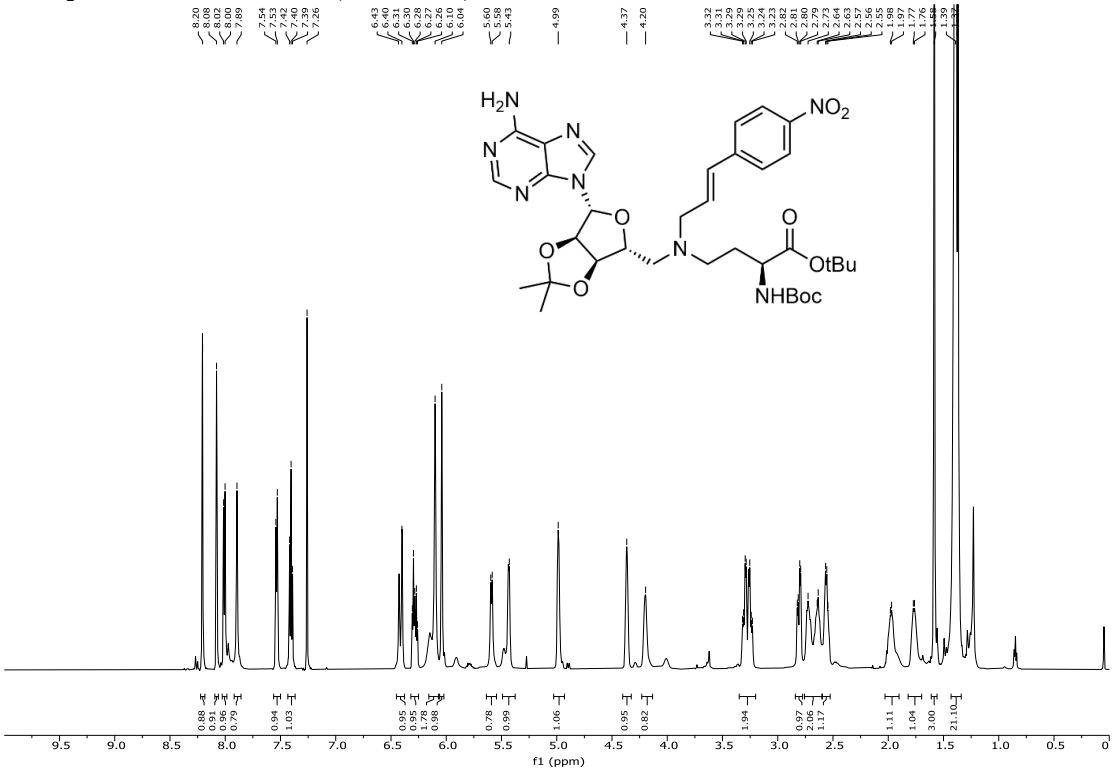

^{13}C NMR (151 MHz) $CDCl_3$

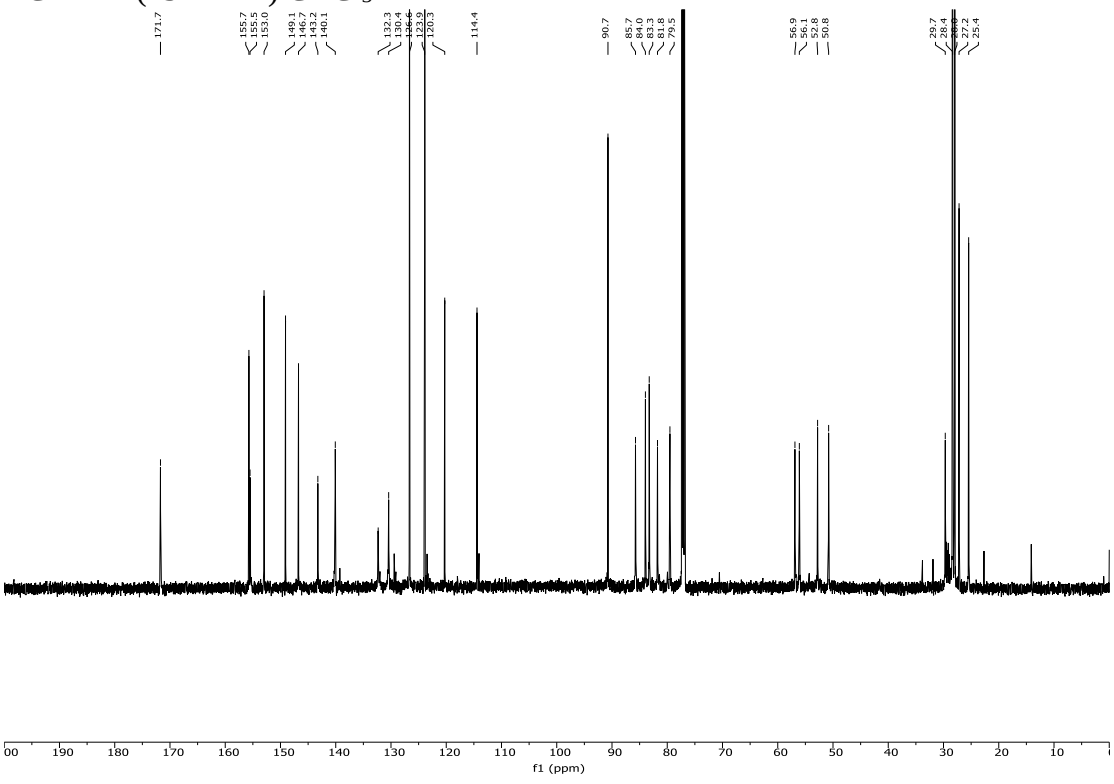

Compound **16s** ^{1}H NMR (600 MHz) $CDCl_3$

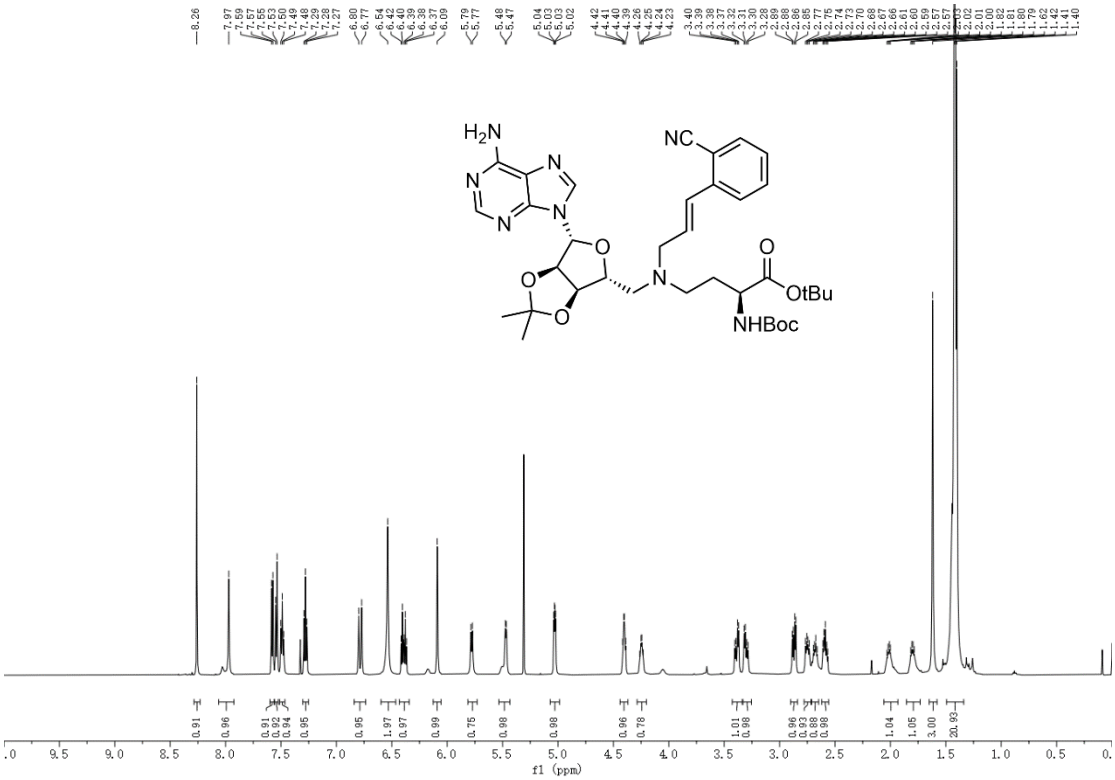

^{13}C NMR (151 MHz) $CDCl_3$

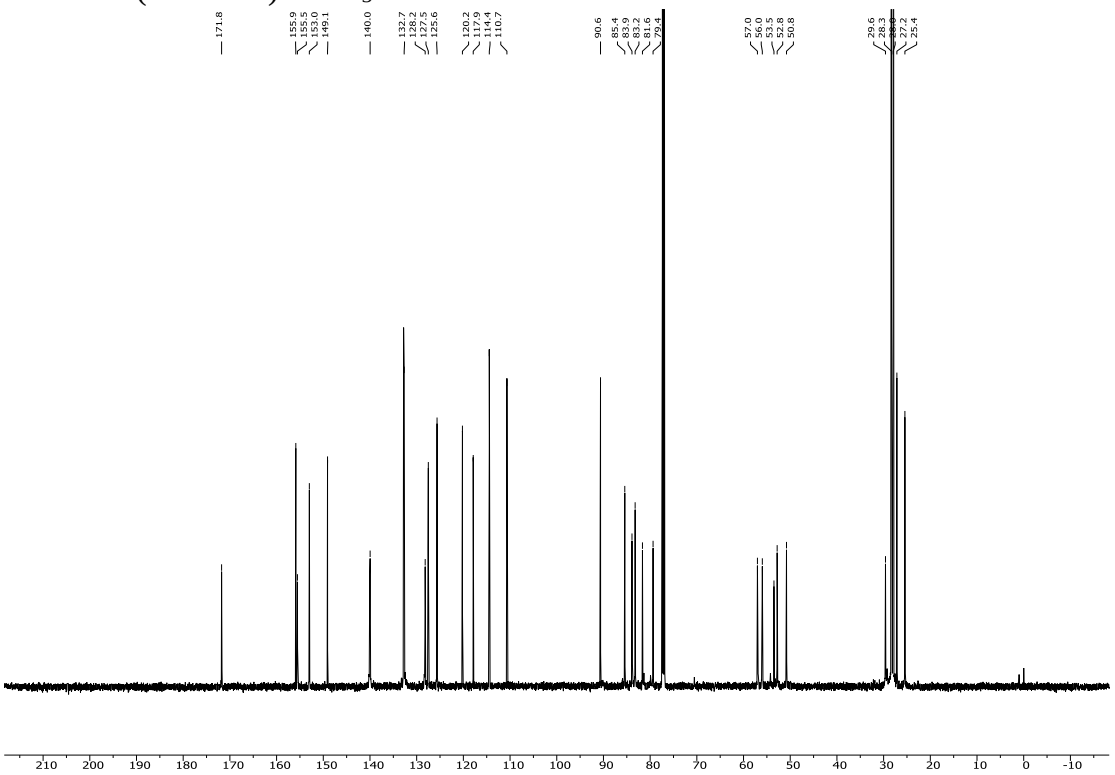

Compound **16t** ^{1}H NMR (400 MHz) $CDCl_3$

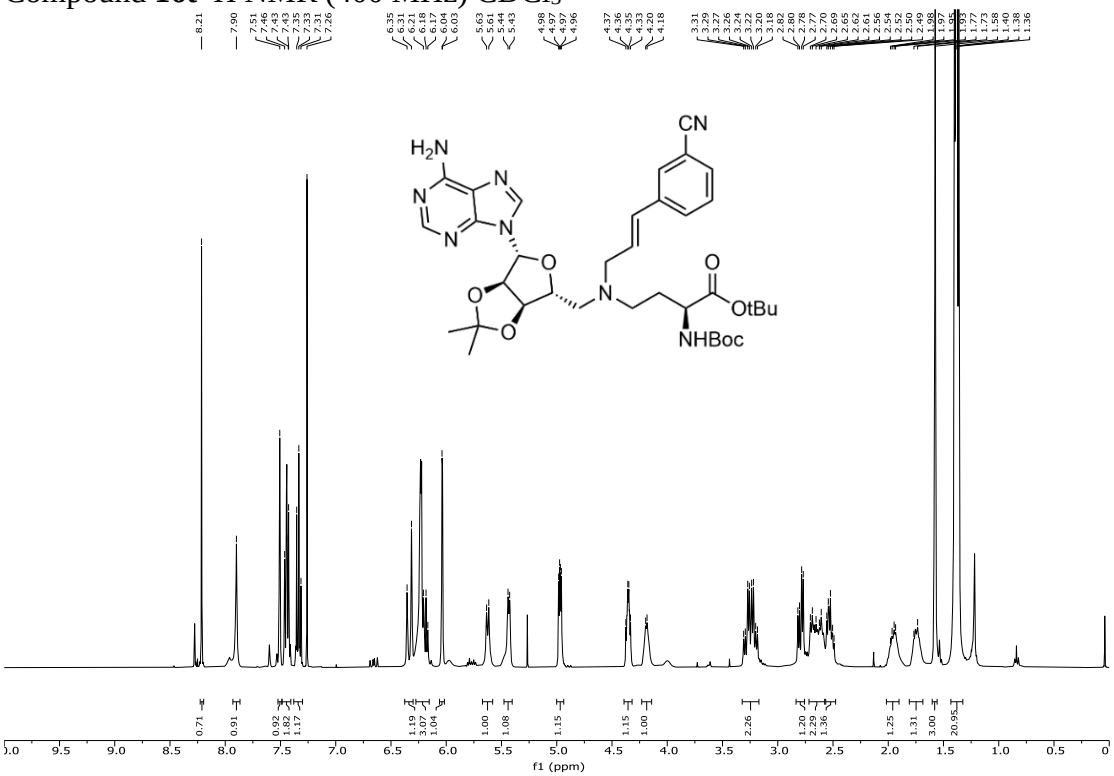

^{13}C NMR (101 MHz) $CDCl_3$

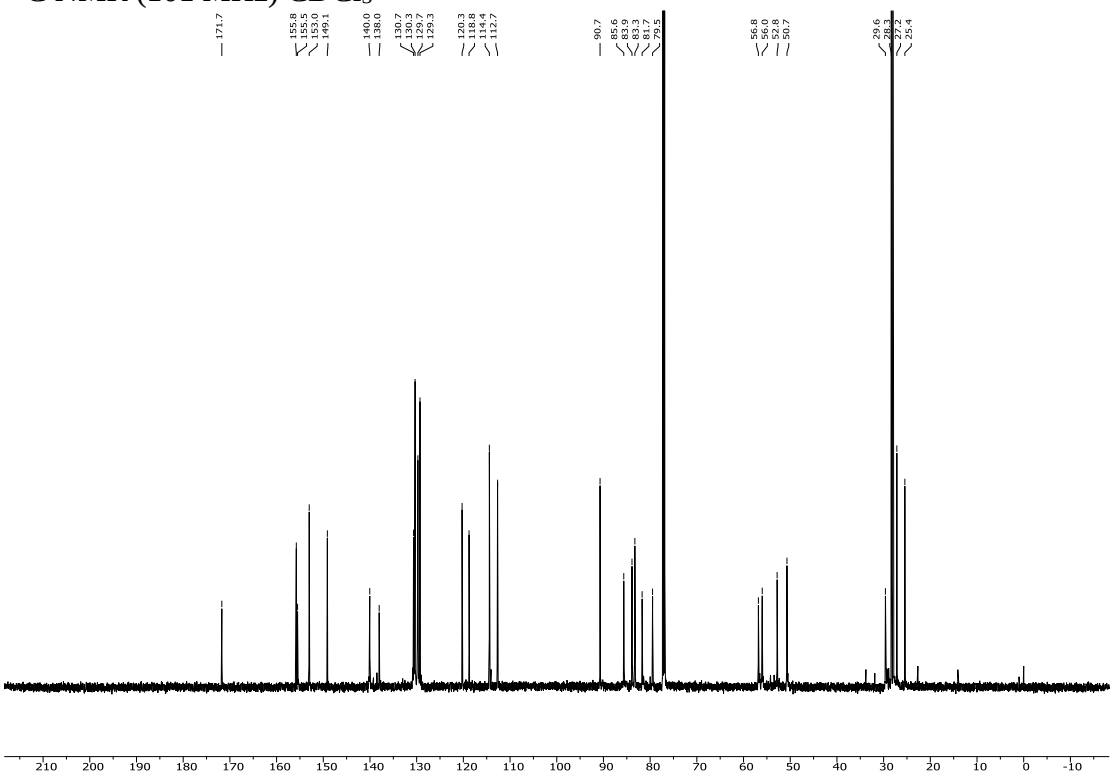

Compound **16u** ^{1}H NMR (400 MHz) $CDCl_3$

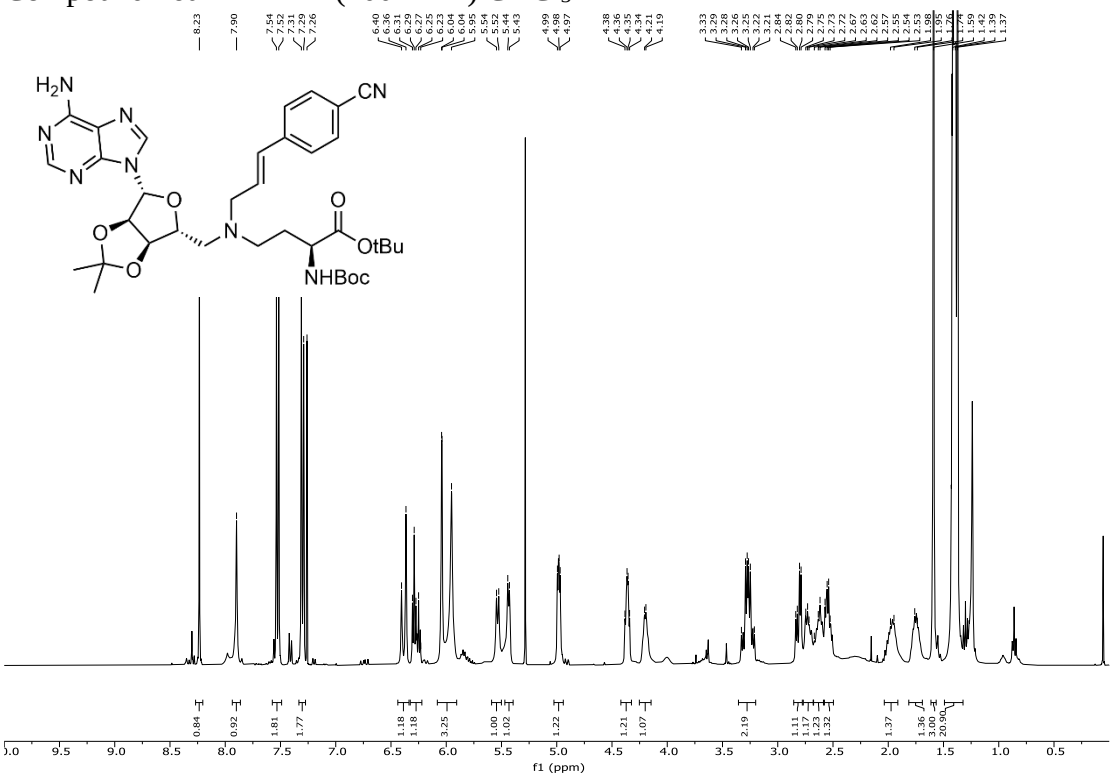

^{13}C NMR (101 MHz) $CDCl_3$

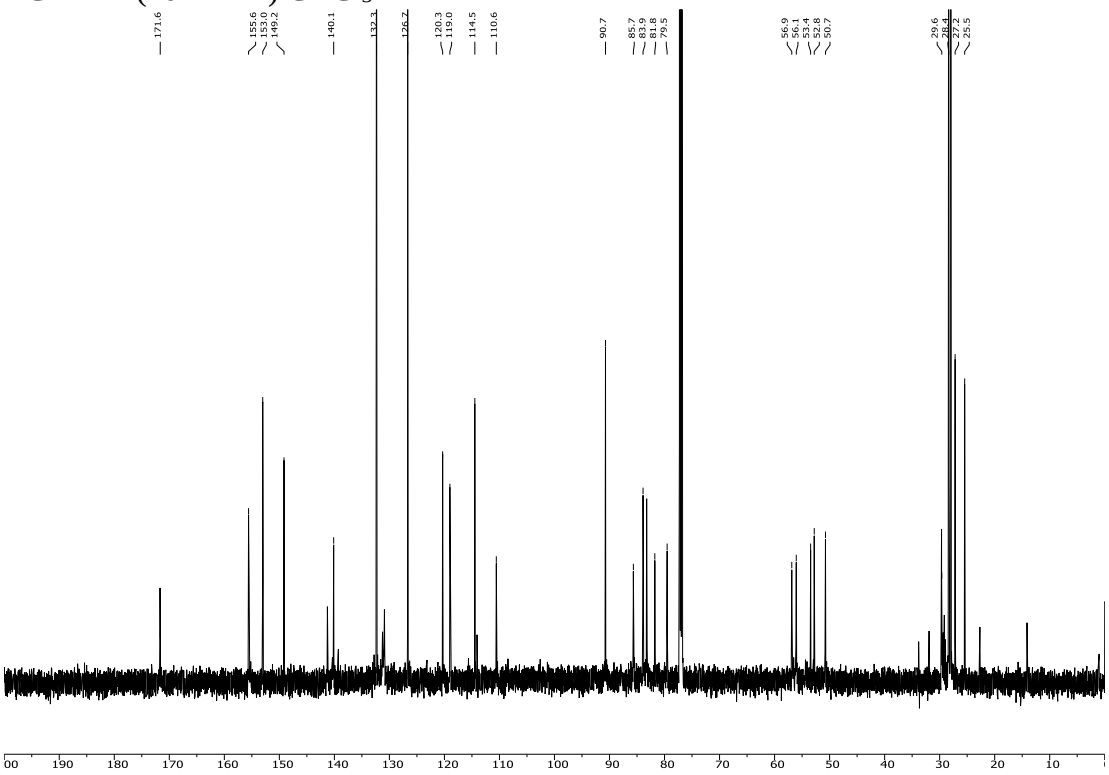

Compound **16v** ^{1}H NMR (400 MHz) $CDCl_3$

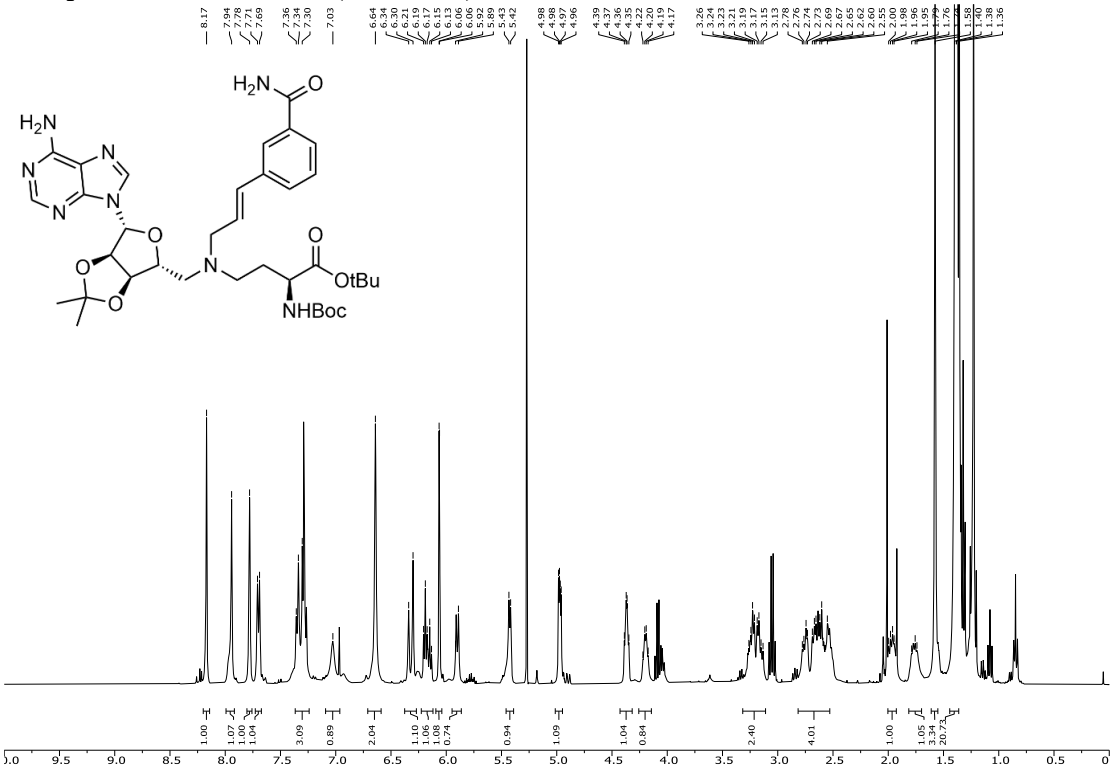

^{13}C NMR (101 MHz) $CDCl_3$

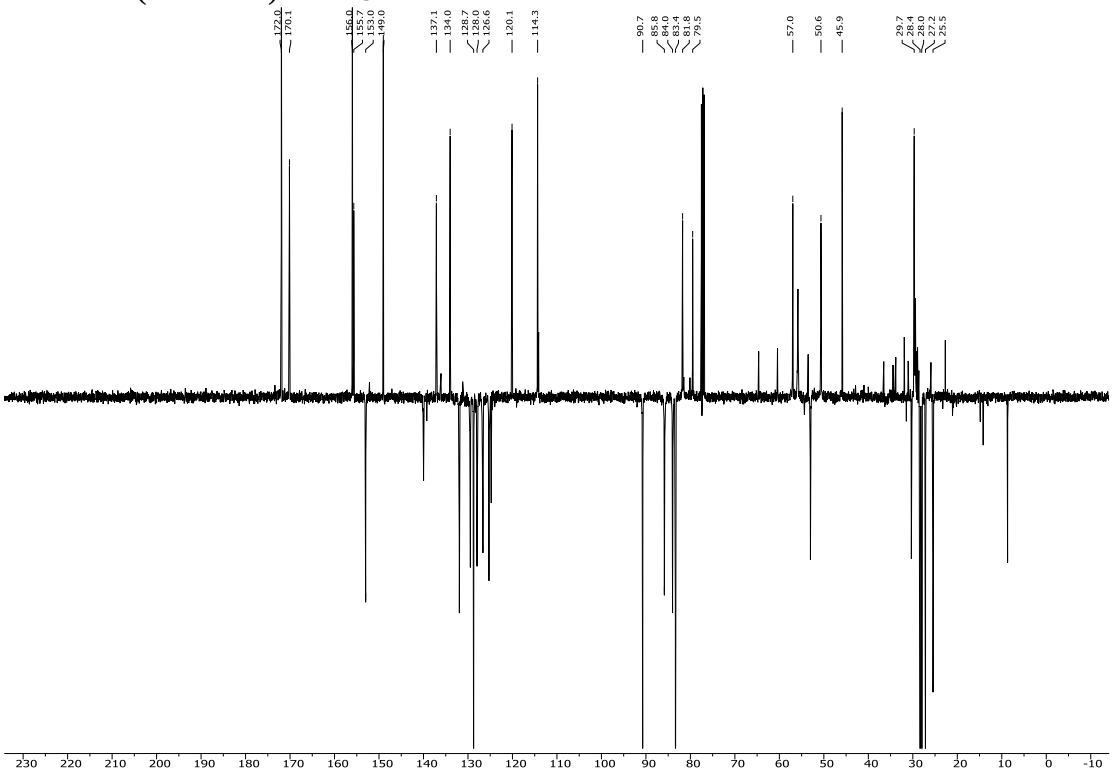

Compound **16w** ^{1}H NMR (400 MHz) $CDCl_3$

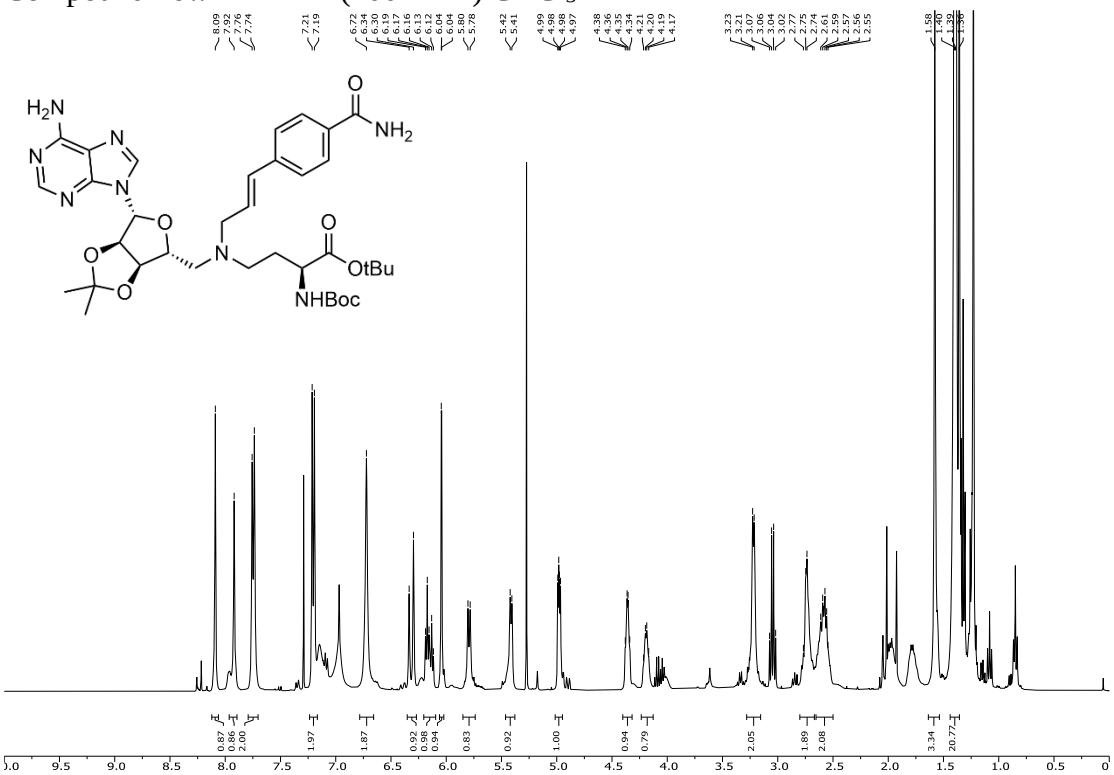

^{13}C NMR (101 MHz) $CDCl_3$

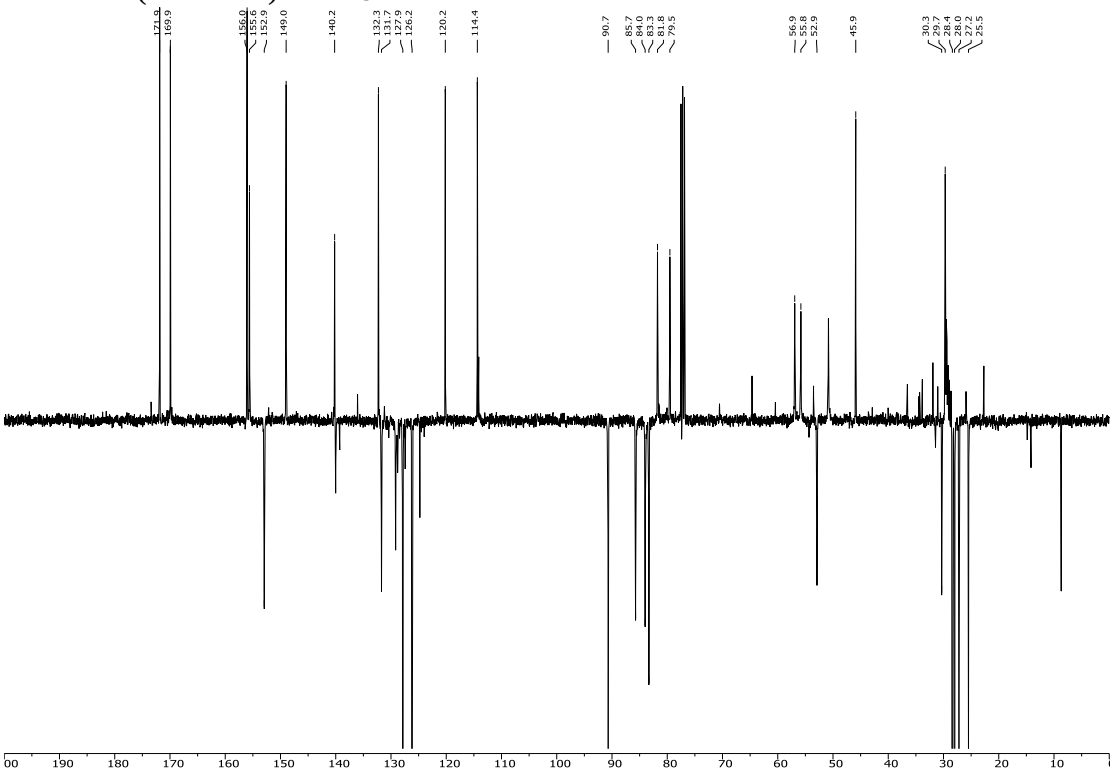

Compound **16x** ^{1}H NMR (400 MHz) $CDCl_3$

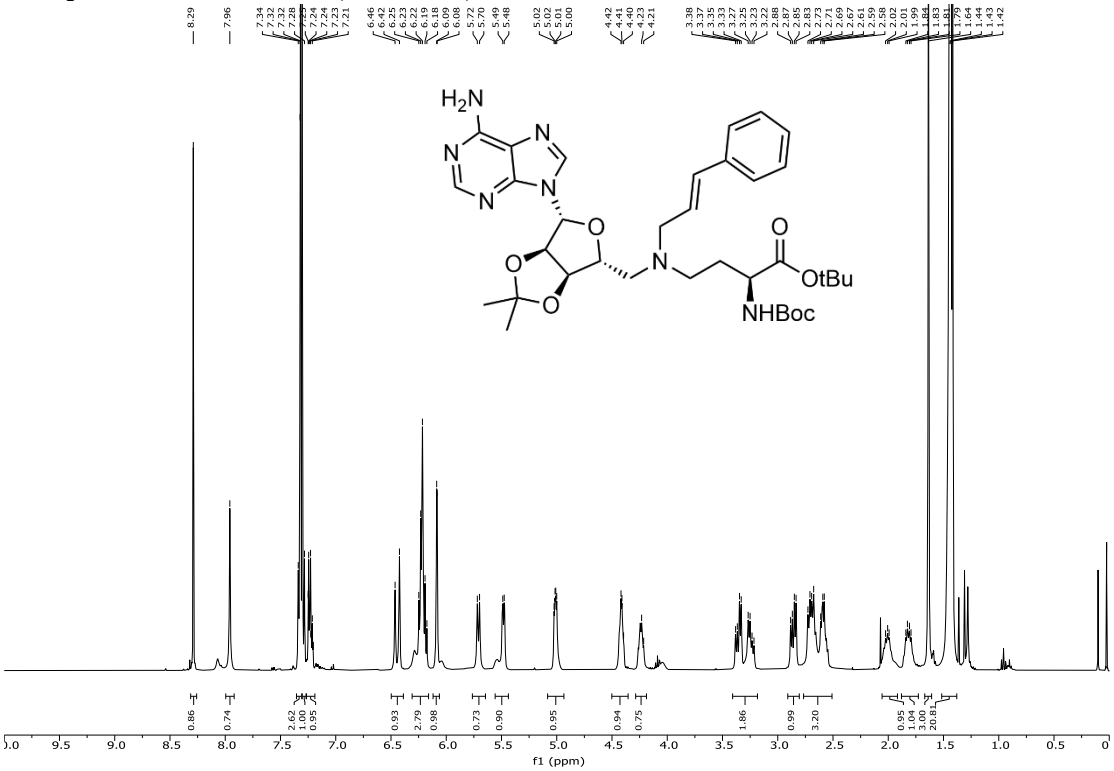

^{13}C NMR (101 MHz) $CDCl_3$

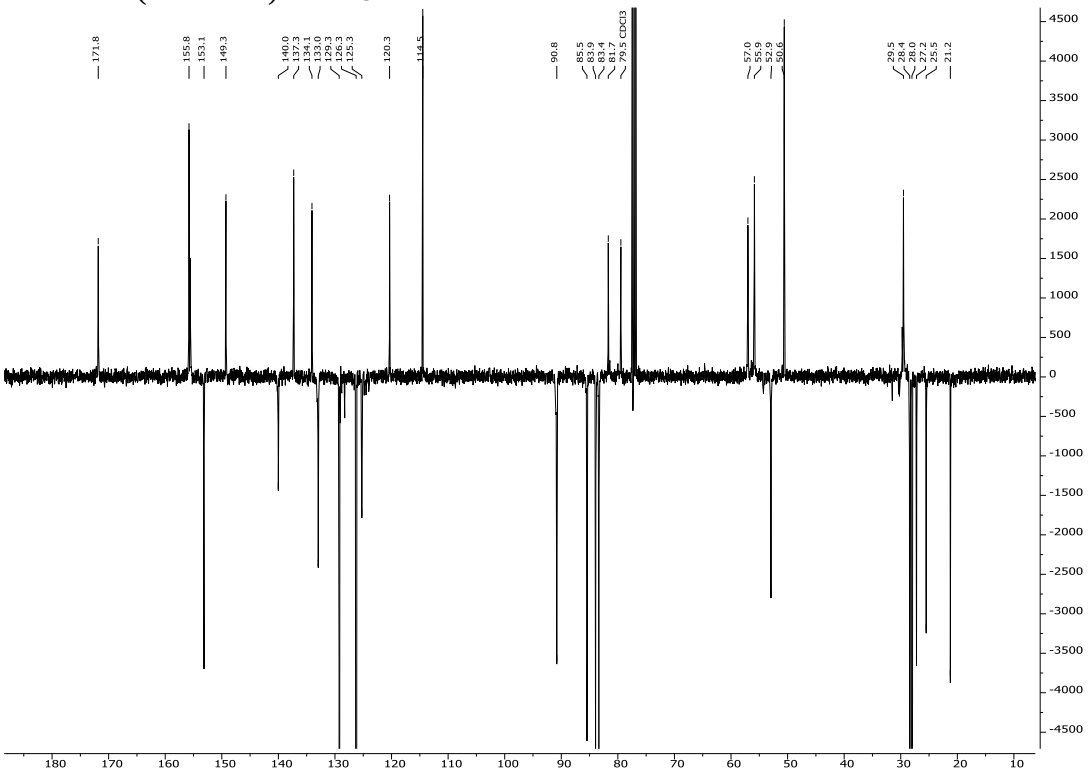

Compound **16y** ^{1}H NMR (400 MHz) $CDCl_3$

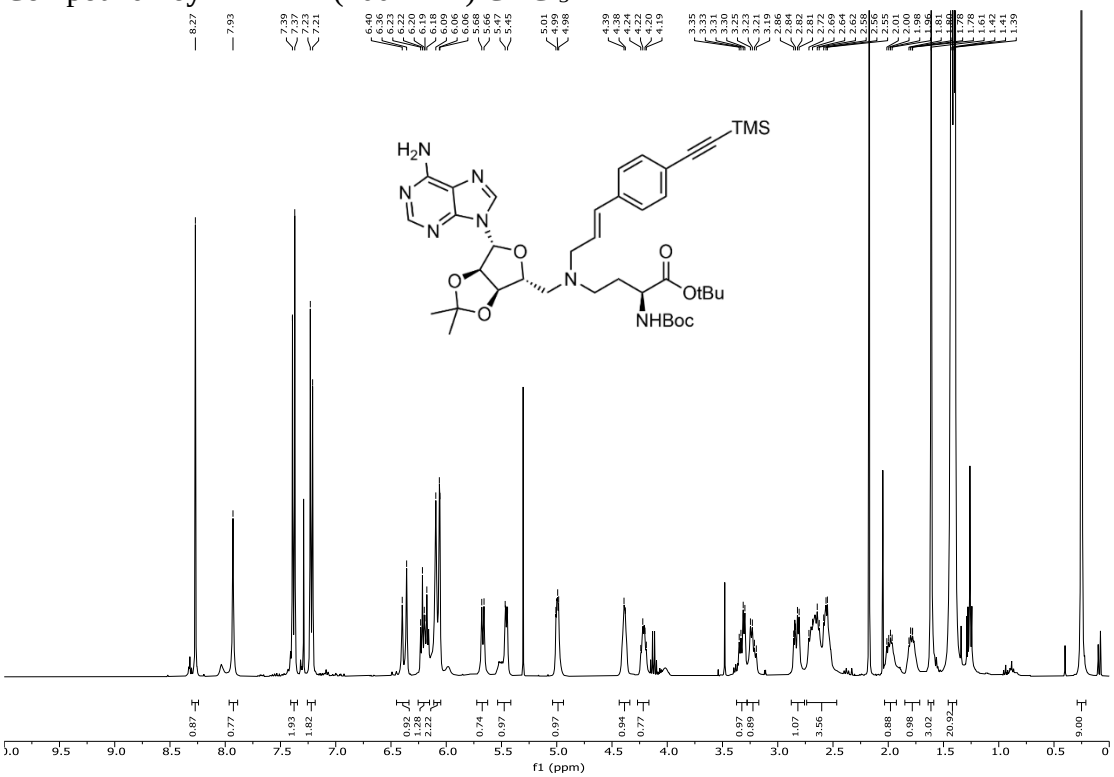

^{13}C NMR (101 MHz) $CDCl_3$

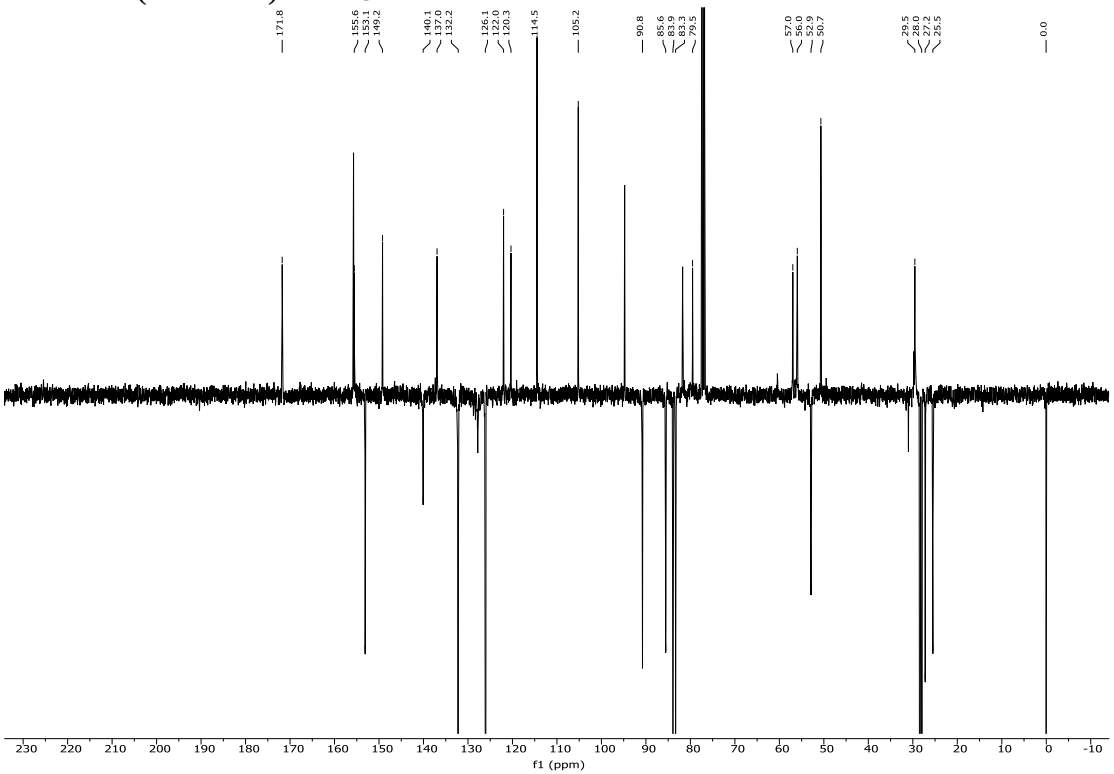

Compound **17a** ^{1}H NMR (400 MHz) CD_3OD

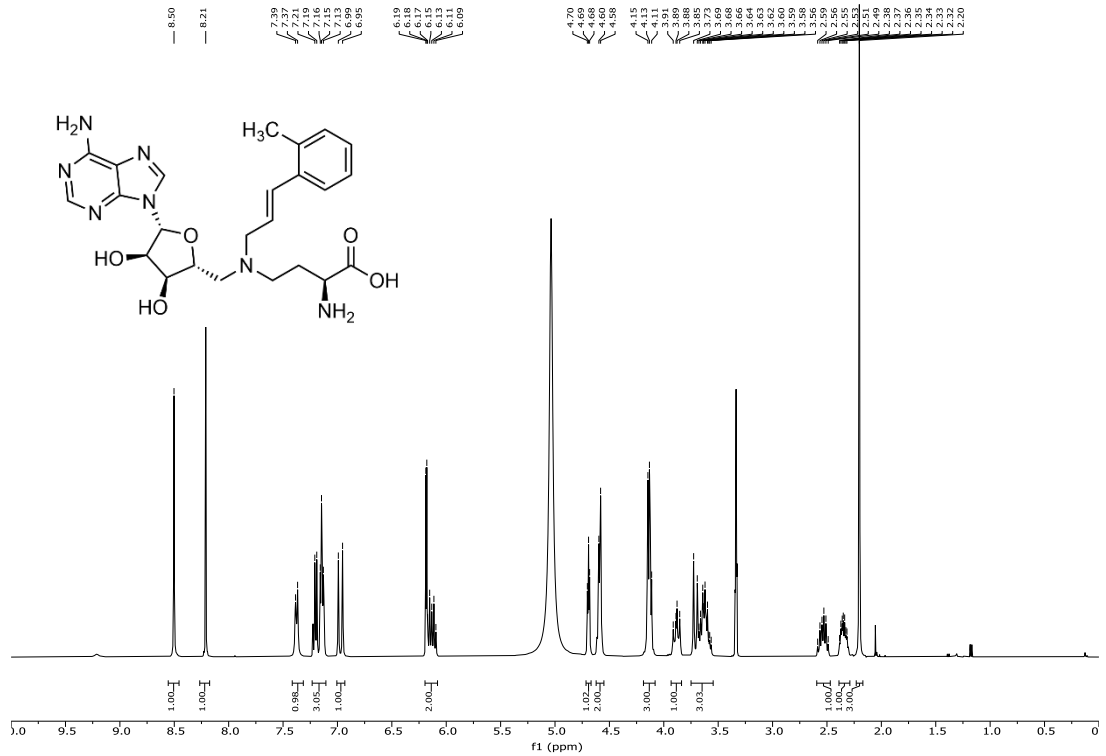

^{13}C NMR (101 MHz) CD_3OD

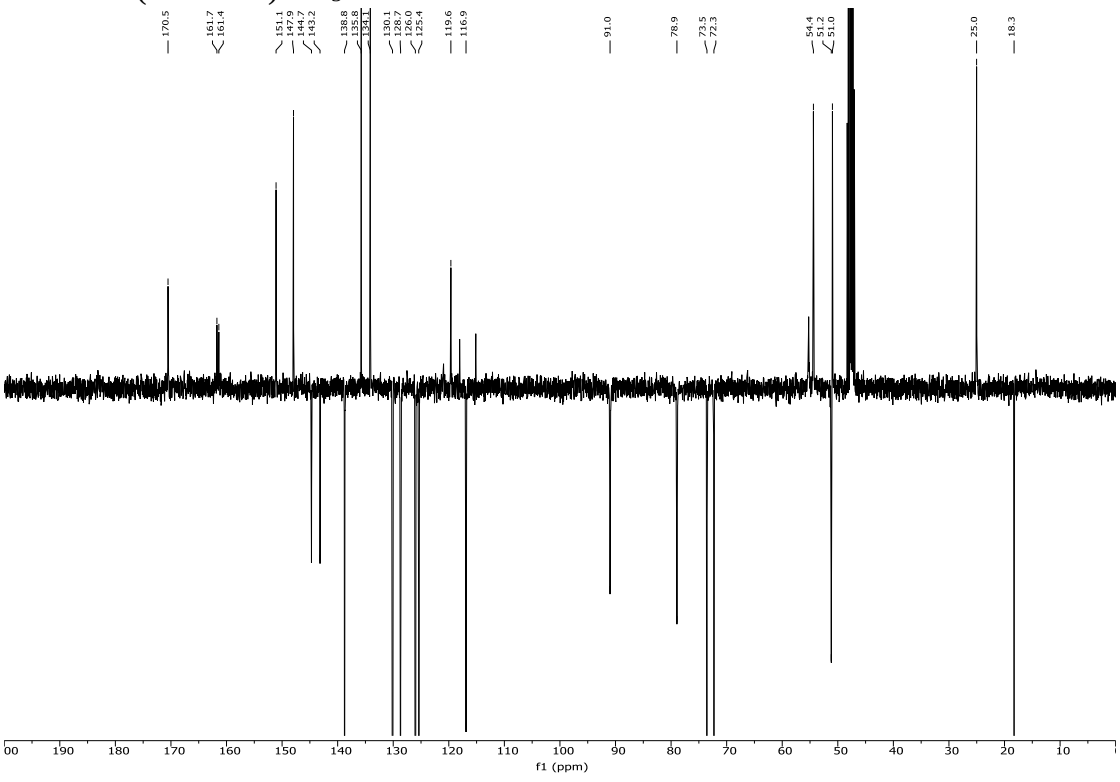

Compound **17b** ^{1}H NMR (400 MHz) CD_3OD

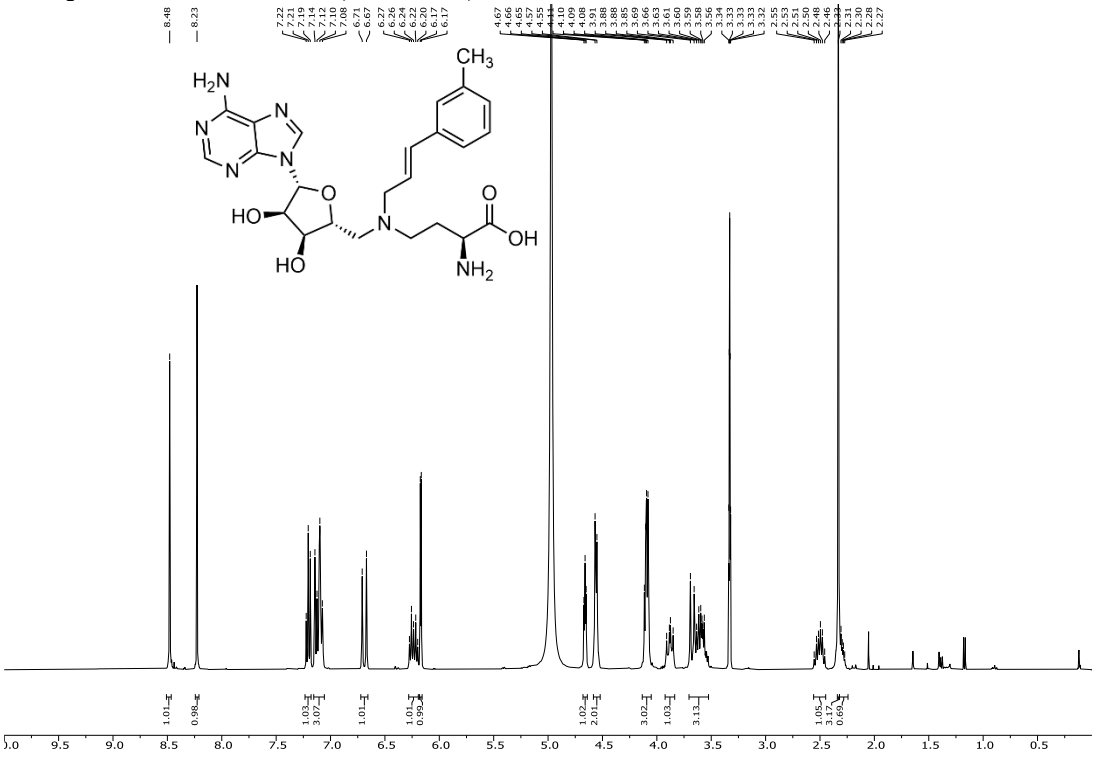

^{13}C NMR (101 MHz) CD_3OD

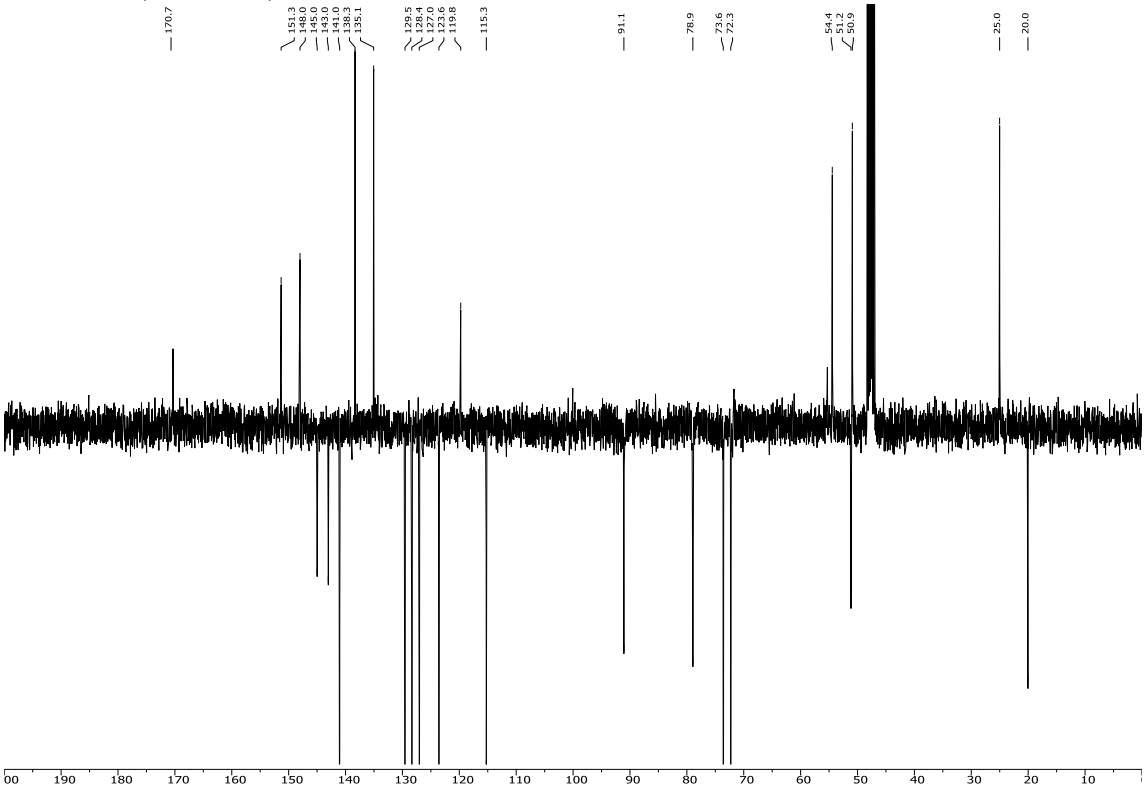

Compound **17c** ^{1}H NMR (400 MHz) D_2O

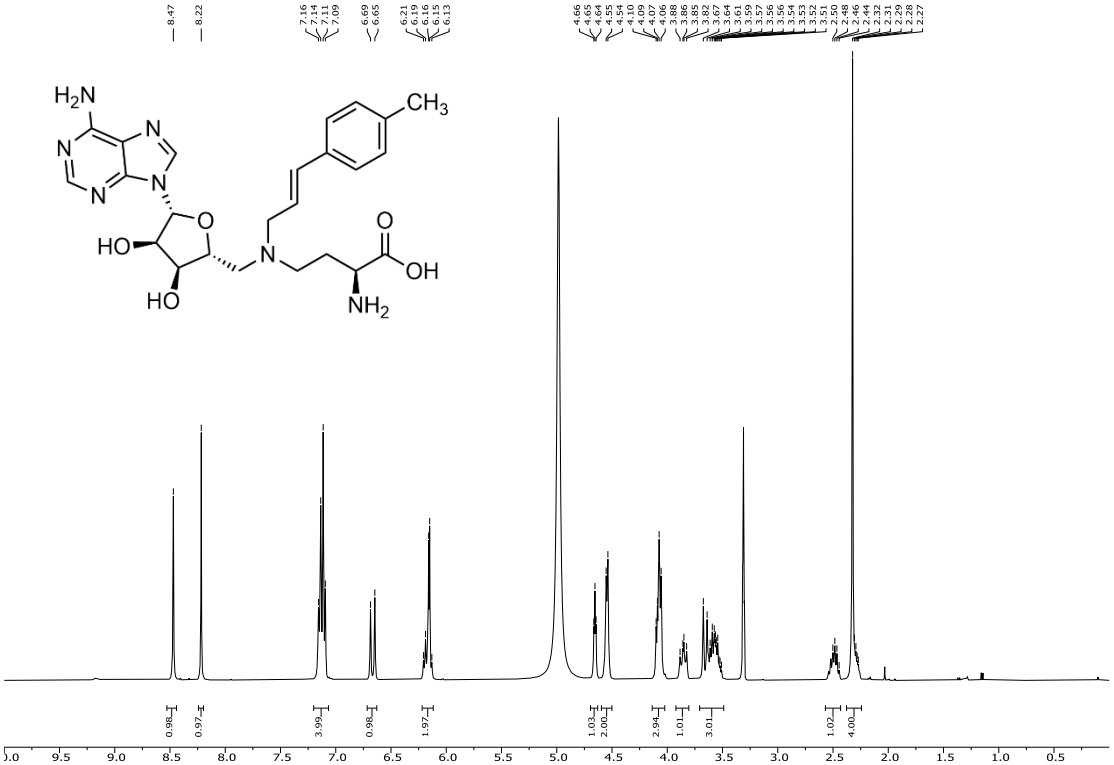

^{13}C NMR (400 MHz) D_2O

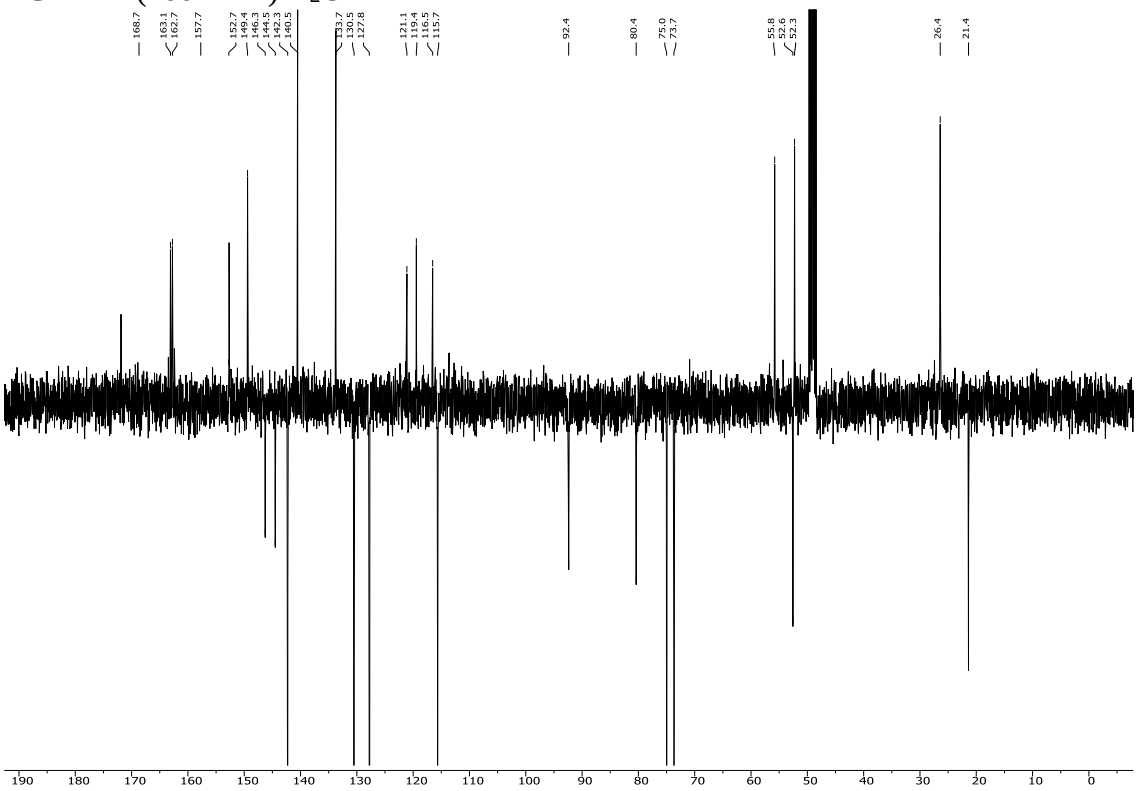

Compound **17d** ^{1}H NMR (400 MHz) CD_3OD

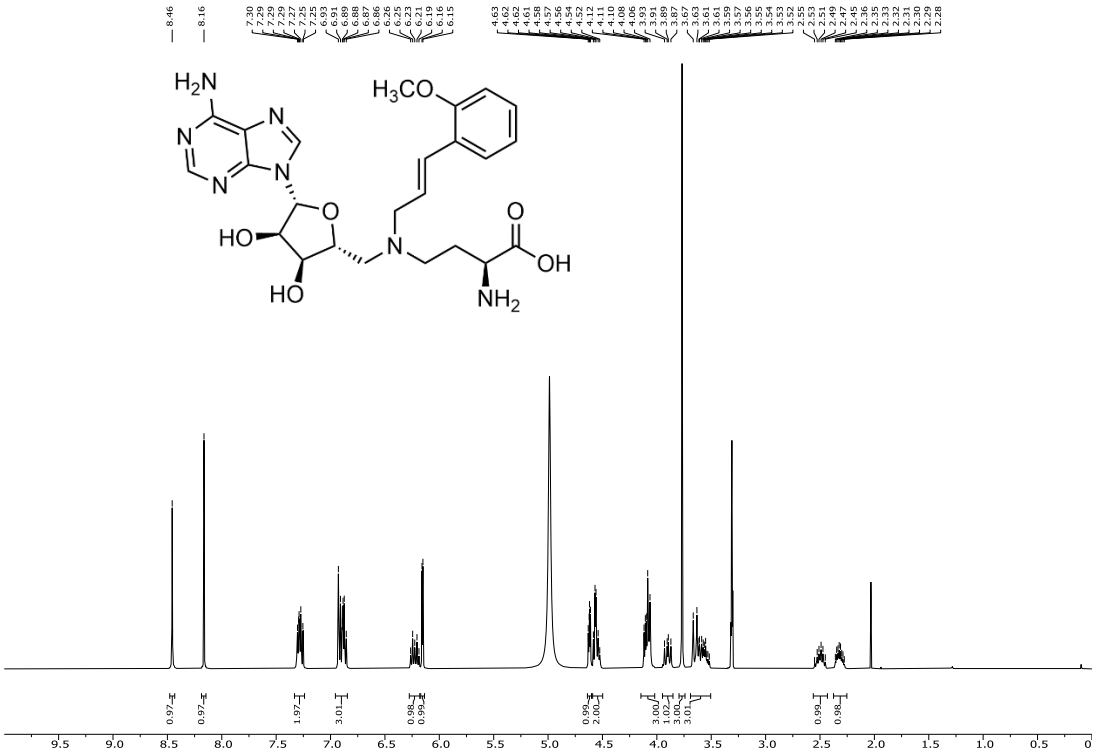

^{13}C NMR (400 MHz) CD_3OD

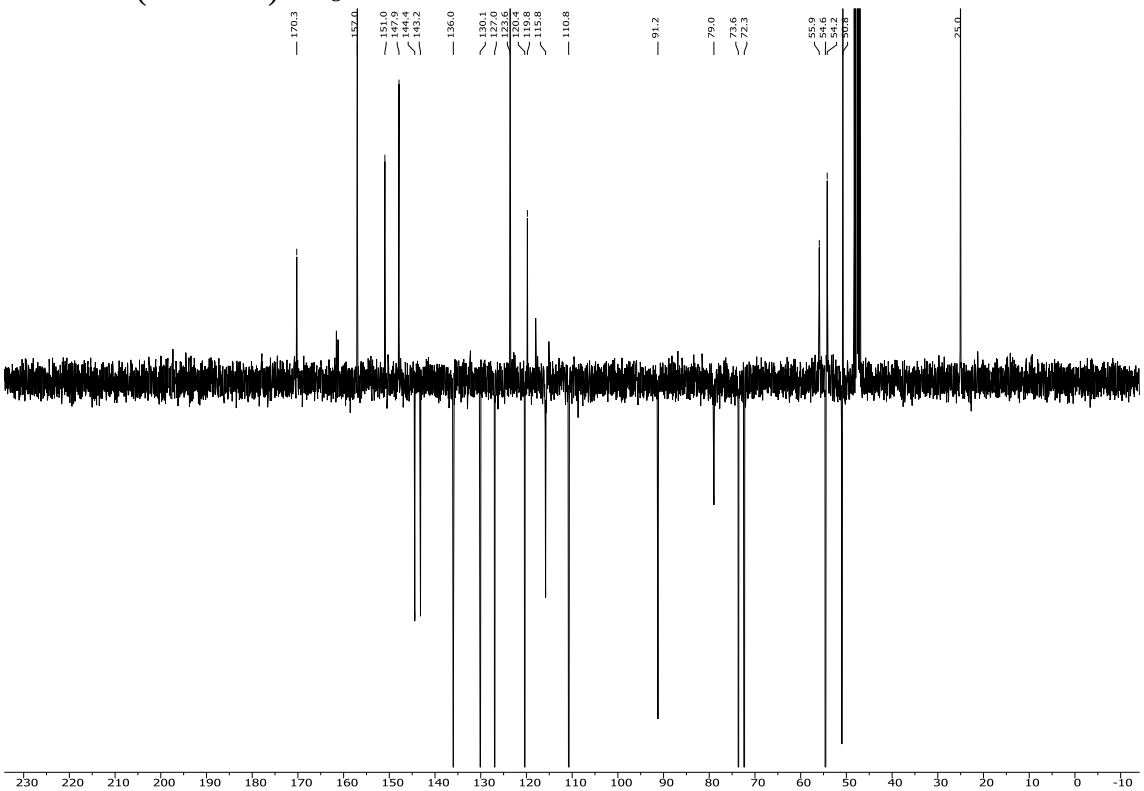

Compound **17e** ^{1}H NMR (400 MHz) CD_3OD

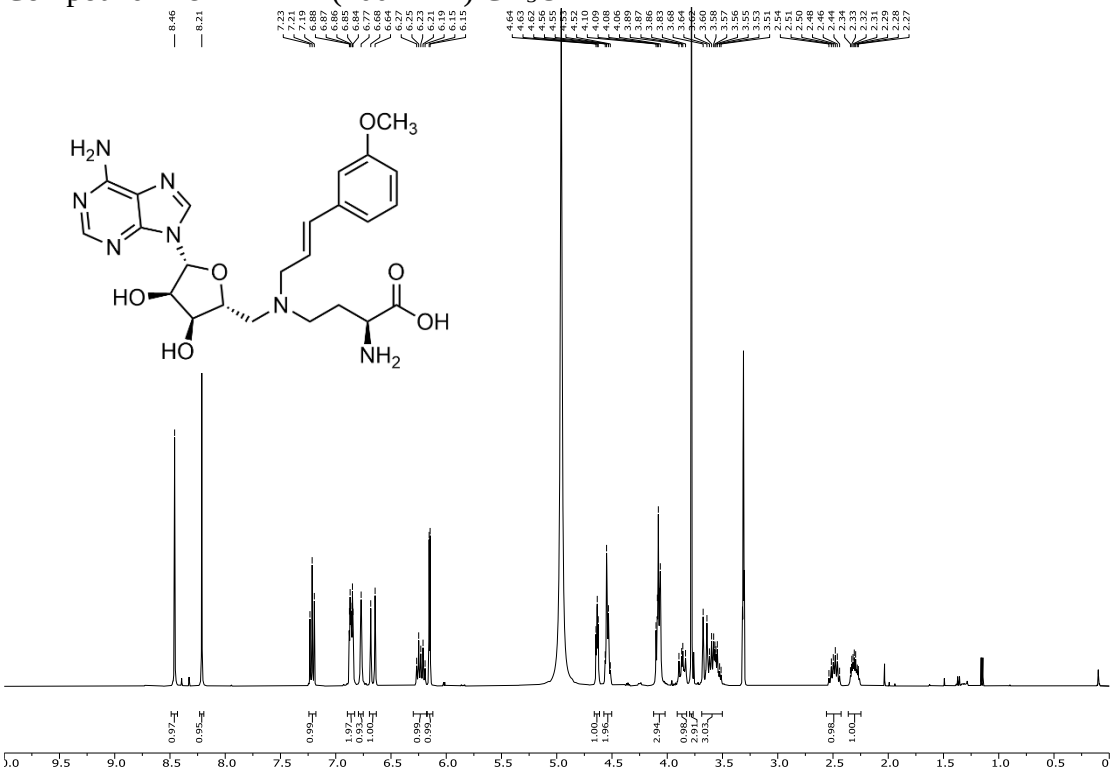

^{13}C NMR (101 MHz) CD_3OD

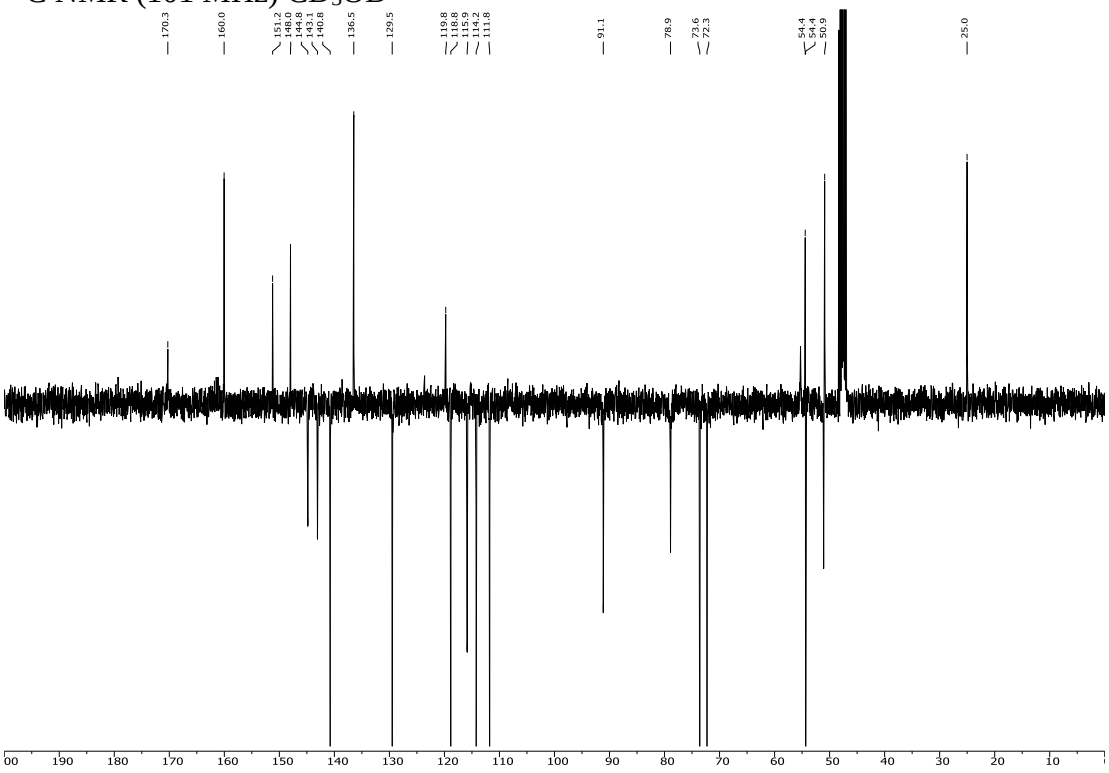

Compound **17f** ^{1}H NMR (400 MHz) D_2O

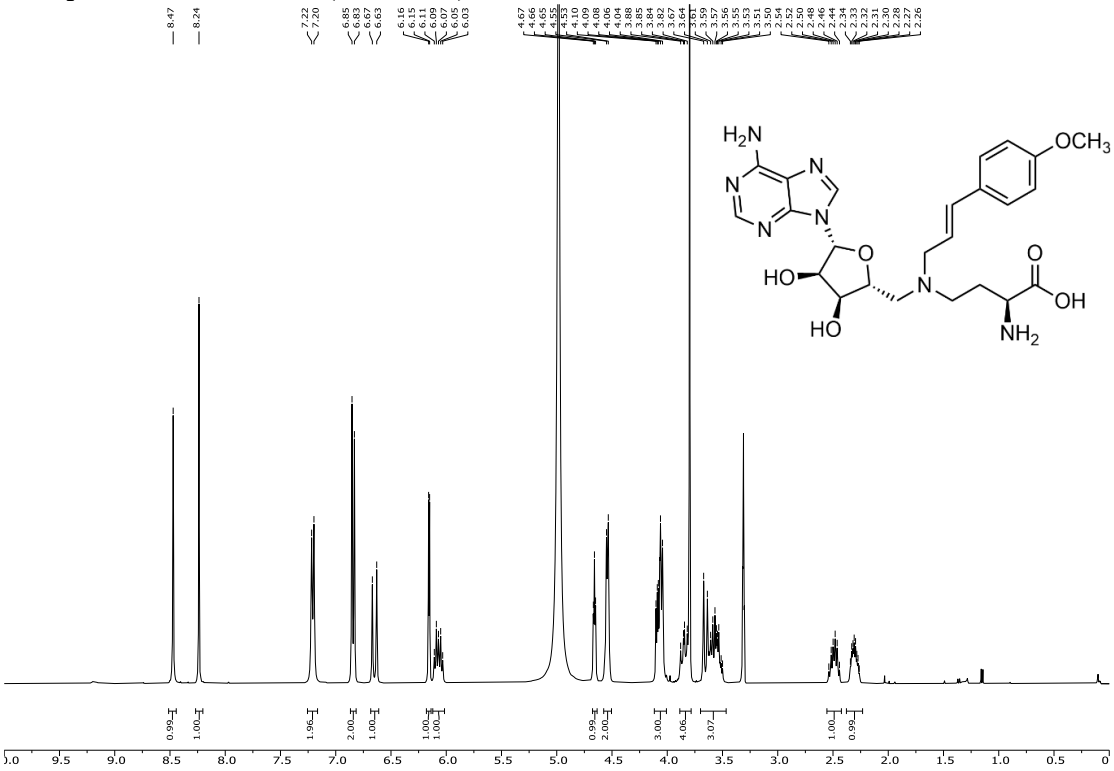

^{13}C NMR (101 MHz) D_2O

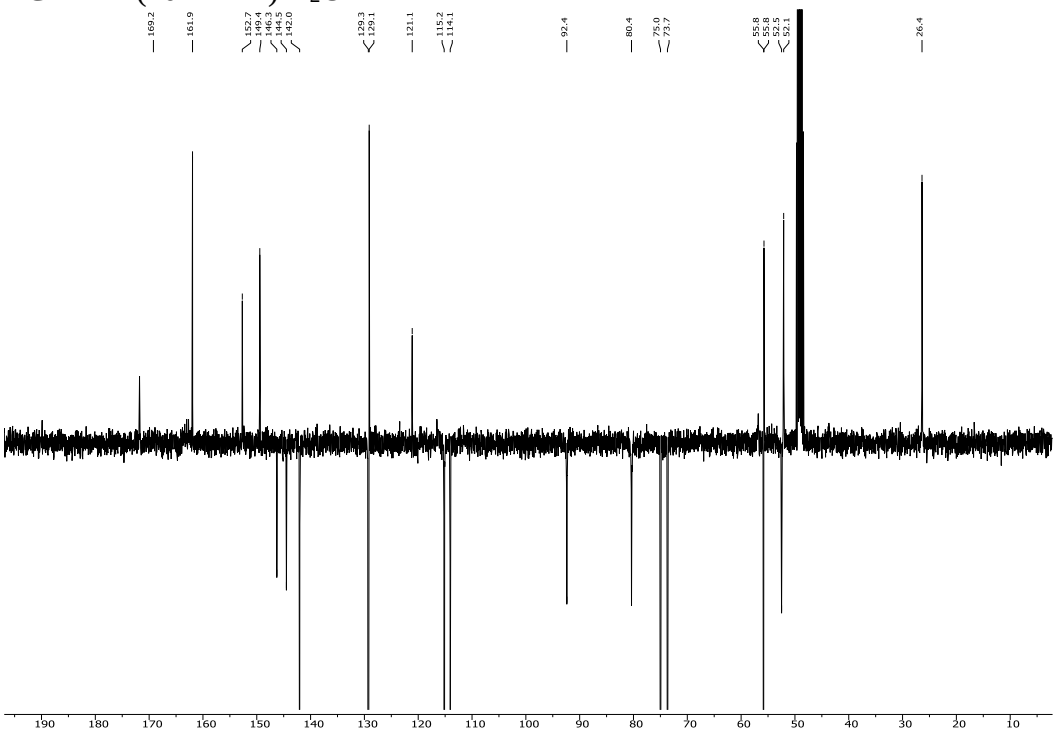

Compound **17g** ^{1}H NMR (400 MHz) D_2O

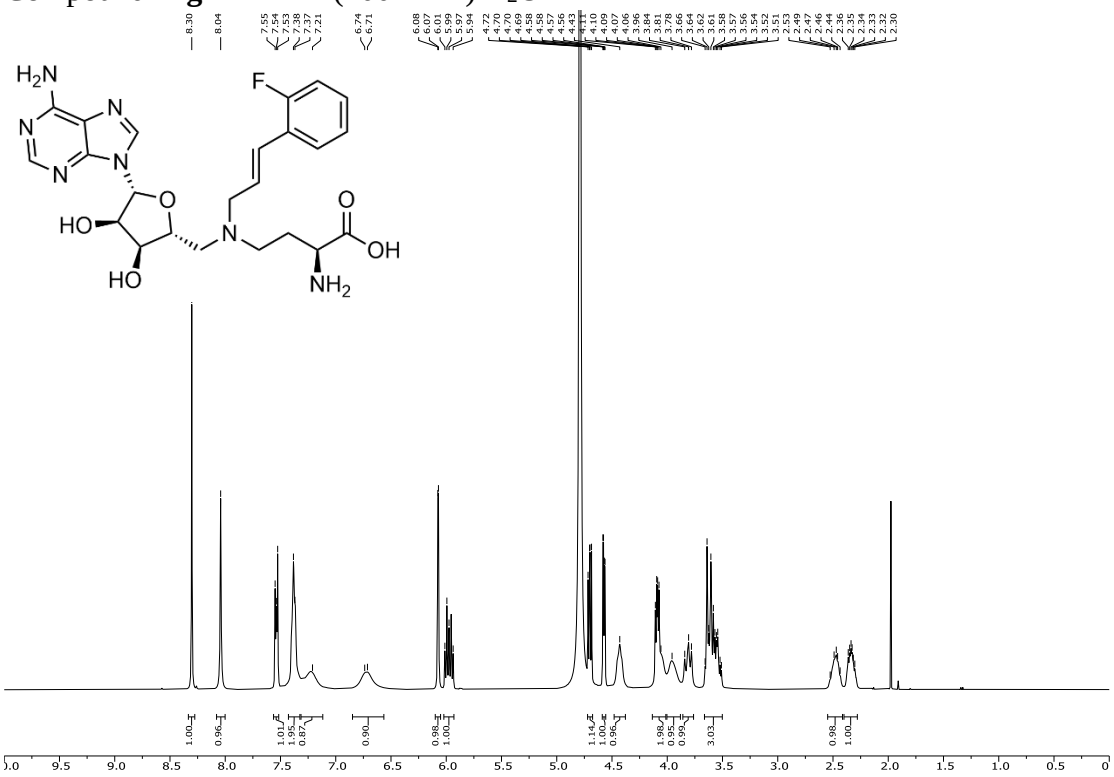

^{13}C NMR (101 MHz) D_2O

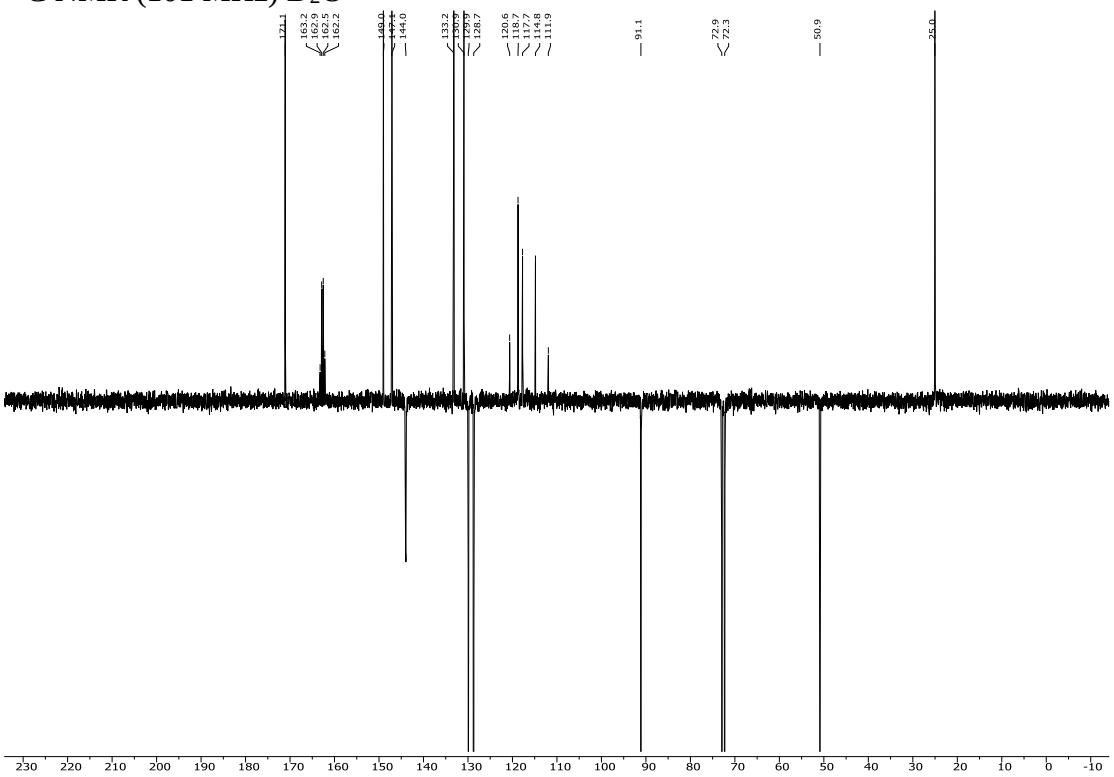

Compound **17h** ^{1}H NMR (400 MHz) D_2O

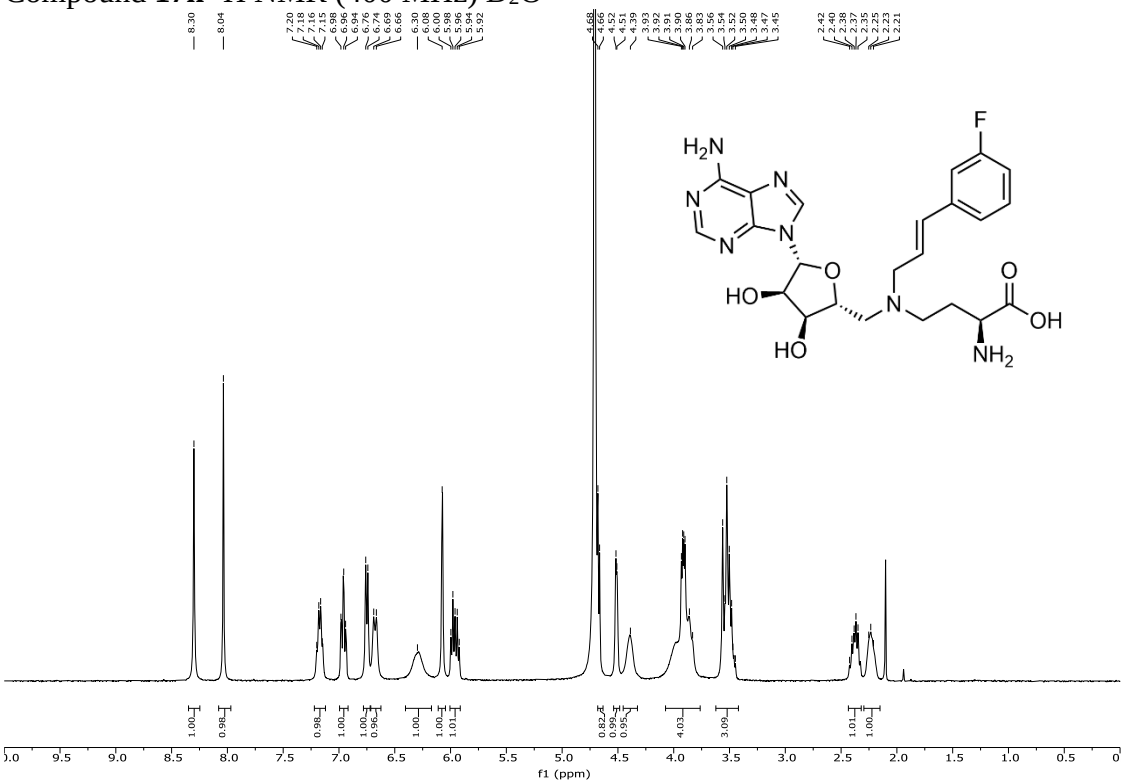

^{13}C NMR (101 MHz) D_2O

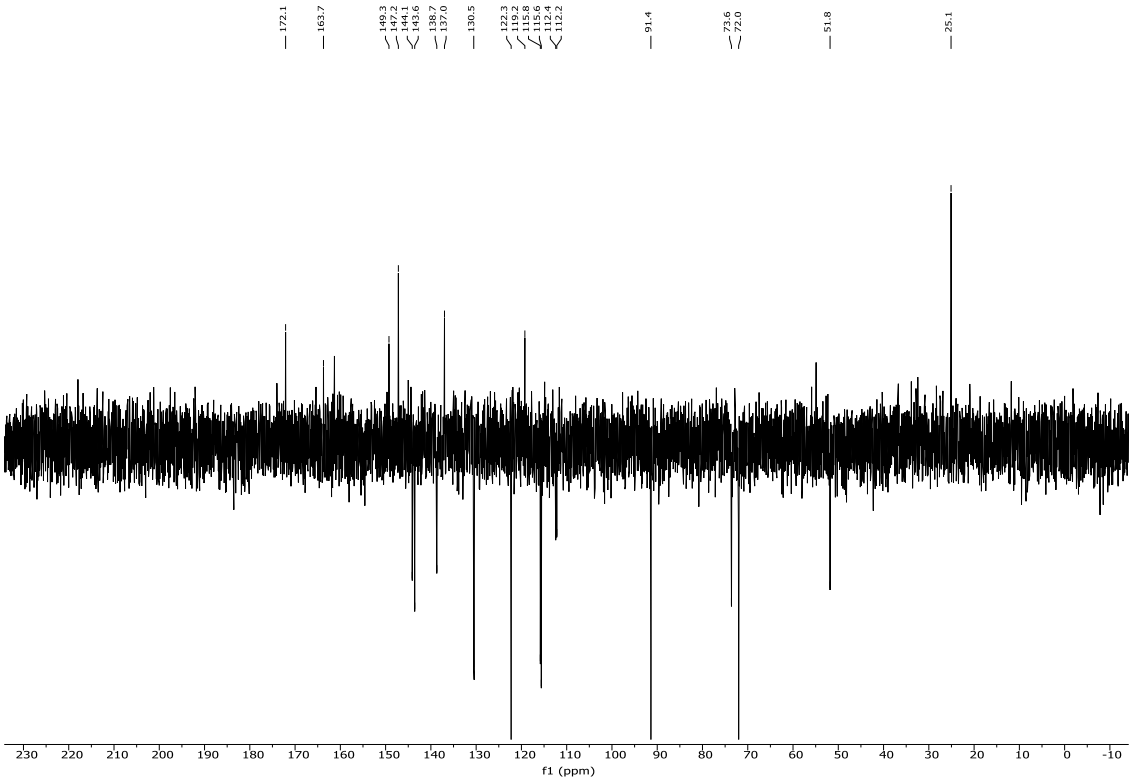

Compound **17i** ^{1}H NMR (400 MHz) D_2O

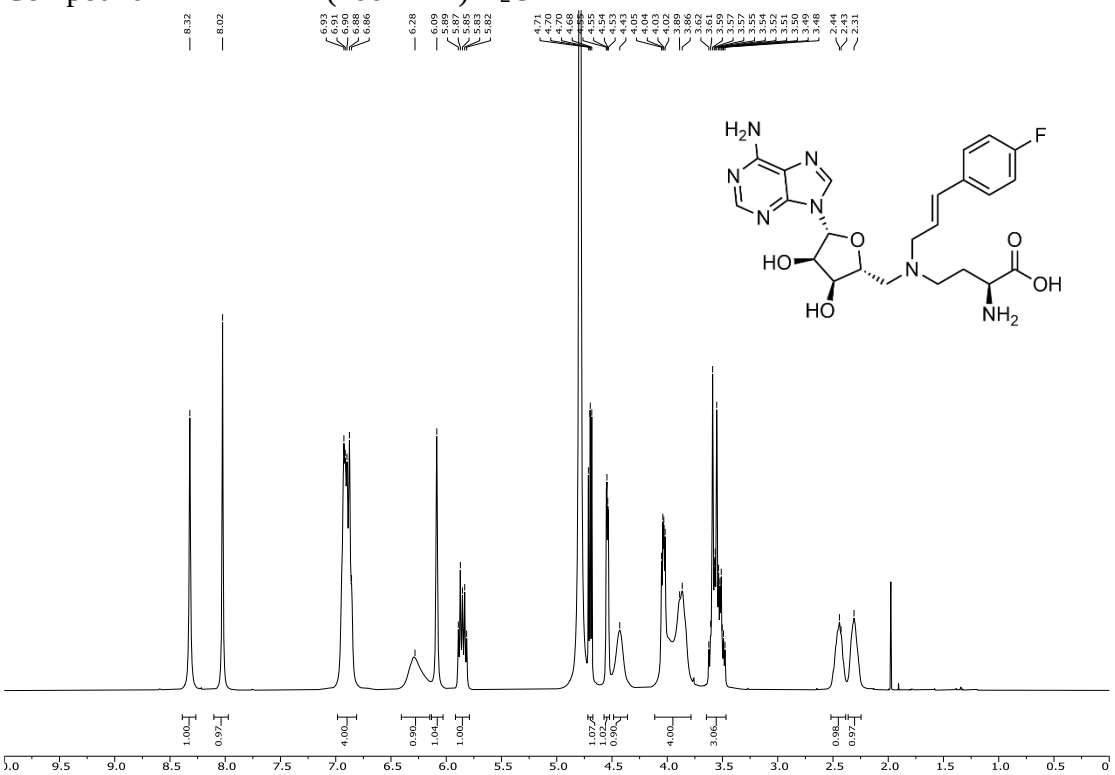

^{13}C NMR (101 MHz) D_2O

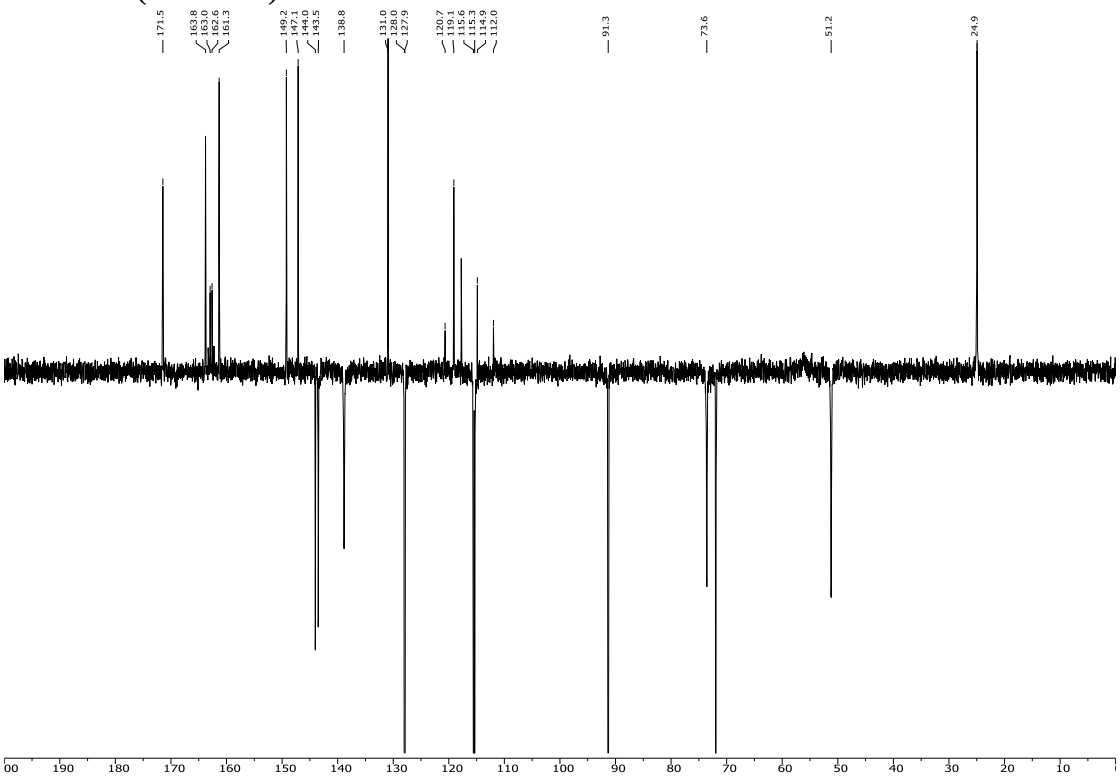

Compound **17j** ^{1}H NMR (400 MHz) D_2O

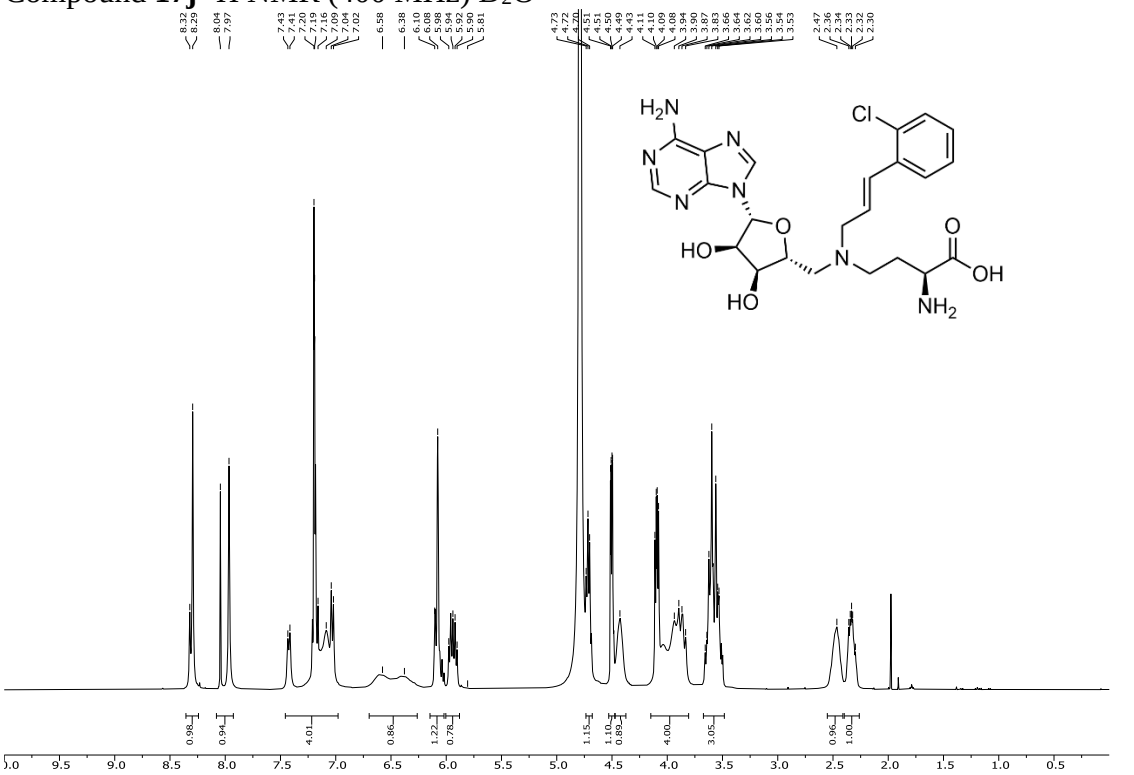

^{13}C NMR (101 MHz) D_2O

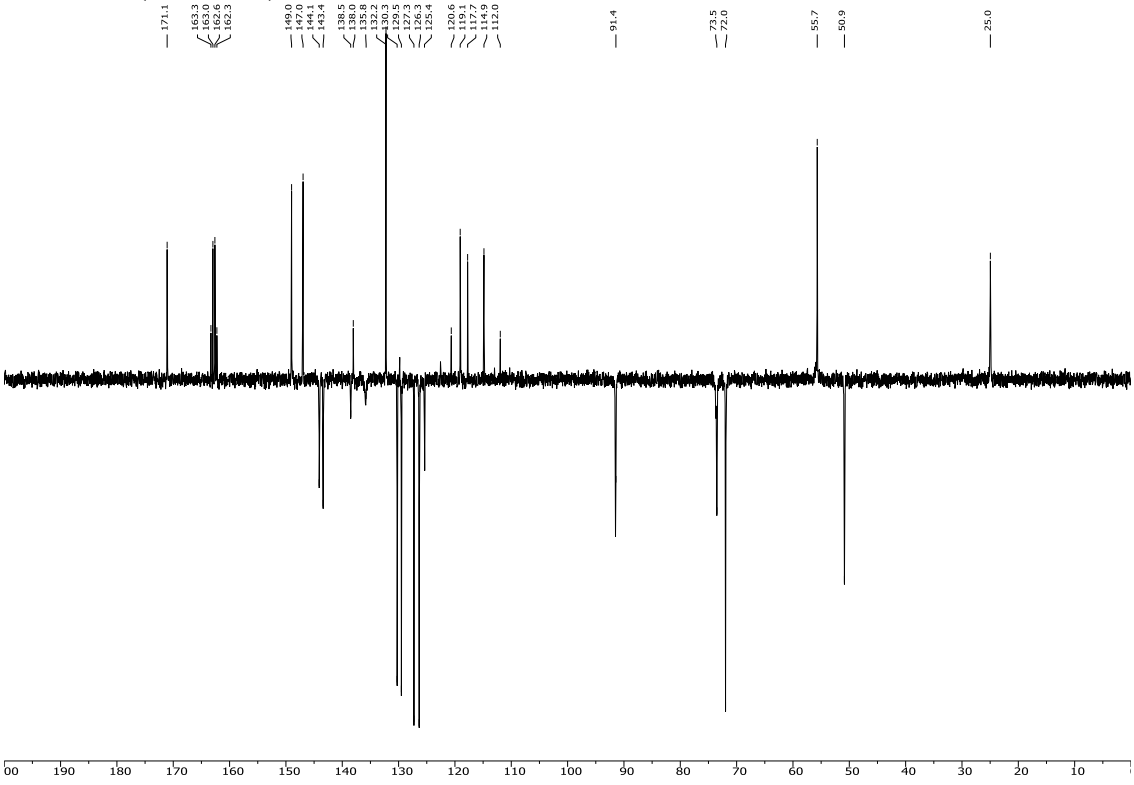

Compound **17k** ^{1}H NMR (400 MHz) CD_3OD

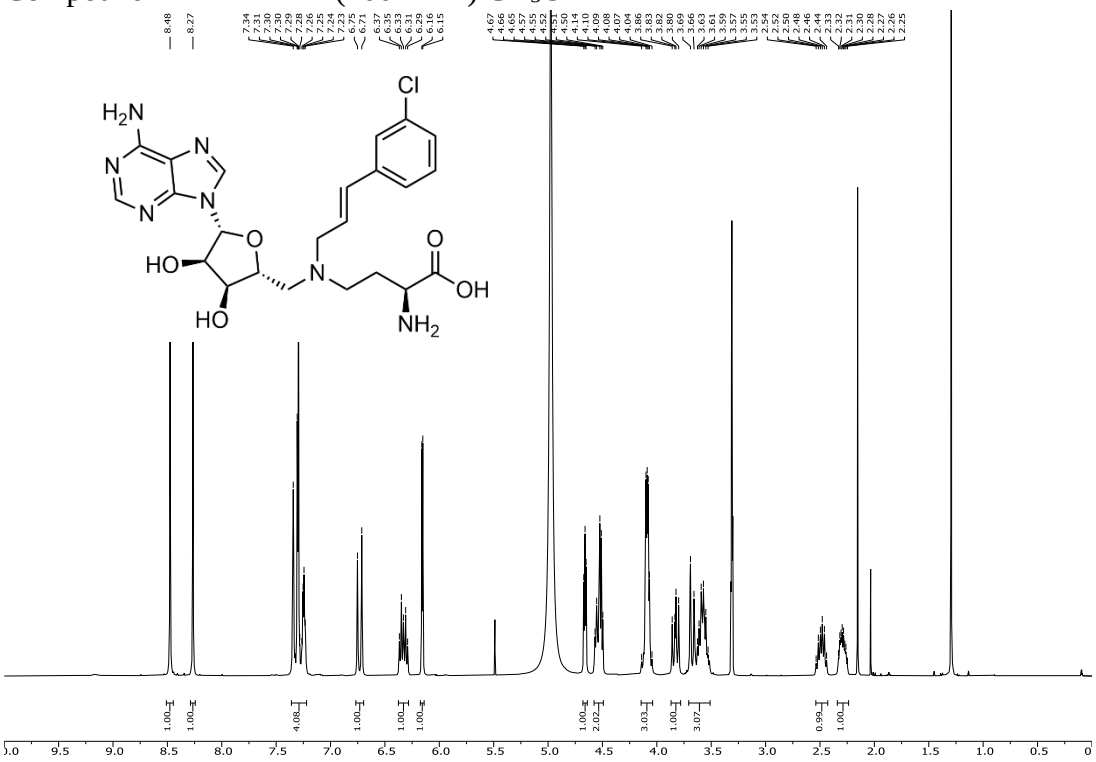

^{13}C NMR (101 MHz) CD_3OD

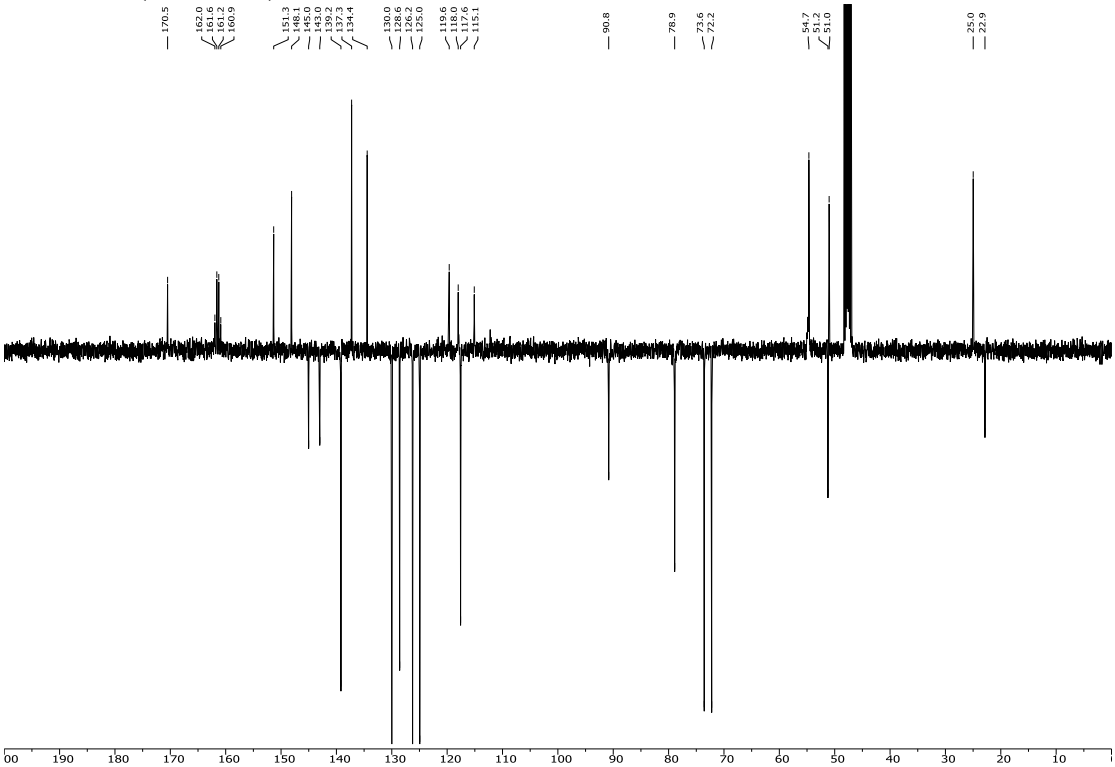

Compound **17l** ^{1}H NMR (400 MHz) D_2O

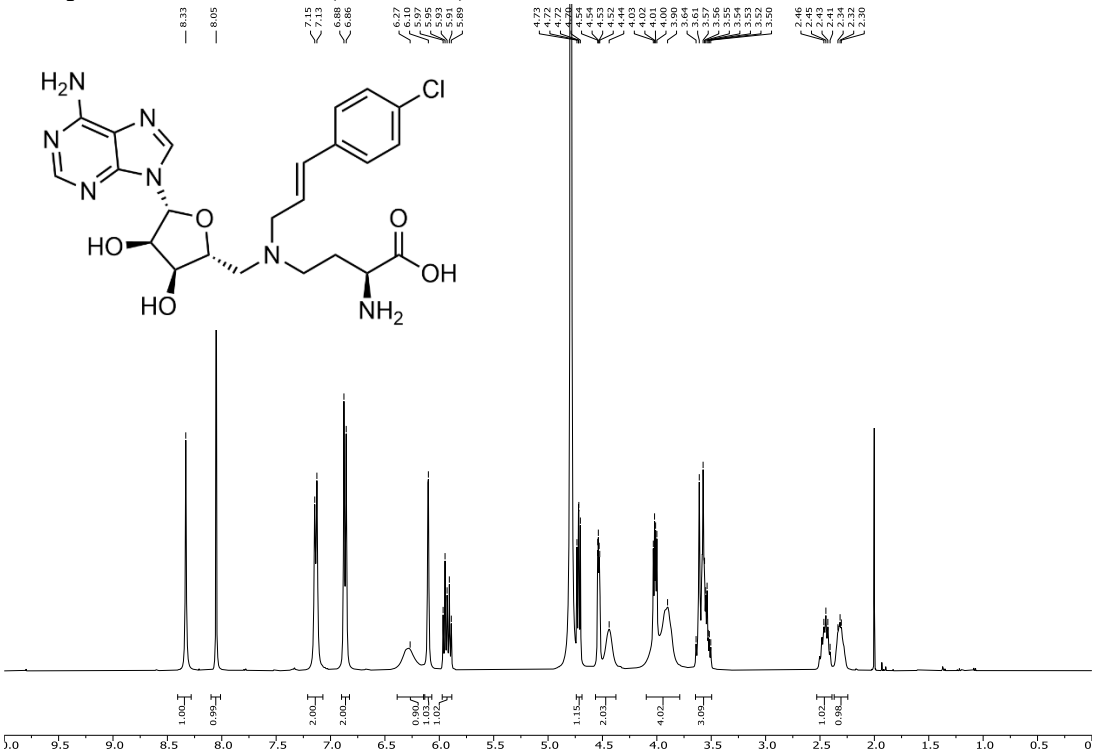

^{13}C NMR (101 MHz) D_2O

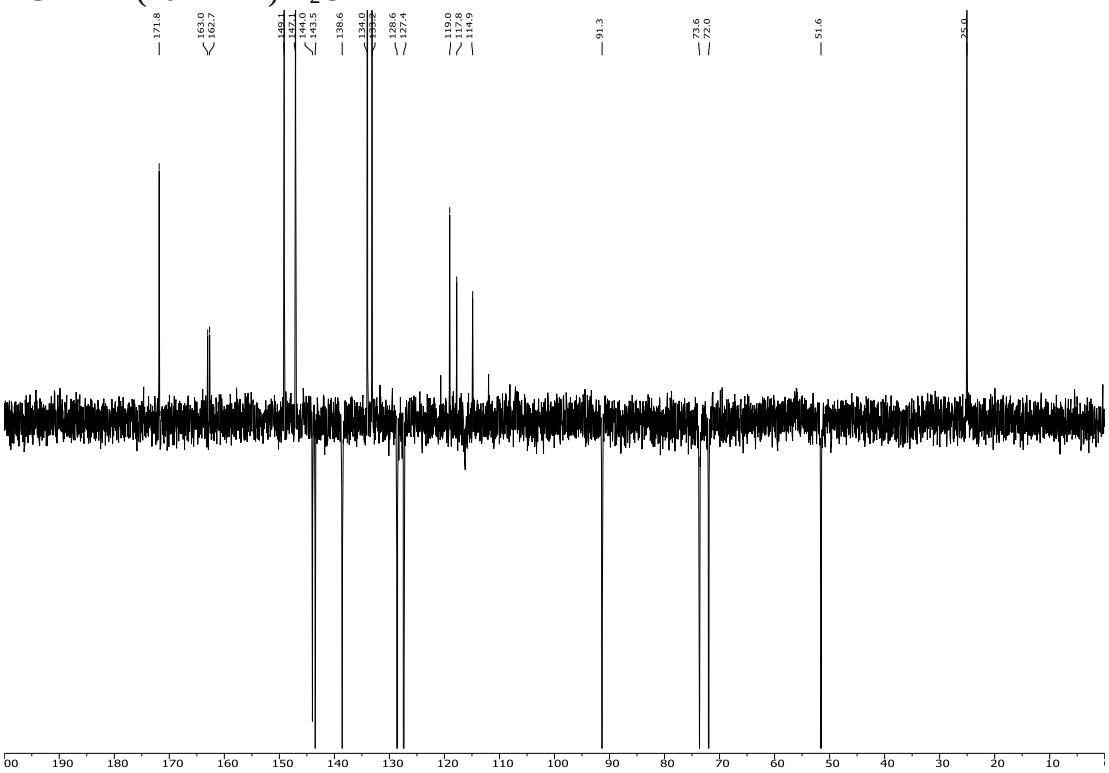

Compound **17m** ^{1}H NMR (400 MHz) D_2O

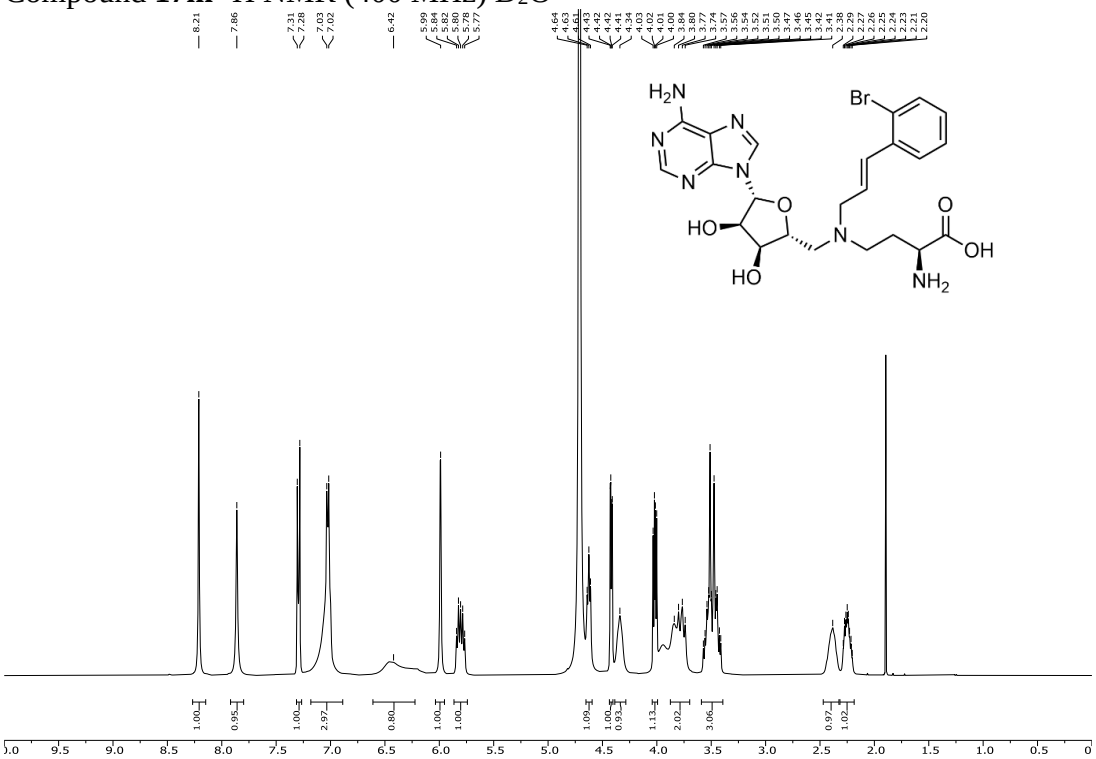

^{13}C NMR (101MHz) D_2O

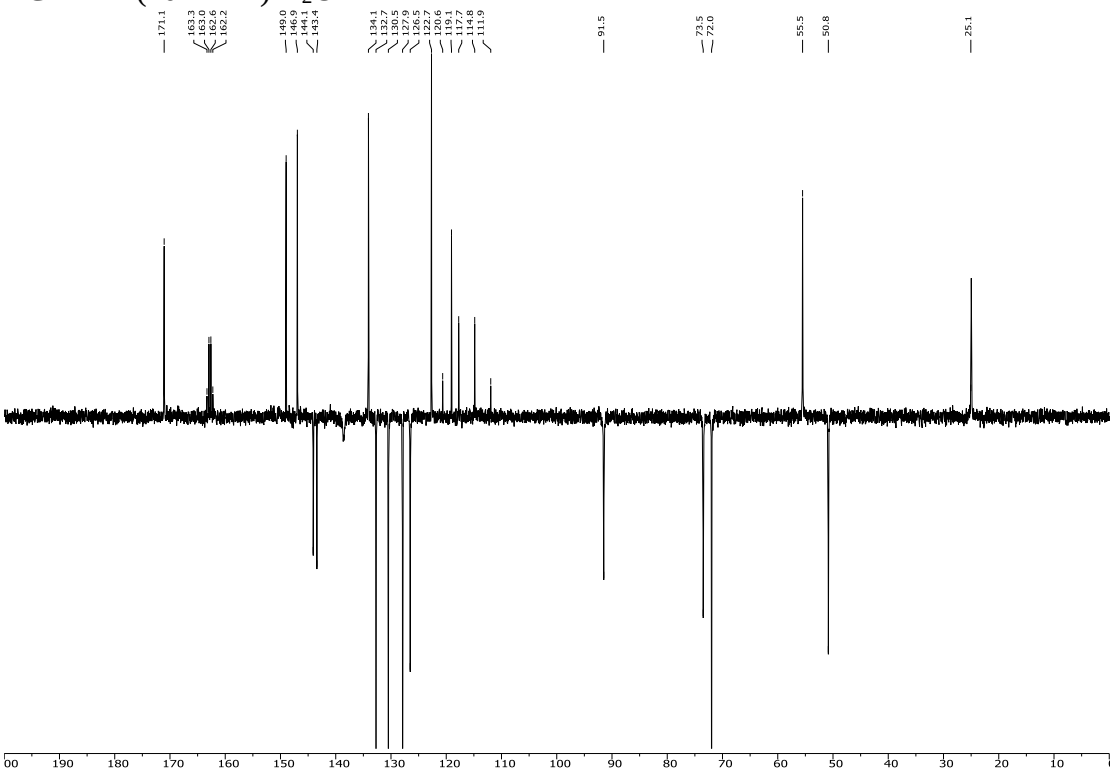

Compound **17n** ^{1}H NMR (400 MHz) D_2O

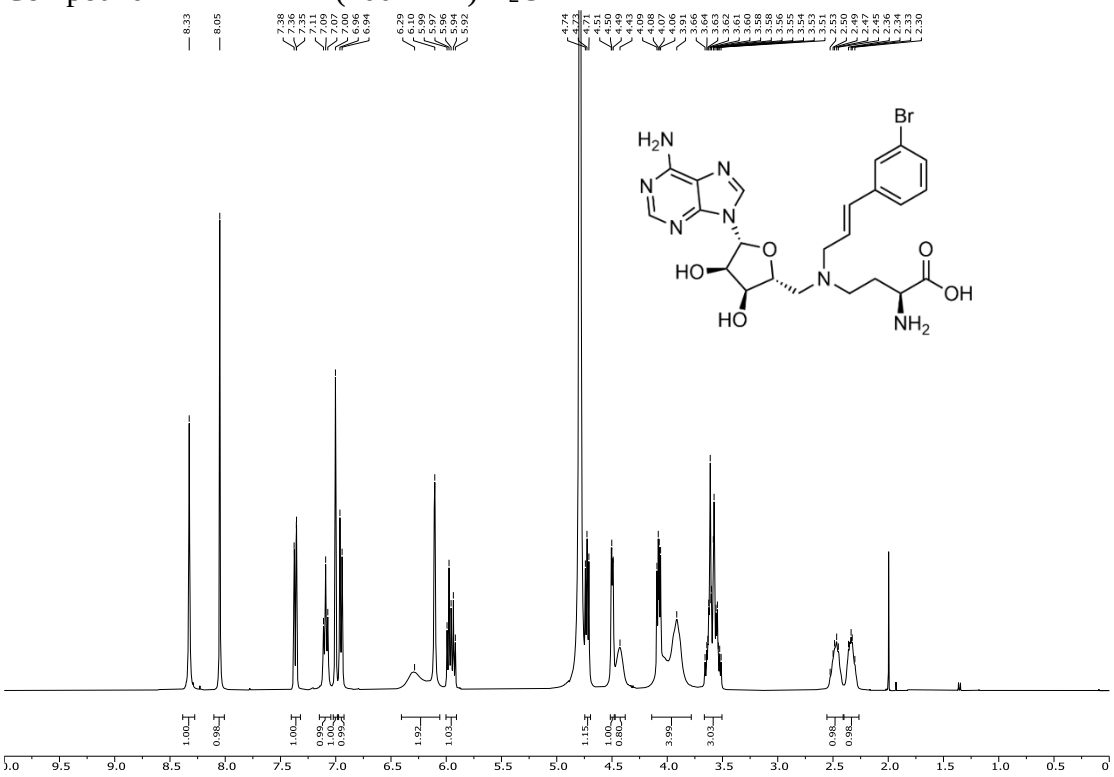

^{13}C NMR (101 MHz) D_2O

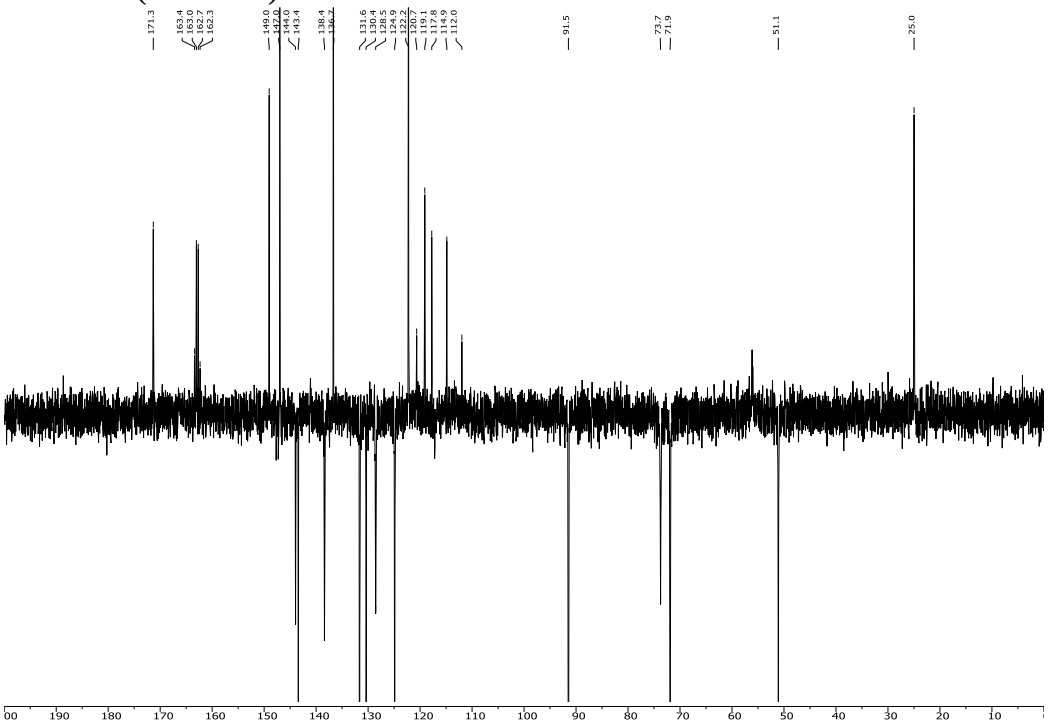

Compound **17o** ^{1}H NMR (400 MHz) D_2O

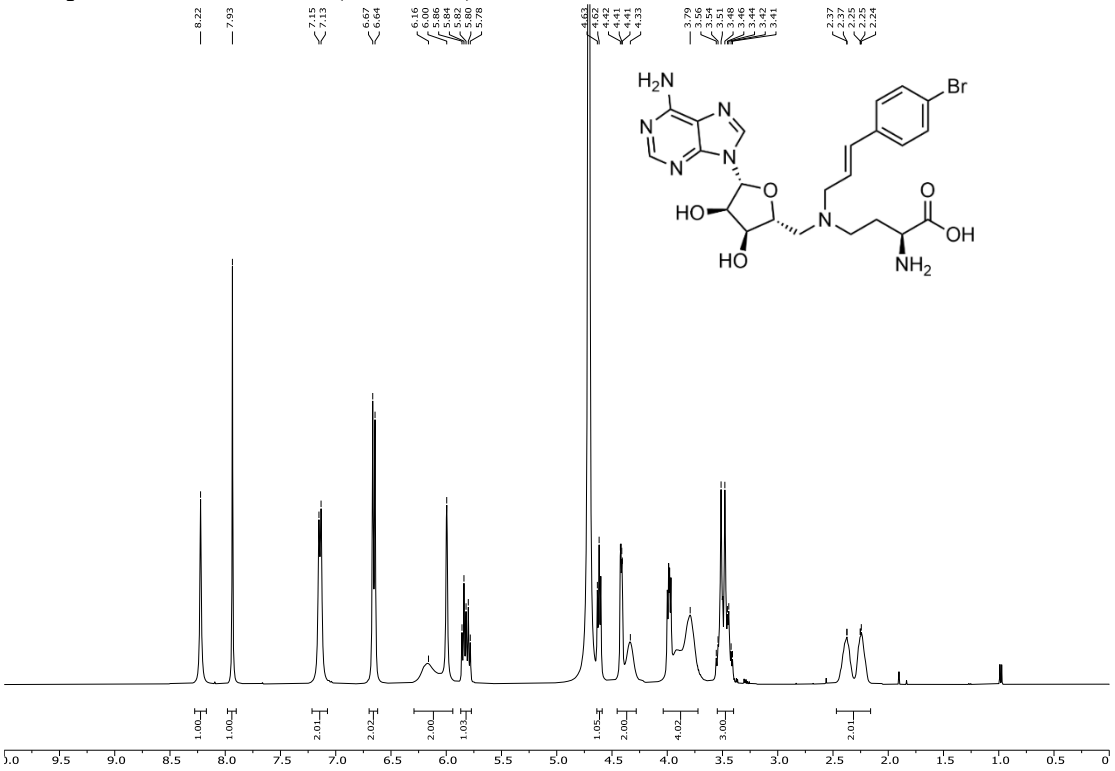

^{13}C NMR (101 MHz) D_2O

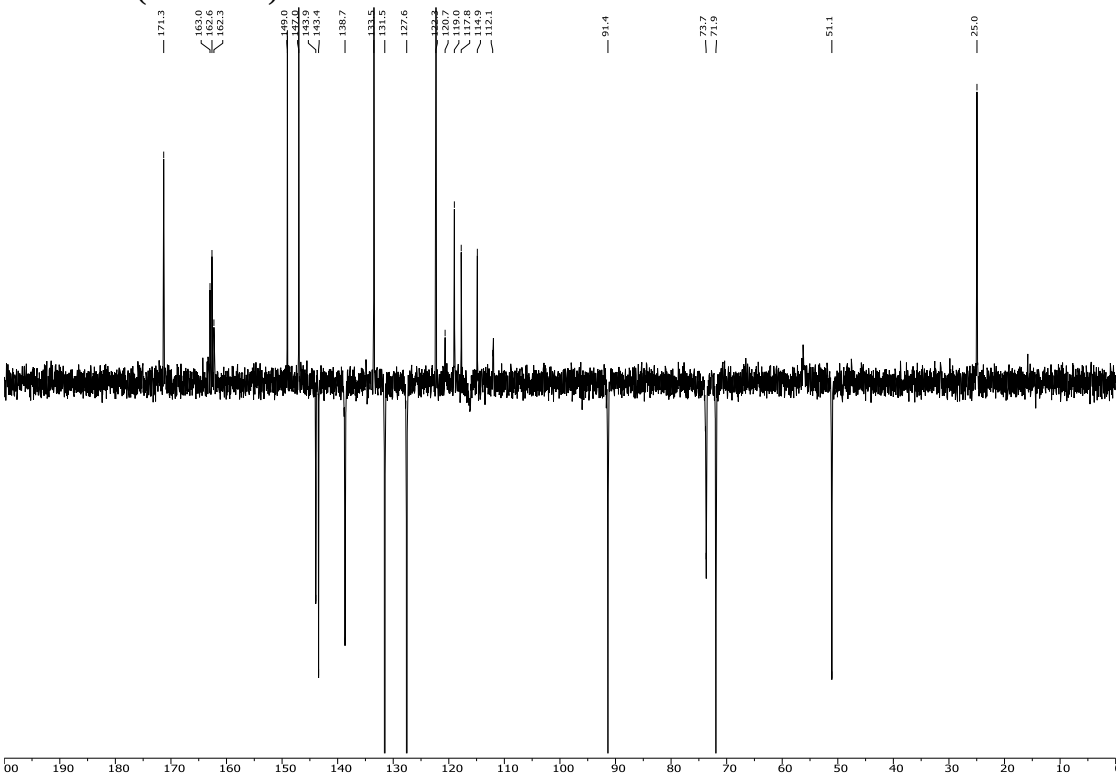

Compound **17p** ^{1}H NMR (400 MHz) D_2O

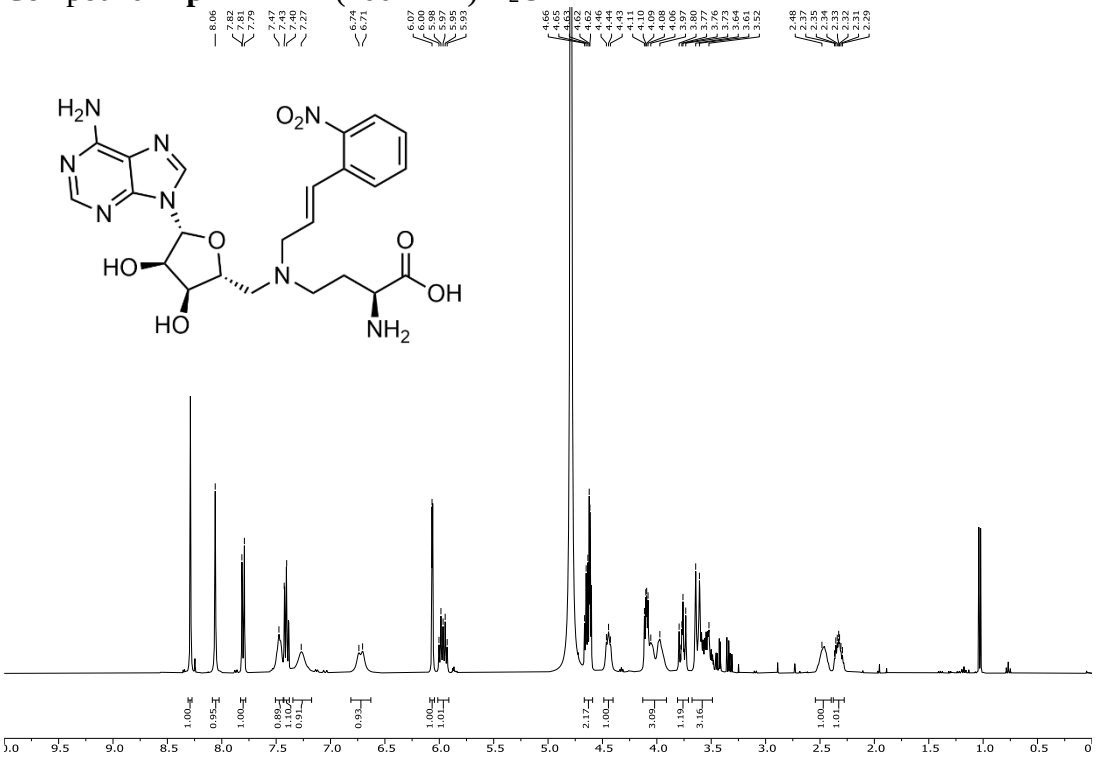

^{13}C NMR (101 MHz) D_2O

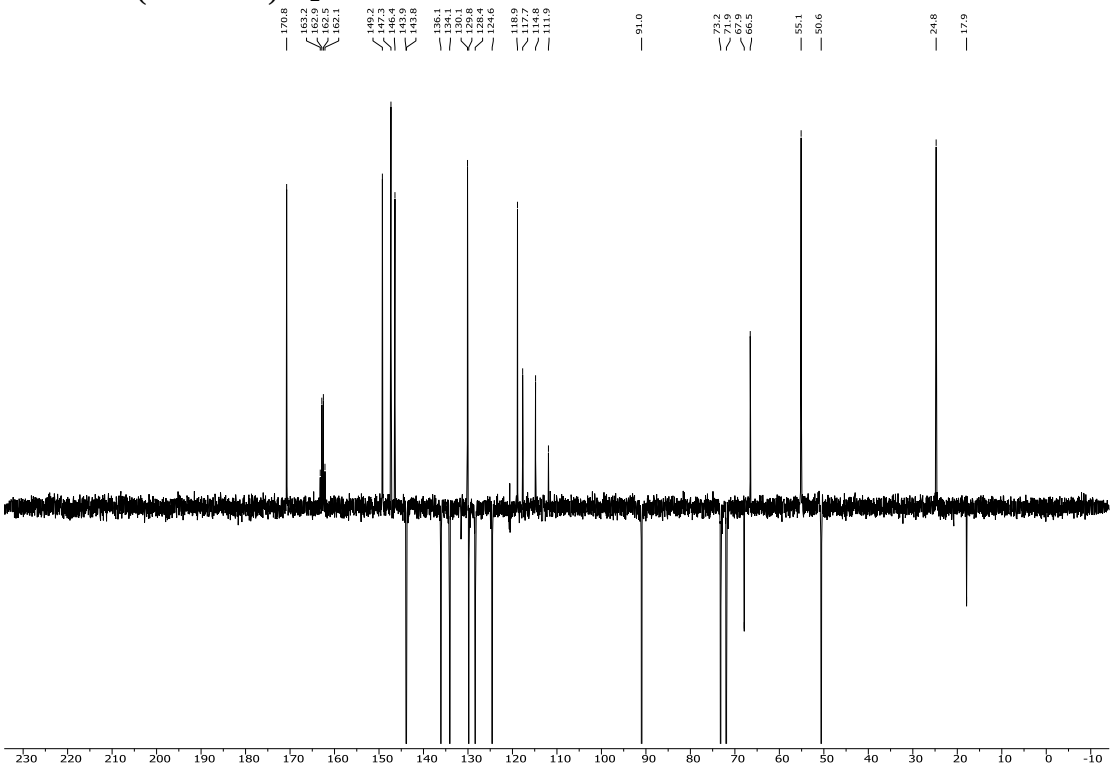

Compound **17q** ^{1}H NMR (500 MHz) CD_3OD

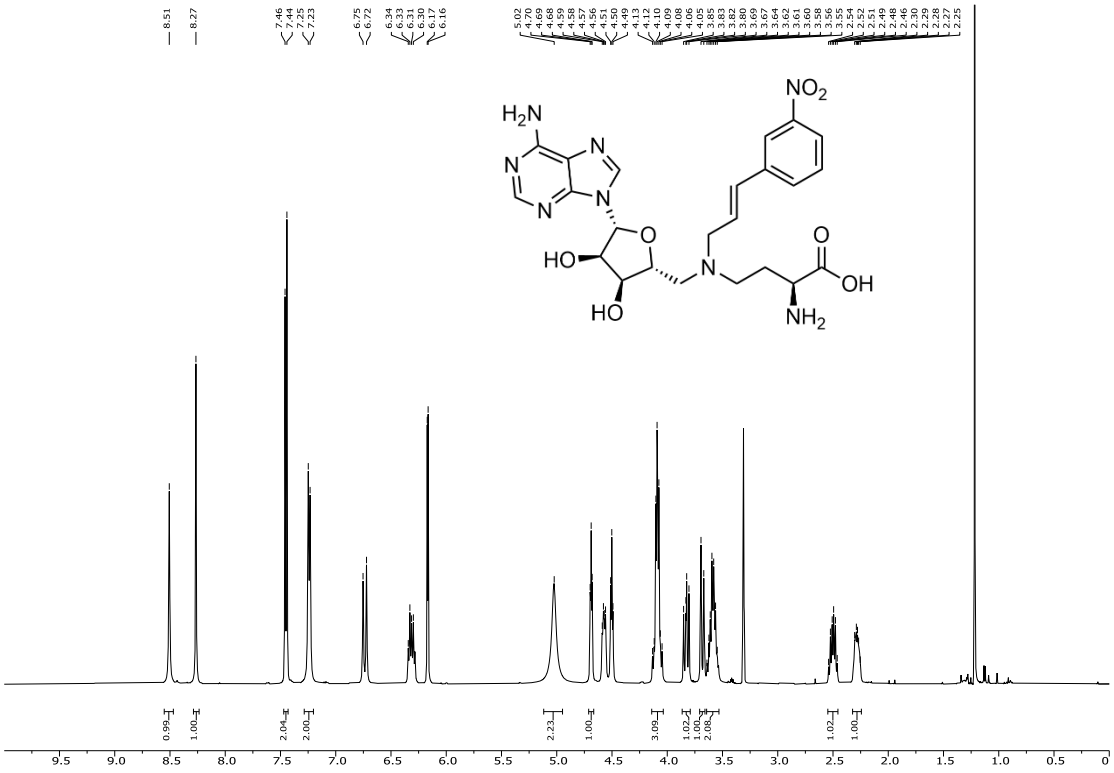

^{13}C NMR (126 MHz) CD_3OD

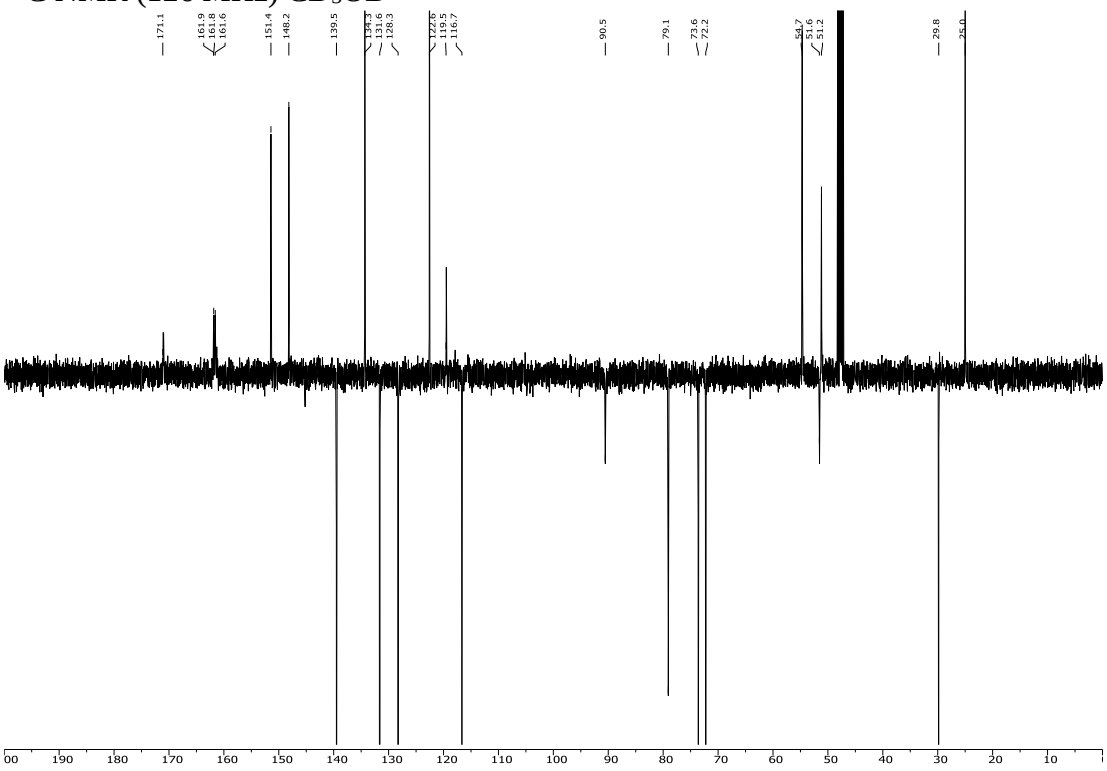

Compound **17r** ^{1}H NMR (400 MHz) CD_3OD

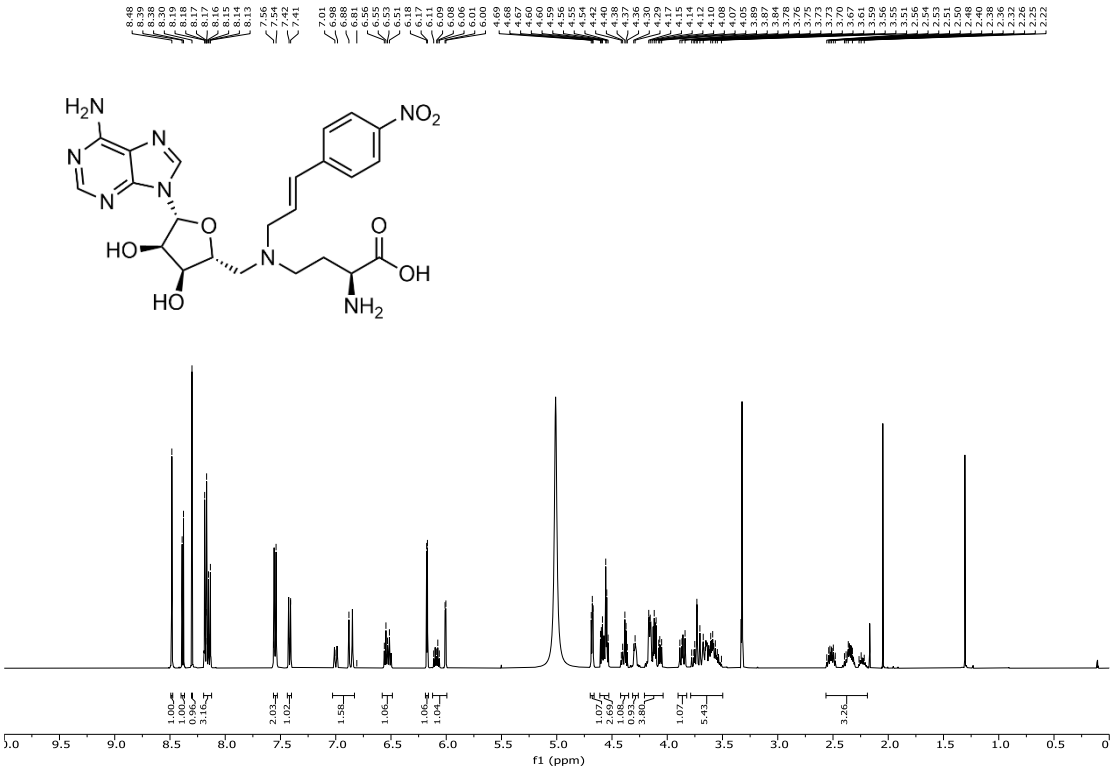

^{13}C NMR (101 MHz) CD_3OD

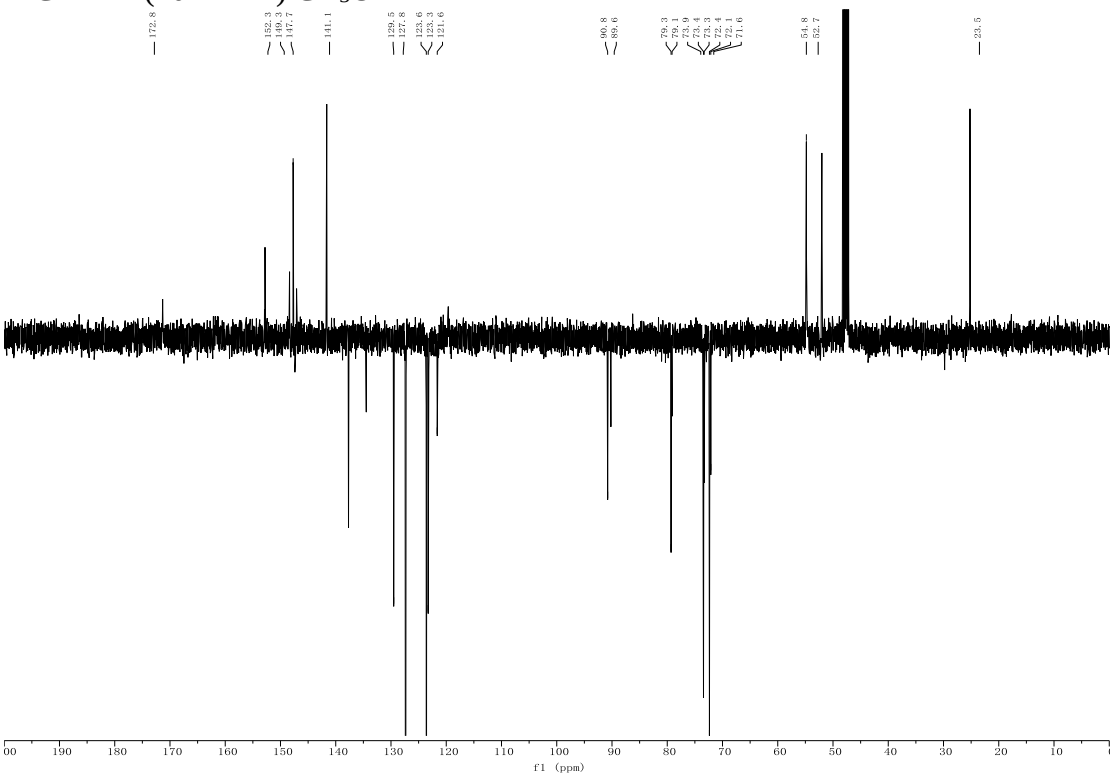

Compound **17s** ^{1}H NMR (400 MHz) D_2O

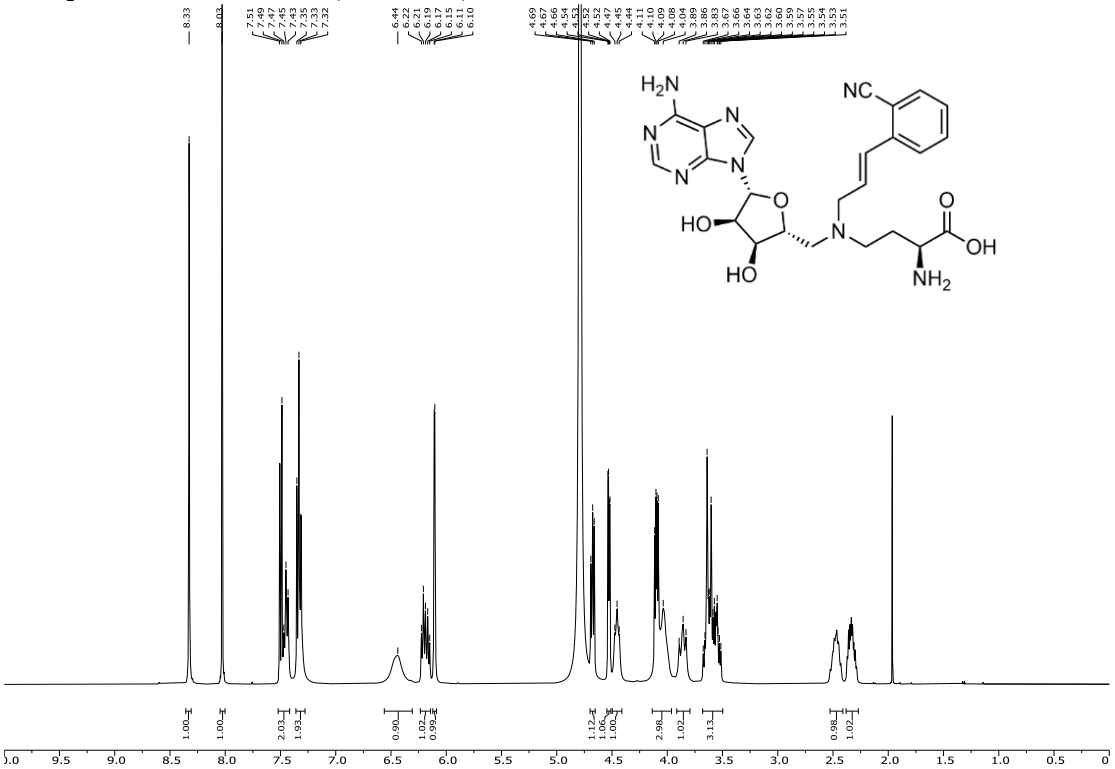

^{13}C NMR (101 MHz) D_2O

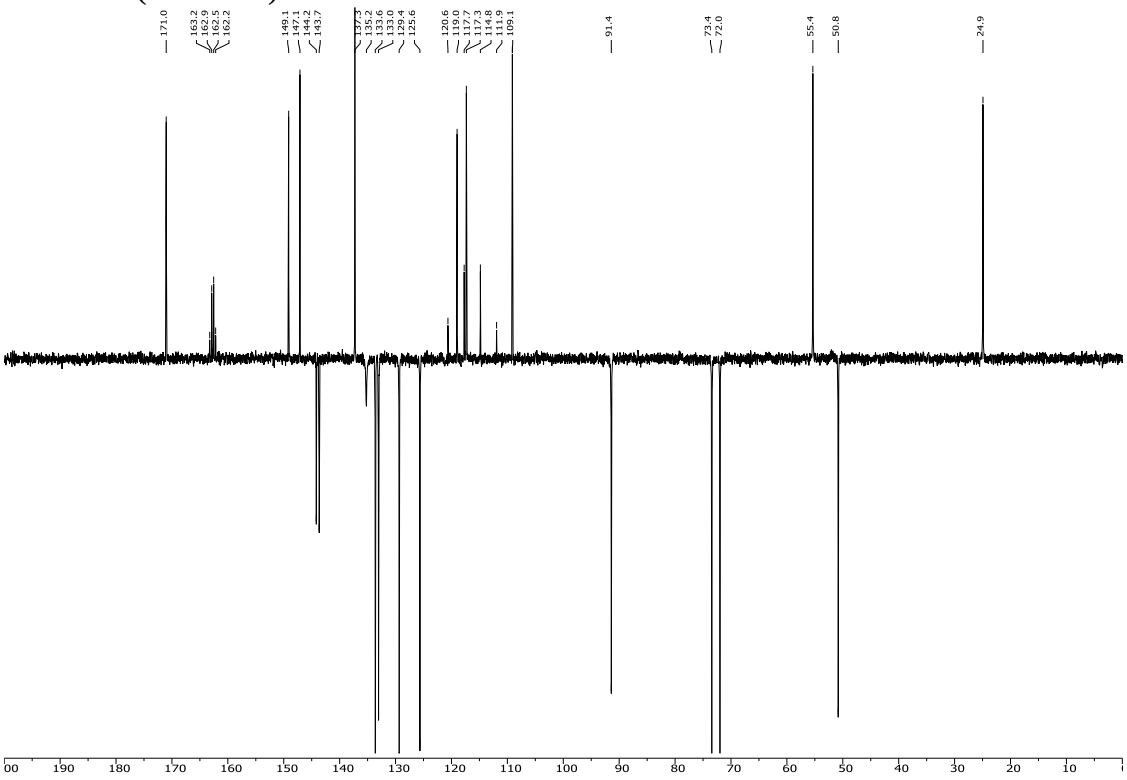

Compound **17t** ^{1}H NMR (400 MHz) D_2O

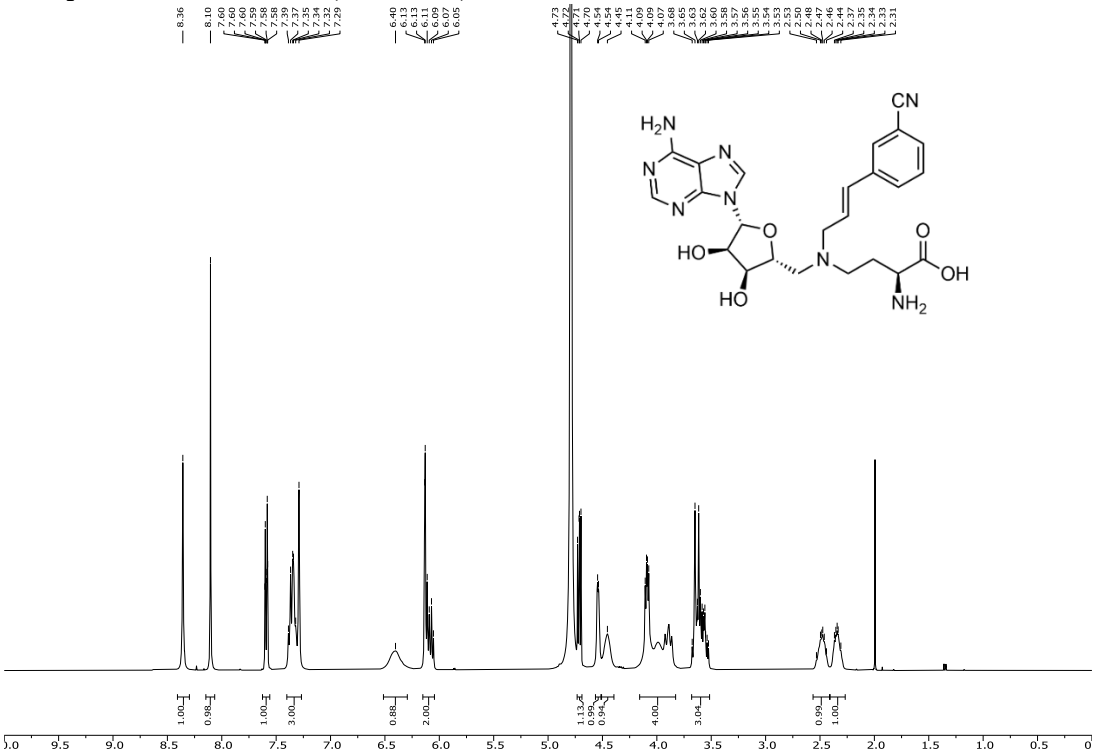

^{13}C NMR (101 MHz) D_2O

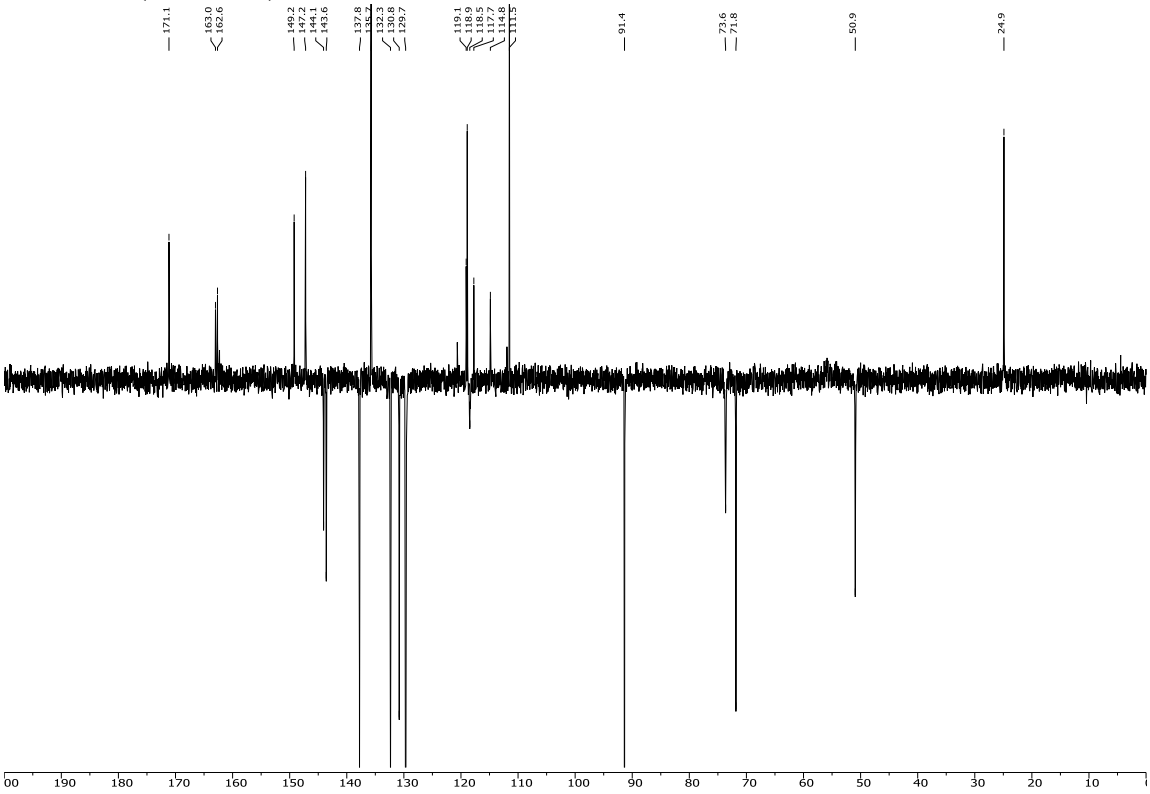

Compound **17u** ^{1}H NMR (400 MHz) D_2O

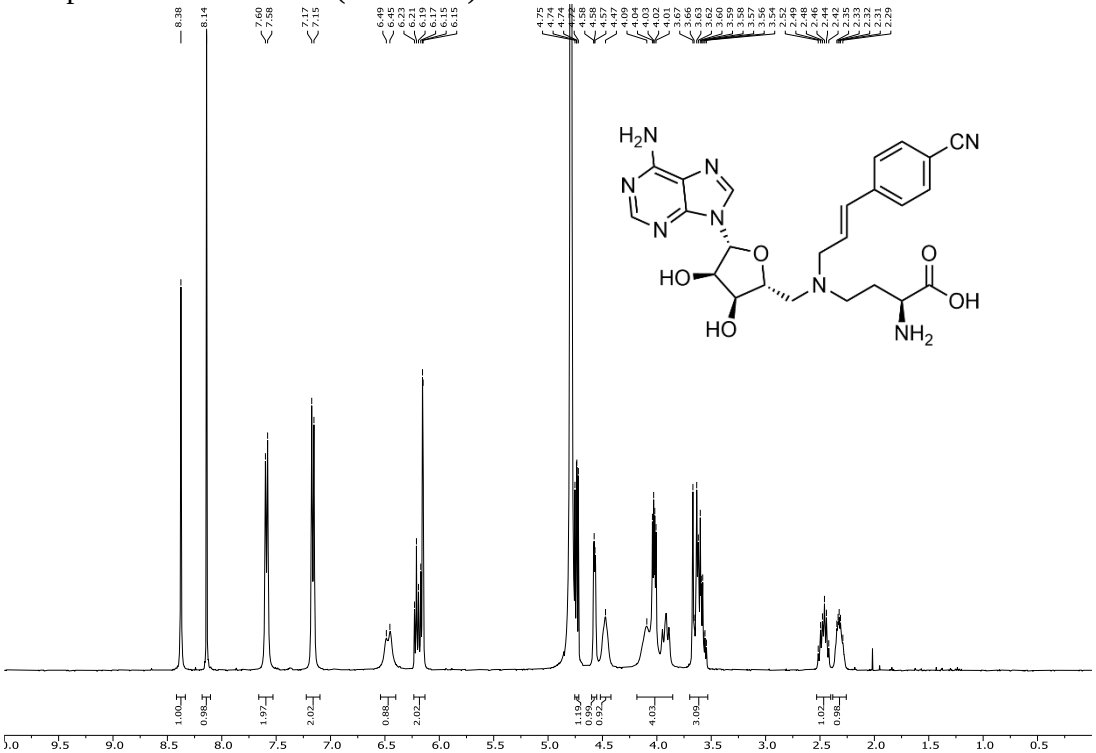

^{13}C NMR (101 MHz) D_2O

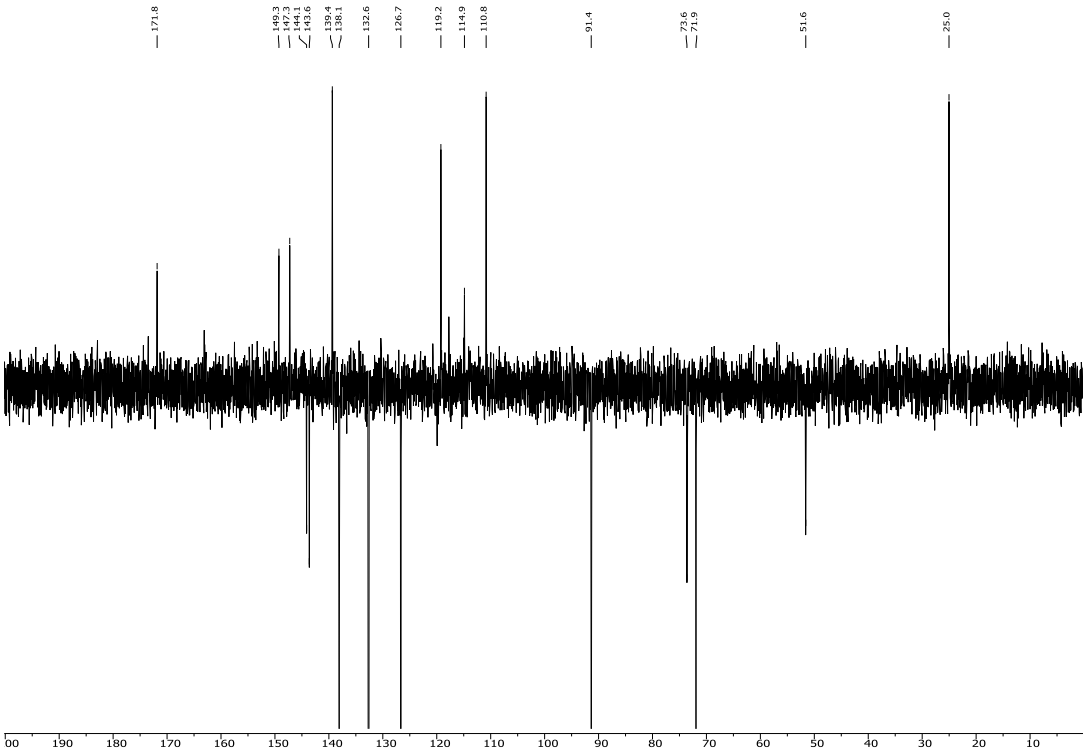

Compound **17v** ^{1}H NMR (400 MHz) CD_3OD

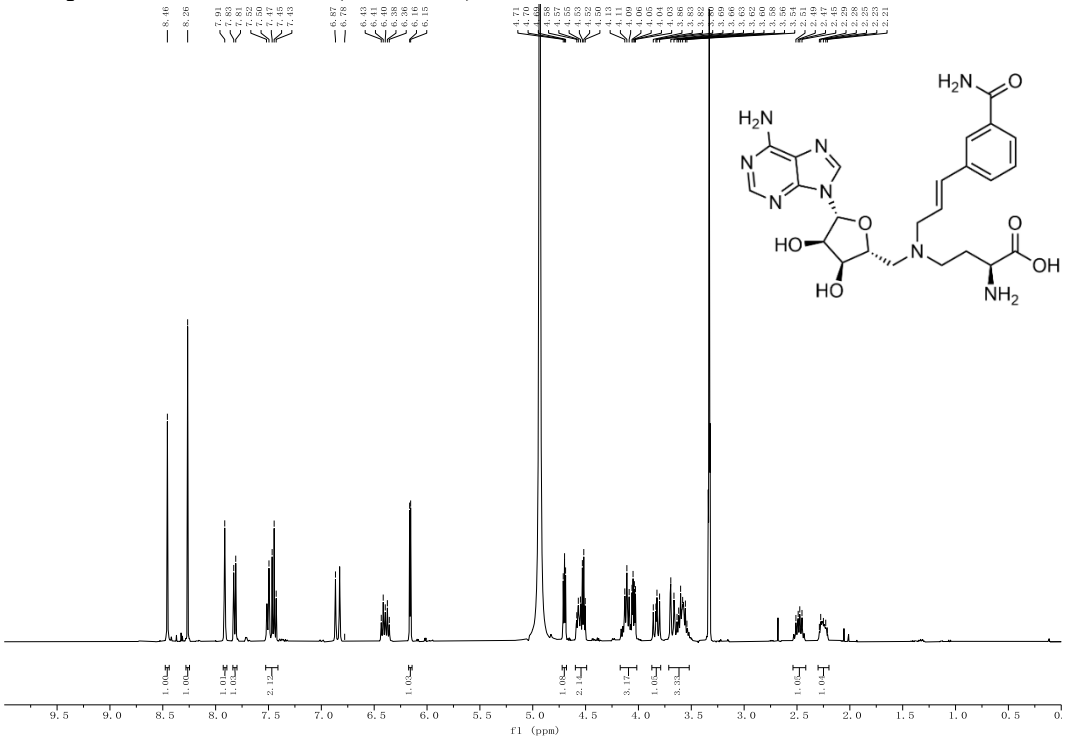

^{13}C NMR (101 MHz) CD_3OD

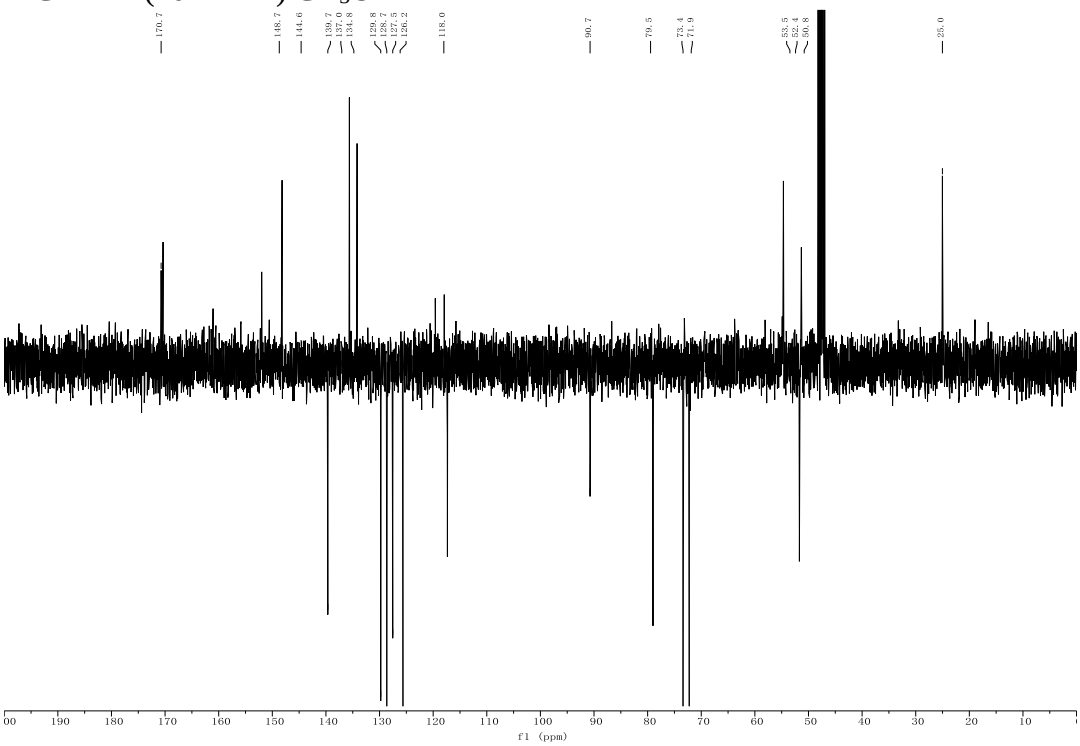

Compound **17w** ^{1}H NMR (400 MHz) CD_3OD

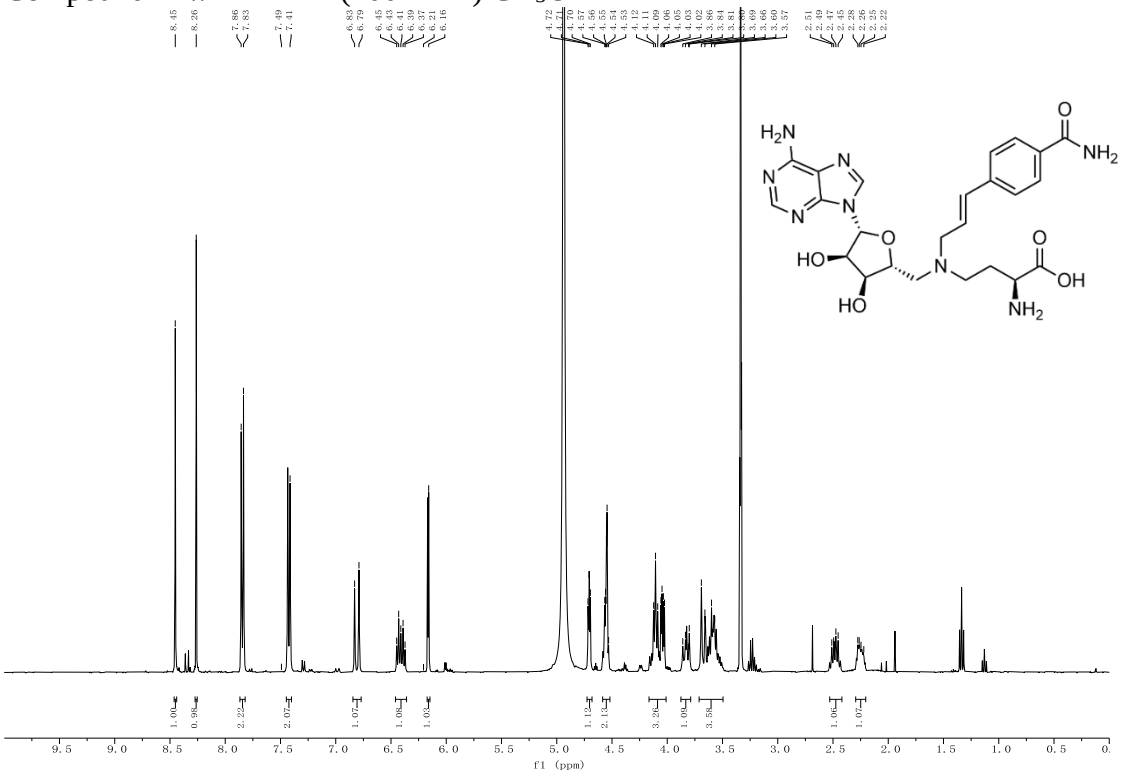

^{13}C NMR (101 MHz) CD_3OD

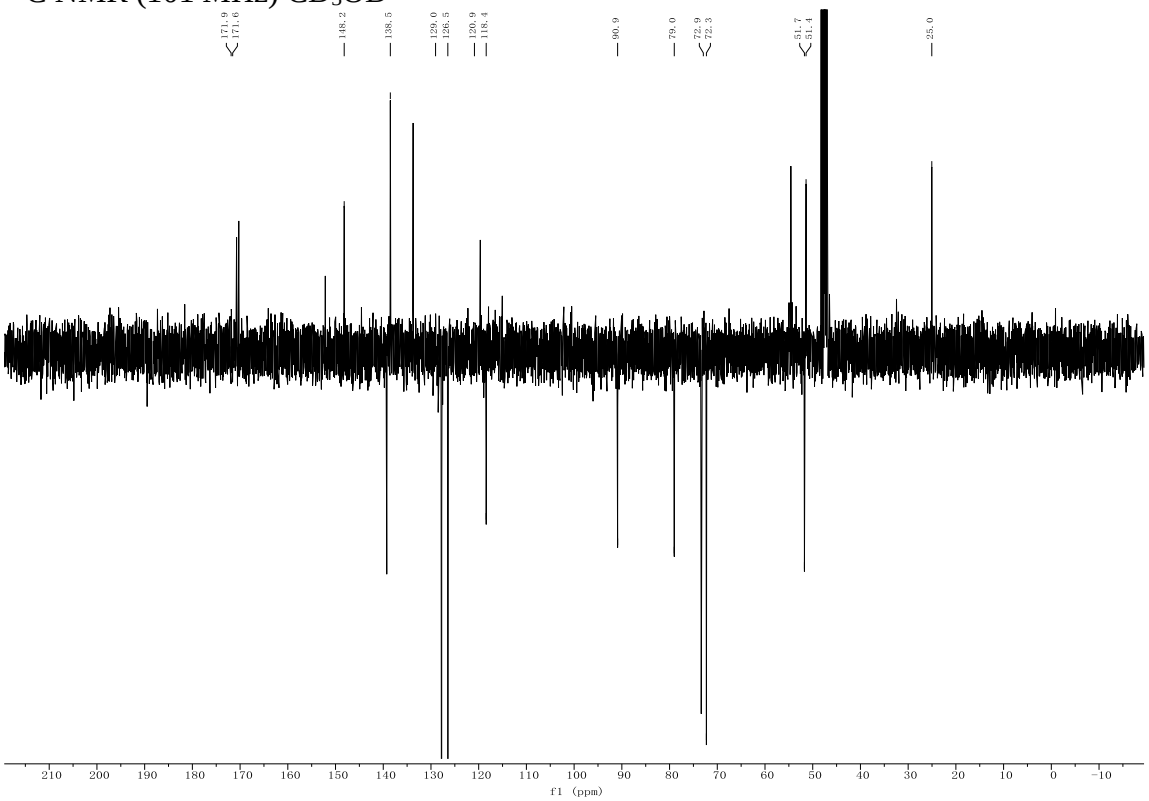

Compound **17x** ^{1}H NMR (500 MHz) CD_3OD

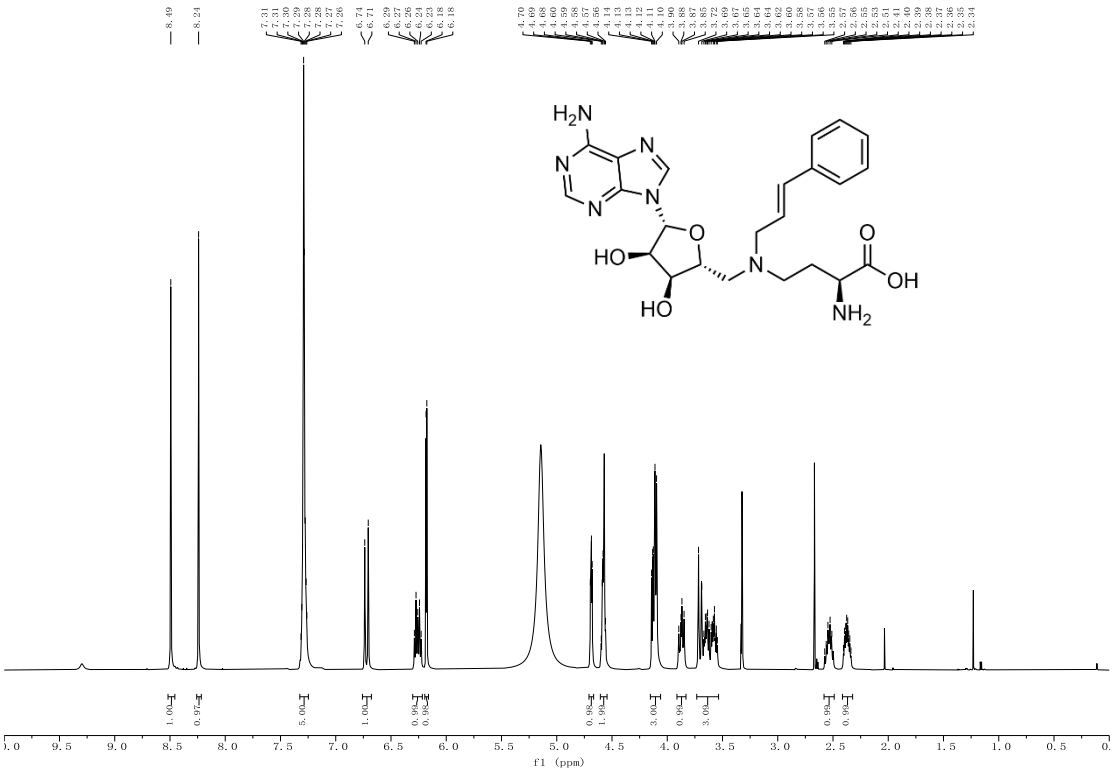

^{13}C NMR (126 MHz) CD_3OD

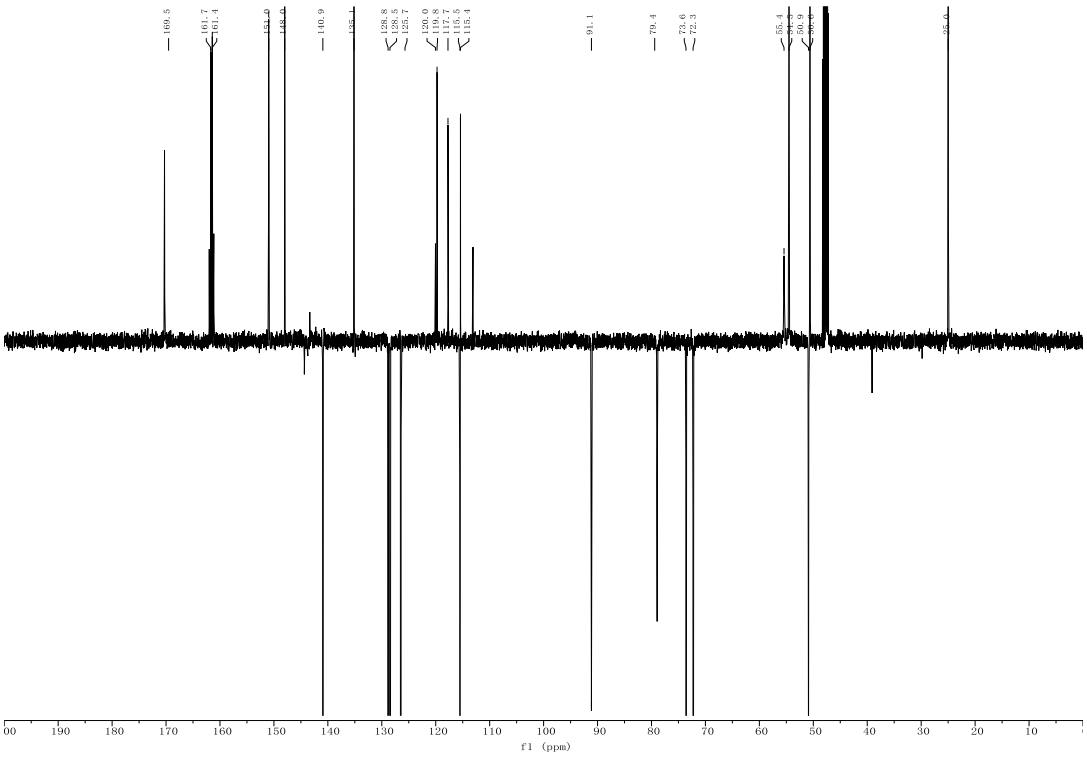

Compound **17y** ^{1}H NMR (500 MHz) CD_3OD

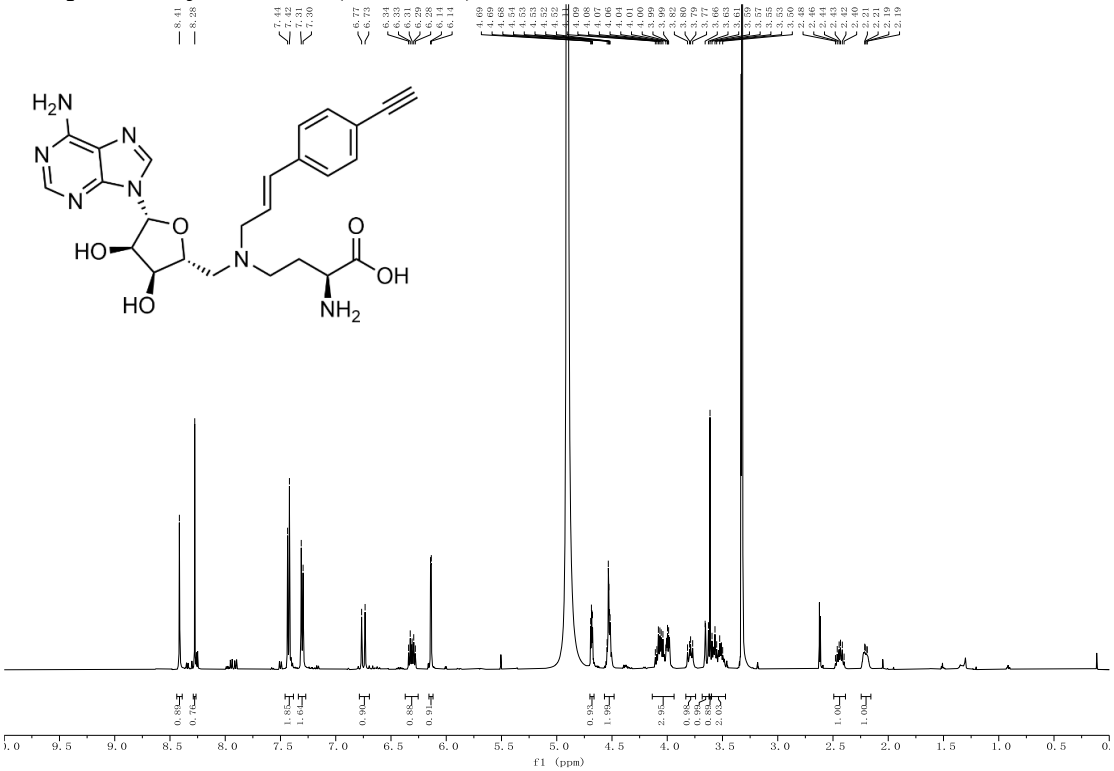

^{13}C NMR (126 MHz) CD_3OD

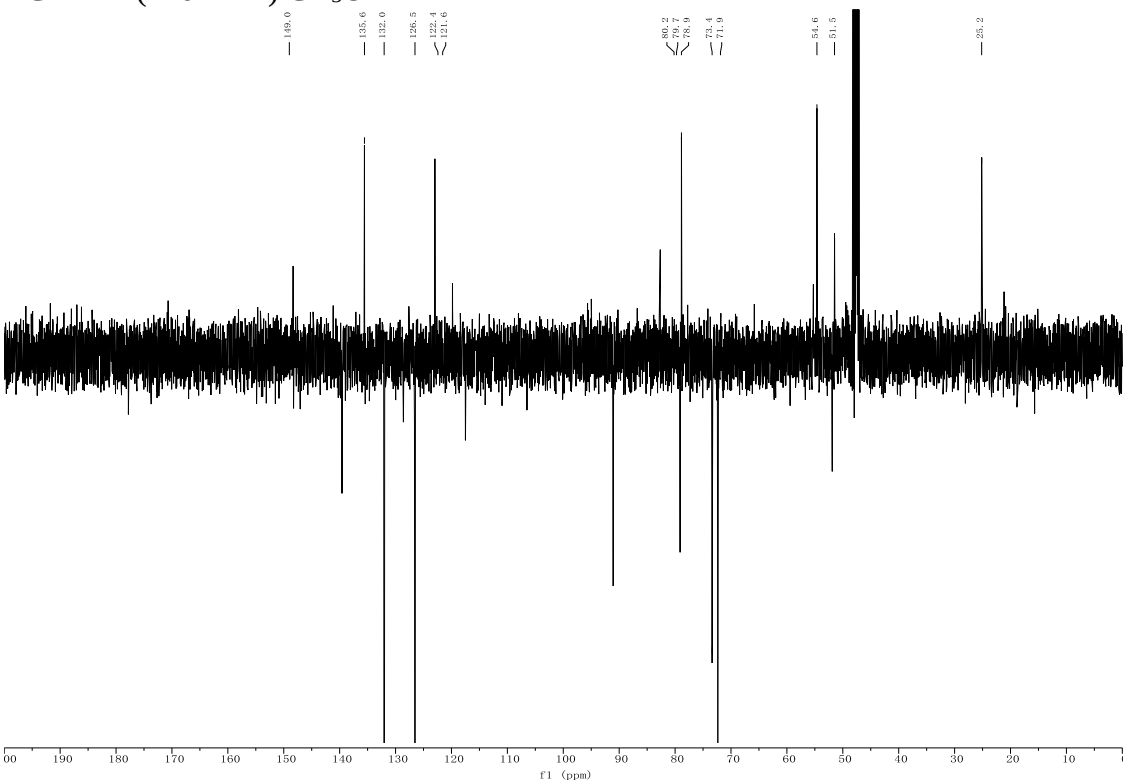

Compound **18** ^{1}H NMR (400 MHz) $CDCl_3$

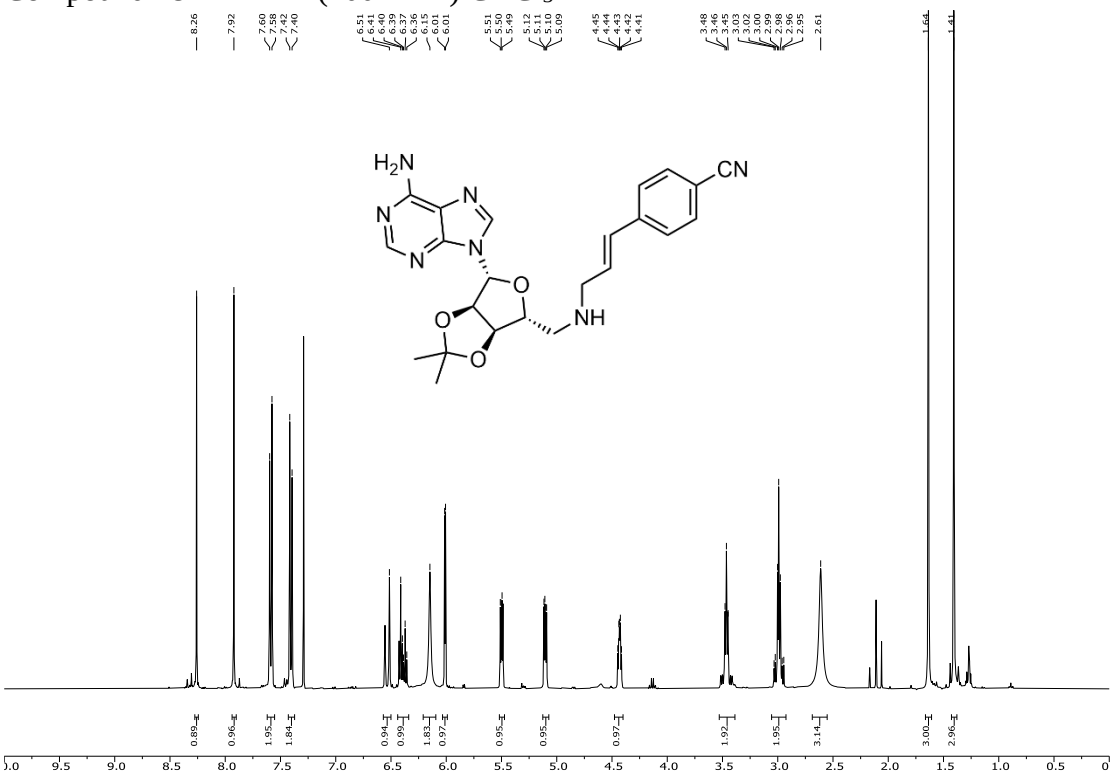

^{13}C NMR (101 MHz) $CDCl_3$

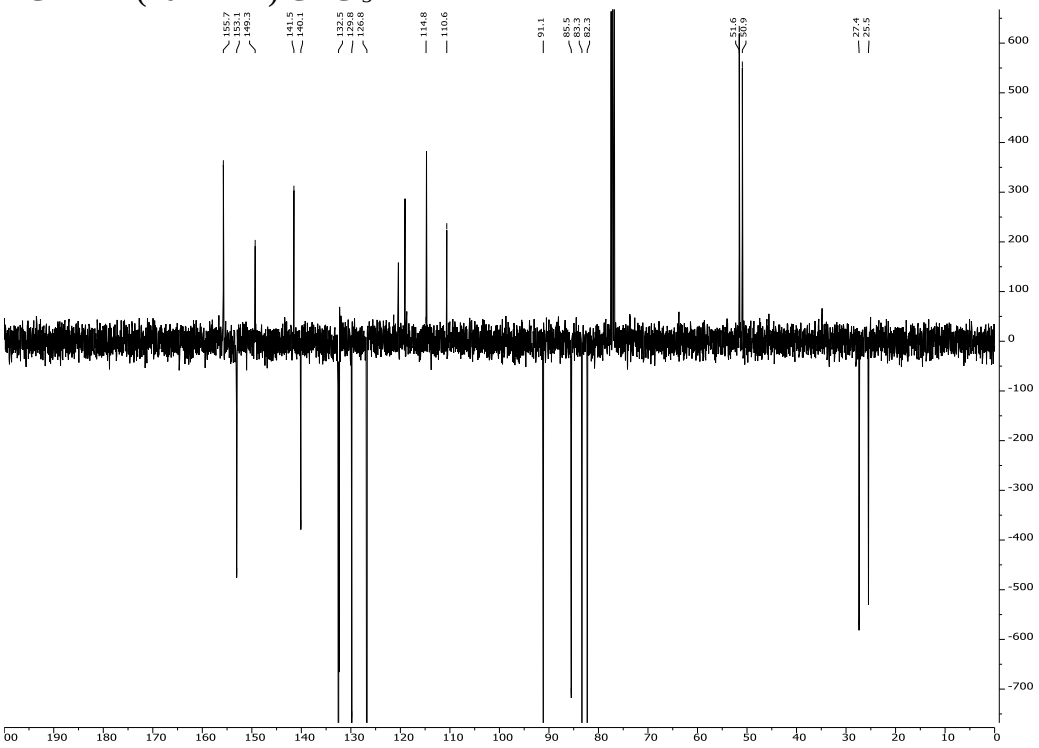

Compound **20a** ^{1}H NMR (400 MHz) $CDCl_3$

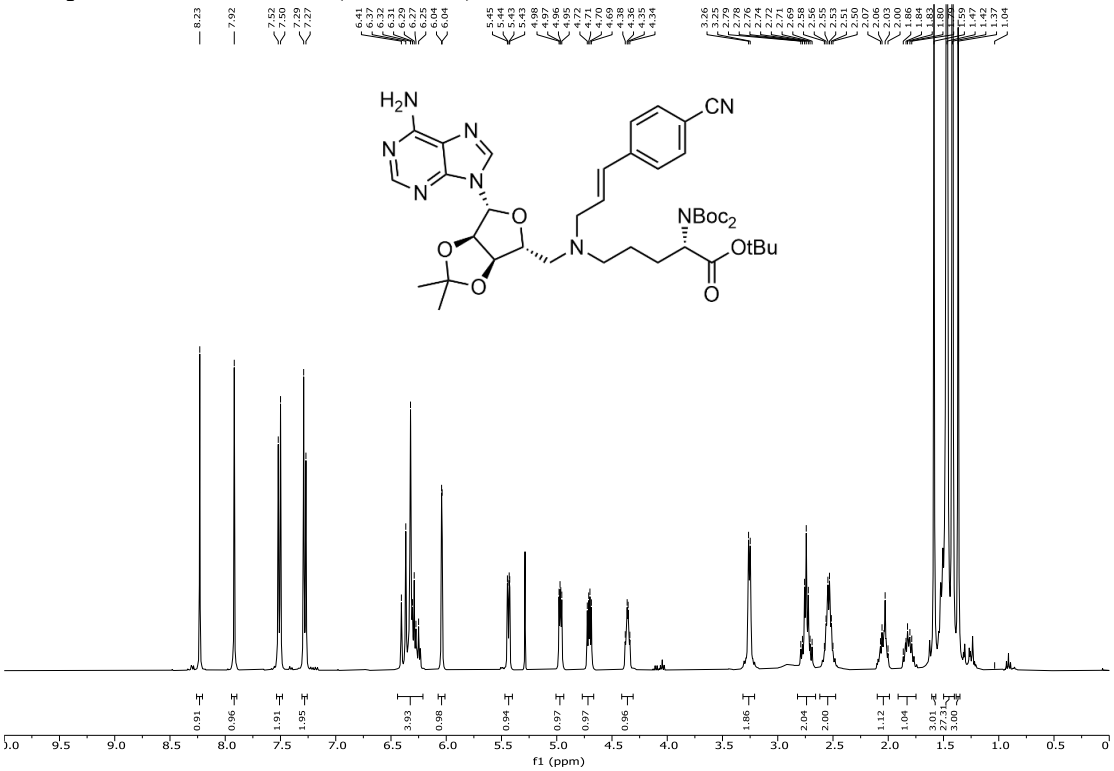

^{13}C NMR (101 MHz) $CDCl_3$

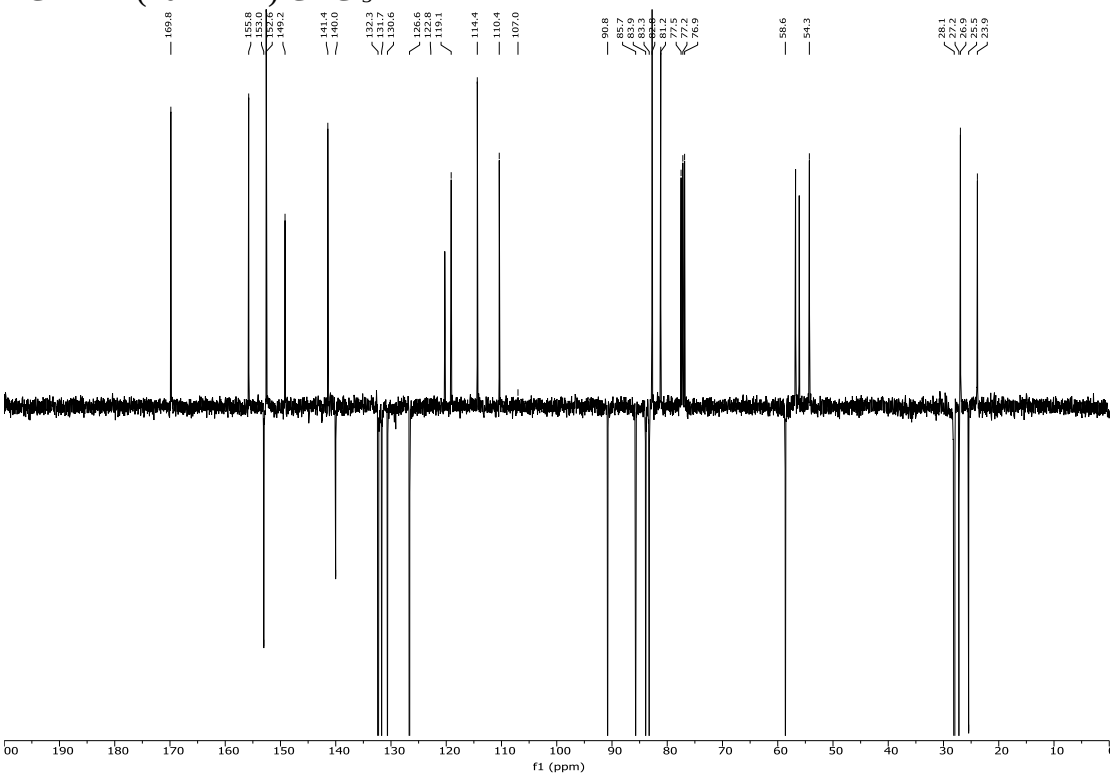

Compound **20b** ^{1}H NMR (400 MHz) $CDCl_3$

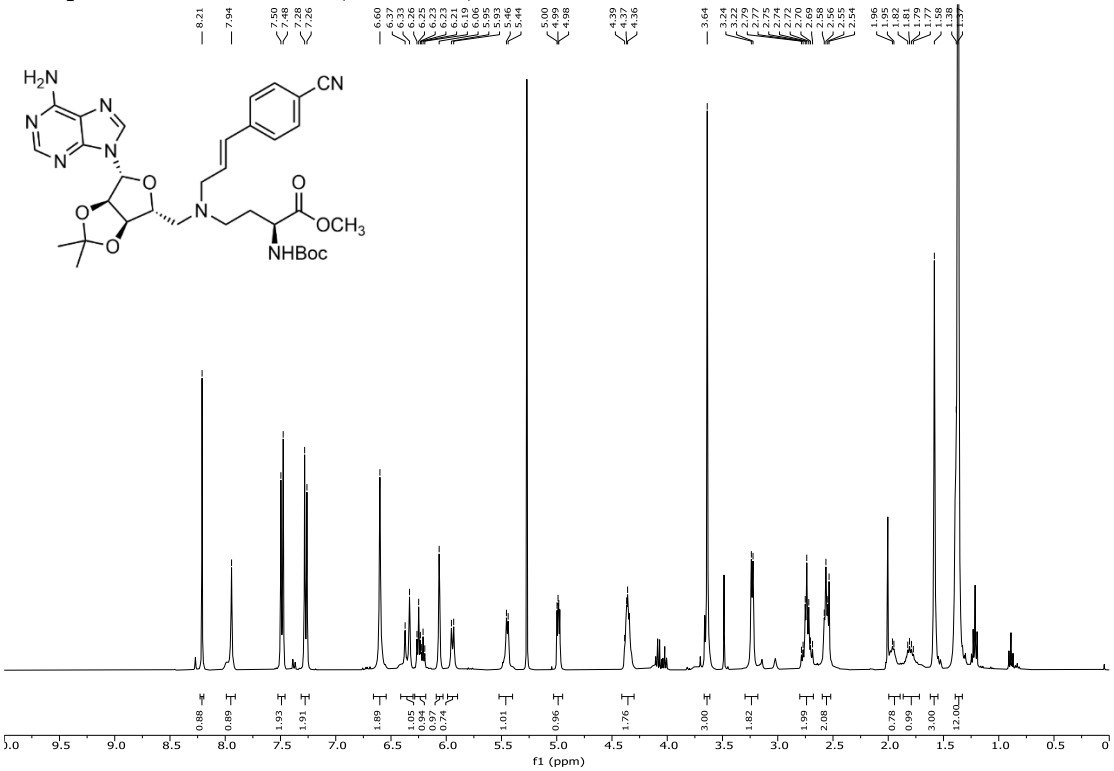

^{13}C NMR (101 MHz) $CDCl_3$

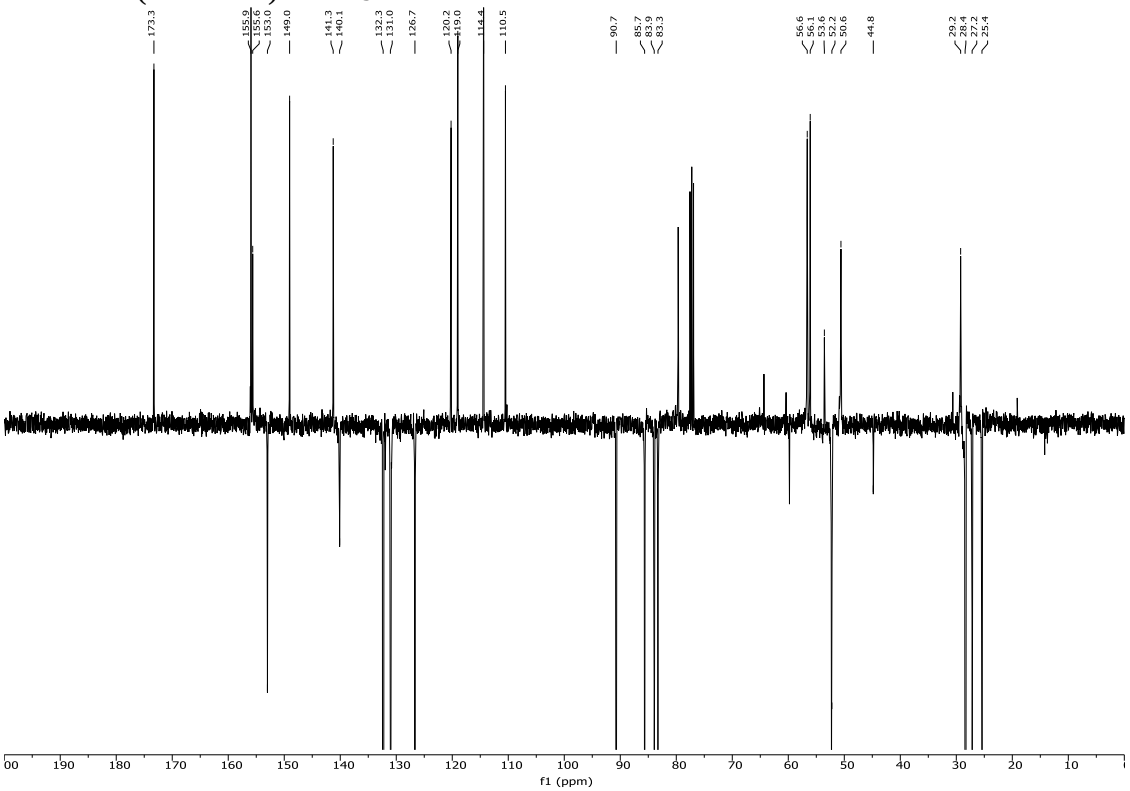

Compound **20c** ^{1}H NMR (400 MHz) $CDCl_3$

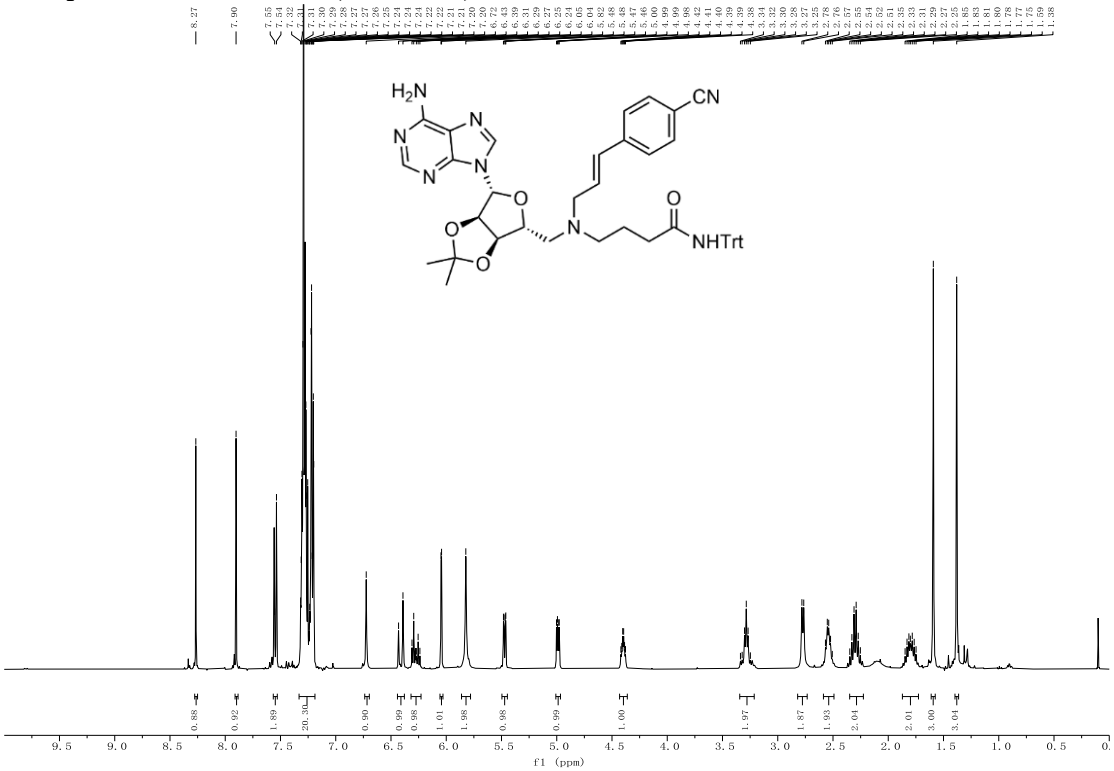

^{13}C NMR (101 MHz) $CDCl_3$

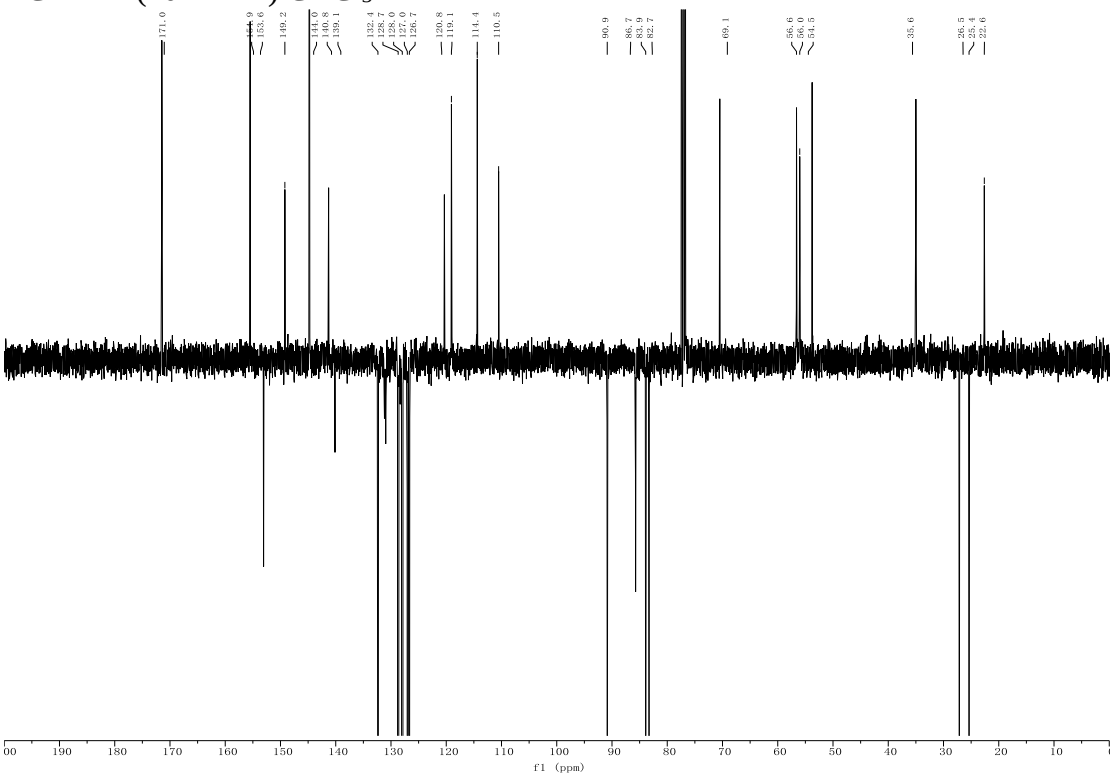

Compound **20d** ^{1}H NMR (500 MHz) $CDCl_3$

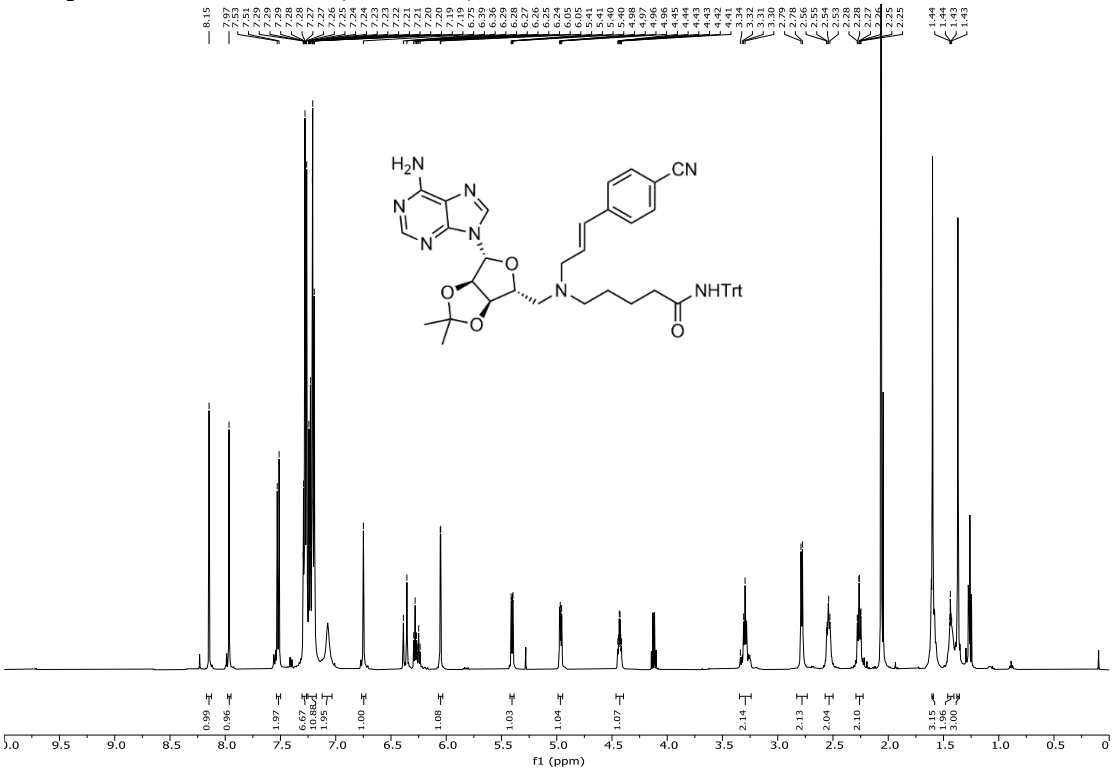

^{13}C NMR (126 MHz) $CDCl_3$

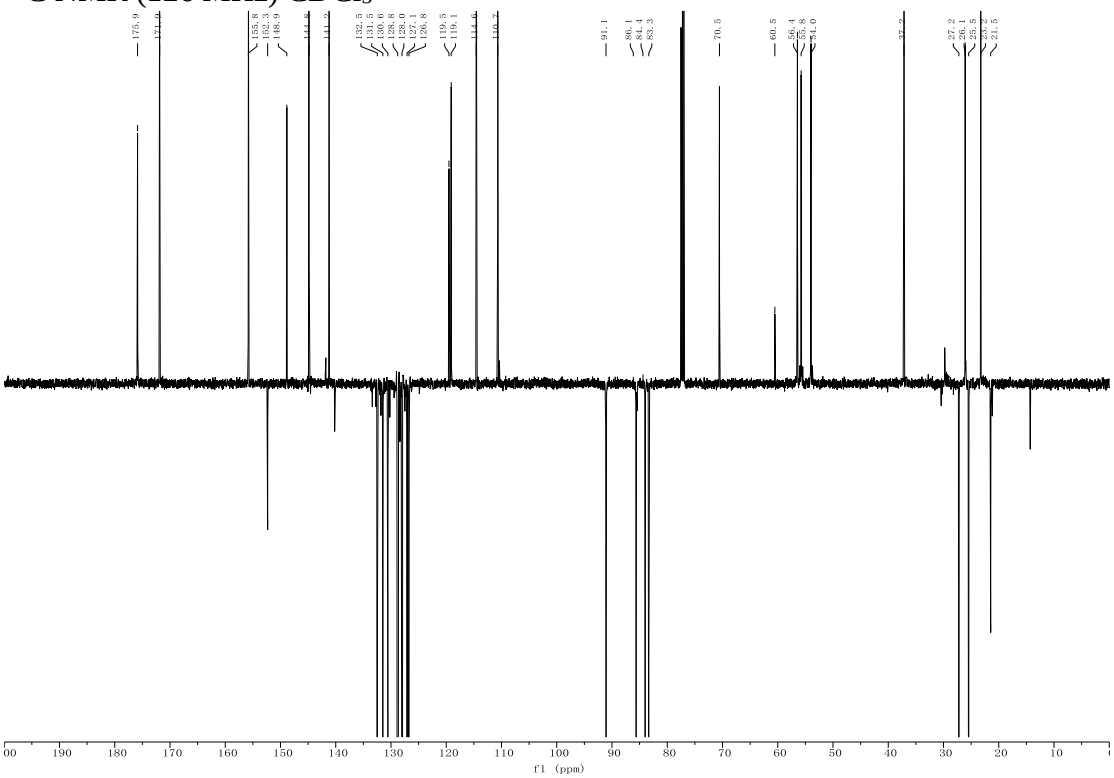

Compound **20e** ^{1}H NMR (500 MHz) $CDCl_3$

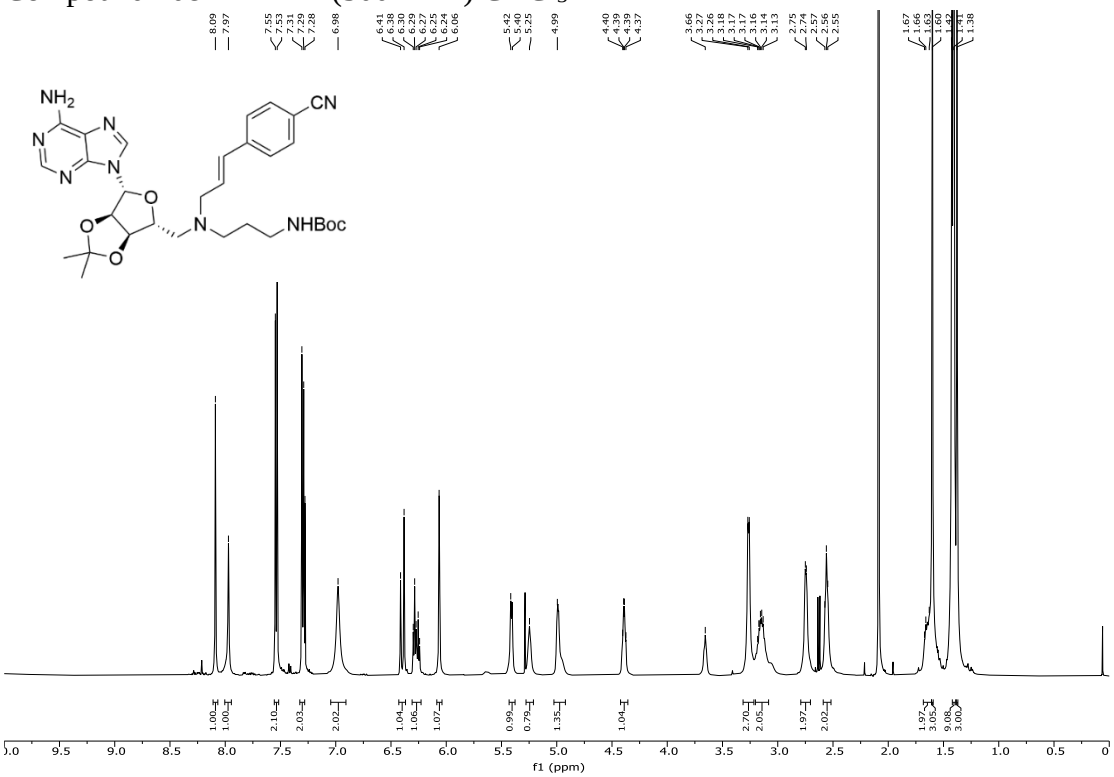

^{13}C NMR (126 MHz) $CDCl_3$

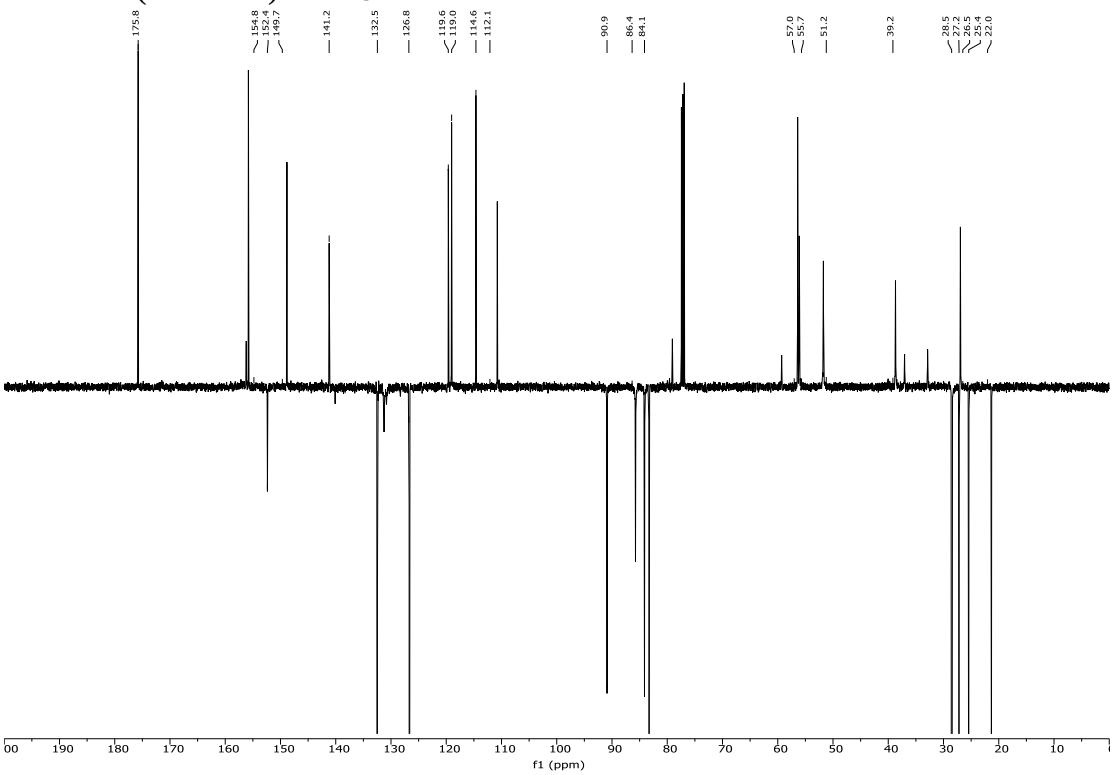

Compound **20f** ^{1}H NMR (400 MHz) $CDCl_3$

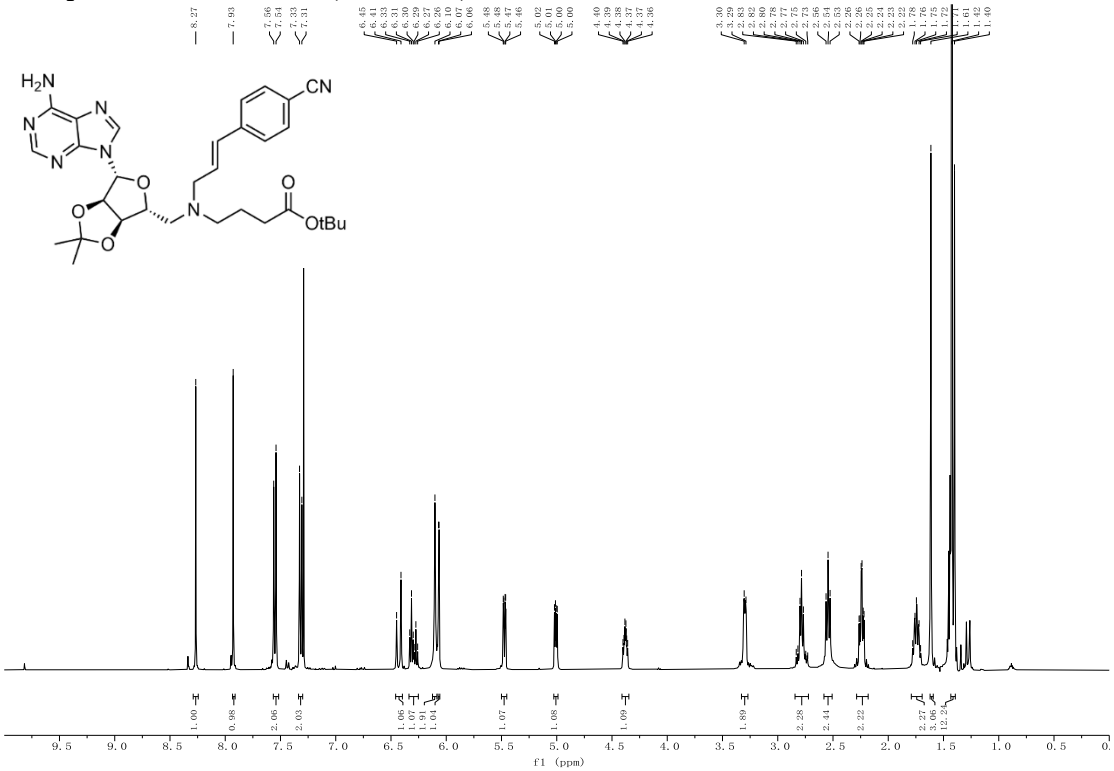

^{13}C NMR (101 MHz) $CDCl_3$

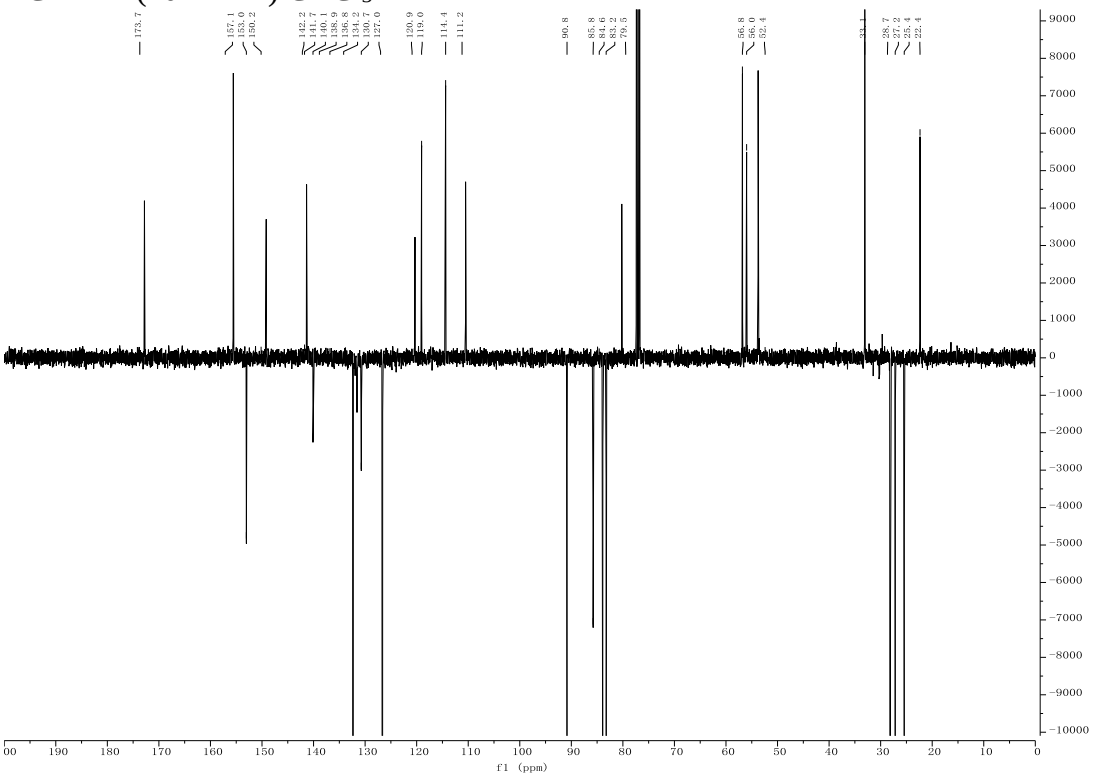

Compound**20g** ^{1}H NMR (500 MHz) $CDCl_3$

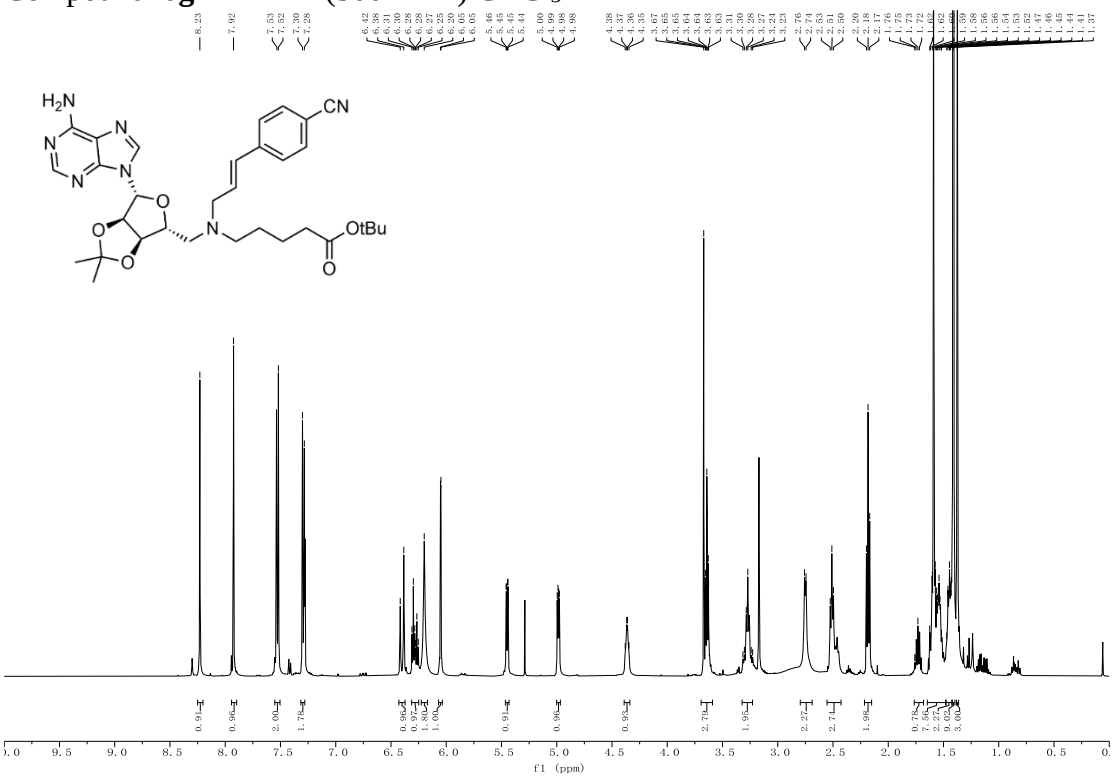

^{13}C NMR (126 MHz) $CDCl_3$

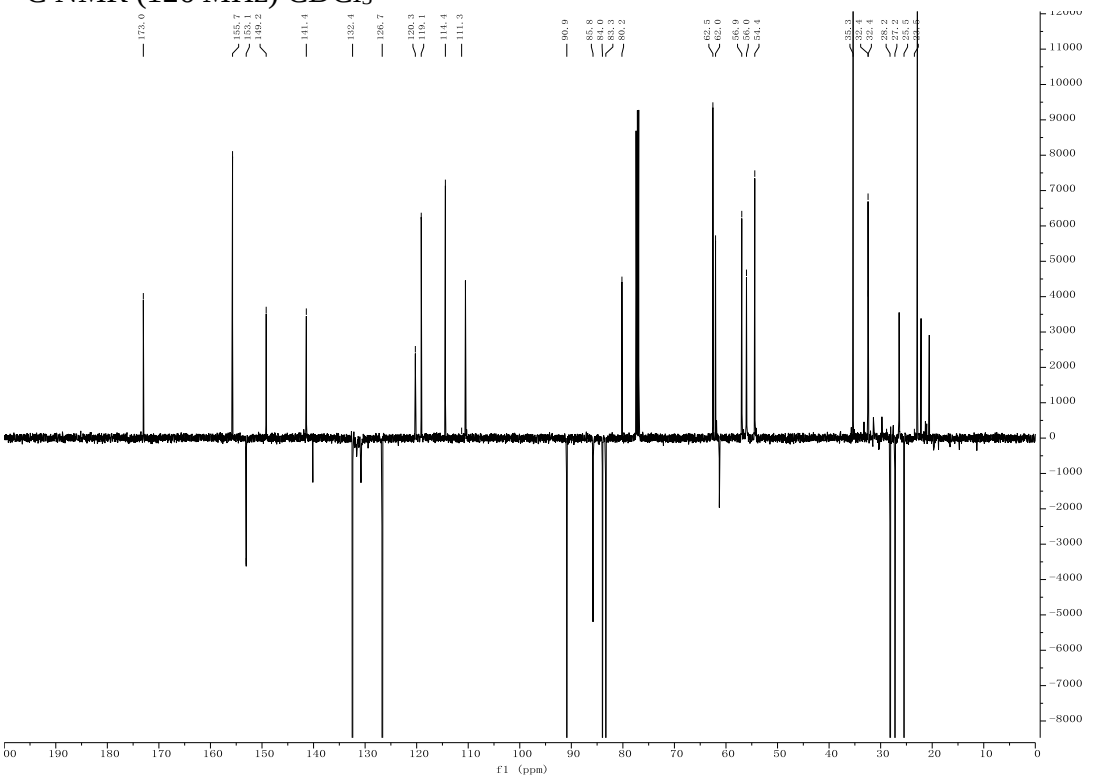

Compound **20h** ^{1}H NMR (400 MHz) $CDCl_3$

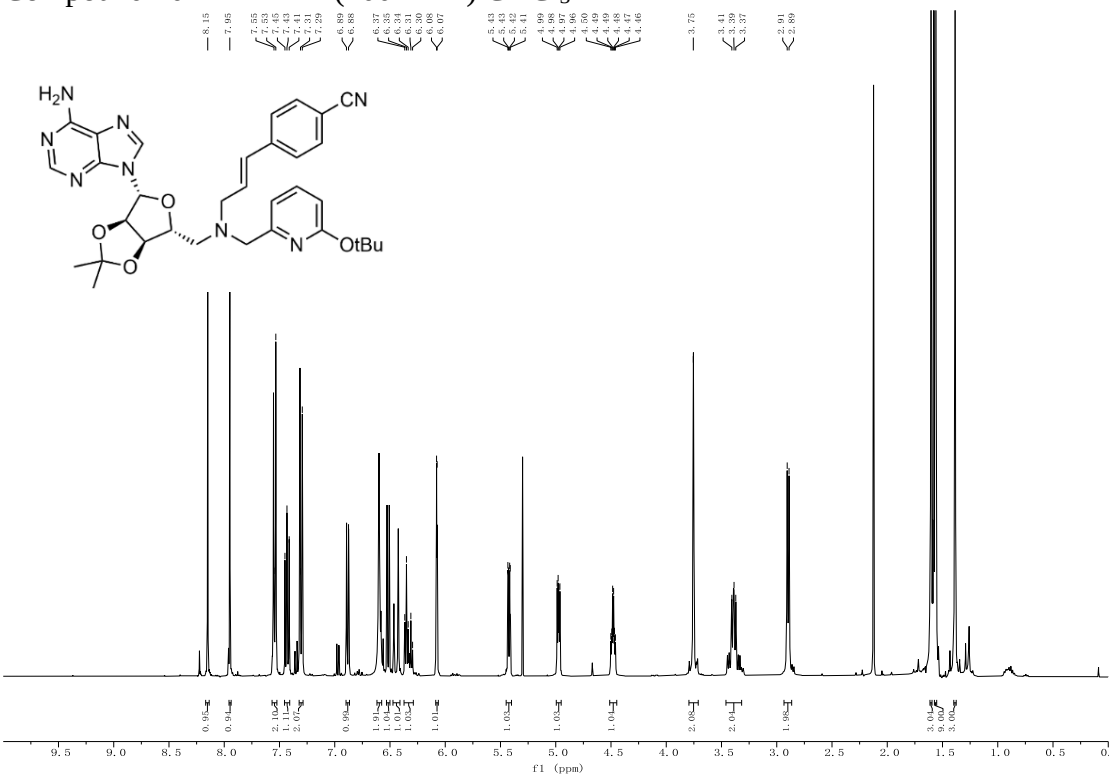

^{13}C NMR (101 MHz) $CDCl_3$

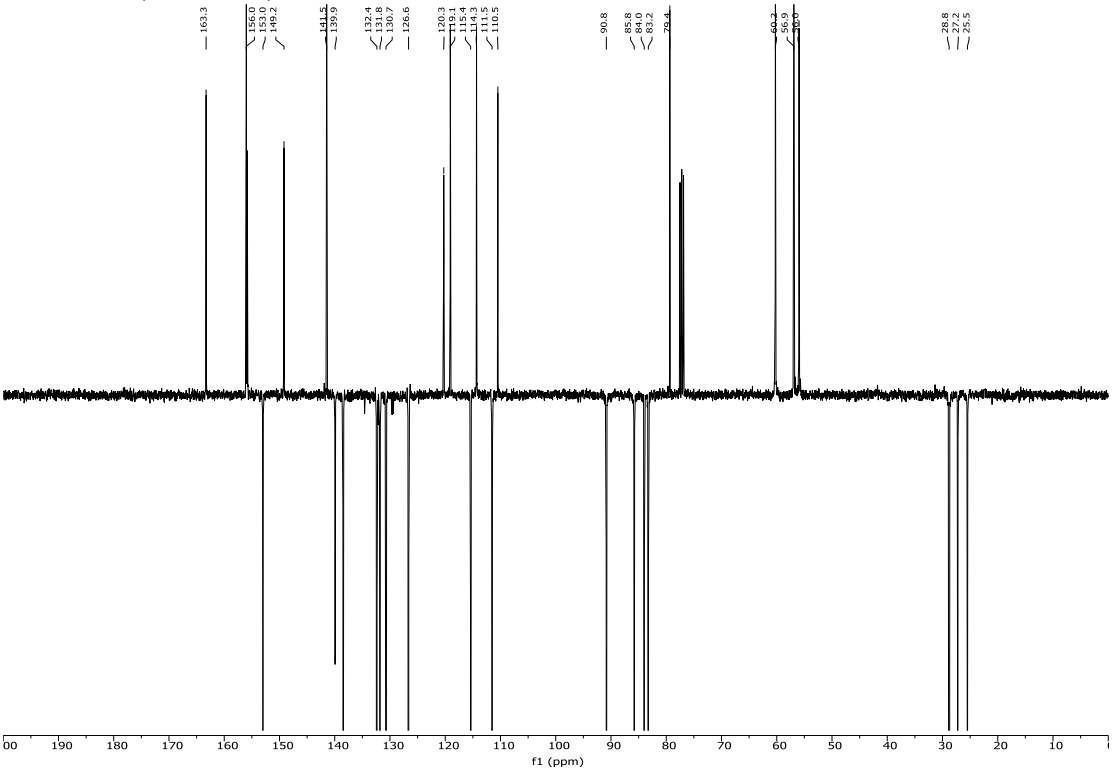

Compound **20j** ^{1}H NMR (400 MHz) $CDCl_3$

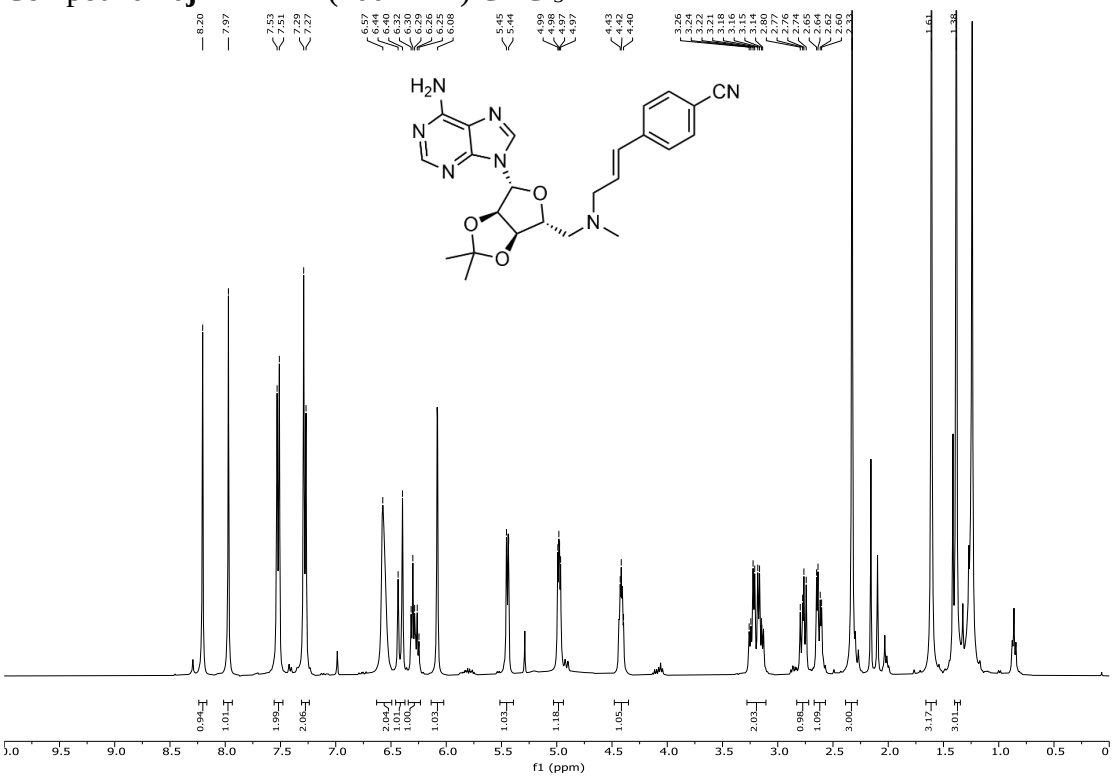

^{13}C NMR (101 MHz) $CDCl_3$

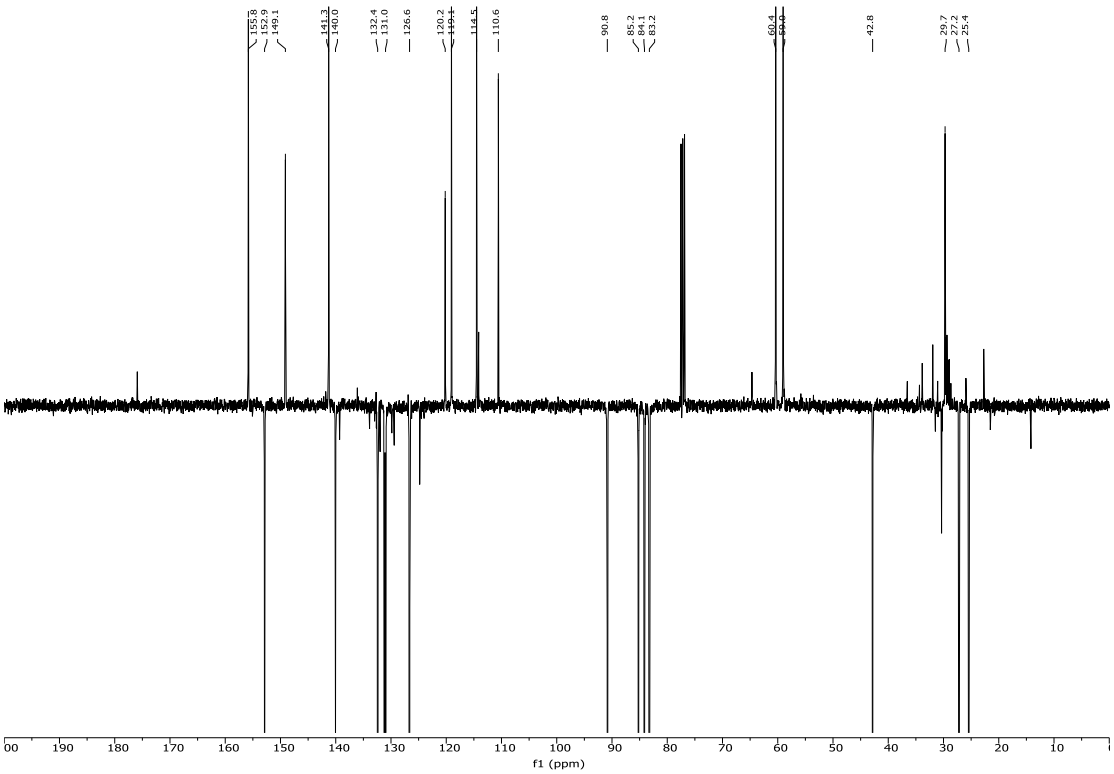

Compound **20k** ^{1}H NMR (400 MHz) $CDCl_3$

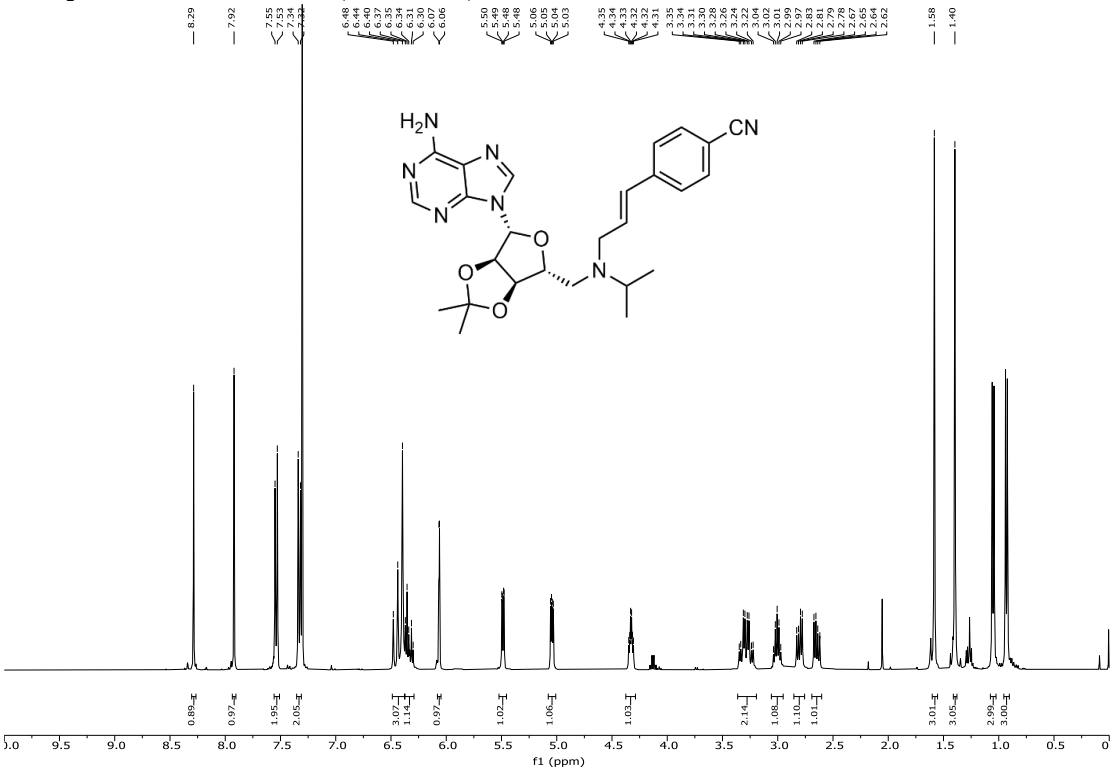

^{13}C NMR (101 MHz) $CDCl_3$

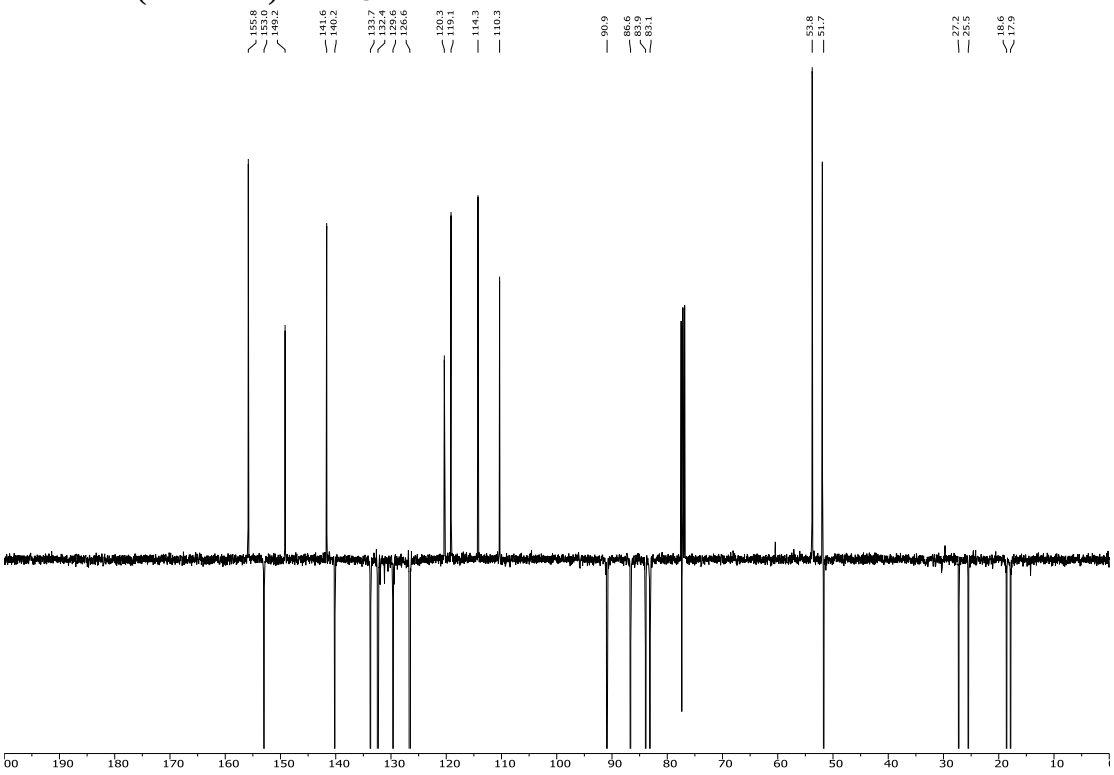

Compound **21a** ^{1}H NMR (400 MHz) CD_3OD

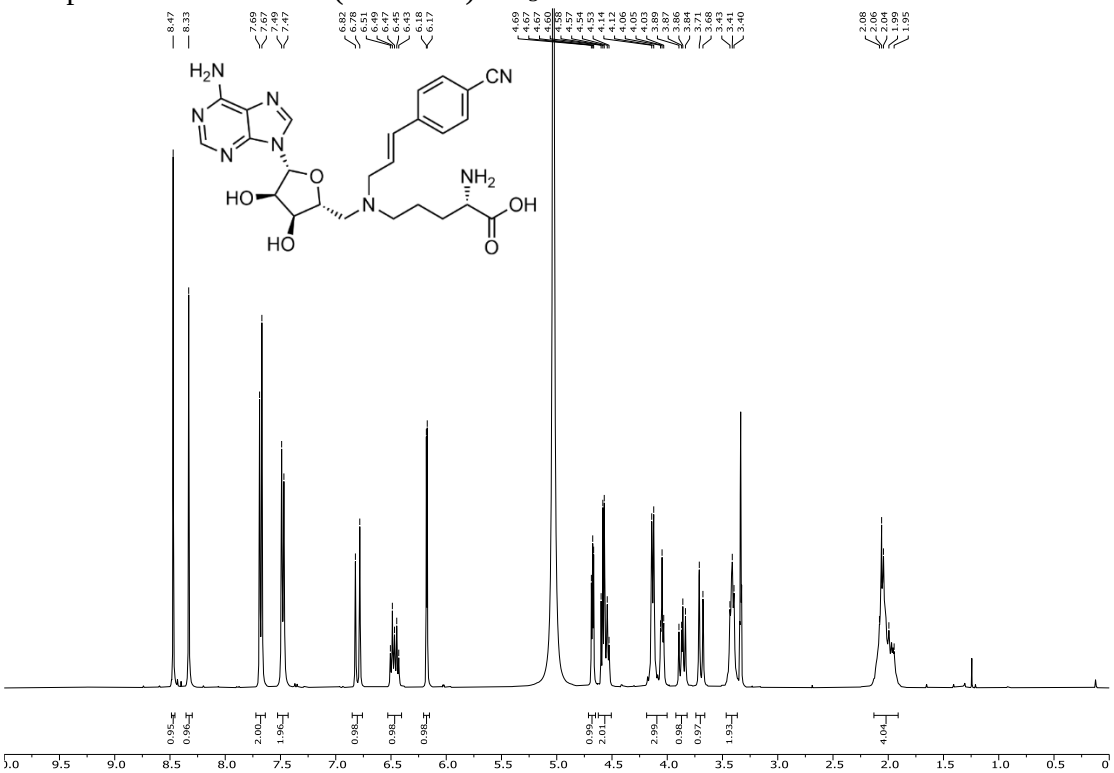

^{13}C NMR (101 MHz) CD_3OD

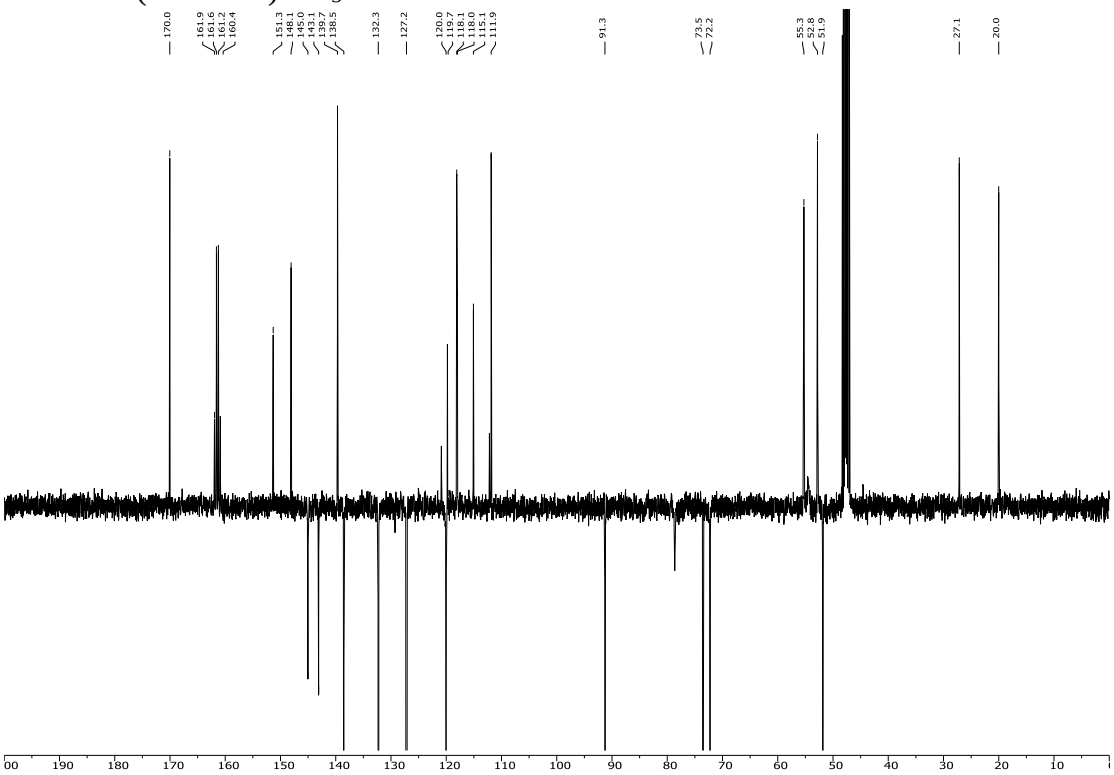

Compound **21b** ^{1}H NMR (400 MHz) CD_3OD

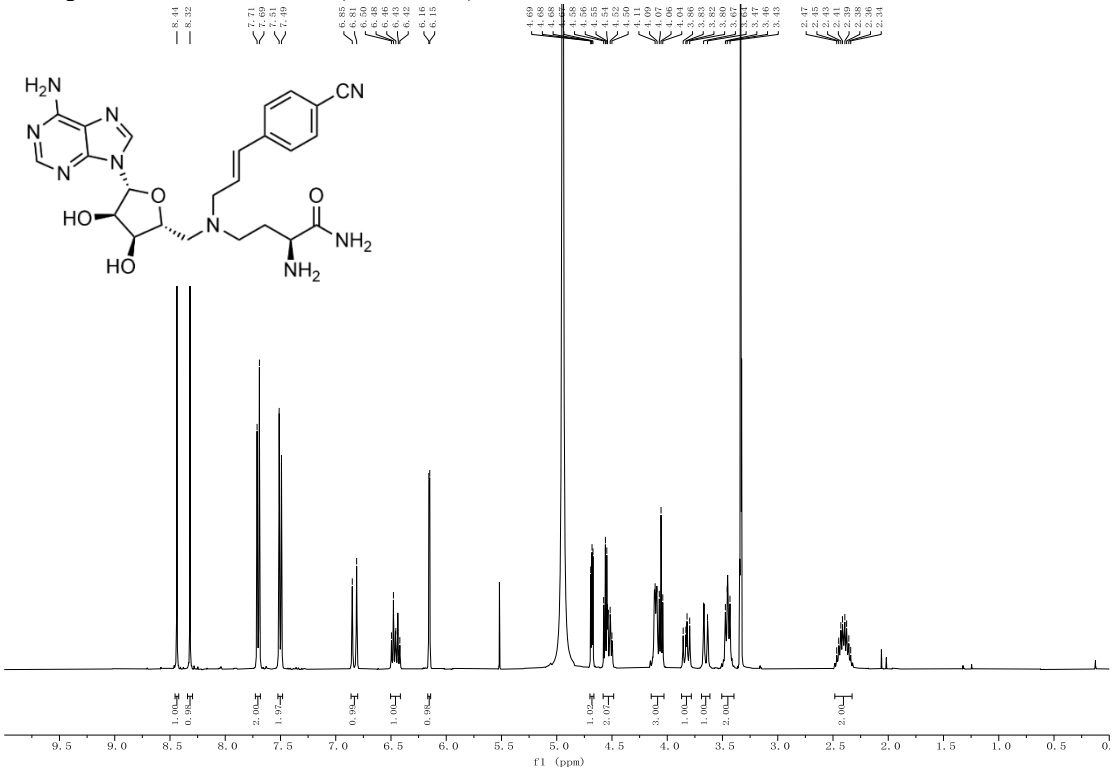

^{13}C NMR (101 MHz) CD_3OD

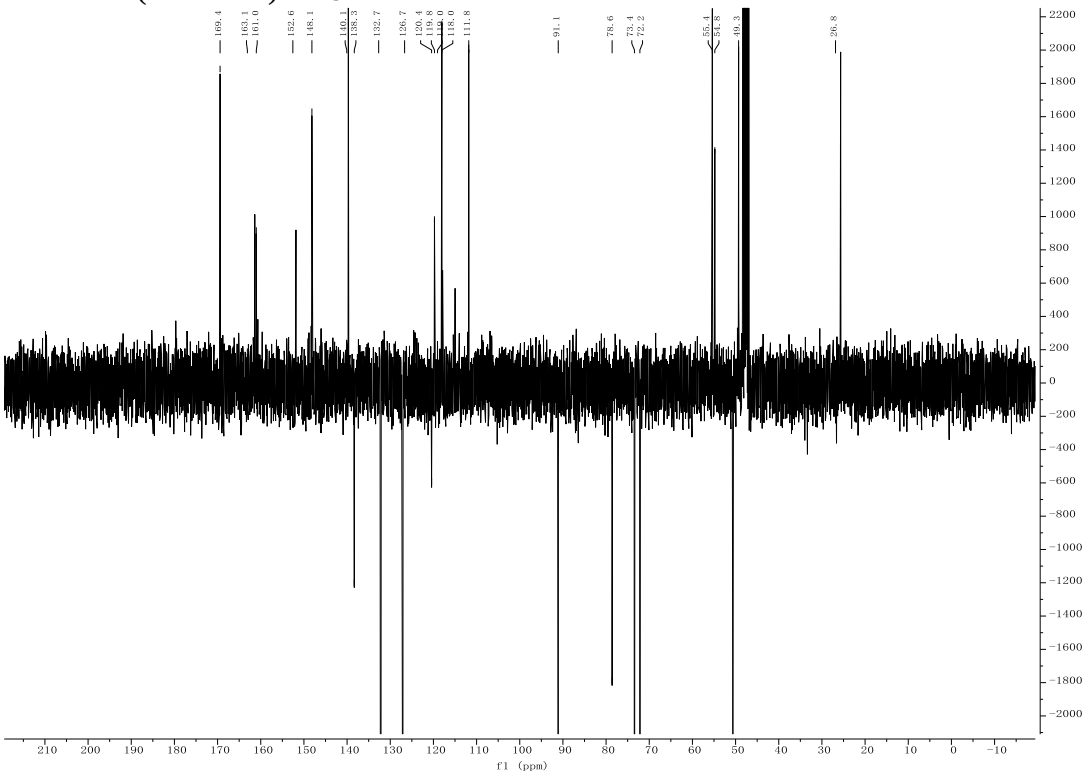

Compound **21c** ^{1}H NMR (400 MHz) CD_3OD

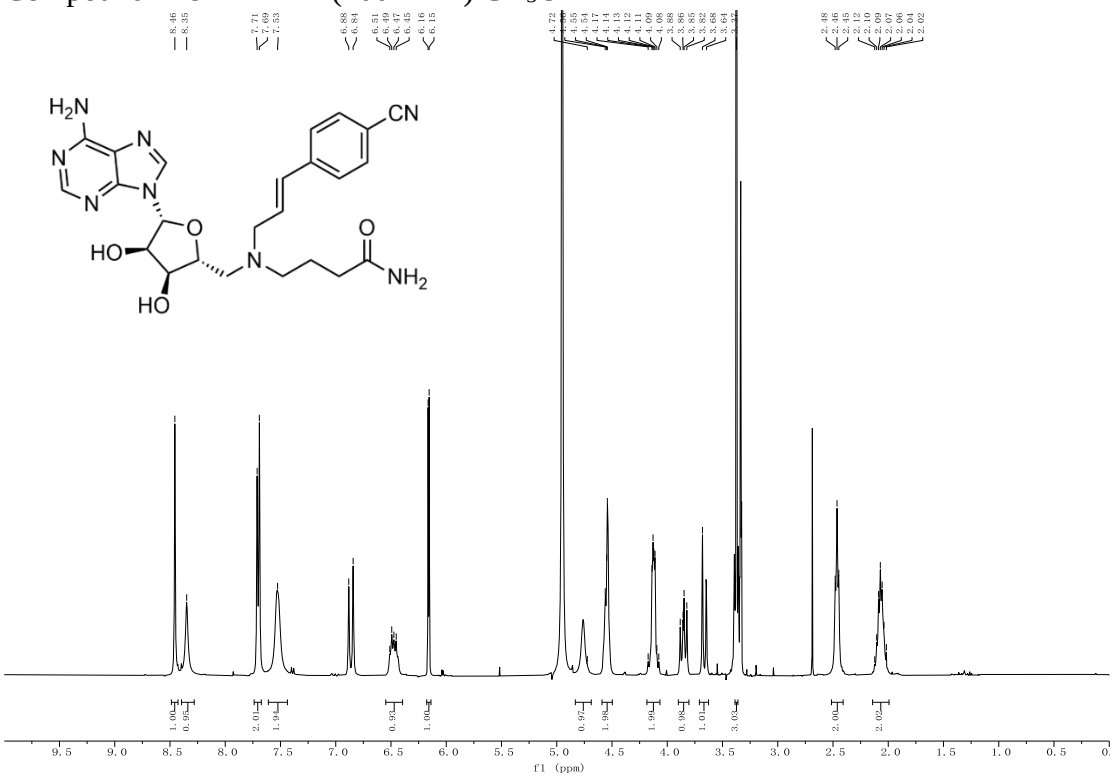

^{13}C NMR (101 MHz) CD_3OD

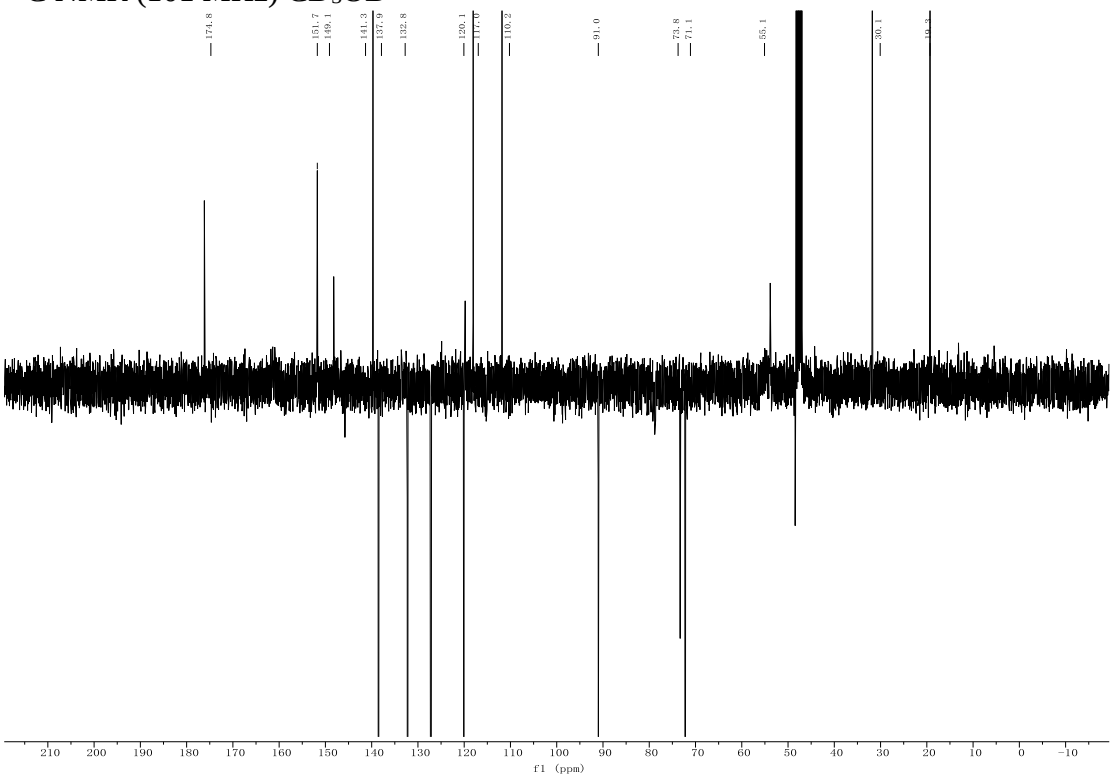

Compound **21d** ^{1}H NMR (400 MHz) CD_3OD

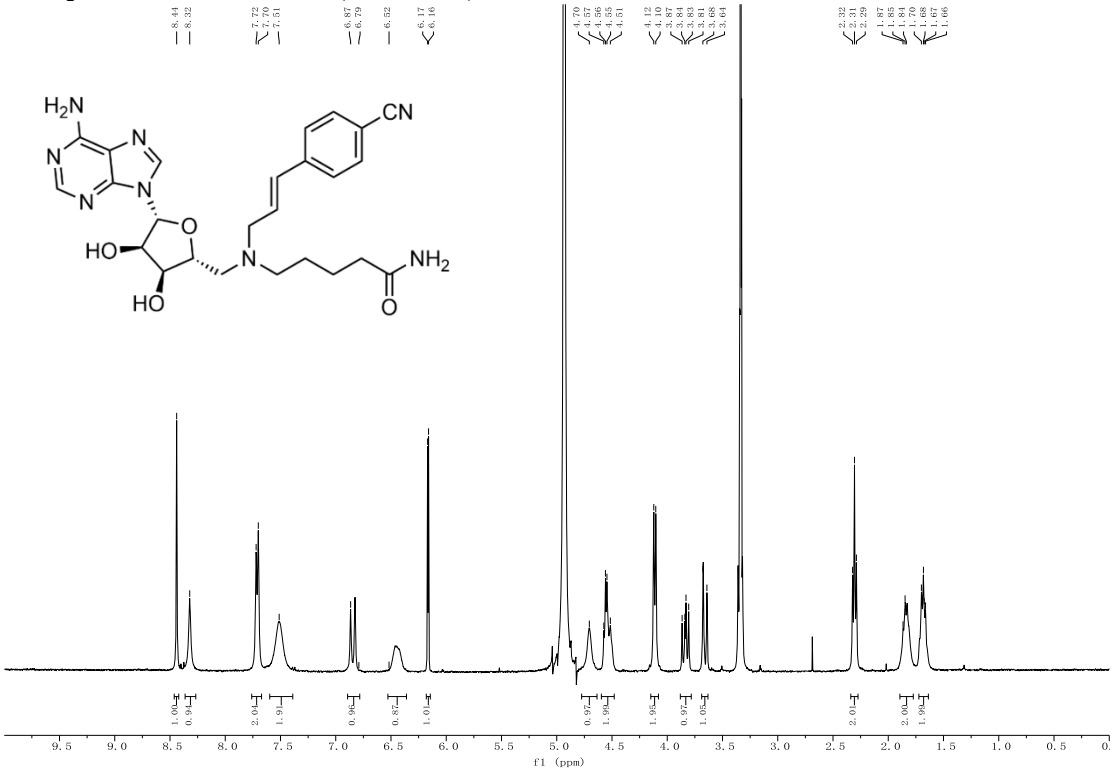

^{13}C NMR (101 MHz) CD_3OD

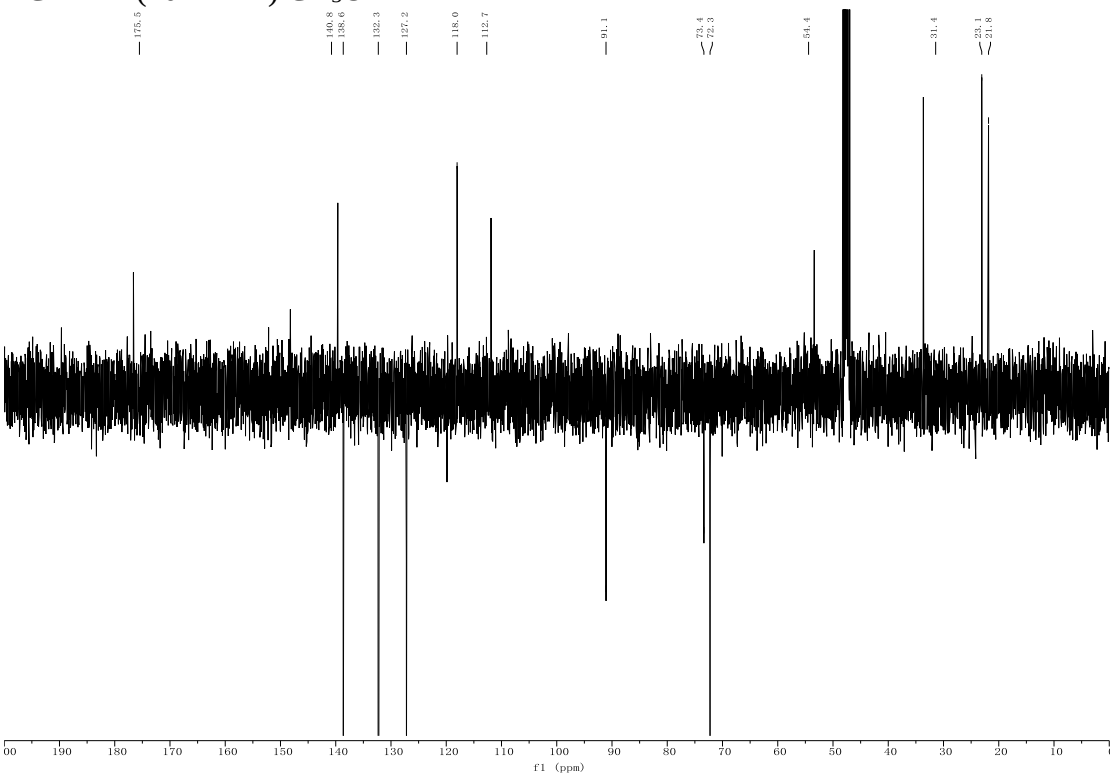

Compound **21e** ^{1}H NMR (500 MHz) CD_3OD

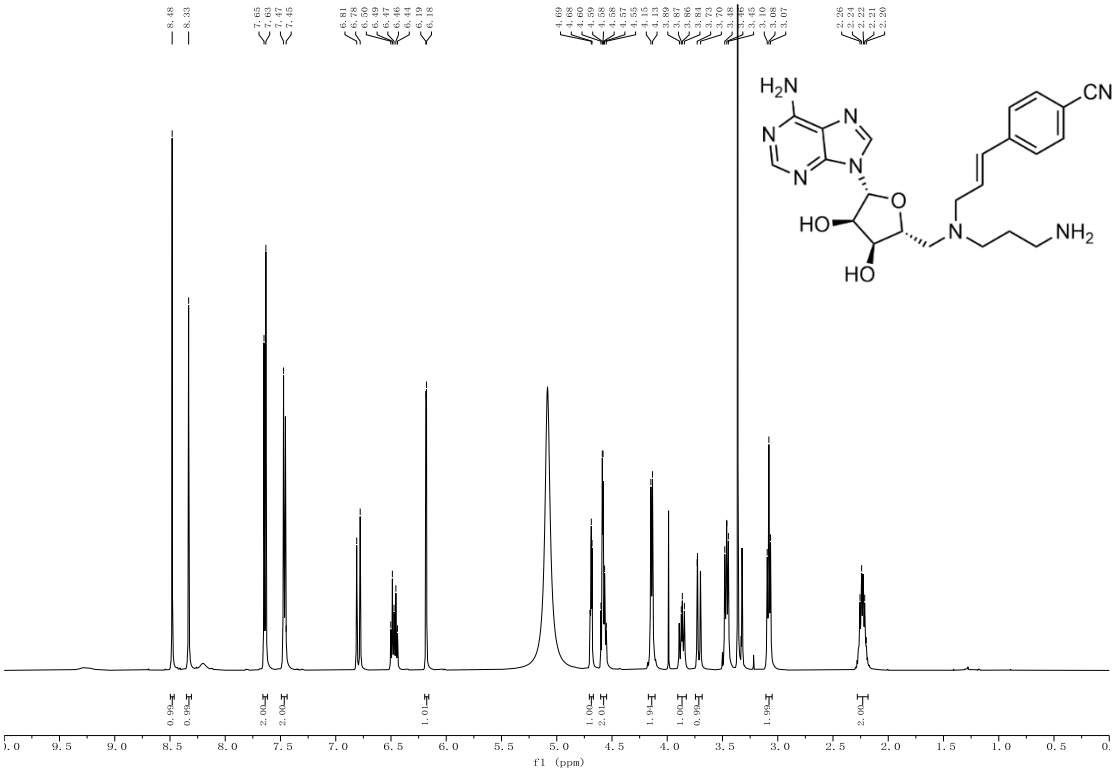

^{13}C NMR (126 MHz) CD_3OD

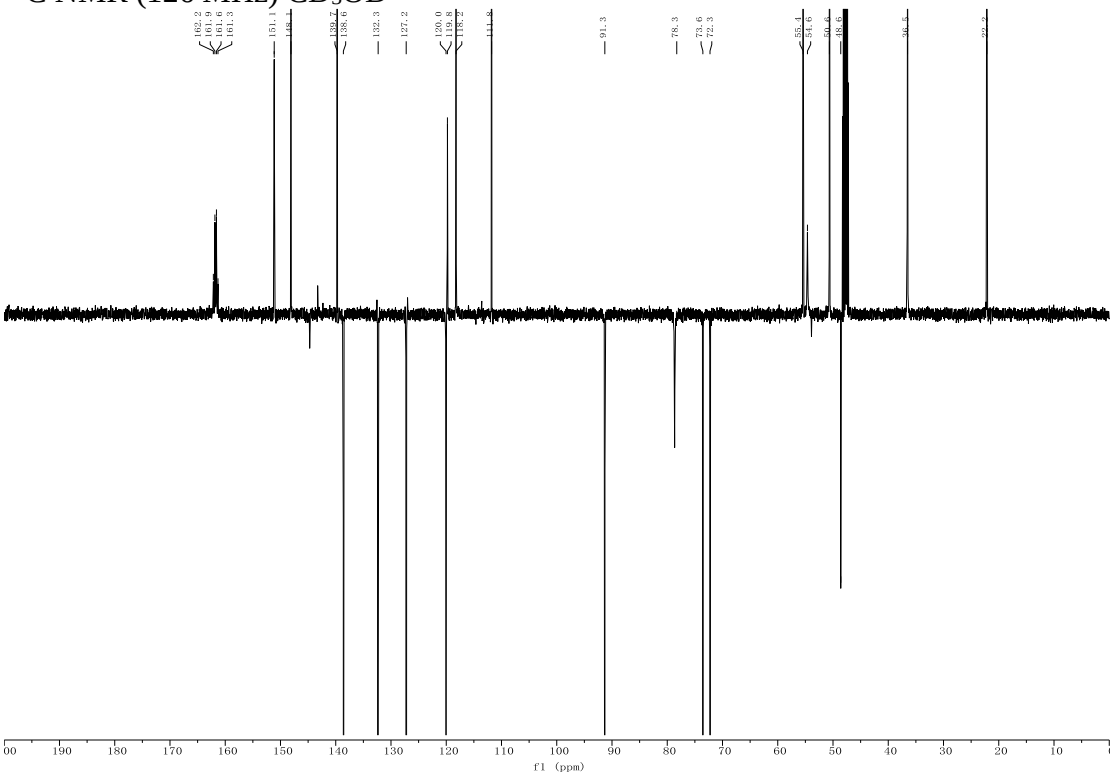

Compound **21f** ^{1}H NMR (400 MHz) CD_3OD

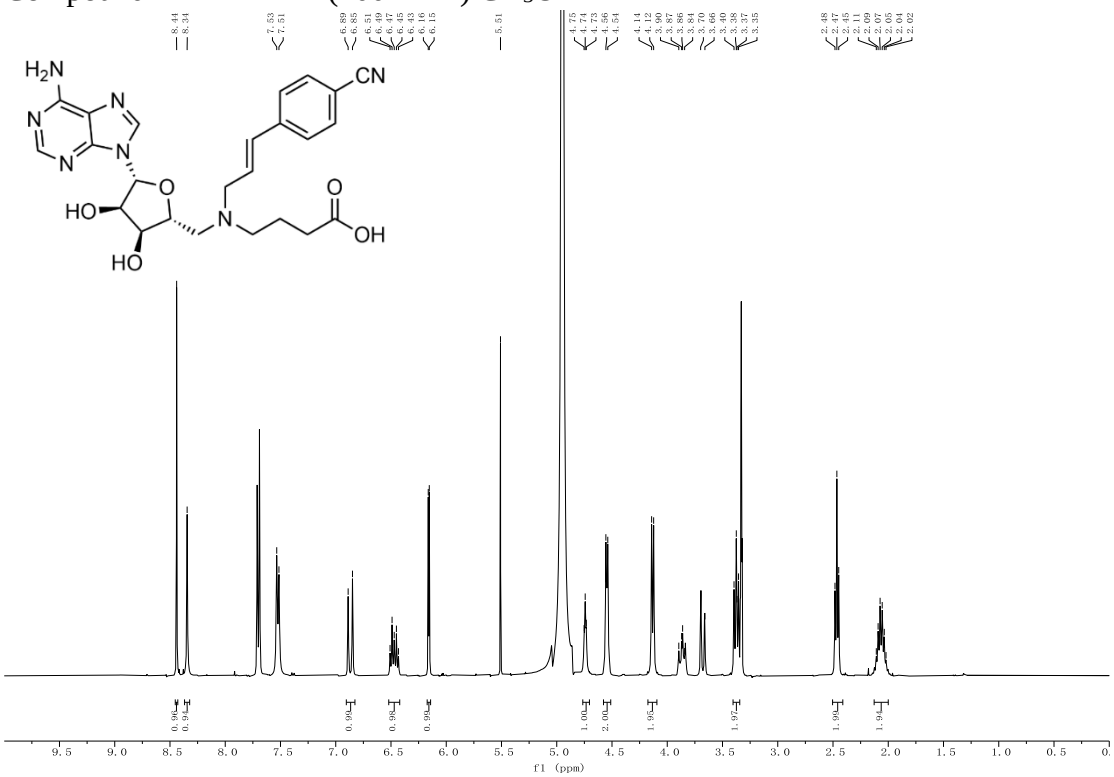

^{13}C NMR (101 MHz) CD_3OD

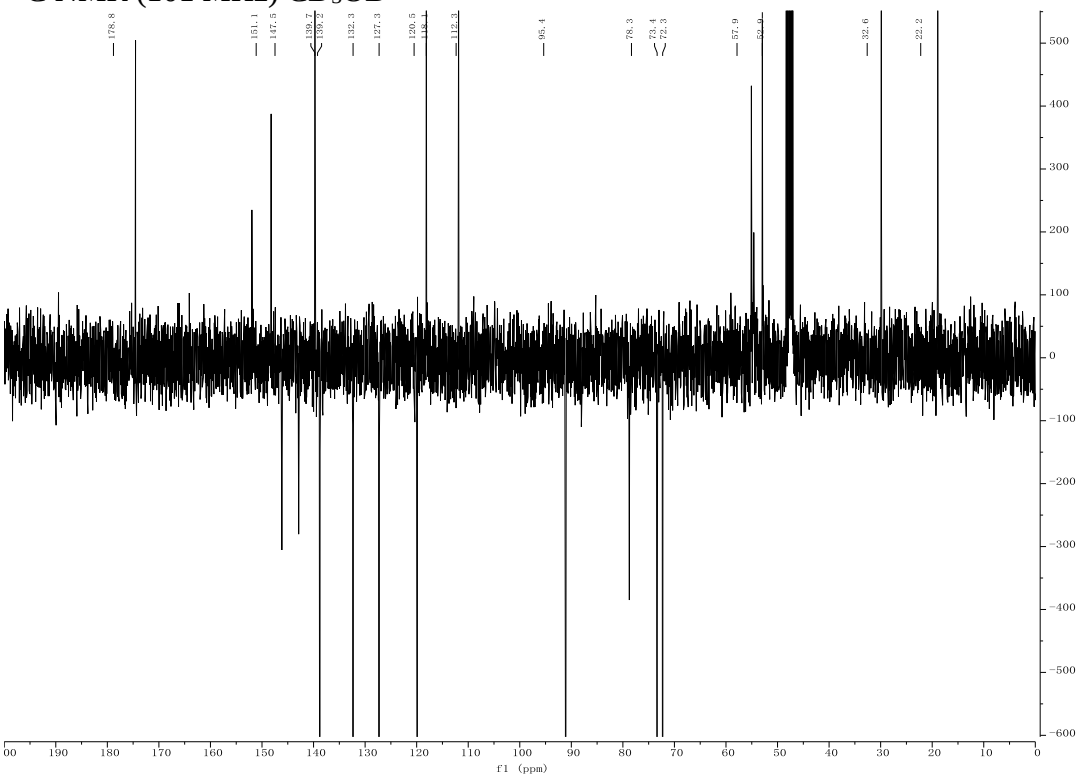

Compound **21g** ^{1}H NMR (400 MHz) CD_3OD

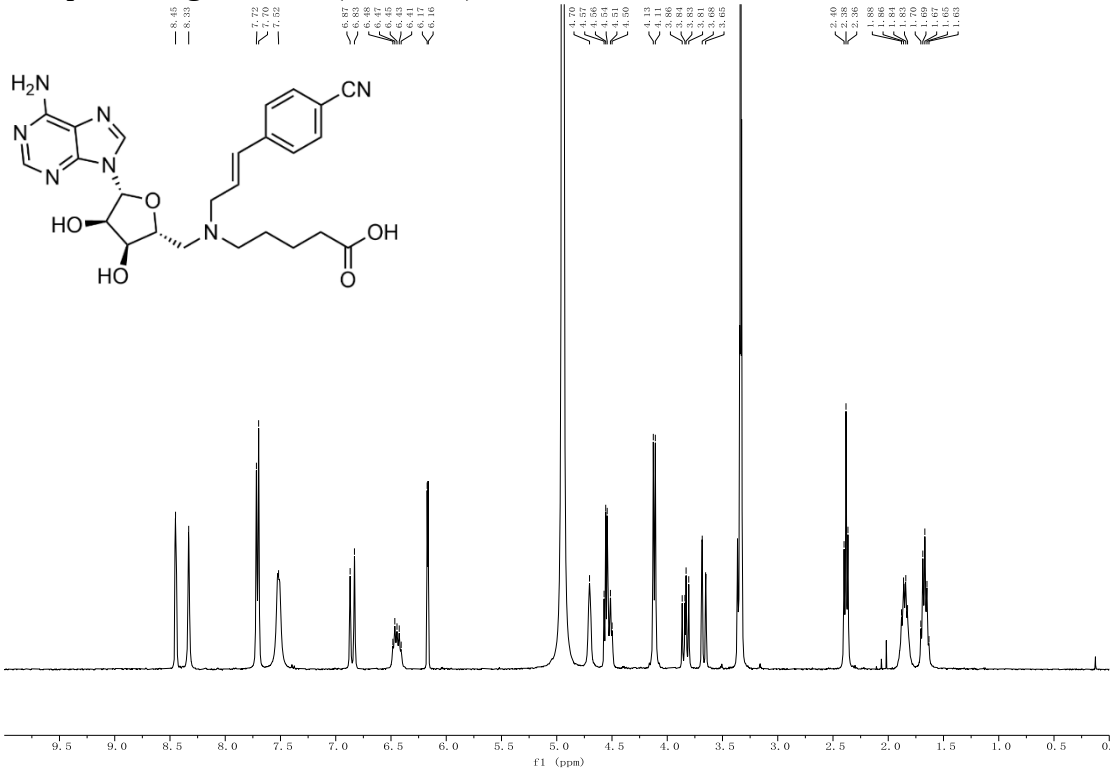

^{13}C NMR (101 MHz) CD_3OD

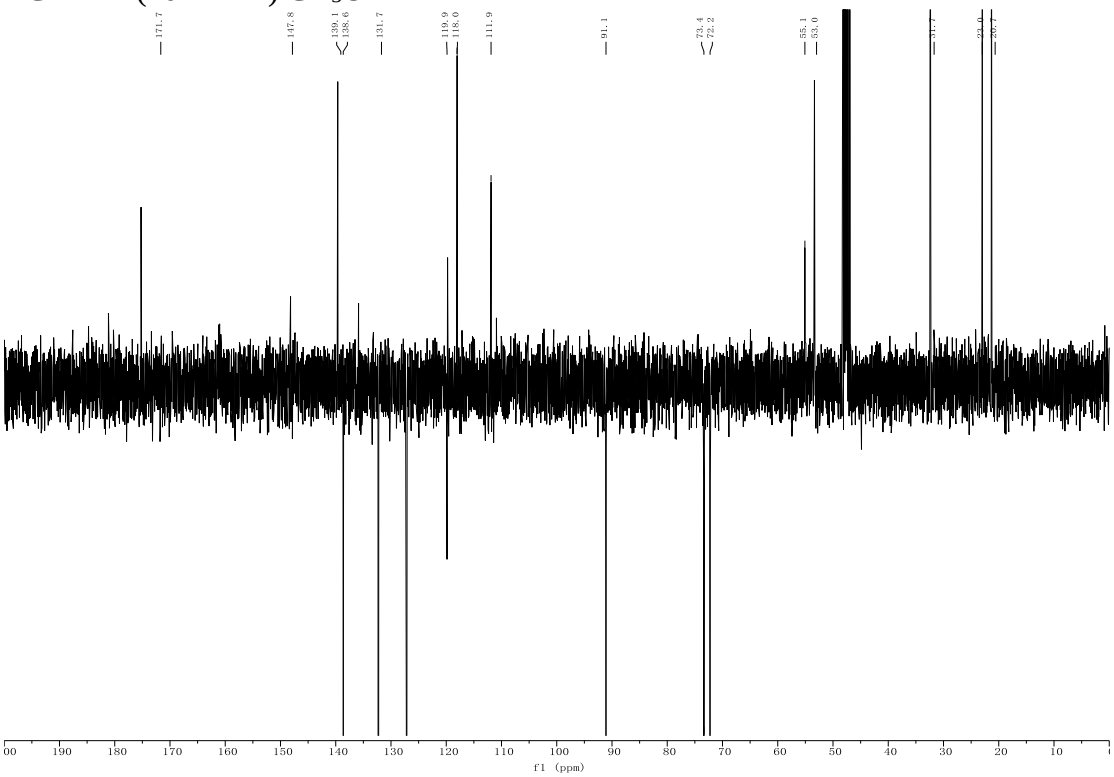

Compound **21h** ^{1}H NMR (400 MHz) CD_3OD

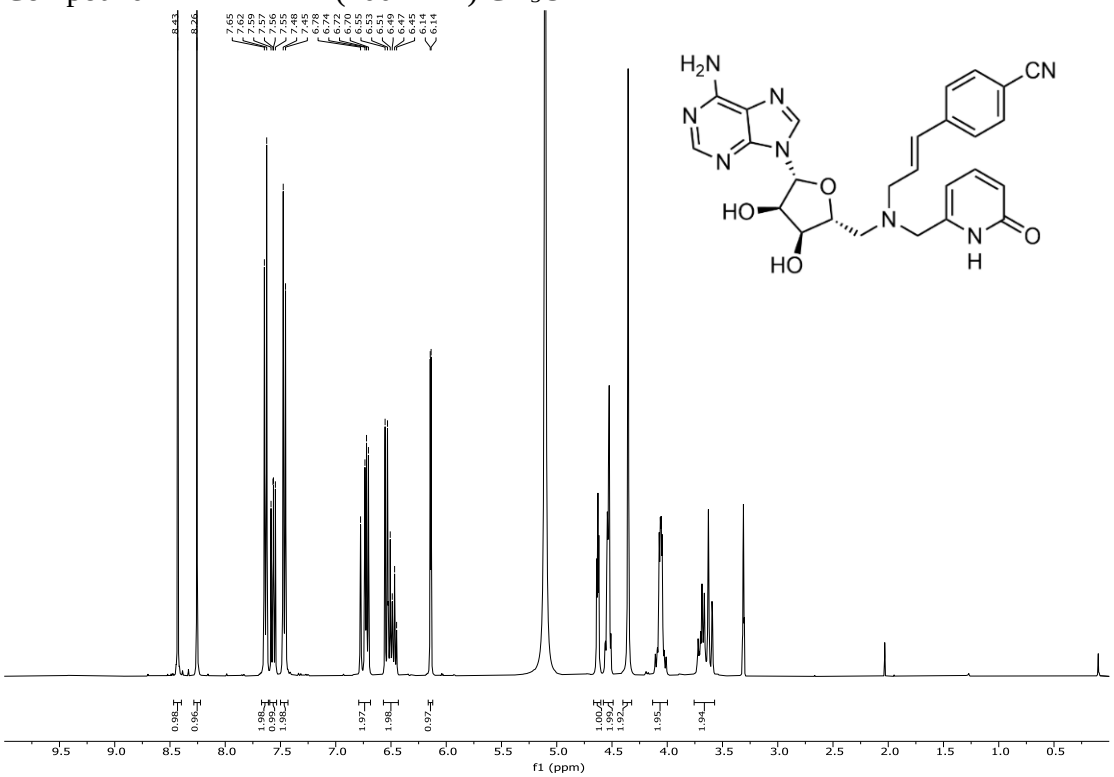

^{13}C NMR (101 MHz) CD_3OD

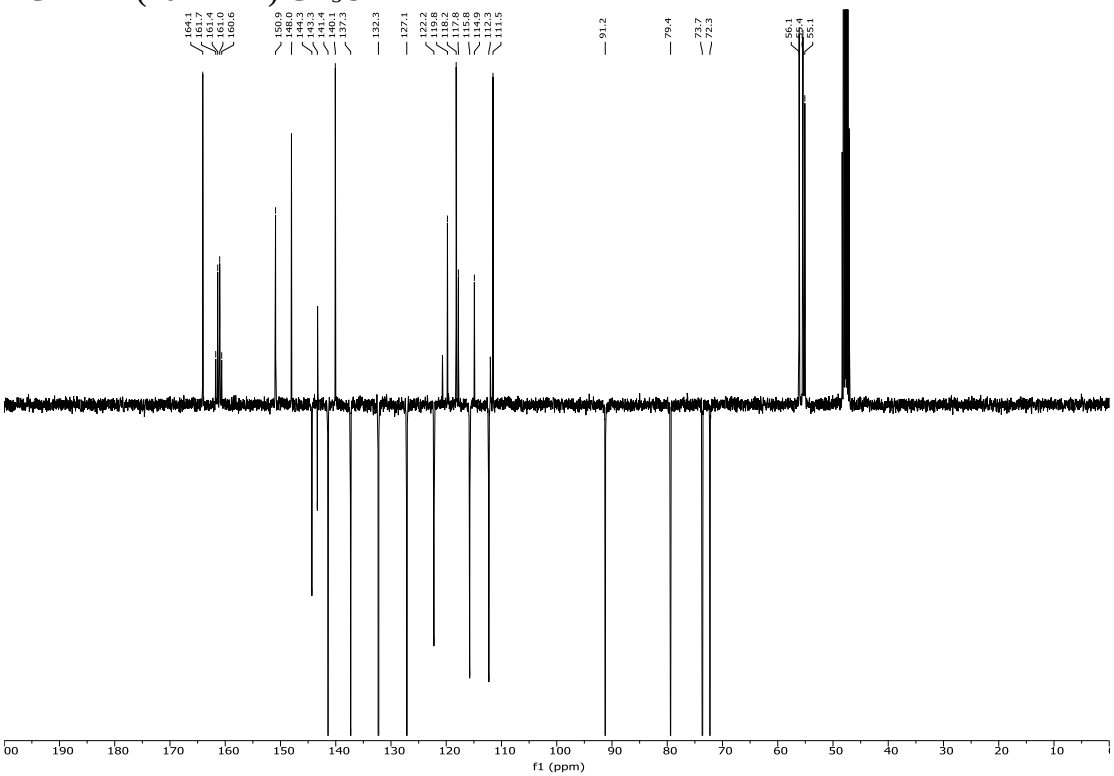

Compound **21i** ^{1}H NMR (500 MHz) CD_3OD

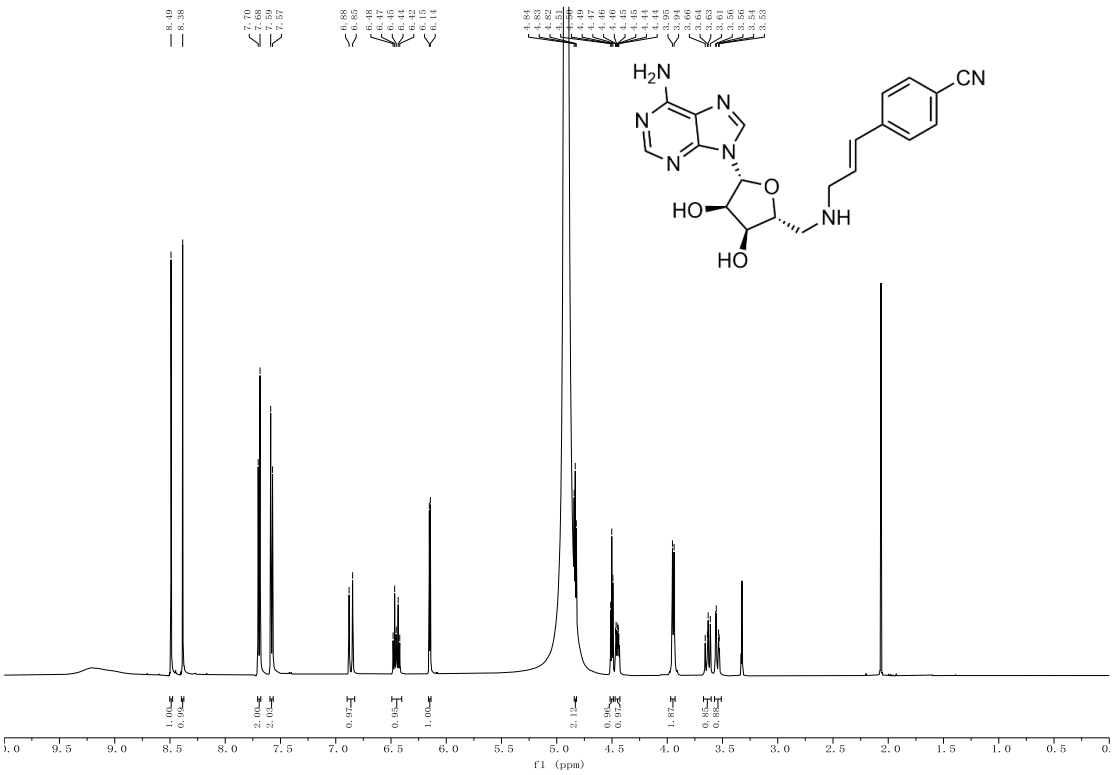

^{13}C NMR (126 MHz) CD_3OD

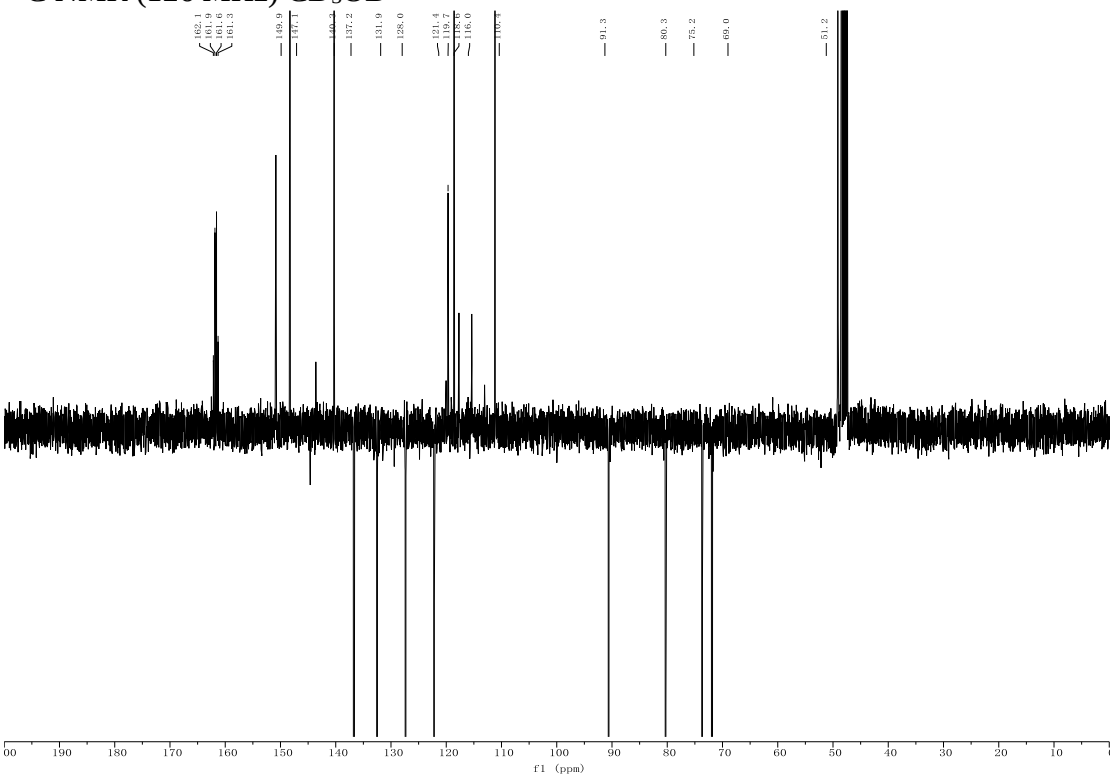

Compound **21j** ^{1}H NMR (400 MHz) CD_3OD

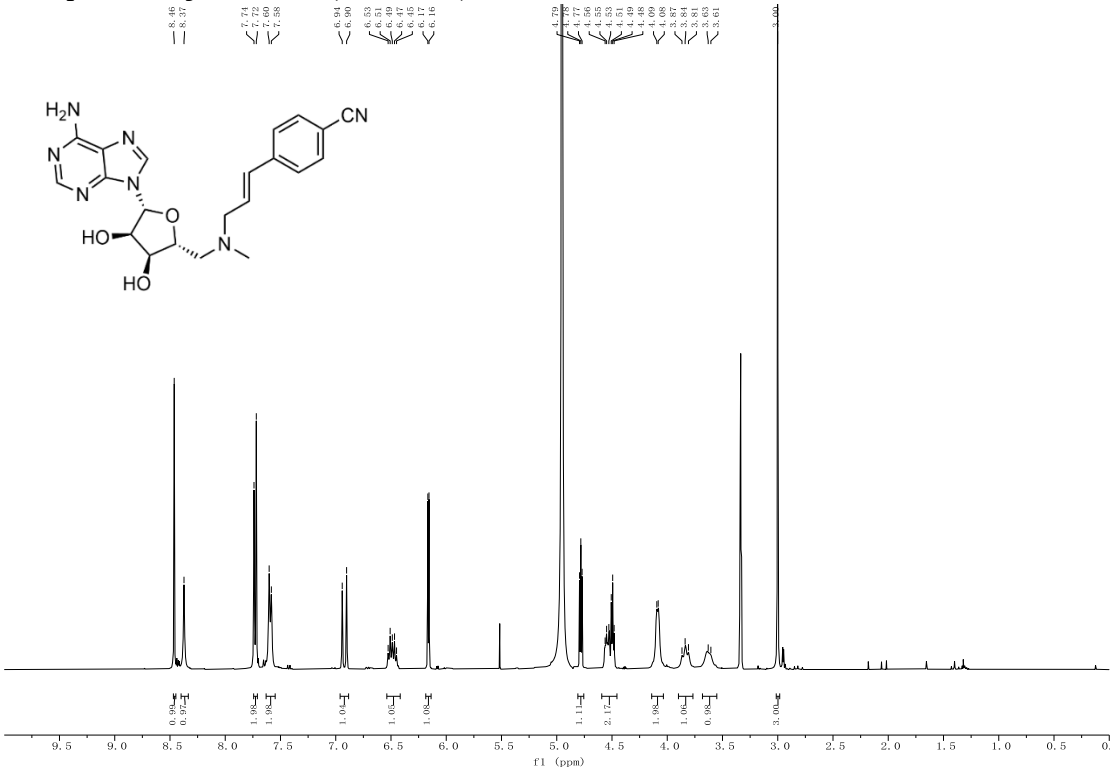

^{13}C NMR (101 MHz) CD_3OD

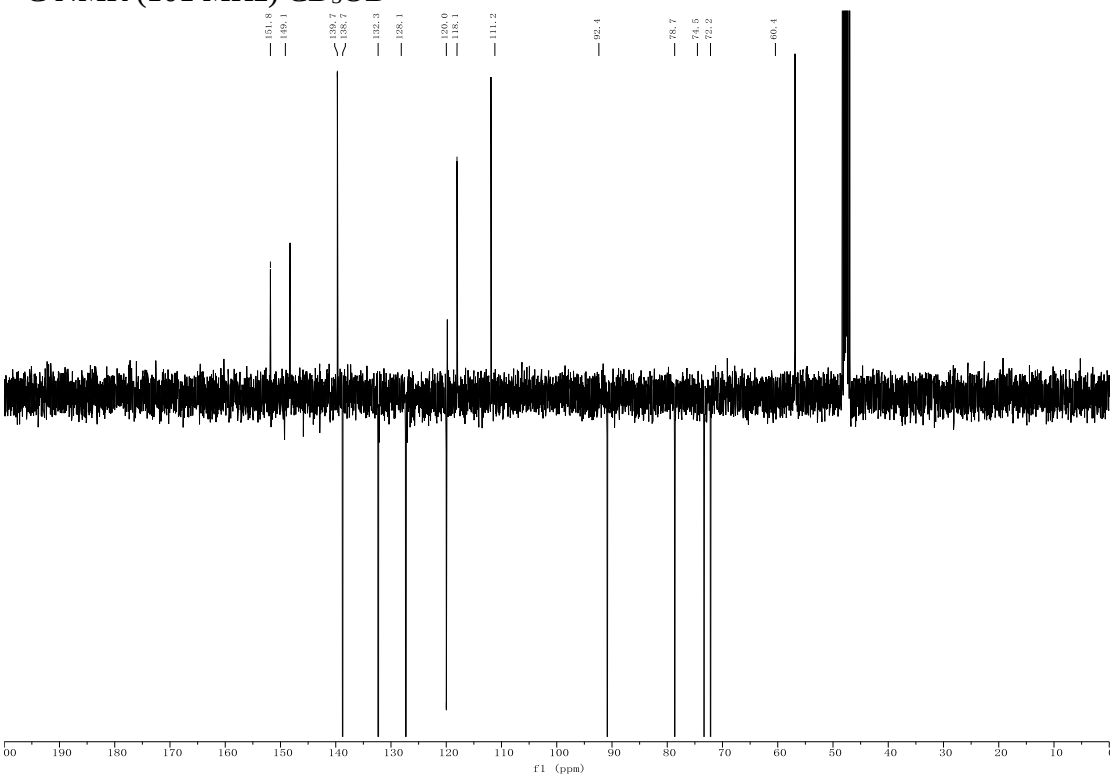

Compound **21k** ^{1}H NMR (500 MHz) CD_3OD

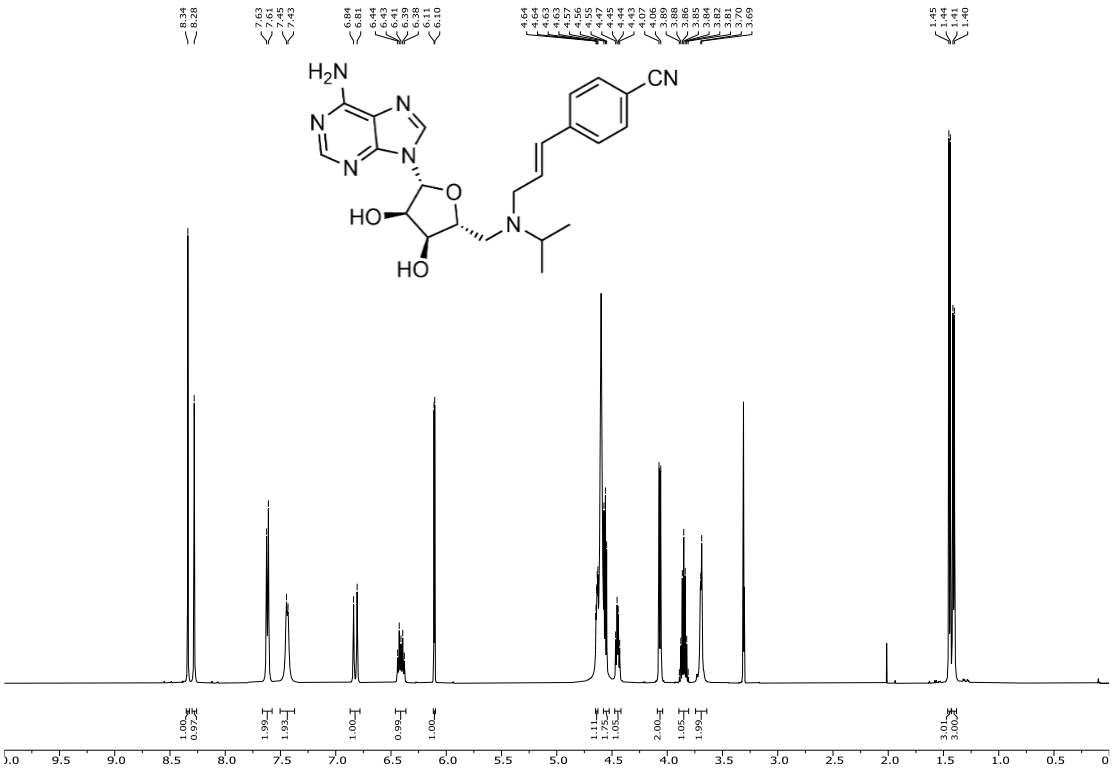

^{13}C NMR (126 MHz) CD_3OD

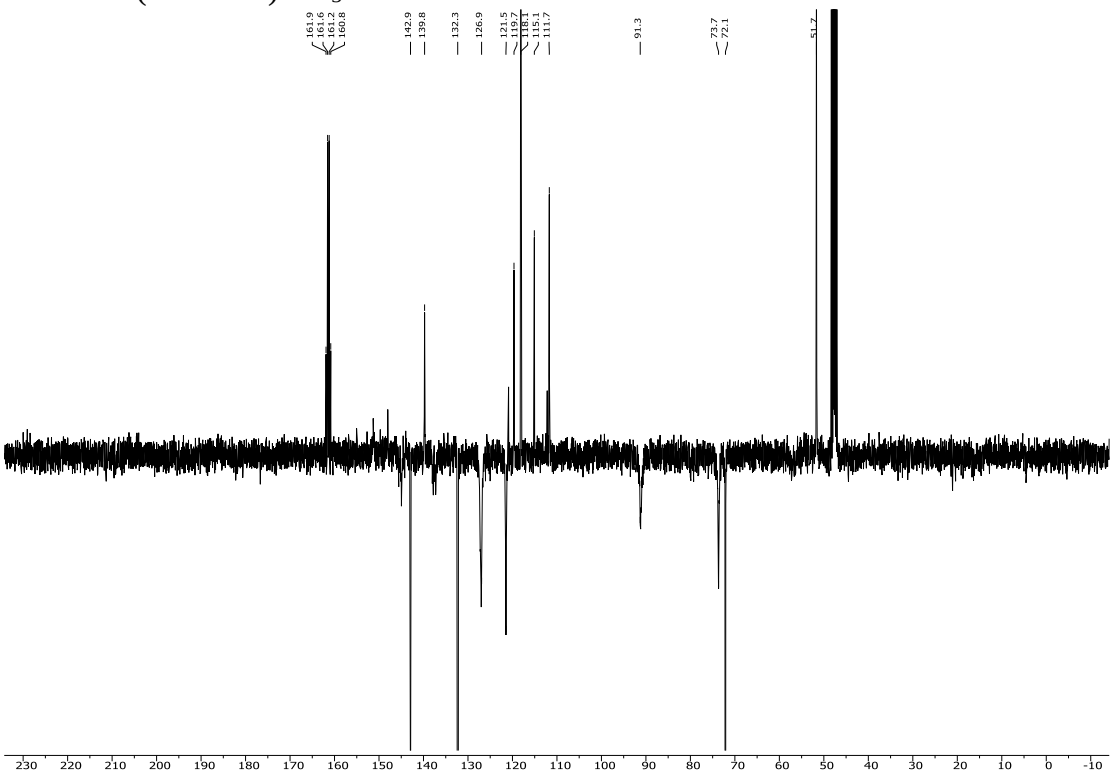

Compound **22b** ^{1}H NMR (400 MHz) CD_3OD

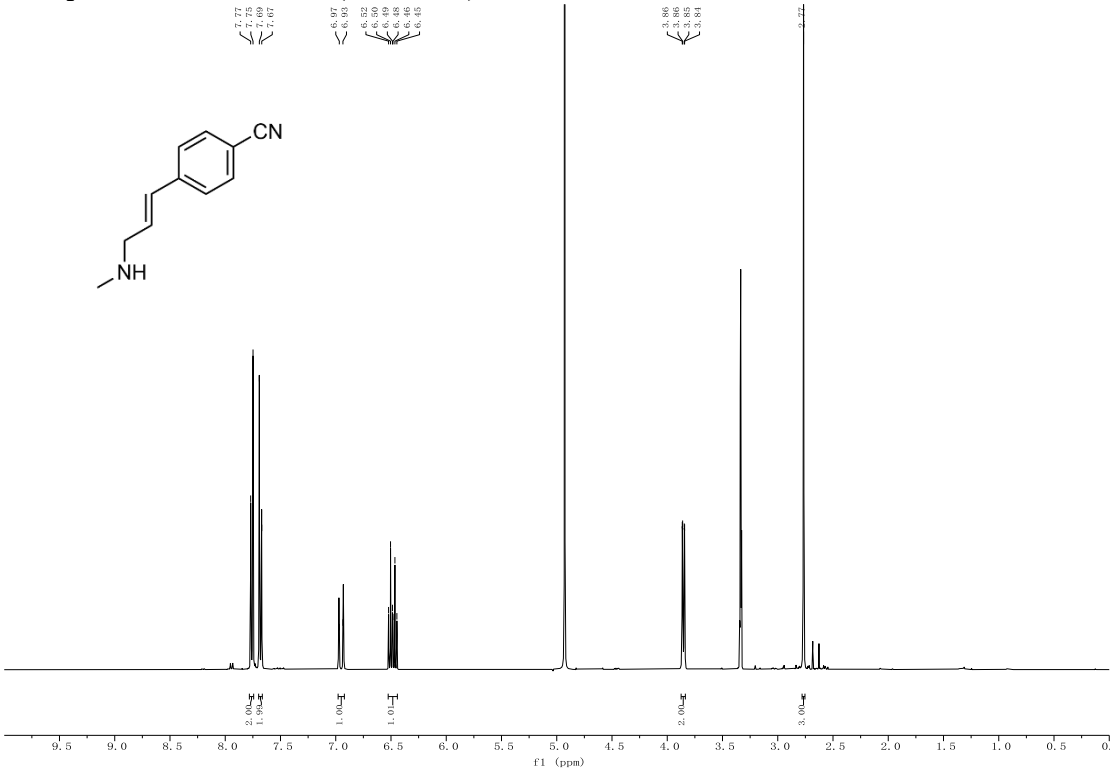

^{13}C NMR (101 MHz) CD_3OD

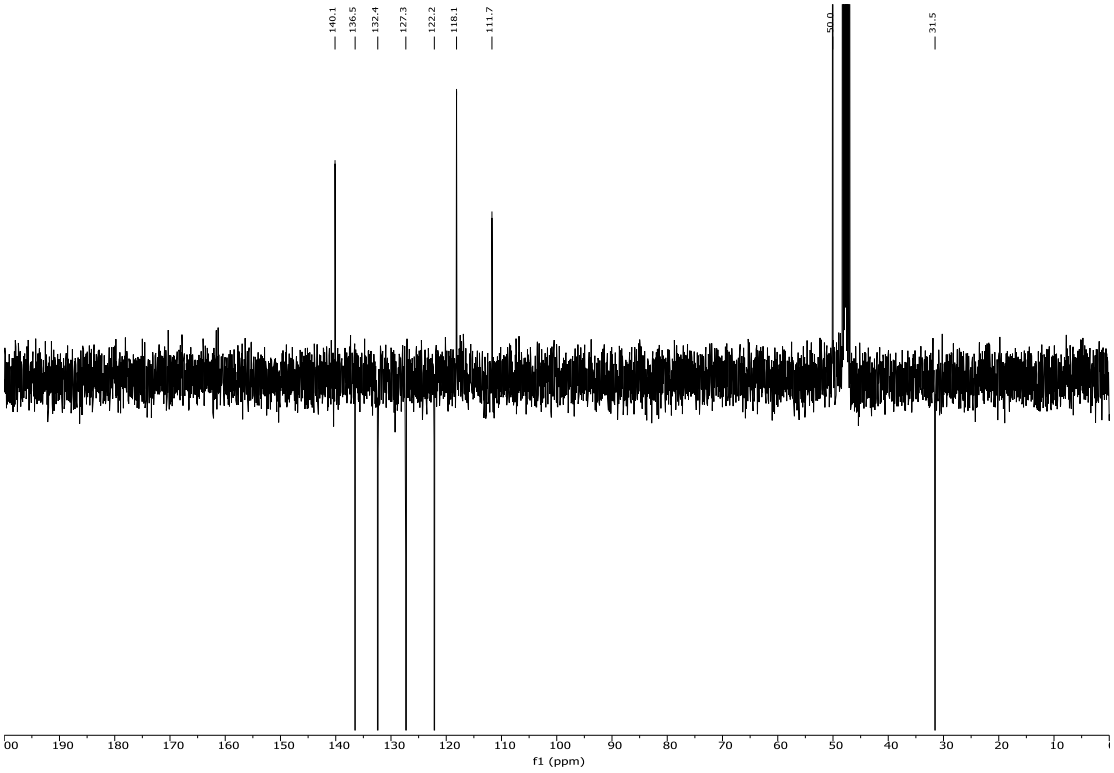

Compound **23a** ^{1}H NMR (400 MHz) $CDCl_3$

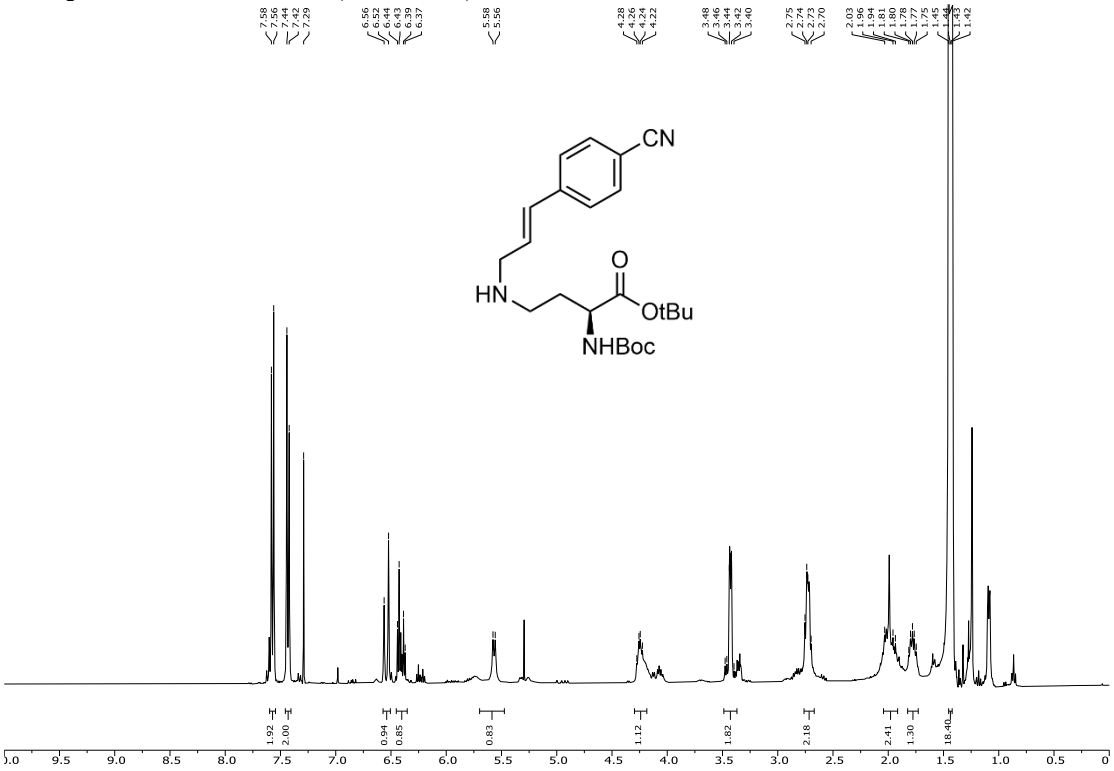

^{13}C NMR (101 MHz) $CDCl_3$

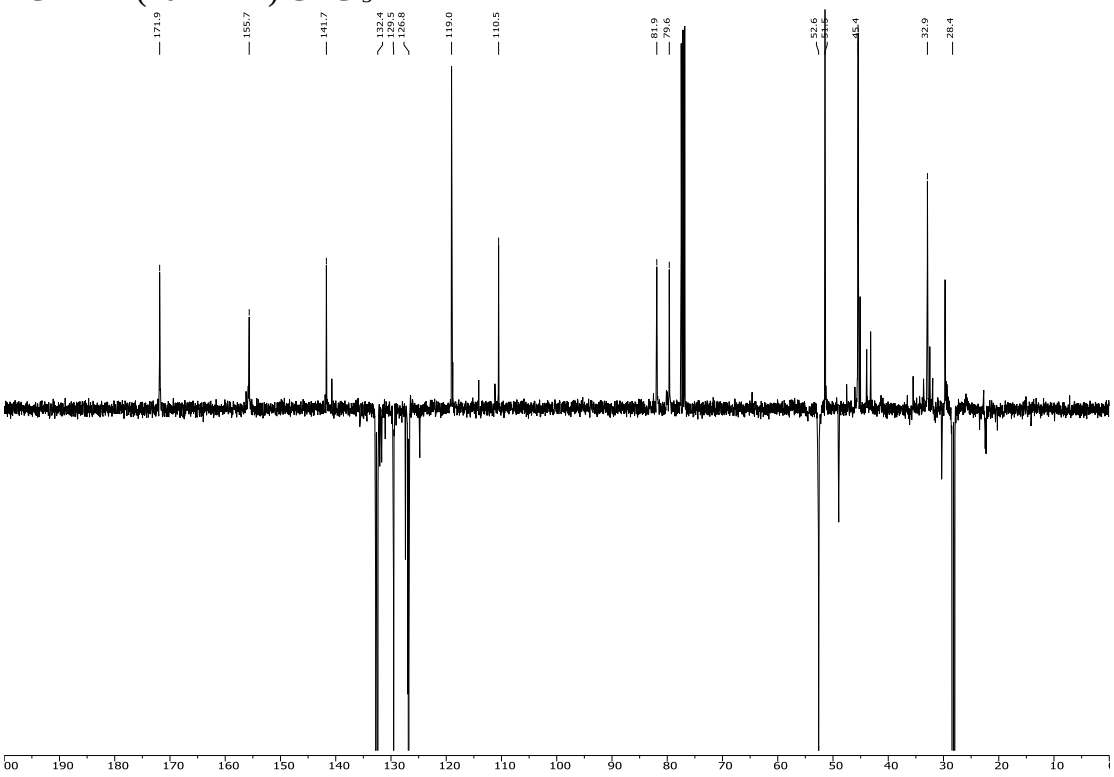

Compound **23b** ^{1}H NMR (400 MHz) $CDCl_3$

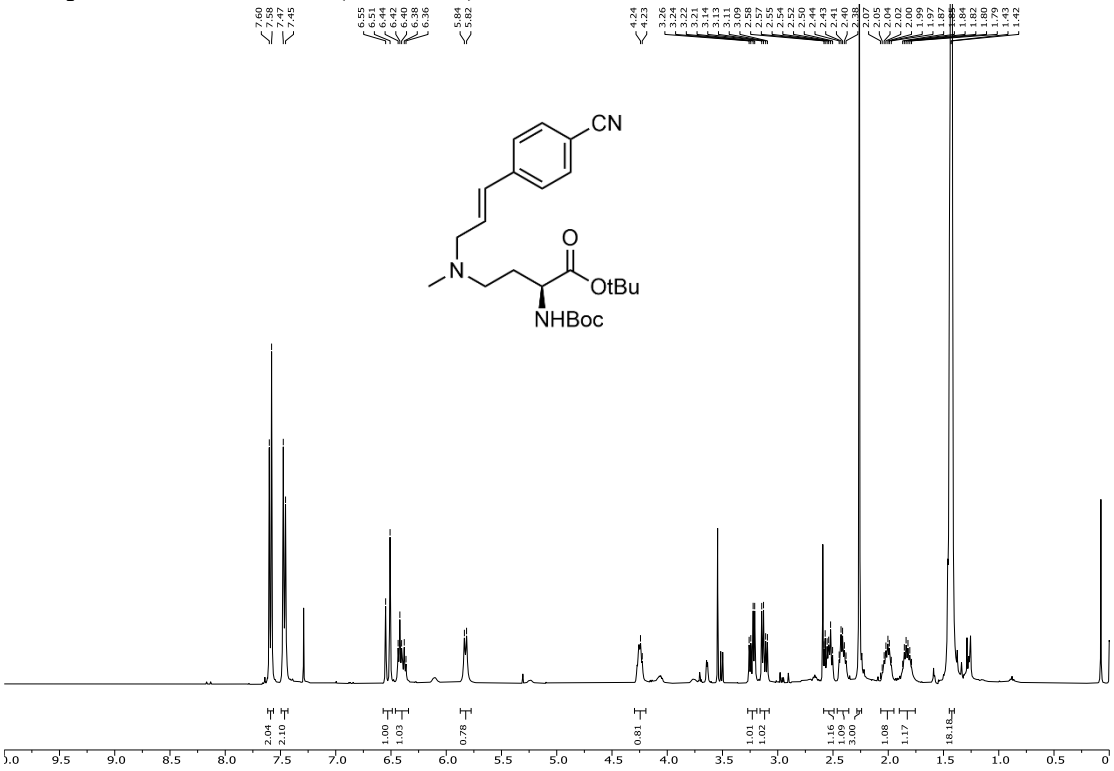

^{13}C NMR (101 MHz) $CDCl_3$

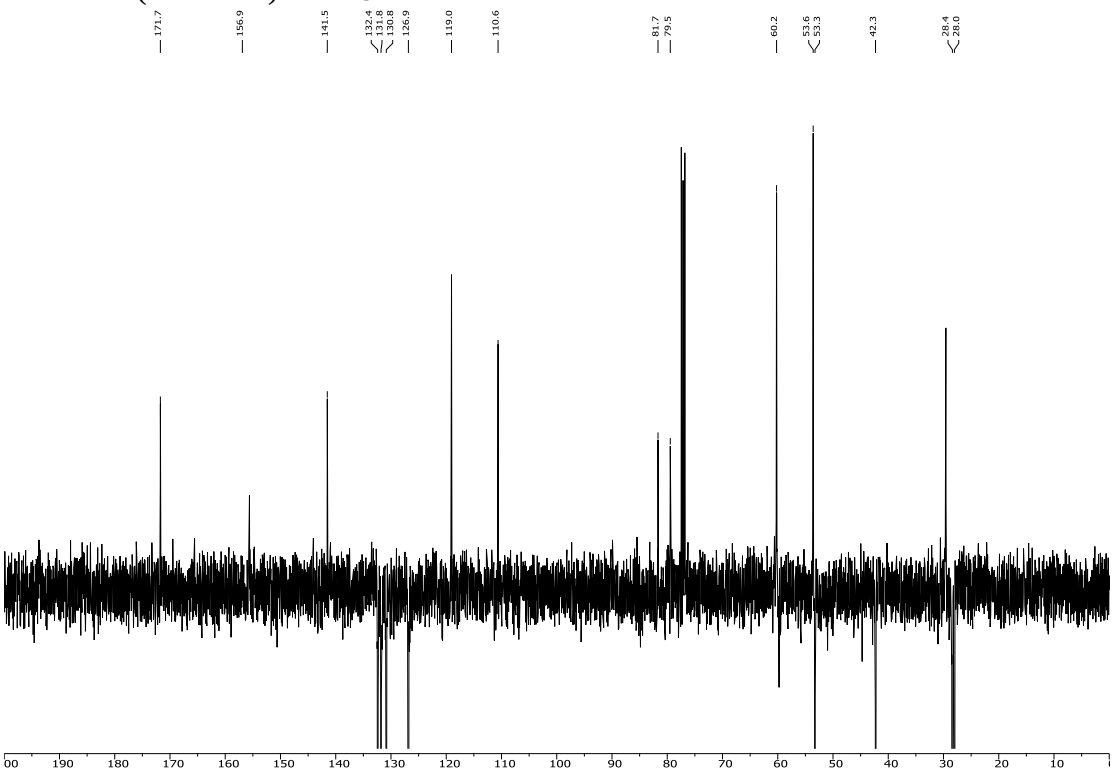

Compound **24a** ^{1}H NMR (400 MHz) CD_3OD

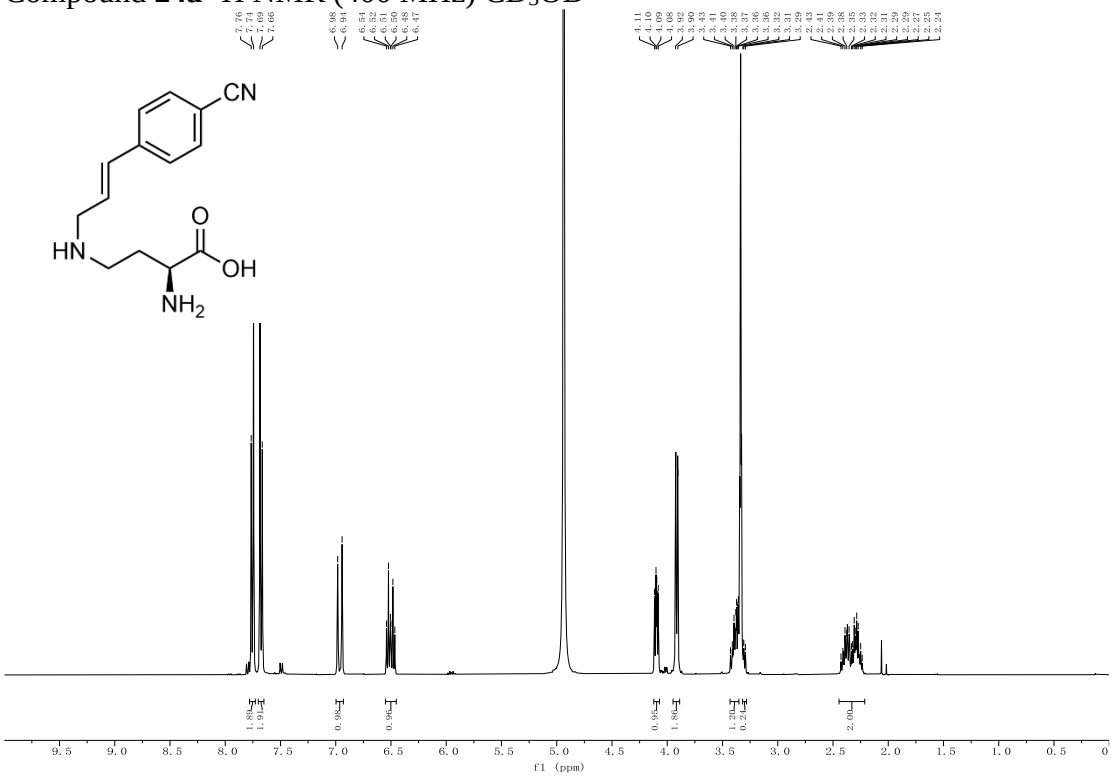

^{13}C NMR (101 MHz) CD_3OD

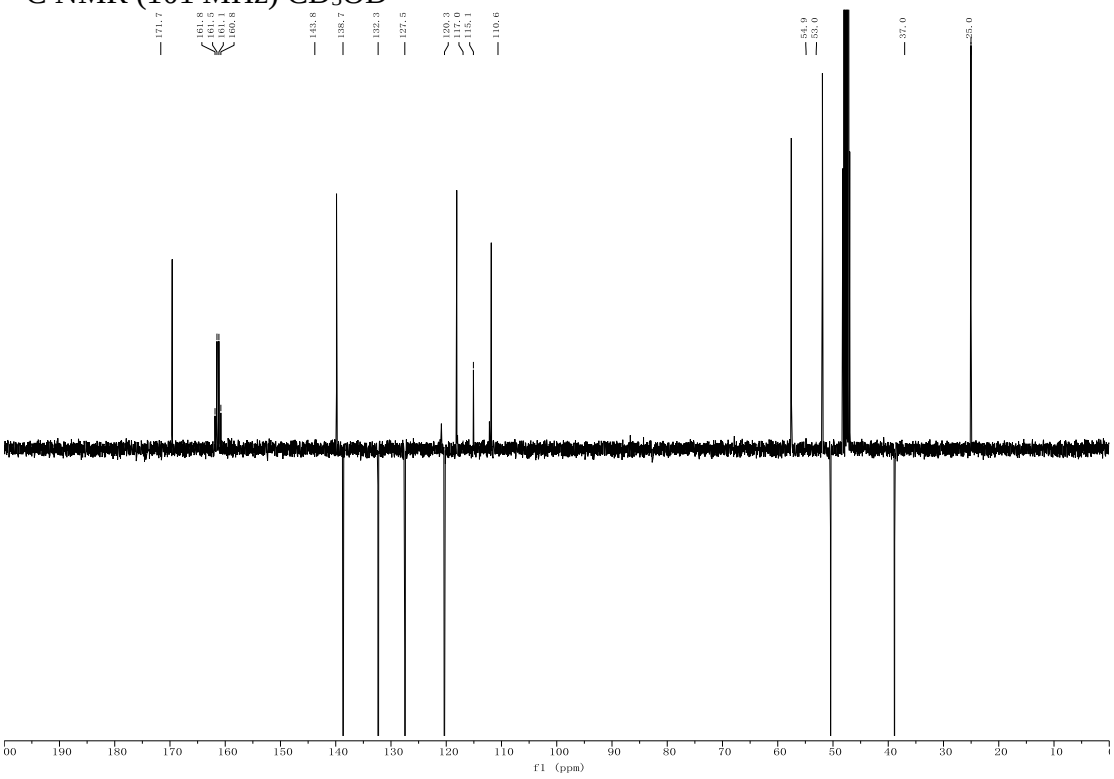

Compound **24b** ^{1}H NMR (400 MHz) CD_3OD

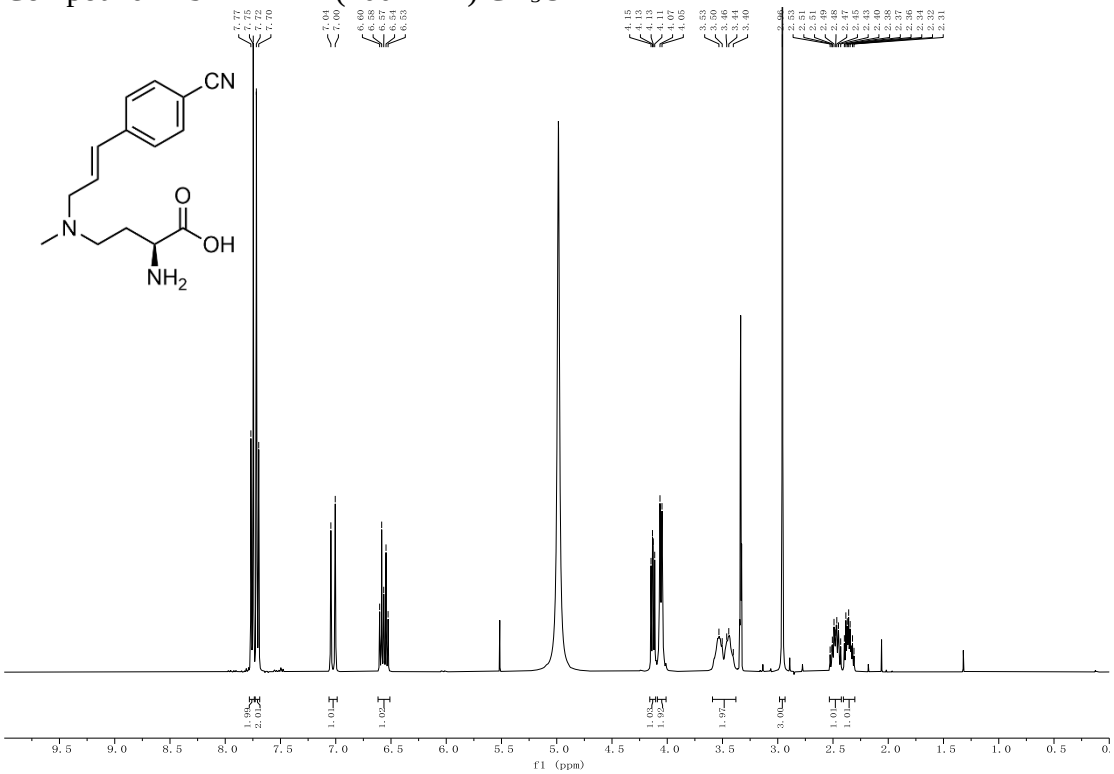

^{13}C NMR (101 MHz) CD_3OD

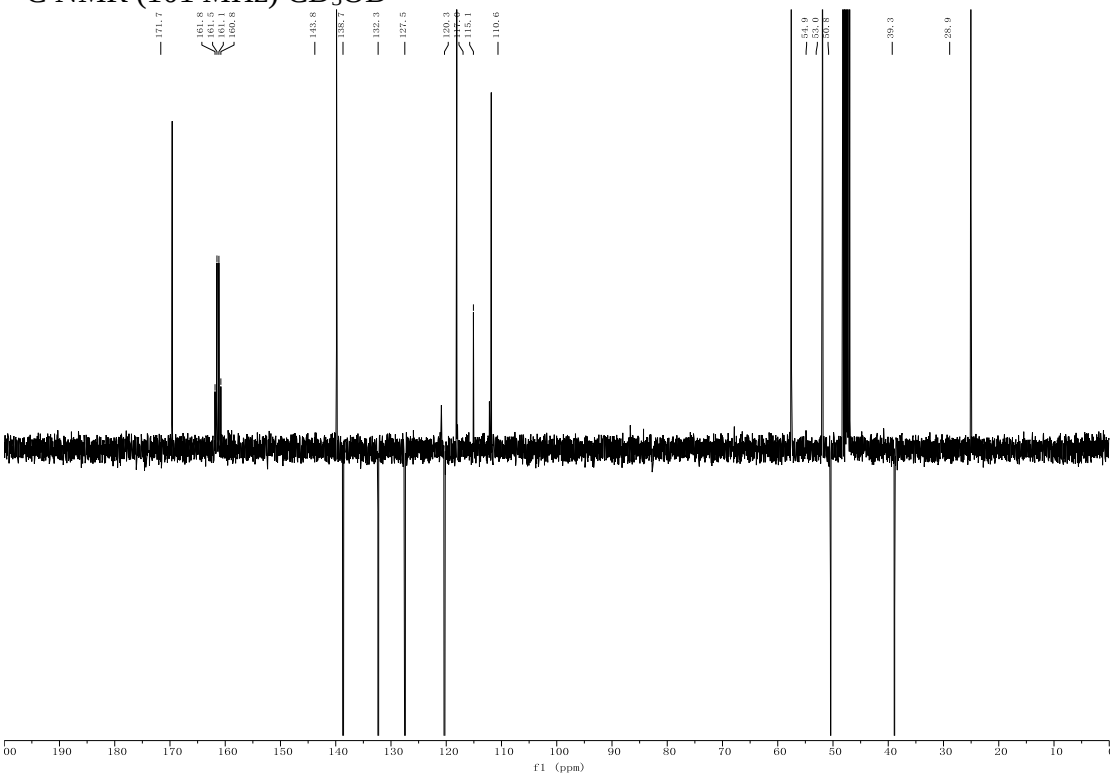

Compound **25a** ^{1}H NMR (500 MHz) $CDCl_3$

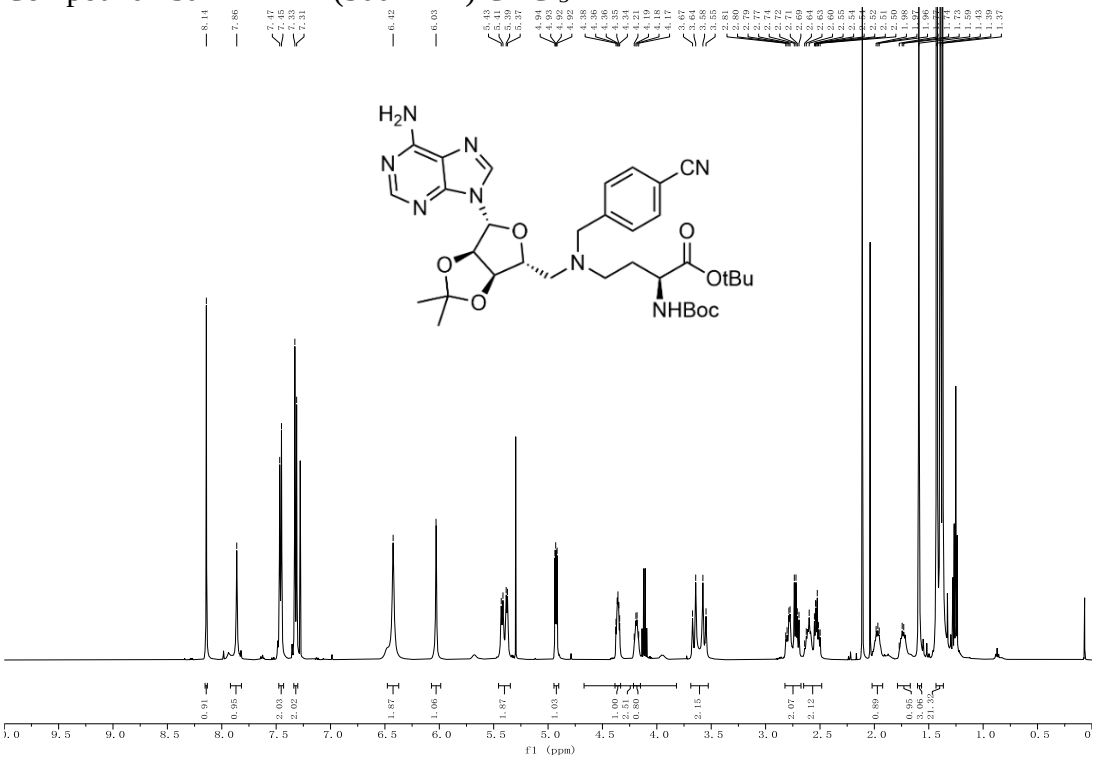

^{13}C NMR (126 MHz) $CDCl_3$

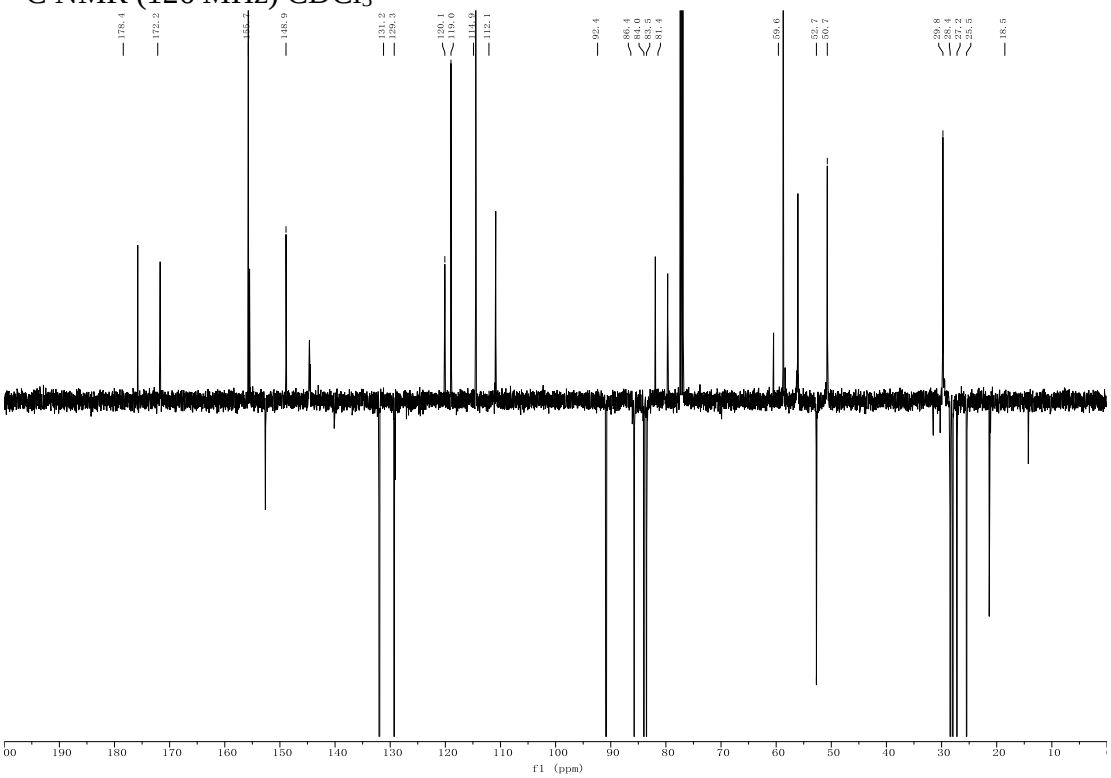

Compound **25** ^{1}H NMR (500 MHz) CD_3OD

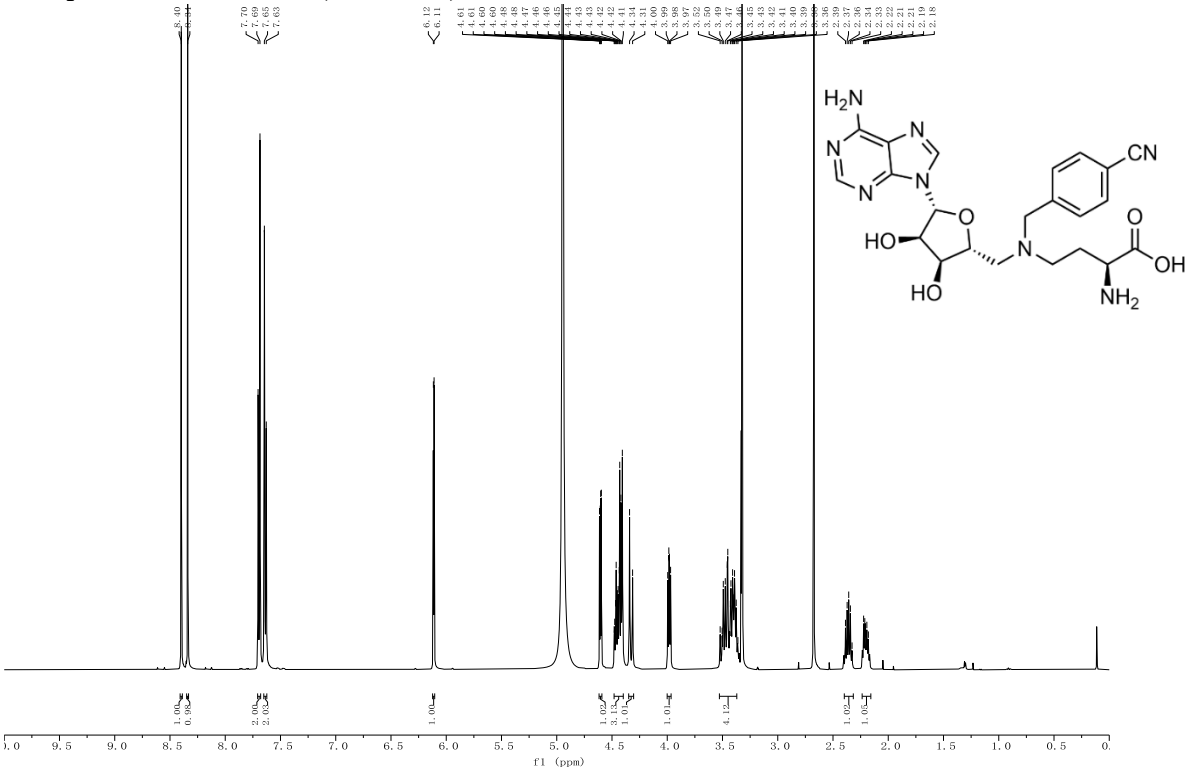

^{13}C NMR (126 MHz) CD_3OD

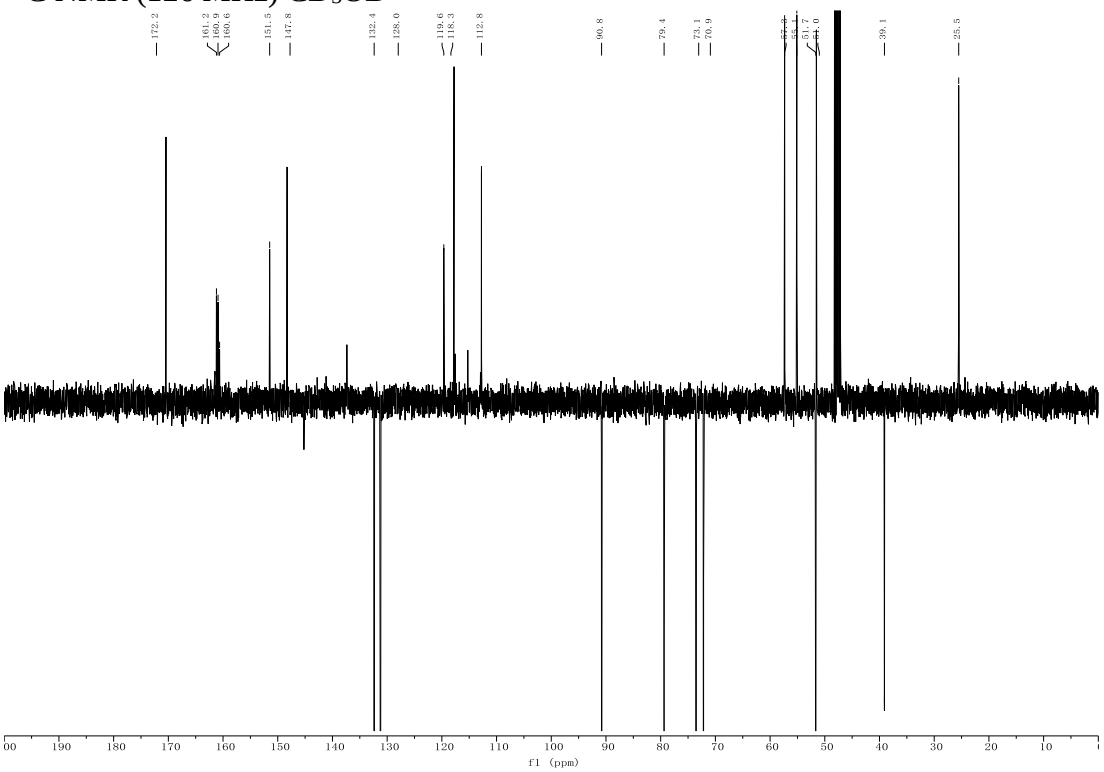

Compound **26a** ^{1}H NMR (400 MHz) $CDCl_3$

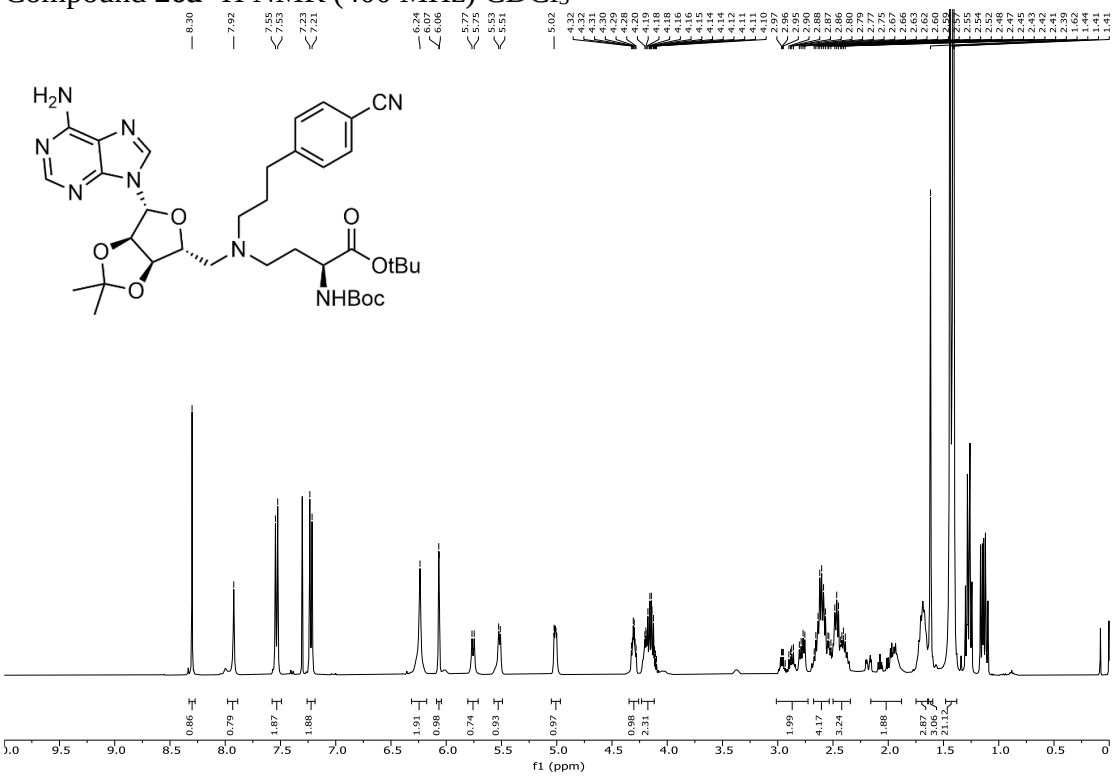

^{13}C NMR (101 MHz) $CDCl_3$

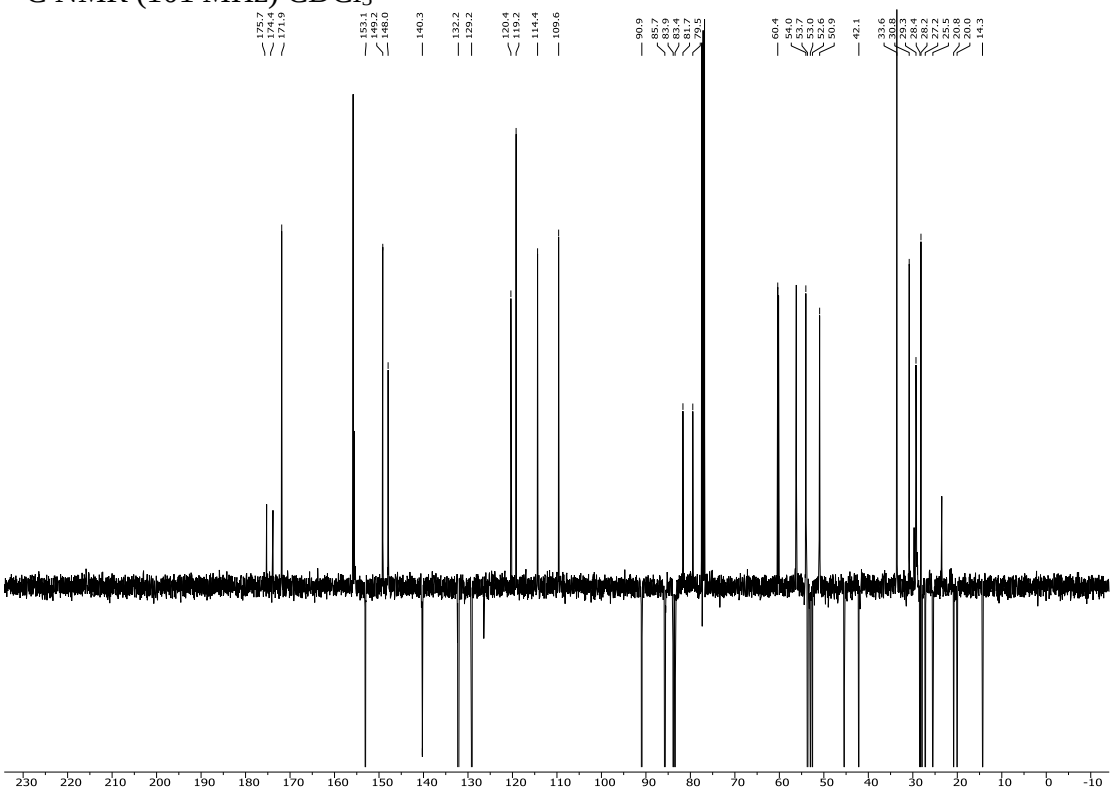

Compound **26** ^{1}H NMR (400 MHz) CD_3OD

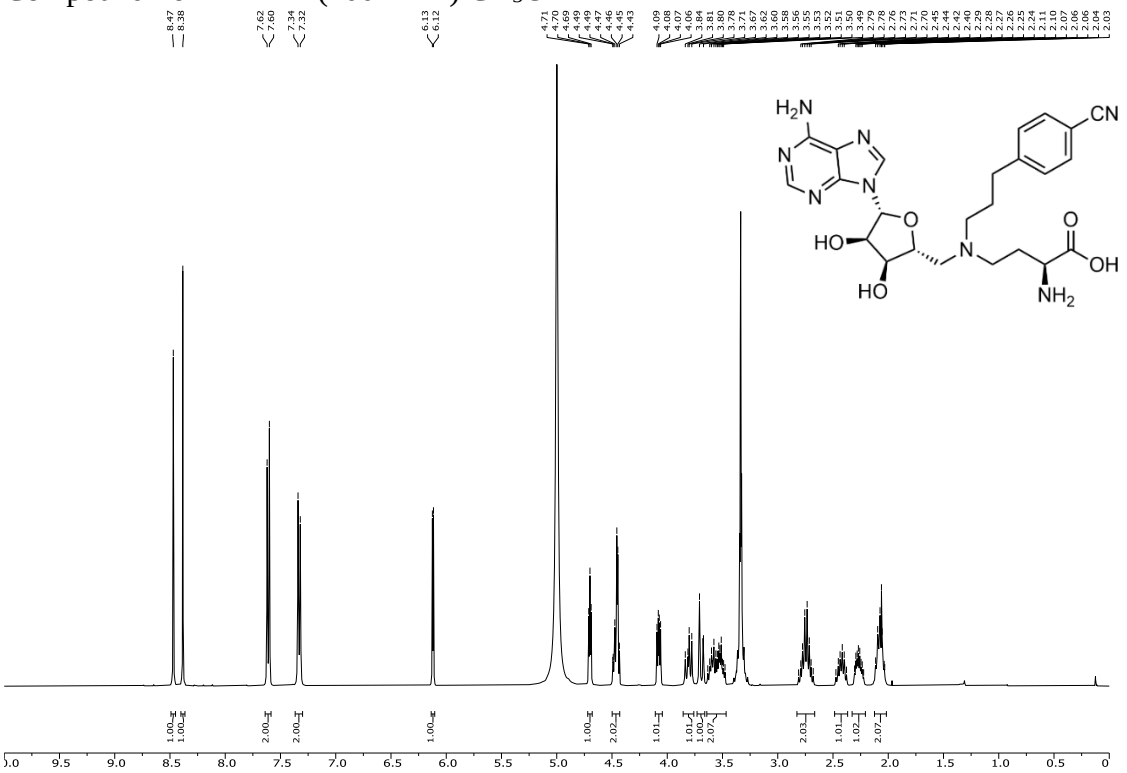

^{13}C NMR (101 MHz) CD_3OD

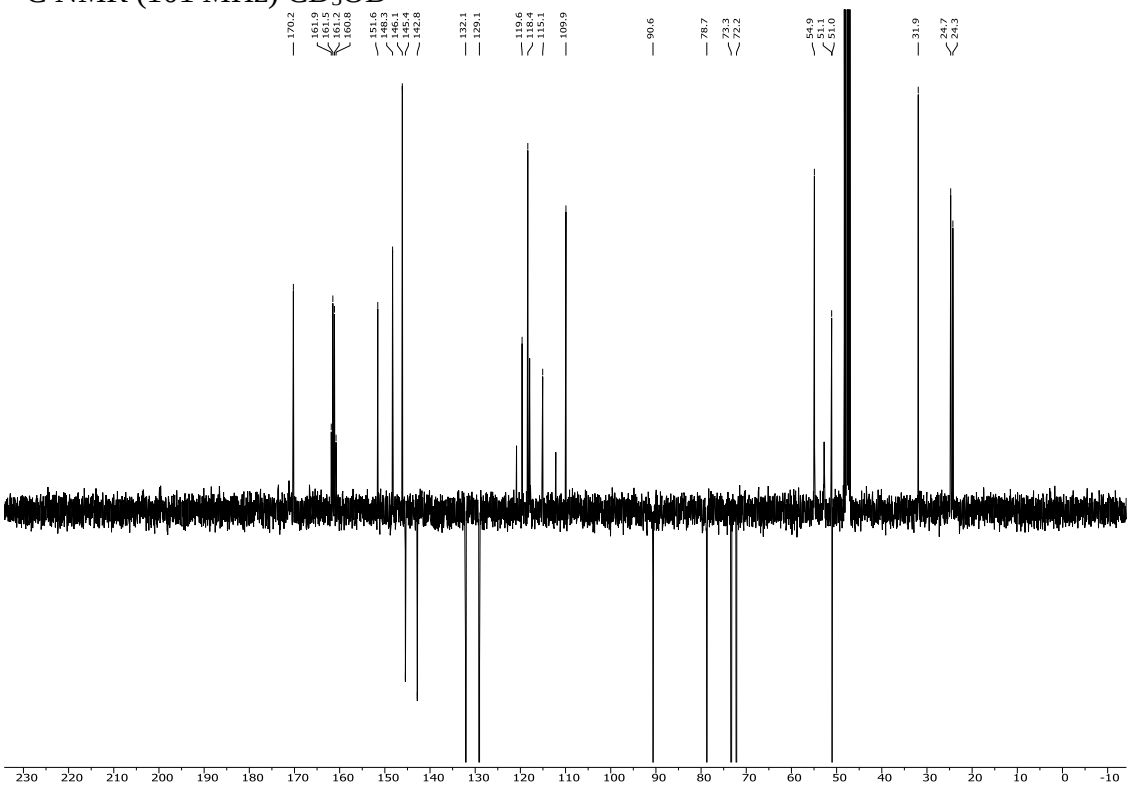

Compound **27** ^{1}H NMR (500 MHz) CD_3OD

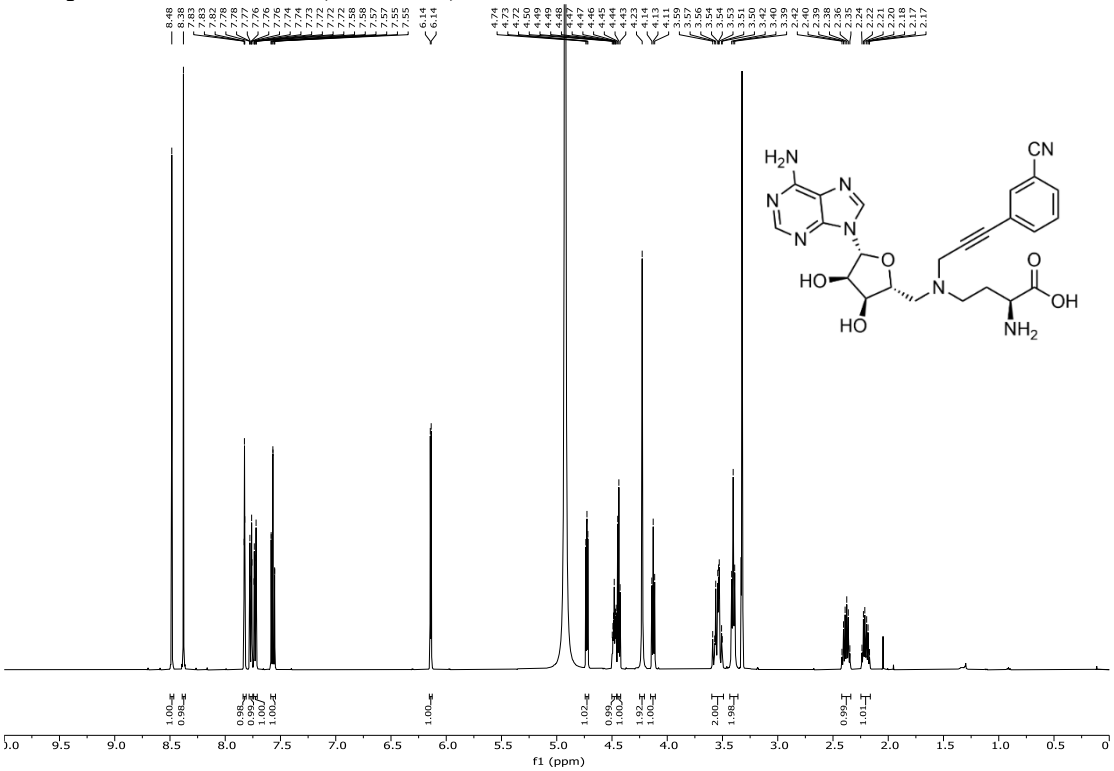

^{13}C NMR (126 MHz) CD_3OD

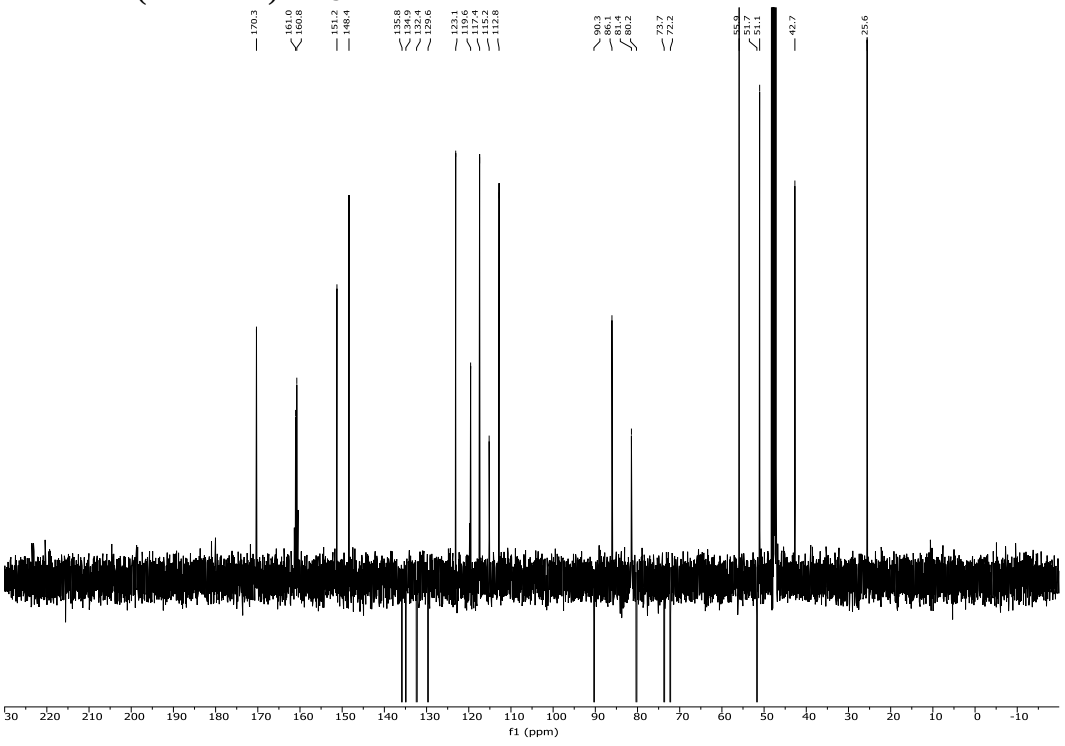

Compound **28a** ^{1}H NMR (500 MHz) $CDCl_3$

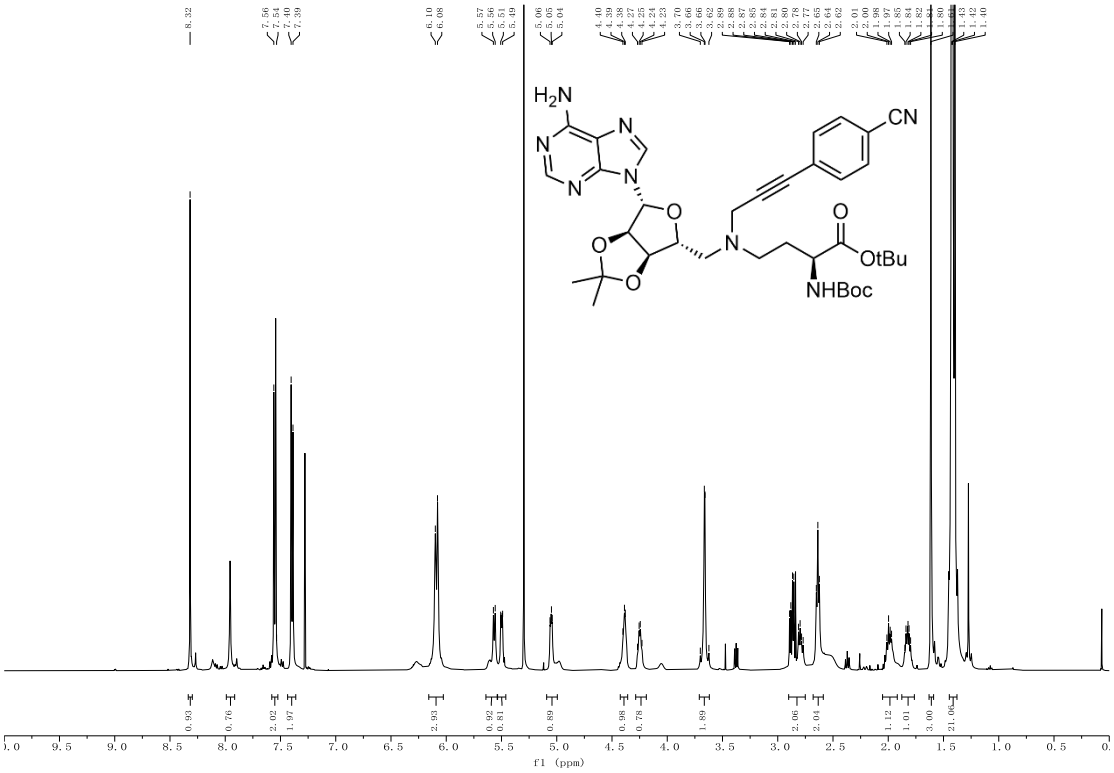

^{13}C NMR (126 MHz) $CDCl_3$

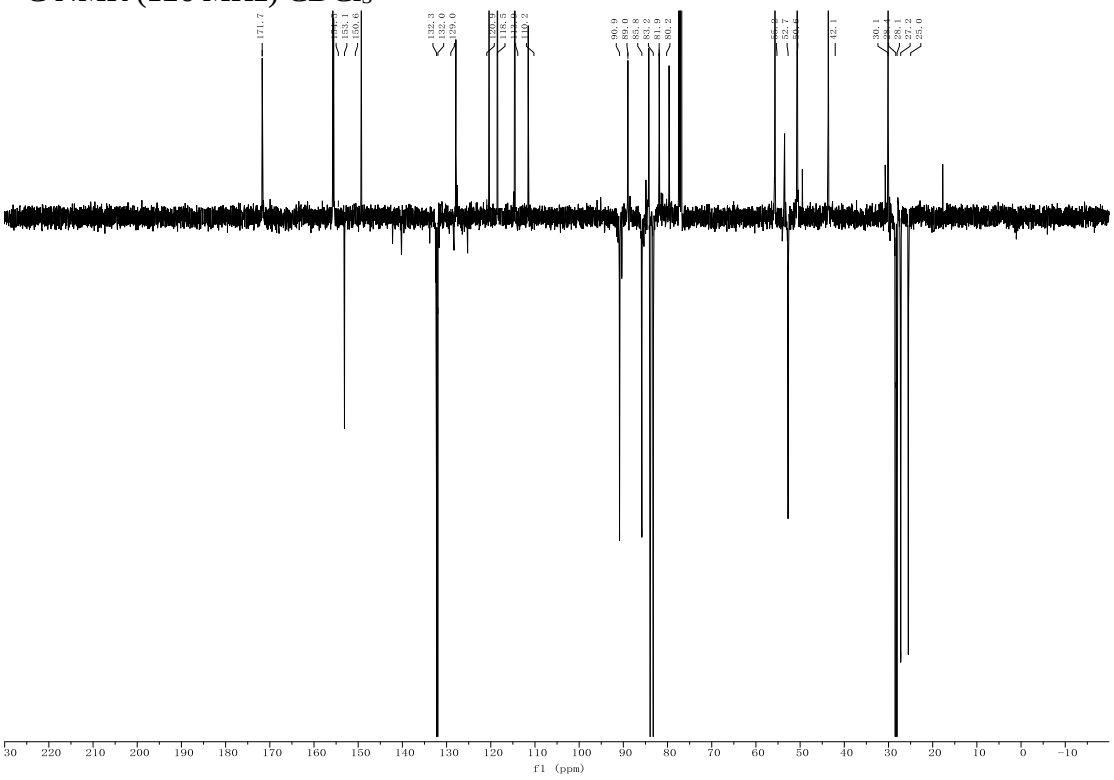

Compound **28** 1H NMR (500 MHz) CD_3OD

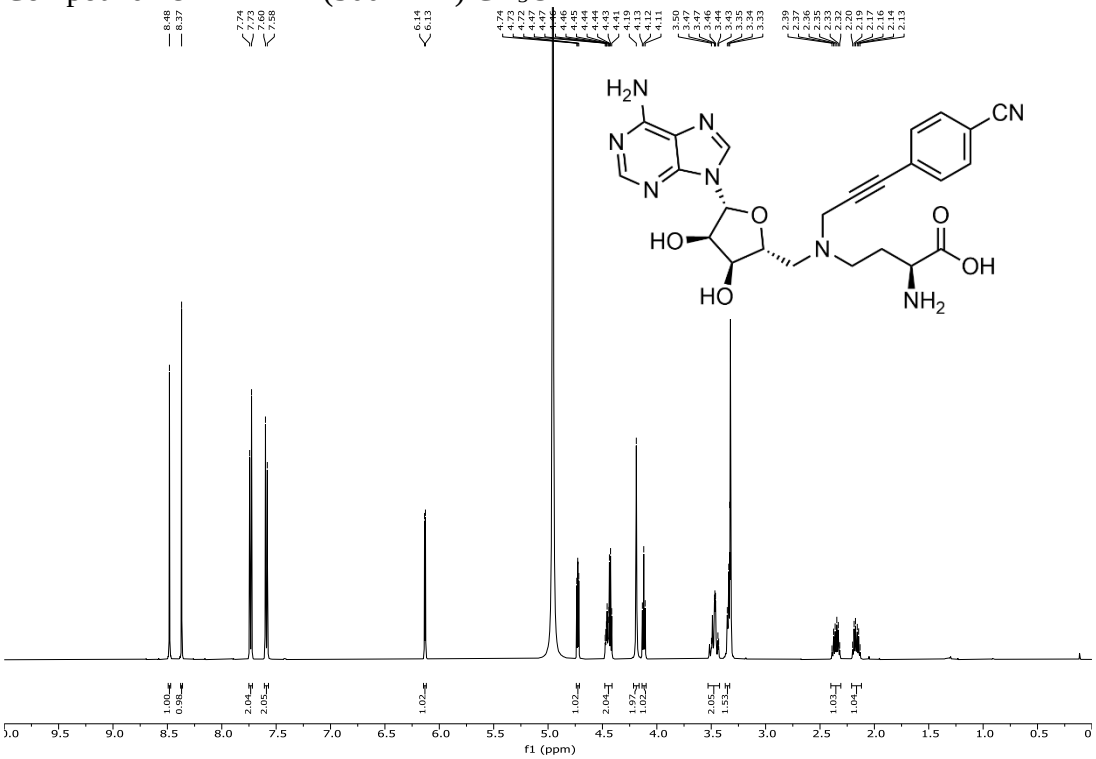

^{13}C NMR (126 MHz) CD_3OD

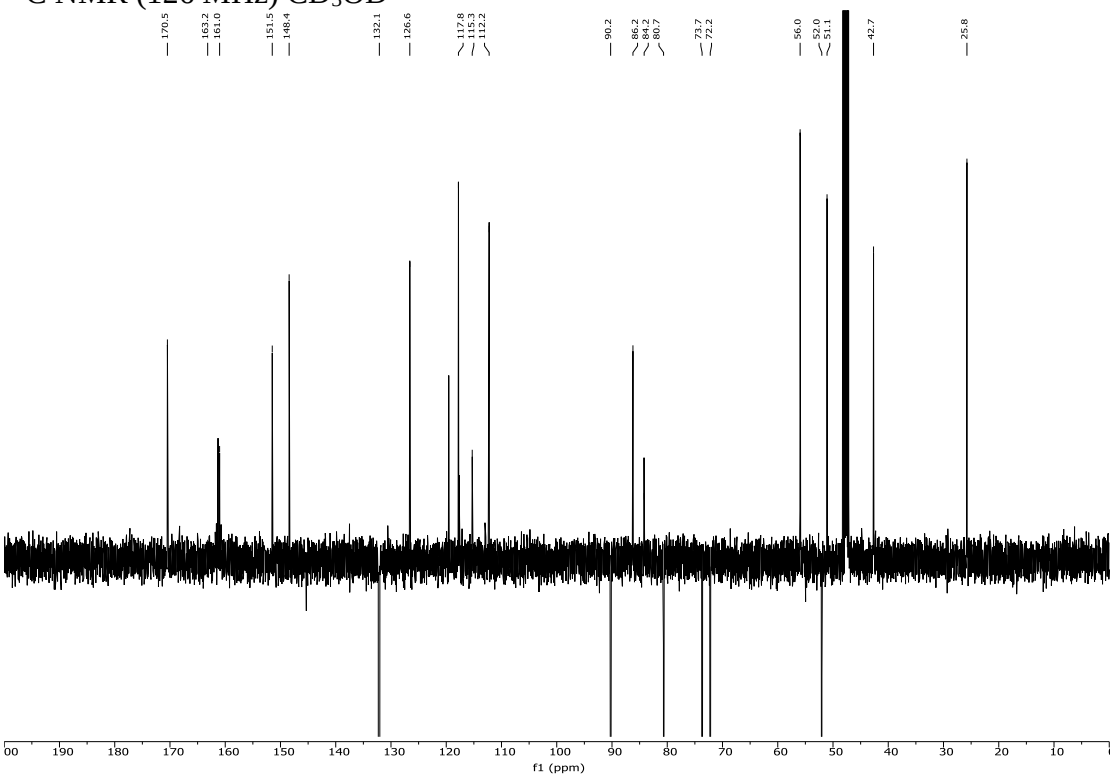

Compound **29a** ^{1}H NMR (400 MHz) $CDCl_3$

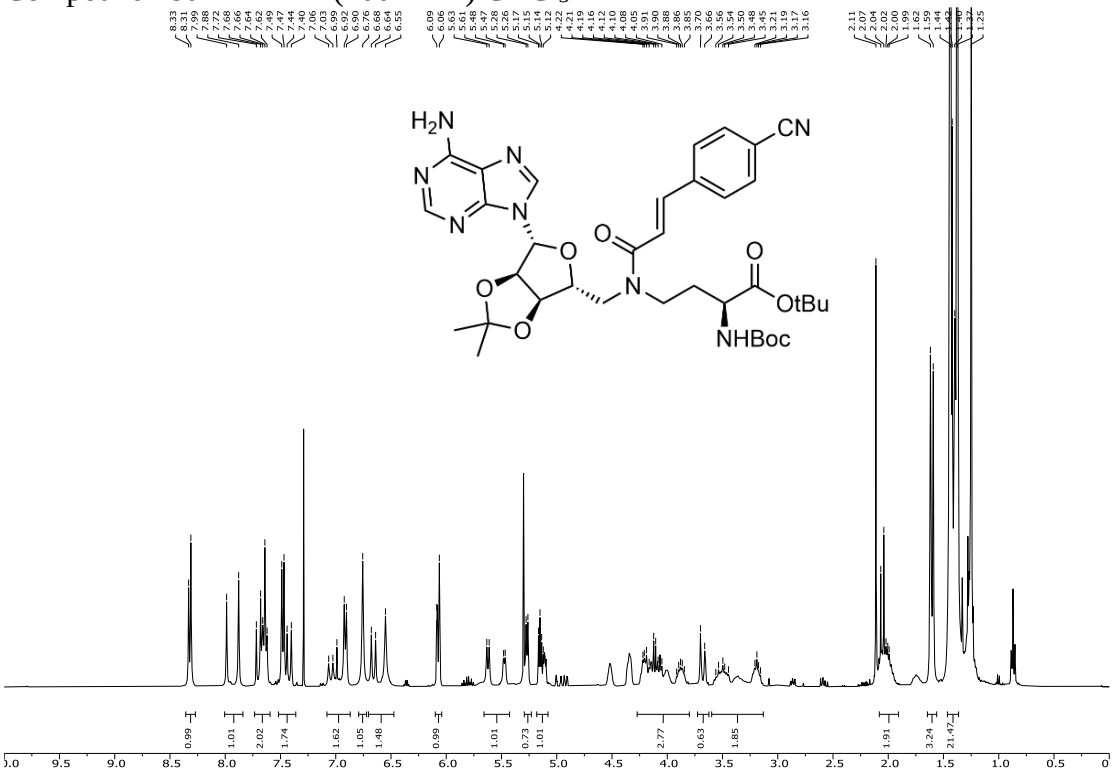

^{13}C NMR (101 MHz) $CDCl_3$

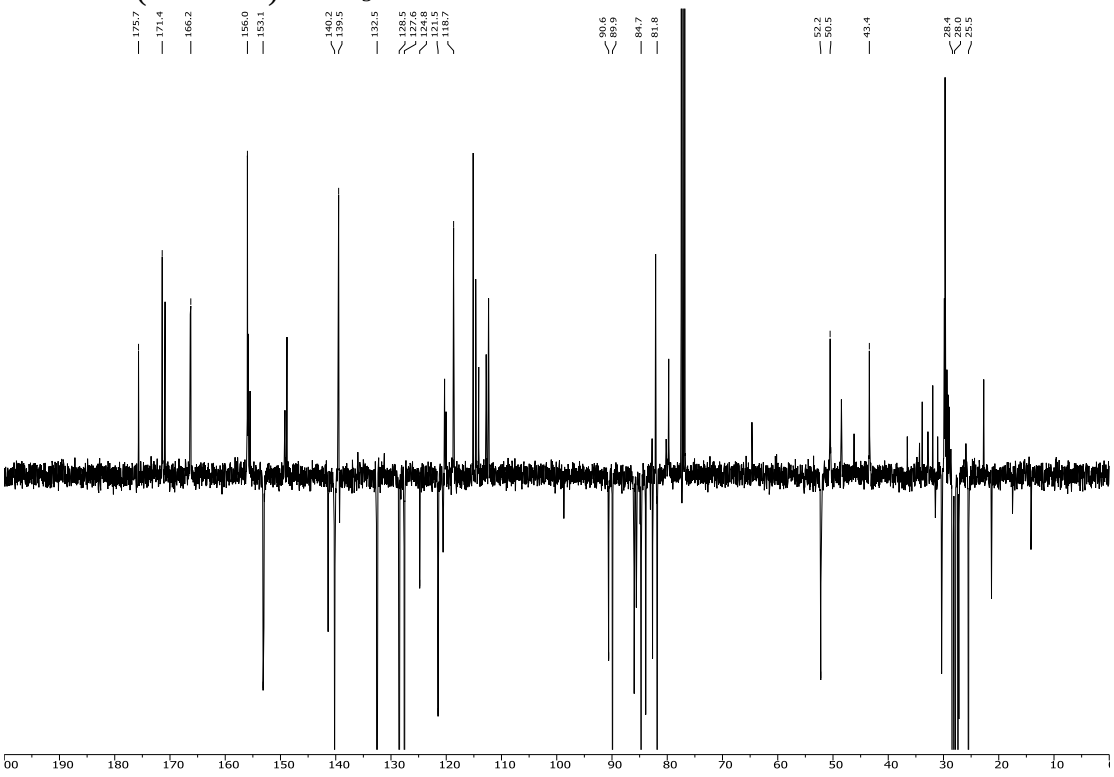

Compound **29** ^{1}H NMR (400 MHz) CD_3OD

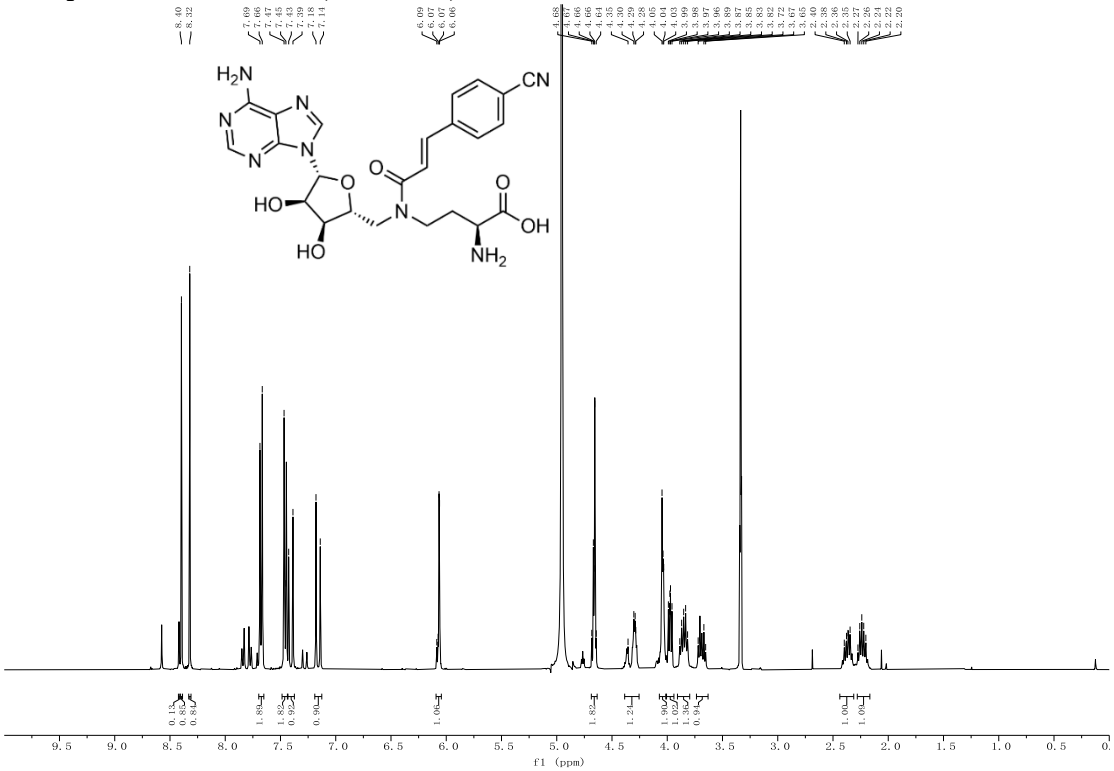

^{13}C NMR (101 MHz) CD_3OD

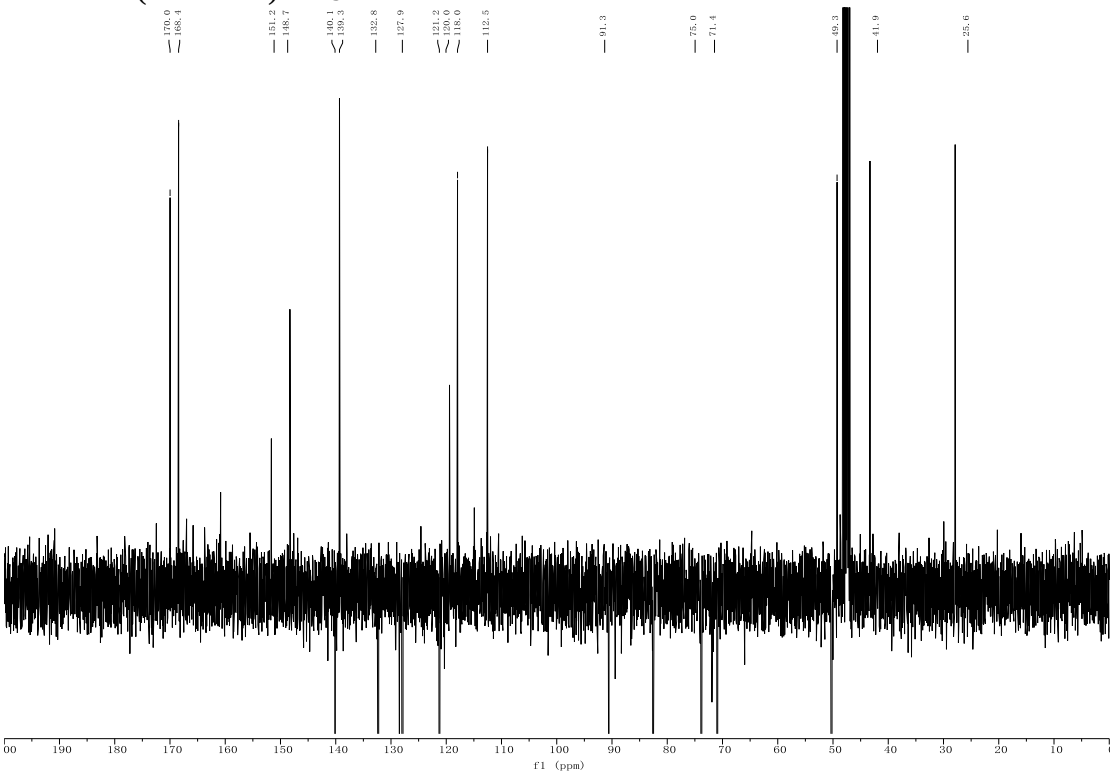

Compound **31a** ^{1}H NMR (400 MHz) $CDCl_3$

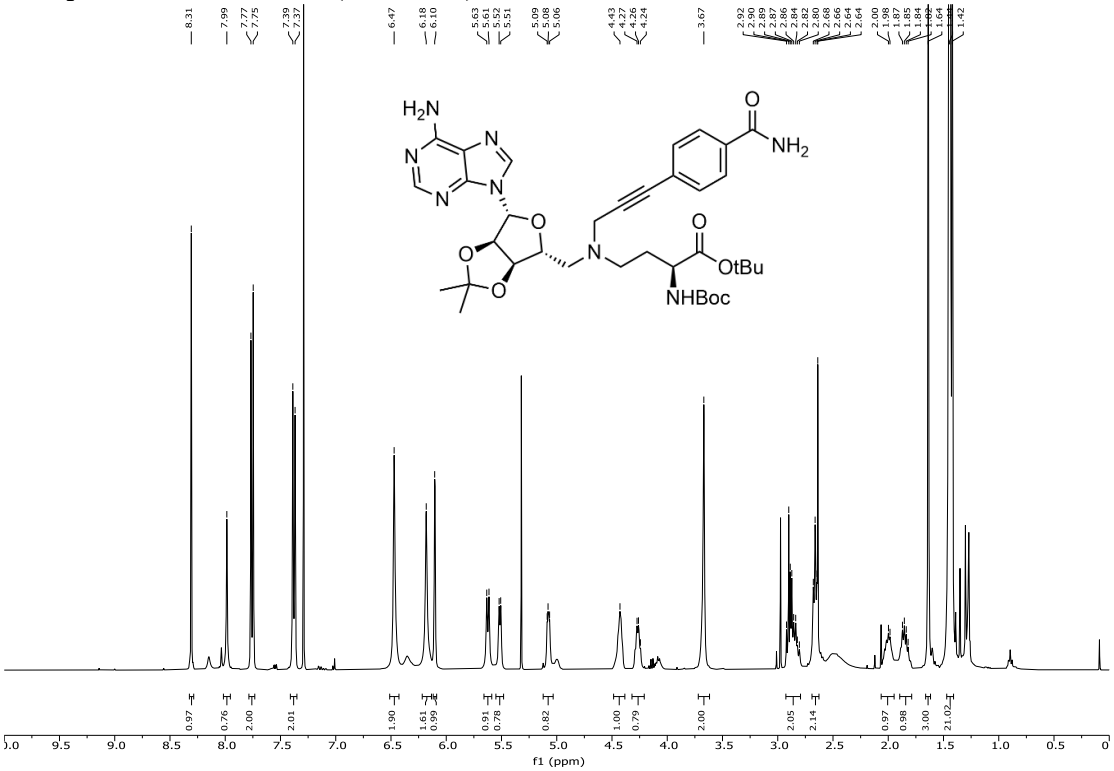

^{13}C NMR (101 MHz) $CDCl_3$

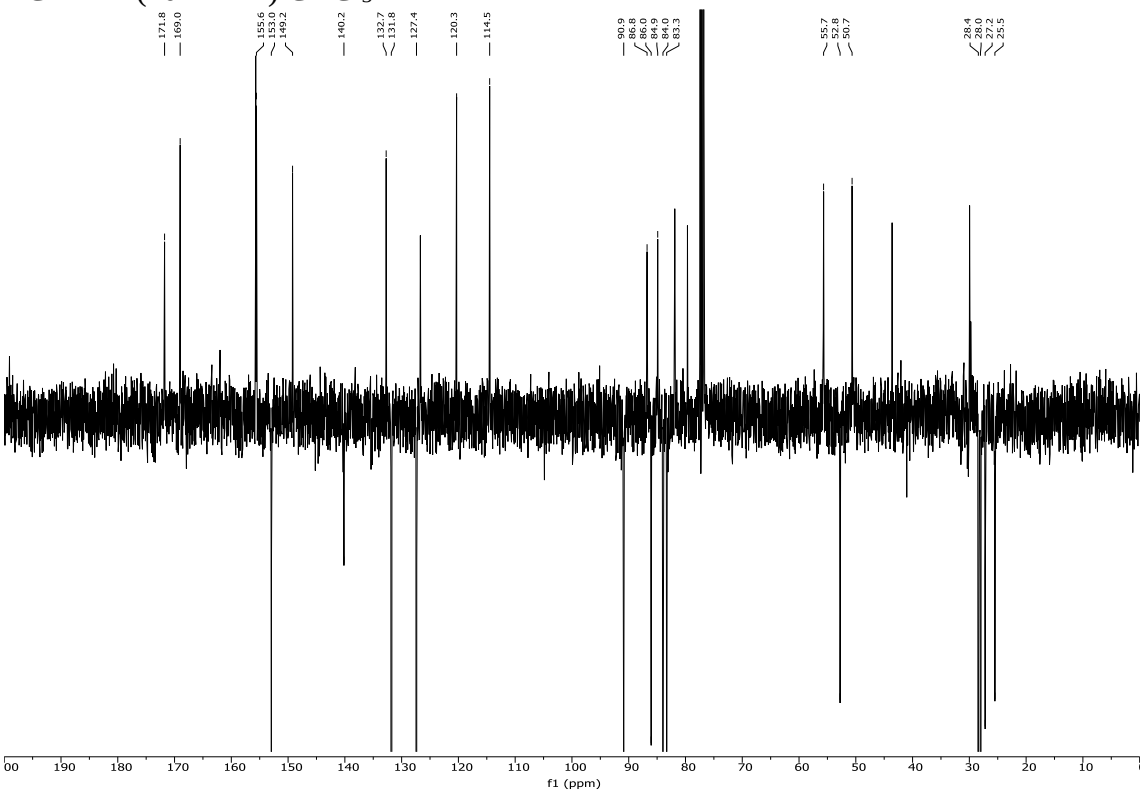

Compound **31** ^{1}H NMR (400 MHz) CD_3OD

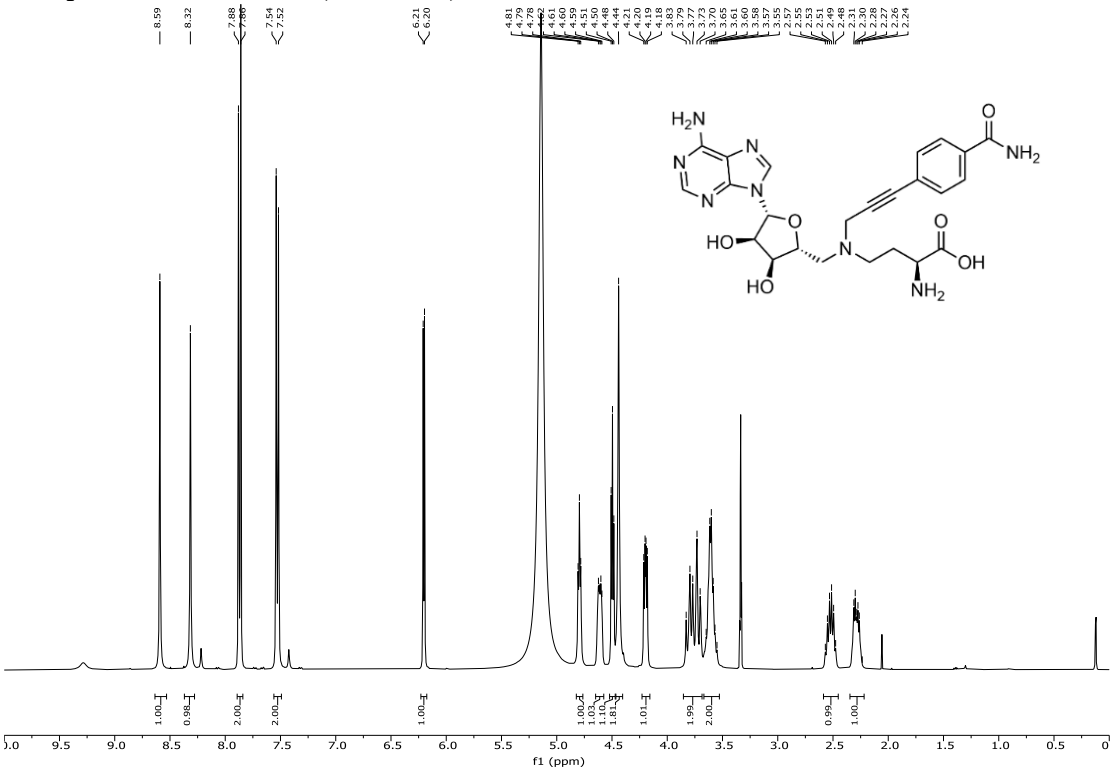

^{13}C NMR (101 MHz) CD_3OD